22 Integrated cross section and tectonic evolution of the Alps along the Eastern Traverse

S.M. Schmid, O.A. Pfiffner, G. Schönborn, N. Froitzheim and E. Kissling

Contents

22.1 Introduction

The Eastern Traverse follows closely the European GeoTraverse EGT (Figure 22-1, inset of Plate 22-1) and is partly based on geophysical data acquired in the framework of the EGT and earlier refraction seismic projects. These data are combined with data obtained during the NRP 20 project (Figure 22-1): line E1, almost parallel to the EGT line (see Pfiffner & Hitz, Chapter 9) and lines S1, S3 and S5 (see Schumacher, Chapter 10, projected into the Eastern Traverse, see also Holliger 1991). Whereas the Central and Western Traverses only offer relatively incomplete information across the entire Alps, both in respect to the geophysical methods used (only a few refraction lines are available) and in respect to their length (the Western Traverse stops well north of the Insubric line), the Eastern Traverse is nearly complete. Hence, to some extent and for certain authors (see Chapters 23 and 24) this section has model character. From a strictly geological point of view the position of the Eastern Traverse is ideal: it follows closely the N–S trending western margin of the Austroalpine nappes, which are largely missing further to the west and which almost completely cover lower structural units further to the east (Figure 22-1, inset of Plate 22-1). Proximity to this margin allows information on the Austroalpine units, projected into the profile. This enlarges considerably the cross section in a vertical direction. For example, in case of the southern Penninic units, downward extrapolation using geophysical data to depths of about 60 km can be complemented by an upward projection of geological units reaching 20 km above sea level. Furthermore, ongoing and very recent research outside the framework of NRP 20 offers further constraints on the geology along this transect: e. g. projects in the Bündnerschiefer (Steinmann 1994), the Adula nappe (Partzsch et al. 1994), the Austroalpine nappes and the Engadine line (Froitzheim et al. 1994, Schmid Froitzheim 1993), the Bergell area (Rosenberg et al. 1994 & 1995) and the Southern Alps (Schönborn 1992).

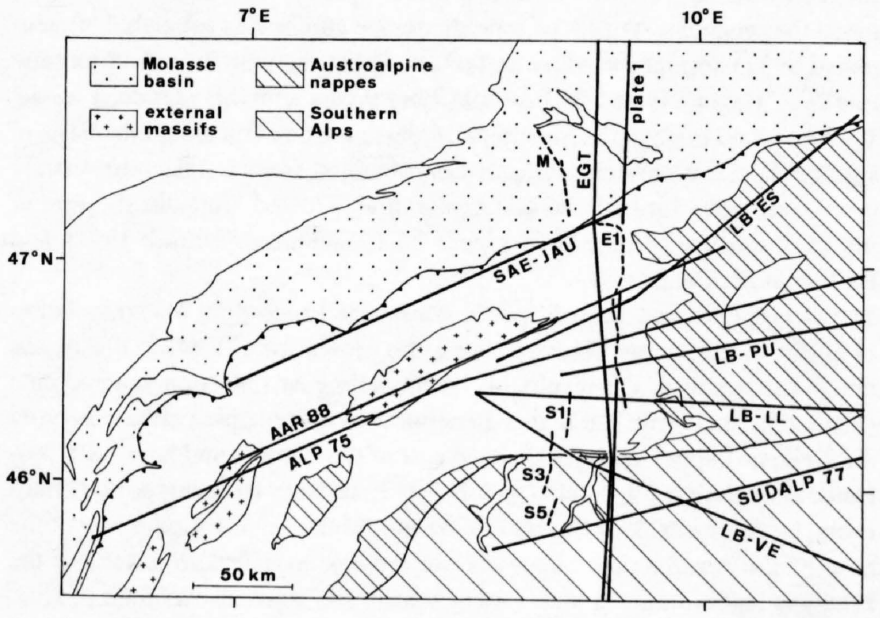

Figure 22-1
Network of seismic lines used for constraining the profile of plate 22-1. Solid lines: refraction profiles; broken lines: reflection profiles.

Plate 22-1 attempts to integrate geophysical and geological data into a single cross section across the Alpine chain. The section runs N–S along grid line 755 of the Swiss topographic map (except for the southernmost part near Milano, see Figure 22-1 and inset of Plate 22-1). As drawn, there is a marked difference between the tectonic style of the shallower crustal levels and that of the lower crustal levels. This difference in style is only partly real. The underlying wedging and associated deformation of the lower crust indeed strongly contrasts with the piling up and refolding of thin flakes of upper crustal material (the Alpine nappes), particularly in the central portion of the profile. This contrast is probably the most spectacular and unforeseen result of NRP 20.

Partly, however, this difference in style reflects the different types of data sets used for compiling this integrated cross section. Upper crustal levels have been drawn on the basis of projected surface information, locally constrained by the results of geophysical modelling (parts of the northern foreland and the Penninic nappes). The geometry of the lower crustal levels, on the other hand, relies entirely on the results of deep seismic soundings which provide a different scale of resolution compared to direct surface observation. It was felt that there was no point in drawing fine details into the deeper parts of the cross section, as is the case for the shallower parts, where such details are drawn according to projected surface information. As a result, lower and upper crustal levels may look more different in style and therefore less related than they probably are.

A word of caution concerns the use of this cross section. Deformation certainly was not plane strain within this N-S-section. Shortening, extension and displacements repeatedly occurred in and out of the section. For example, faults with a strike-slip component such as the Insubric line, currently juxtapose crustal segments whose internal structures may have developed elsewhere. Because this chapter is concerned primarily with a discussion of Plate 22-1, it will focus strongly on the cross-sectional view. However, the 3D problem will also be addressed. An appreciation of 3D problems in the Alps may be found in Laubscher (e. g. 1988,1991). For a discussion of 3D problems from a geophysical point of view the reader is referred to Pfiffner & Hitz (Chapter 9) and Valasek & Mueller (Chapter 23). An attempt to correlate different NRP 20 transects through the Alps from a geological point of view is found in Marchant & Stampfli (Chapter 24). Certain details of the Eastern Traverse interpretation in Chapter 24 differ from those given in this chapter.

22.2 Methods and data used for the compilation of the integrated cross section

The different parts of the cross section have been obtained by a variety of construction and projection methods. These methods, as well as the nature and quality of the geological and geophysical data, need to be outlined briefly for a better appreciation of the assumptions behind the methods and the nature of the data sources. After the discussion of the parts of the profile exhibiting the deep structure (compare also Valasek & Mueller, Chapter 23) the different parts of the higher structural levels will be discussed, proceeding from north to south.

22.2.1 Geophysical data used to compile features of the deep structure

The solid lines labelled "crustal model along EGT" denote the position of the upper and lower boundary of the lower crust, which is generally characterized by a significant increase in P-wave velocity and often high reflectivity.

These lines are similar, but not identical to the C1/C2 (top of the lower crust) and M1/M2 (Moho) interfaces as defined in Chapters 9 and 23 and Valasek (1992). In Plate 22-1 the positions of these interfaces are drawn after the results of refraction work (Ye, 1992; Buness, 1992) and an integrated interpretation of both refraction and reflection seismic data (Holliger & Kissling 1992). This allows the reader to assess the degree of compatibility with the results obtained by the reflection method, also displayed in Plate 22-1. The positions of these interfaces depicted in Plate 22-1 do not differ significantly from those given by Valasek (1992). Positions where the interfaces are not well constrained are indicated by broken lines.
Only well-constrained seismic velocities from Ye (1992) are indicated in Plate 22-1 where they do not spatially overlap with the drawing of geological features. For clarity some of the fine details presented by Ye (1992) have been deleted. Velocities of around 6.5 to 6.6 km/s typical for the lower crust (with a notable exeption for the lower crust in the northern foreland according to Ye, 1992), contrast with values between 6.0 and 6.2 km/s in the lower parts of the upper crust. Layers characterized by lower velocities than those indicated in Plate 22-1, including velocity inversions, are observed at relatively shallow depth (Ye 1992). Low velocity layers (about 5.8 km/s) are found beneath the external Molasse basin at a depth of about 10km and also within the lower Penninic nappes and underneath the Southern Alps (see Ye 1992 for details).
The solid lines denoting the interfaces of the lower crust are constrained by migrated wide-angle reflections (modified after Hollinger & Kissling 1992 and Ye 1992). The position of these reflections is very strongly controlled by the availability of seven refraction profiles oriented parallel to the strike of the chain (Figure 22-1, see also Holliger & Kissling 1991, 1992, Baumann 1994). All these profiles intersect the profile of Plate 22-1 and the EGT refraction profile (Ye 1992), hence there is considerable 3D control on the position of these reflections. The depth migration procedure within the EGT profile (almost identical with the cross section of Plate 22-1) integrates new data by Ye (1992) and is outlined in Holliger (1991) and Holliger & Kissling (1991, 1992).

We chose to superimpose the results of reflection seismic work directly onto the features arrived at by refraction seismics in order to graphically visualize the degree of compatibility between these two data sets. Major deep reflections from the E1, S1, S3 and S5 lines (Figure 22-1) have been converted into digitized line drawings by a procedure outlined in Hollinger (1991). These digitized line drawings were projected onto the EGT line before migration in the N–S section. The eastward projection of data from the Southern Traverses was necessary in order to complete the profile along the Eastern Traverse, because E1 terminates well north of the Insubric line. The chosen procedure for eastward projection needs to be briefly discussed.
Any projection method assumes lateral continuity of the structures projected. However, if structures from different tectonic levels do depart from each other in terms of direction and plunge of the projection vector, the question will then arise, which structure one assumes to be laterally continuous. Marchant (1993) and Marchant & Stampfli (Chapter 24) put the large dimensions of the Adriatic lower crustal wedge below the Penninic nappes (at a depth of 20 to 50km in the center of Plate 22-1) into question by arguing that the N-wards flattening Insubric line, well imaged along S1, has to be projected to the east by using the axial dip of the Adula nappe. By cylindrically projecting the Adula and underlying Penninic nappes, including the Insubric line above the Adriatic lower crustal wedge, to the E, there is of course no room for such a large wedge. This is because the S-dipping lower crust of the northern foreland does not exhibit such an axial dip to the E. Conversely, if one projects those parts of the lower crustal wedge covered by S1, including the Insubric line, subhorizontally to the east (Hollinger 1991) there is no room for Penninic units below the Leventina-Lucomagno nappe along the Eastern Traverse, as depicted in Plate 22-1.

Holliger (1991) and Holliger & Kissling (1991, 1992) have argued that the geometry of middle to lower crustal material is appropriately constrained by Bouguer gravity data (corrected for the effects of the Ivrea body, Kissling 1980, 1982). This gravity map reflects the integrated effects of such deep crustal features. This then ultimately (i.e. after migration) leads to the configuration depicted in Plate 22-1. The following major arguments additionally support the procedure chosen: (1) There is independent evidence for the existence of such a large lower crustal wedge from the refraction work carried out along the EGT line (Ye 1992) and the compatibility of the refraction-based model of Ye (1992) with the projected and migrated line drawings of the major reflections is good as can be seen in Plate 22-1. (2) The axial dip of the Alpine nappes to the east is discordant to the European lower crust and the Moho, independently indicating strong decoupling between lower and upper crust. In the light of this decoupling the use of a cylindrical projection of upper crustal flakes is, in our view, not justified for projecting lower crustal features such as the Adriatic wedge.

In a second step, the projected digitized line drawings were migrated according to a velocity model which needs no projection since it is based on strike-parallel profiles (Holliger 1991). This velocity model (figure 4 in Holliger and Kissling 1992) is the same as that used for the migration of the wide-angle reflections discussed earlier. The picture emerging from this procedure shows excellent consistency between refraction and reflection data and one geological feature which can be traced to great depth: the Insubric line.

Except for a reflectivity gap beneath the internal Aar massif and the Gotthard "massif" there is excellent agreement between the position of the lower crust of the northern foreland derived from refraction work (solid lines in Plate 22-1) and the zone of high reflectivity. The reason for this gap in near-vertical reflections is not completely understood but it is unlikely to represent a gap in the European Moho as postulated by Laubscher (1994). On the contrary, wide-angle data from the EGT profile and from several orogen-parallel profiles (Figure 22-1) show strong seismic phases from the Moho in this region (Kissling 1993; Ye et al. 1995), whose position is indicated by a solid line in Figure 22-2a (Holliger and Kissling 1991). By applying a NMO (normal-move-out) correction, Valasek et al. (1991) displayed these wide-angle Moho reflections along the EGT profile in a manner commonly used for near-vertical reflection data (Figure 22-2b). Hence, Figure 22-2 clearly documents the continuity of the Moho beneath the northern foreland and the entire Penninic realm.
The gap in the lower crustal reflections in the near-vertical reflection profile is at least partly due to the projection and migration procedures: The northern termination of the southern portion of high reflectivity coincides with the northern termination of profile S1 and is thus a projection artefact. The southward termination of the northern part of reflective lower crust is most likely caused by imaging problems (Holliger 1991, Valasek 1992).
The reflections from the lower crustal Adriatic wedge cross each other in many places, indicating discontinuities within the wedge or, alternatively, problems with the projection and/or migration procedures. As pointed out by Holliger & Kissling (1992) the lower crustal wedge may have a complicated internal structure representing a mixture of predominantly Adriatic lower crust and oceanic crust, having a density slightly higher than that of "normal" lower crust. It is clear, however, that this zone of high reflectivity is largely contained within the lower crustal wedge of the refraction-based EGT crustal model (solid lines in Plate 22-1) except for some gently N-dipping reflections at a depth of 20–25km, slightly above the upper boundary of the lower crustal wedge according to refraction work (solid line below grid 140 in Plate 22-1). Prominent steeply inclined reflections recorded along line S1 commonly related to the Insubric line (Bernoulli et al. 1990, Holliger 1991, Holliger and Kissling 1991, 1992) project into a surface location 5–10km north of the Insubric line in Plate 22-1 (within the northern part of the southern steep belt, near the axial trace of the Cressim antiform). However, due to inaccuracies in the projection and migration techniques, the exact location of some of these reflections in relation to the Insubric mylonite belt remains speculative. In view of the parallelism between the Insubric mylonite belt and the southern steep zone (Schmid et al. 1989) these reflections can be taken to document a flattening of the Insubric mylonite belt from the 70° inclination measured at the surface (Schmid et al. 1987, 1989) to about 45° at some 20km depth.

22.2.2 Helvetic nappes and northern foreland

The top of basement is only accessible to surface observation in the Vättis window (Aar massif) along the profile of Plate 22-1. The geometry chosen for the structure of the top of basement is that of model 1, discussed in Stäuble & Pfiffner (1991 b) and Pfiffner et al. (Chapter 13.1). These authors compared the seismic responses of four alternative geometries (models 1-4) generated by 2D normal-incidence and offset ray tracing with the reflection seismic data. They produced the best-matching events with this particular model 1. Thrusts and folds in the Subalpine Molasse are constructed on the basis of surface data and projected information obtained from a reflection seismic profile, recorded for hydrocarbon exploration, situated immediately west of the EGT traverse (profile M in Figure 22-1; Stäuble & Pfiffner 1991a and Pfiffner et al., Chapter 8).
The Helvetic nappes are only partly constructed according to extrapolation of surface information obtained along the profile trace. Certain details are drawn according to the results of 3D modelling of reflection seismic data (Stäuble et al. 1993). The higher Penninic and Austroalpine units overlying the Helvetic nappes are only exposed east of the transect and have been projected onto the profile parallel to a N 70° E azimuth by using profiles published by Allemann & Schwizer (1979) and Nänny (1948). Updoming of the base of the Austroalpine nappes above the Aar massif corresponds to the Prättigau half window in map view (Cadisch 1950; see also Pfiffner & Hitz, Chapter 9). Its geometry was obtained by stacking a series of profiles across the Prättigau half window (Nänny 1948). Stacking did not use a fixed axial plunge, but instead resulted from lateral correlation between individual pro-

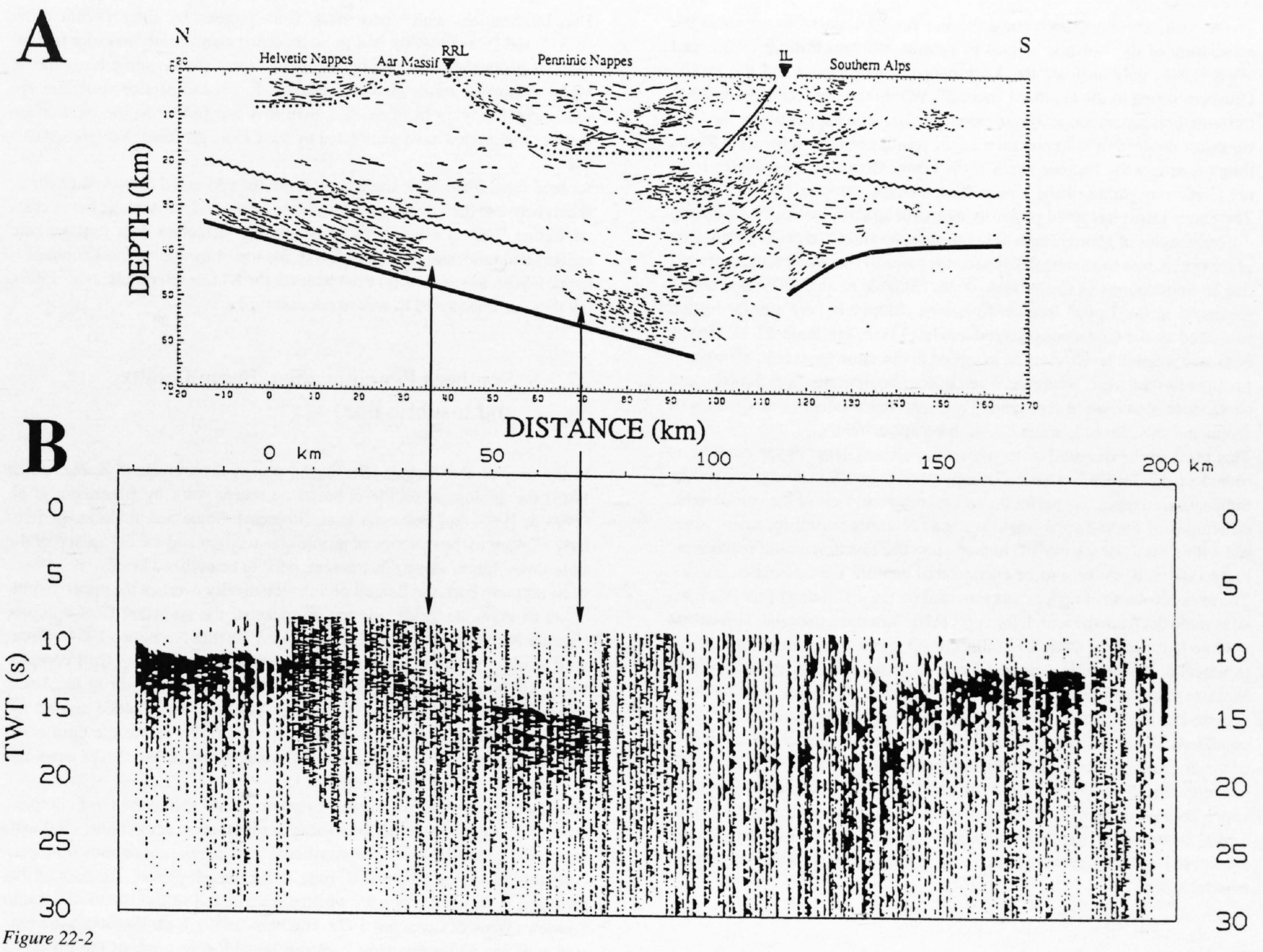

Figure 22-2
Summary of seismically determined crustal structure and Moho depth along the Eastern Traverse (see plate 22-1).
a: Migrated near-vertical reflections along the Eastern Traverse and generalized seismic crustal structure derived from orogen-parallel refraction profiles (Hollinger & Kissling 1992). Solid line: position of Moho, derived from orogen-parallel refraction profiles; wiggly line: top lower crust; dotted line: base of Penninic and Helvetic nappes; thin solid line: Insubric Line (IL); RRL: Rhine-Rhone Line.
b: Normal incidence representation of the wide-angle Moho-reflections in the EGT refraction profile perpendicular to the orogen and across the eastern Swiss Alps (Valasek et al. 1991).

files. The geometry thus obtained (Plate 22-1) results in an average plunge of 15° for the culmination of the base of the Austroalpine units, as can be determined from the vertical and horizontal distances between a point situated in the Vättis window and the eastern termination of the Prättigau half window near Klosters. This angle agrees closely with the plunge of the axial culmination of the Aar massif, based on the network of the seismic profiles E1, E7, E8, E9 and E10 (Hitz & Pfiffner 1994 and Chapter 9).

22.2.3 The Gotthard "massif" and the transition into the lower Penninic nappes

Very strong reflections dipping southward from 2.5 to 4.0 s TWT along line E1 between Canova and Thusis (reflector D in plate 4 of Pfiffner et al., 1990b) have been interpreted in Plate 22-1 (between grid lines 175 and 190) to be due to the allochthonous cover of the southern Gotthard "massif" (Etter 1987). The existence of the small Tavetsch massif as far east as our transect is considered unlikely, as discussed in more detail in Chapter 9. However, an alternative interpretation, such as model A of Pfiffner et al. (1990 b), which attributes this band of S-dipping strong reflections to the top of the Aar massif, cannot be ruled out. According to this alternative model the Gotthard "massif" would wedge out west of the transect discussed here (but see Chapter 9).
The Penninic basal thrust is placed immediately above the inferred allochthonous cover of the Gotthard "massif" (labelled "Triassic, Lower and Middle Jurassic cover slices" in Plate 22-1) according to the final 3D model of the Penninic units given by Litak et al. (1993). Earlier interpretations based on N-dipping reflections visible under the Gotthard massif (northern termination of reflection group E in plate 4 of Pfiffner et al. 1990b), advocating backthrusting and/or backfolding of the Gotthard massif (model C in Pfiffner et al. 1990 b) are abandoned. Seismic modelling showed that these N-dipping reflections may be caused by a synform situated at the base of the Adula nappe near the northern termination of the Simano nappe (see Plate 22-1).
According to the geological interpretation given in Plate 22-1, the basal thrust of the Gotthard "massiv", the Urseren-Garvera zone, is steeply inclined and is therefore not imaged seismically. Regardless of the uncertainties in interpreting the exact shapes of the southernmost Aar massif and the Gotthard "massif", and based on the geometry constrained by 3D seismic modelling (Figure 3a in Litak et al. 1993), the Penninic basal thrust is not shown to be strongly backfolded but merely steepened up in Plate 22-1. This is important since it marks a substantial change in structural style from the Lukmanier area (Etter 1987, Probst 1980). In the Lukmanier area, a late deformation phase (Figure 22-3) linked to the formation of the Chiera synform (D3 of Etter 1987) and to the Carassino phase in the frontal Adula nappe (Löw 1987) leads to substantial backfolding. Such backfolding is even more pronounced in the southern part of the external massifs of the Western Traverse (see Alpine cross section by Escher et al. presented in Chapter 16). This severe overprint by backfolding apparently dies out eastward.
The Gotthard "massif" is considered as a lowermost Penninic, or more exactly a "Subpenninic" nappe (Milnes 1974), in a structural sense. These Subpenninic units also include the Lucomagno-Leventina and Simano nappes, whose geometry will be discussed later. There is a serious problem with the use of terms like "Helvetic" and "Penninic" in that, for historical reasons, they may refer to paleogeographic domains and/or structural units. Whereas the Lucomagno-Leventina and Simano nappes, and according to our interpretation also the Gotthard "massif", may be described as Penninic in a structural sense, it is very likely that some of this crystalline basement represents basement to the Helvetic and Ultrahelvetic cover nappes. This is supported directly by the facies of the overturned allochthonous cover of the southern Gotthard "massif" (Etter 1987, Jung 1963, Frey 1967) which has close affinities with the Helvetic sediments. Use of he term "Subpenninic" helps to resolve this dilemma.

To the west, Trümpy (1969) considers the Tavetsch massif to represent the substratum of the Helvetic nappes in general, whereas Pfiffner (1985) and Wyss (1986) only attribute the Axen nappe to this massif and the Säntis-Drusberg nappe to the Gotthard "massif". Within the transect of Plate 22-1, the structural separation amongst individual Helvetic nappes above the Glarus thrust diminishes in importance. In the profile considered here, the Säntis thrust separates the Jurassic strata of the Lower Glarus nappe complex from the Cretaceous strata of the Upper Glarus nappe complex (Pfiffner 1981). The Säntis thrust has acted primarily as a structural discontinuity separating different styles of shortening within the Jurassic and Cretaceous strata. Displacement across the Säntis thrust decreases steadily southward and eastward due to imbrications in the Jurassic strata (Stäuble et al. 1993). Bed length measured in the Upper Jurassic limestone (38 km) is very similar to that measured in the Cretaceous Schrattenkalk (33 km, see Plate 22-1). Hence, both stratigraphic levels must be assigned to the same basement, contrary to findings further west, where the Axen nappe incorporates both Jurassic and Cretaceous strata while the Säntis-Drusberg nappe consists of Cretaceous sediments only, Jurassic strata having been left behind.

This leads to the question as to wether the entire Glarus nappe complex is rooted in the Tavetsch massif (Trümpy 1969), or alternatively, within the Subpenninic nappes. We prefer the second option in view of the considerable difficulties of finding appropriate volumes of upper crustal basement material within the Tavetsch massif. In map view, the Tavetsch massif pinches out eastward and is unlikely to be encountered beneath the transect of line E1. The excess volume of upper crust provided by the updoming of the Aar massif is ruled out from the search for appropriate basement material. This excess volume is caused by some 27 km of crustal shortening post-dating the detachment of the Helvetic nappes and related to imbrications in the Subalpine Molasse (Burkhard 1990, Pfiffner 1986, Pfiffner et al. 1990b). In order to accommodate the 38 km bed-length of Helvetic nappes (assuming plane strain conditions and an upper crustal thickness of 15km) an area of about 570 km^2 of upper crustal material has to be identified somewhere in Plate 22-1. This suggests that both the Gotthard "massif" and the Lucomagno-Leventina nappe (occupying about 540 km^2 in our section) may represent this upper crustal basement of the Helvetic nappes, their original cover having been substituted by sediments of a more southerly provenance during early phases of detachment.

22.2.4 The northern and central parts of the Penninic zone

Most of the surface data used for constructing this part of the profile (Plate 22-1) have been presented in Chapter 14. This information has been supplemented by data from Steinmann (1994) covering the area of the North-Penninic Bündnerschiefer. Details concerning the orogenic lid (the Austroalpine units) have been improved in respect to an earlier version of parts of this profile (figure 2 in Schmid et al. 1990) using new data from Froitzheim et al. (1994), Handy et al. (1993), and Liniger (1992).

In a first step all major tectonic boundaries have been projected strictly parallel to a N 70° E direction up and down plunge. This direction approximates best the azimuth of most large-scale fold structures in this region. A series of sections parallel to N 70° E, constructed on the basis of structure contour maps, allowed for projections with variable plunge (10-35°). Units were projected into the profile along these strike-parallel sections by assuming that their thicknesses do not change along strike. Geological details within projected units are drawn according to the geometries found where these units are exposed.

In a second step this part of the profile was adjusted to conform to the 3D model based on seismic information (Litak et al. 1993 and Pfiffner & Hitz, Chapter 9). These adjustments were relatively minor at shallower depths and above the Adula nappe. The most important modification concerns the Misox zone, which has a considerable thickness and which is shown to be continuous southward, joining up with the Chiavenna ophiolites exposed at the surface. This is in contrast to surface geology exposed west of the profile, where the Misox zone is cut out near the Forcola pass due to top-to-the-east movements along the Forcola normal fault. The Chiavenna ophiolite is portrayed as a long continuous slab, about 1km thick, which caused high-amplitude reflections consistent with a gneiss/ophiolite interface (Litak et al. 1993).

The overall geometry of the Adula and Simano nappes follows that given in figure 3a of Litak et al. (1993). Ornamentation in the Adula nappe is based on the data of Löw (1987). A considerable amount of speculation led to the depicted geometry of the top of the Gotthard "massif" and the Lucomagno-Leventina units. While their overall position below the Penninic basal thrust is constrained by the model of Litak et al. (1993), the portrayed structural details are based on surface information a long way west of the transect. This information, which was taken from profiles by Etter (1987), Löw (1987), and Probst (1980), had to be modified significantly in order to conform to constraints imposed by the geometry of the Penninic basal thrust. Major synformal zones such as the Scopi, Piora, and Molare structures appear more flat-lying in Plate 22-1 than they are further to the west, since they are interpreted to be unaffected by the Chiera synform as discussed earlier.

As seen from Plate 22-1, there is no room for additional Subpenninic thrust sheets between the Lucomagno-Leventina nappe and the Adriatic lower crustal wedge. This is a corollary of combining refraction data (top Adriatic wedge) and reflection data (position of the top of the Leventina-Lucomagno nappe). Such lower units do exist beneath the S3 line (Bernoulli et al. 1990), but they are interpreted to wedge out eastward.

22.2.5 Southern Penninic zone, Bergell pluton and Insubric line

In the area of the Bergell (Bregaglia) pluton (Trommsdorff & Nievergelt 1983) the geological profile is based on recent work by Rosenberg et al. (1994 & 1995) and Davidson et al. (in press). Some new findings, particularly relevant to the methods of profile construction and the discussion of the tectonic evolution along this transect, need to be outlined briefly.

In its northern part, the Bergell pluton tectonically overlies the upper amphibolite to granulite grade migmatitic rocks of the so-called Gruf complex (Bucher-Nurminen & Droop 1983, Droop & Bucher-Nurminen 1984). Structural work in progress unambiguously demonstrates that the Gruf complex continues into the migmatites forming the southernmost part of the Adula nappe (Hafner 1994). These migmatites have been backfolded around the Cressim antiform (Plate 22-1, Heitzmann 1975). Therefore the Gruf complex, including the window below the Bergell pluton at Bagni di Masino, has to be considered part of the Adula nappe.

Whereas quartzo-feldspatic gneisses predominate within the Gruf complex, a variety of other lithologies consisting of ultramafics, amphibolites, calc-silicates and alumo-silicates is concentrated in an almost continuous band concordantly following the tonalitic base of the Bergell pluton. The base of this intrusion is exposed along its western margin and in the Bagni di Masino window (Wenk & Cornelius 1977, Diethelm 1989). Near Vicosoprano a narrow antiform within the Gruf complex immediately south of the Engadine line (indicated in Plate 22-1 according to work in progress) is interpreted to connect these lithologies at the base of the pluton with the Chiavenna ophiolites. The Chiavenna ophiolites overlie the Gruf complex along a steeply north-dipping faulted contact (Schmutz 1976), which is possibly related to movements along the Engadine line. Hence, this band of ultramafics and metasediments found on top of the Gruf complex is tentatively interpreted to be the southern continuation of the Chiavenna ophiolites and the Misox zone.

Based on this interpretation, and independent of the correlation between the Adula nappe and Gruf complex, the Bergell pluton appears to occupy a similar structural position to that of the Tambo and Suretta nappes north of the Engadine line. Recent mapping near Vicosoprano has revealed the following geometry shown in Plate 22-1, which supports this conclusion: The granodiorite cuts discordantly through the remnants of both theTambo and Suretta nappes that are preserved south of the Engadine line. Over the short distance between Vicosoprano and the Maloja pass the northern contact of the Bergell pluton reaches higher tectonic levels exposed along its eastern margin (i. e. Avers Bündnerschiefer and Forno-Lizun ophiolites).

Magmatic, submagmatic and solid state deformational fabrics in tonalite, granodiorite, and country rocks show that the Bergell pluton was emplaced and solidified during a regional tectonic event. This synmagmatic deformation first produced a very strong (mylonitic) fabric found at the base of the pluton and, subsequently, led to large-scale folds that shortened this basal contact (Plate 22-1). One of these folds can be traced directly into the Cressim antiform (Hafner 1994, Plate1).

Initial stages of vertical movement along the Insubric mylonite belt affected the tonalitic tail of the southern Bergell pluton and were coeval with deformation in the presence of melts (Rosenberg et al. 1995). This conclusion is contrary to earlier interpretations, which regarded all movements along the Insubric line to postdate the Bergell intrusion (Schmid et al. 1987). It also shows that final intrusion, backfolding and initial stages of backthrusting along the Insubric line were contemporaneous and related to ongoing N–S shortening. The north-dipping Insubric mylonite belt was extrapolated to depth by assuming that it parallels the migrated reflections attributed to the Southern Steep Belt (Plate 22-1). The vertical, brittle Tonale fault (as exposed in a spectacular gorge near Gravedona, Fumasoli 1974) is related to later strike-slip movements along the Insubric line.

Considerable vertical extrapolation is possible thanks to the pronounced ax-

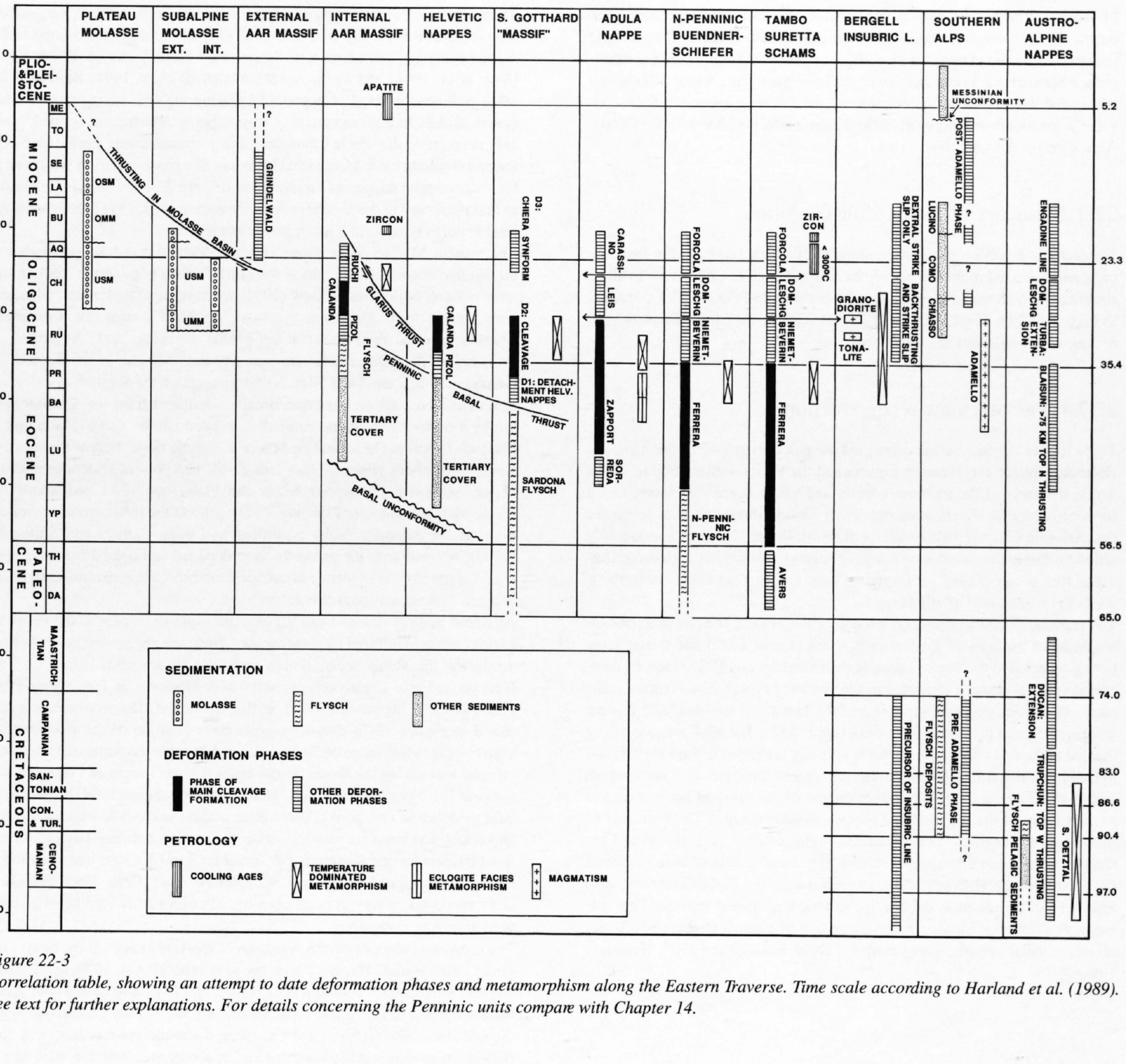

Figure 22-3
Correlation table, showing an attempt to date deformation phases and metamorphism along the Eastern Traverse. Time scale according to Harland et al. (1989). See text for further explanations. For details concerning the Penninic units compare with Chapter 14.

ial plunge of the Bergell pluton indicated by structural (Rosenberg et al. 1994 & 1995) and petrological (Reusser 1987) data. In a first step, the Tambo and Suretta nappes were projected southward and upward by using structure contour maps (Pfiffner et al. 1990a, partly modified by new field data). At a point situated near Vicosoprano, east of the transect (projecting well above sea level in Plate 22-1) the geometries of Tambo, Suretta and overlying nappes were displaced vertically across the Engadine line by 4 km, in accordance with the kinematic model for this line proposed by Schmid and Froitzheim (1993). Using this kinematic model, the position of the Tambo and structurally higher tectonic units was anchored to their position immediately south of the Engadine line where these nappes were cut by the Bergell intrusion.

The position of the base of the Bergell intrusion was evaluated by projecting auxiliary profiles located east of Plate 22-1. This projection used structure contour maps (Davidson et al., in press) of the base of the pluton, deformed by NE–SW striking folds. The roof of the intrusion was placed at the structural level presently exposed at the eastern margin of the pluton. This is a minimum altitude, since the eastern contact represents the side rather than the roof of this pluton (Rosenberg et al. 1995, Spillmann 1993). The geometry of the "Ultrapenninic" (in the sense of Trümpy 1992) or Austroalpine Margna and Sella nappes, including the continuation of the southward outwedging Platta ophiolites and the Corvatsch-Bernina nappes, is drawn after Liniger (1992) and Spillmann (1993). However, this geometry is exposed approximately 25 km east of the transect and may be substantially different in our transect. This geometry was projected nevertheless in order to illustrate the southward connection of the orogenic lid to the Austroalpine Tonale series exposed in the Southern Steep Belt north of the Insubric line.

22.2.6 Southern Alps

The Southern Alps part of the section was taken without modification from Schönborn (1992, cross section B of his enclosure) except for the northernmost region where compatibility with the shape of the Insubric fault necessitated very minor adjustments. This section in Schönborn (1992) almost coincides with N–S grid line 755, departing from a N–S orientation only south of E–W grid line 60 in order to incorporate well data published by Pieri & Groppi (1981).

The profile is balanced and retro-deformability was established at all stages by forward modelling. The deeper parts of the profile were kept as simple as possible and drawn according to geometrical rules of ramp and flat geometry observed for basement and cover the surface. More intensive dissection by thrusting and/or ductile lobes, comparable to those proposed for the Aar massif, is to be expected, but has not been drawn because of the lack of subsurface data. However, the mass balance within the basement, the top of which is well constrained by well data in its undeformed portion in front of the Milan thrust belt (Plate 22-1) is unaffected by geometrical details. The total amount of shortening (about 80km) within the sediments necessarily leads to the postulate that parts of the upper crustal and all of the lower crustal excess volume must now occur within the Adriatic wedge situated below the Penninic nappes and the depth extrapolation of the N-dipping Insubric line. The volume of crustal material available south of the Insubric line is insufficient (Schönborn 1992, Pfiffner 1992). Substantial thinning of the Adriatic lower crust during Jurassic rifting and passive continental margin formation cannot be held responsible for this volume deficit because the Southern Alps were in a lower plate margin situation at that time (Lemoine et al. 1987, Froitzheim and Eberli 1990).

In order to allow for a change in structural style within the deeper basement, ductile shear zones have been schematically drawn at depth. These shear zones are expected to merge with a major detachment zone situated at the interface between the upper and lower Adriatic crust. This major detachment allows for the northward indentation of the Adriatic lower crust, or conversely, for southward transport of the Insubric line, together with the Central Alps, over the Adriatic lower crust.

22.3 Summary of the tectonic evolution

The tectonic evolution of the Alps along the Eastern Traverse (the Penninic units are discussed more extensively by Schmid et al. in Chapter 14) will be summarized with the help of the profiles presented in Figure 22-7 (identical to Figure 14-21). The timetable of Figure 22-3 (identical to Figure 14-20) provides the available time constraints.

22.3.1 Paleotectonic reconstruction

Three former oceanic basins controlled the paleogeography of the Alps: the Hallstatt-Meliata, the Piemont-Liguria and the Valais oceans (Figure 22-4). While remnants of the Piemont-Liguria and Valais oceans are found in the form of ophiolitic slivers along the cross section discussed here (compare discussion in Chapter 14), remnants of the Hallstatt-Meliata ocean are only found further to the east (Eastern Alps of Austria, Carpathians). However, because this ocean played an important role during Cretaceous orogeny, it needs to be discussed briefly here.

The Hallstatt-Meliata ocean opened during the Middle Triassic in a position southeast of the present Austroalpine realm (Kozur 1992) and it may have been connected to the Vardar ocean of the Dinarides and Hellenides. Its paleogeographic position is indicated in the sketch of Figure 22-4. Triassic sediments of the Austroalpine units record the history of the shelf and passive margin of Apulia that faced this ocean (Lein 1987). The Mid-Triassic rifting that led to the opening of this ocean is spatially unrelated to the Late Triassic to Early Jurassic rifting leading to the opening of the Piemont-Liguria ocean which will form at the northwestern margin of the Apulian microcontinent (western part of the Austroalpine nappes, Southern Alps). The remnants of this ocean did not reach the region of the profile of Plate 22-1. However, Cretaceous or "Eoalpine" orogeny resulting from continental collision following the closure of the Hallstatt-Meliata ocean during the Early Cretaceous also affected the Austroalpine and South-Penninic units in our transect. This collision was followed by westward propagation of a thrust wedge towards our area of interest in eastern Switzerland (Thöni and Jagoutz 1993, Neubauer 1994).

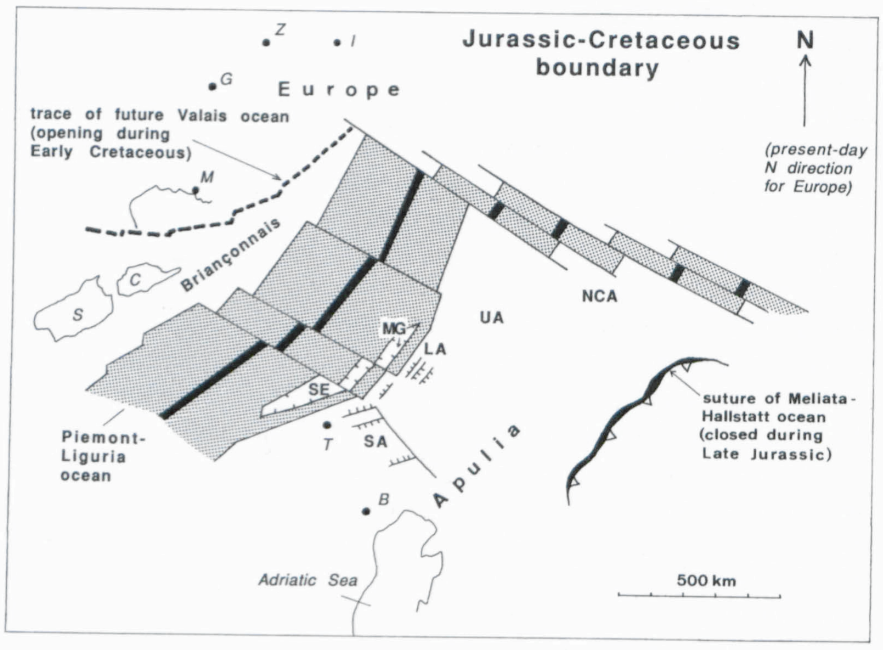

Figure 22-4
Paleogeographic reconstruction of the Piemont-Liguria (South Penninic) and the Hallstatt-Meliata ocean and their margins at the Jurassic-Cretaceous boundary, after Dercourt et al. (1986) and Stampfli (1993). SE: Sesia-Dentblanche extensional allochthon; MG: Margna extensional allochthon; SA: passive continental margin of Southern Alps; LA: Lower Austroalpine realm; UA: Upper Austroalpine realm; NCA: Northern Calcareous Alps. Geographical reference points are: S (Sardinia), C (Corsica), M (Marseille), G (Geneva), Z (Zürich), I (Innsbruck), T (Torino) and B (Bologna).

The passive continental margin along the northwestern edge of the Apulian microcontinent is locally well preserved in spite of crustal shortening in the Austroalpine nappes of eastern Switzerland (Froitzheim & Eberli 1990, Conti et al. 1994) and in the Southern Alps (Bertotti 1991, Bertotti et al. 1993, Schumacher et al., Chapter 15). During the final rifting phase (Toarcian to Middle Jurassic) a system of west-dipping detachments formed, probably penetrating the whole lithosphere and accommodating simple-shear extension (Froitzheim & Manatschal in press). The passive margin preserved in the Austroalpine nappes of Graubünden (Figure 22-5) is amazingly similar to that preserved in the Southern Alps (Bernoulli et al. 1993); both areas exhibit features typical for a lower plate margin.

The present Margna-Sella nappe system occupied a special position near the passive continental margin at the northwestern edge of the Apulian microcontinent. Following Trümpy (1992) we have separated these "Ultrapenninic" units from the lower Austroalpine nappes with the Corvatsch-Bernina units at their base in the profile of Plate 22-1. According to Froitzheim & Manatschal (in press) the Margna-Sella nappes in Graubünden and the Dent Blanche-Sesia units of the Western Alps represent extensional allochthons that became separated from the Apulian margin by a narrow intervening zone of denudated mantle rocks (Platta unit in Plate 22-1) before the formation of a mid-oceanic ridge west of these extensional allochthons (Figures 22-4 and 22-5). The present structural position of the Margna-Sella nappes below the Platta ophiolites and above the Forno-Malenco ophiolites (Figure 22-6b) reflects the influence of complications in the paleogeography according to Liniger (1992) and Spillmann (1993). According to the reconstruction depicted in Figure 22-5 there is no need for the former existence of an additional spreading centre south of the Margna-Sella extensional allochthon.

An upper plate position of the Briançonnais unit in respect to the Piemont-Liguria ocean is inferred by most authors. However, the geometry of the margin facing the Valais ocean, which probably did not open before the Late Jurassic to Early Cretaceous (Frisch 1979, Florineth & Froitzheim 1994, Stampfli 1993, Steinmann 1994), is ill-constrained. The reconstruction depicted in Figure 22-7a shows an upper-plate position of the Briançonnais with respect to the Valais ocean in order to minimize the volume of continental crust underlying the Briançonnais facies domain (compare Figure 14-8 in Chapter 14). Note, however, that Florineth & Froitzheim (1994) present local field evidence in favour of a lower-plate margin at the NW edge of the Briançonnais. Evidence for sinistral strike slip motion between Europe and the Briançonnais terrane (Stampfli 1993) and for local sinistral transpression in the Schams nappes (discussion in Chapter 14, Rück 1990, 1995, Schmid et al 1990) points to very oblique opening, not necessarily leading to a single predominating asymmetry.

The proposed paleogeographic situation of the Adula nappe at the distal margin of stable Europe (Figure 22-7a; see also Schmid et al. 1990, and Chapter 14) has far-reaching consequences regarding the timing of eclogite facies metamorphism in the Adula nappe (a Tertiary rather than Cretaceous age is the corollary), the width of the European distal margin that has been subducted (more than usually assumed and in accordance with the estimates of Marchant & Stampfli, Chapter 23), and the very high rates of subduction and subsequent exhumation of the Adula eclogites. In order to minimize the amount and rate of Tertiary subduction, a width of only 50km was assumed for that part of the Valais or North-Penninic Bündnerschiefer basin that was originally underlain by oceanic crust (Figure 22-7a).

22.3.2 Cretaceous (Eoalpine) orogeny

Figures 22-5 and 22-6 illustrate that the Austroalpine nappe pile in eastern Switzerland was assembled by oblique east-over-west imbrication of the NW passive margin of the Apulian microcontinent (Froitzheim et al. 1994, Handy et al. 1993, Schmid & Haas 1989). The associated deformation (Trupchun phase in Figure 22-3; see Froitzheim et al. 1994) also affected structurally lower units, such as the Arosa-Platta ophiolites, the "Ultrapenninic" Margna-Sella nappes and the Lizun-Forno-Malenco ophiolites underlying the Margna nappe (Ring et al. 1988, Liniger 1992, Spillmann 1993). During Tertiary orogeny a basal thrust displaced all these structurally highest units that were previously affected by Cretaceous orogeny to the north by at least 75km (Froitzheim et al. 1994). This orogenic lid in the sense of Laubscher (1983) overrode the present day Engadine window and the Prättigau half-window (between coordinates 190 and 210 in the profile of Plate 22-1) only after Cretaceous orogeny. Sedimentation in the Briançonnais and Valais domains through to the Early Tertiary precludes Cretaceous orogeny within these lower structural units.

We propose separate orogenies during the Cretaceous and Tertiary, rather than two separate deformation phases during progressive convergence for the following reasons:

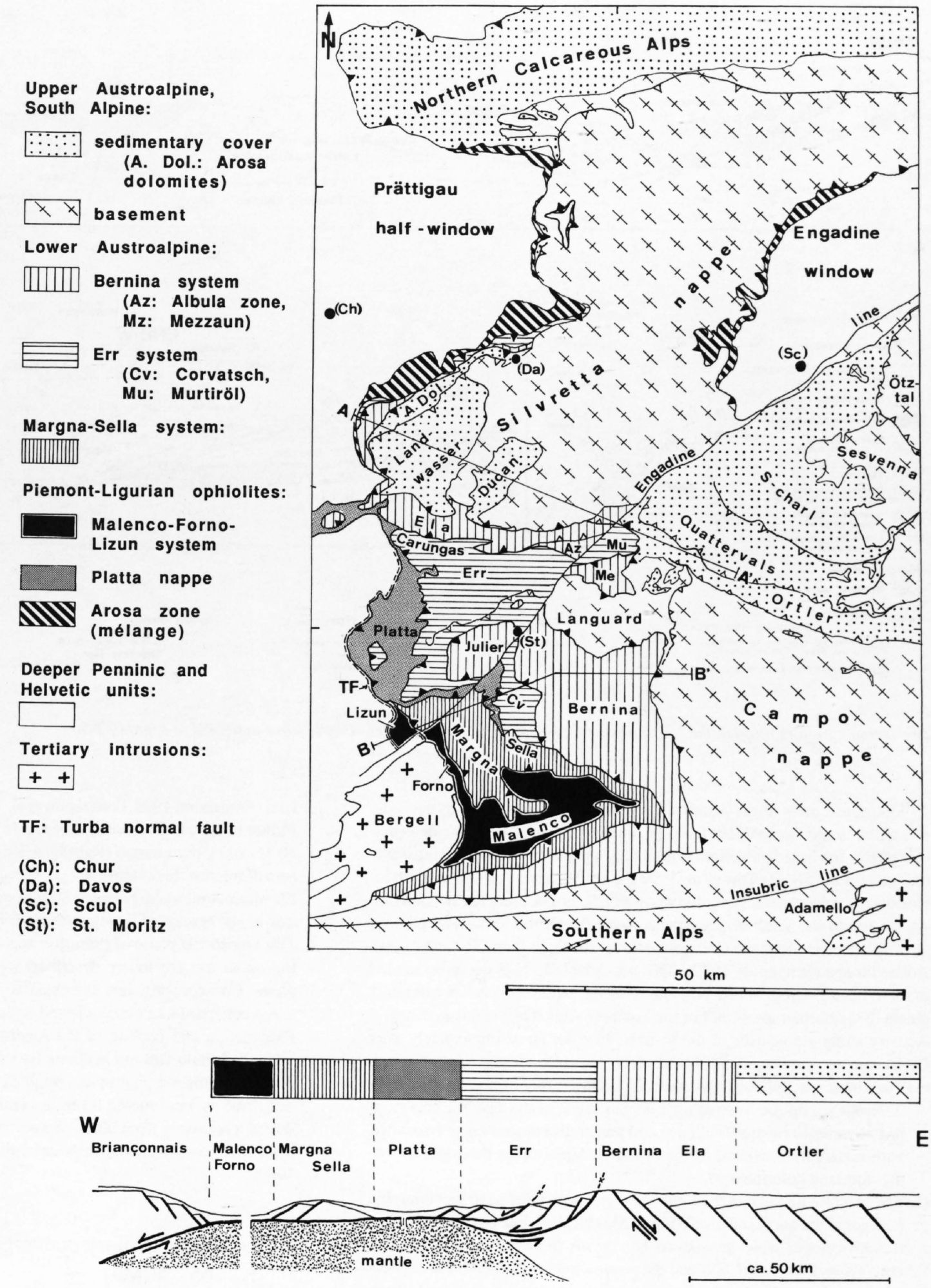

Figure 22-5
Reconstructed E–W section through the passive margin preserved in the Austroalpine units of Graubünden (bottom figure from Froitzheim et al. 1994) and map of the tectonic units in the Austroalpine realm, representing westwardly dislocated fragments of this passive continental margin. Small triangles along tectonic boundaries point in the direction of the structurally higher unit, irrespective of the nature of the boundary (thrust or normal fault; for details see Froitzheim et al. 1994).

(1) The kinematics (top to the W–WNW imbrication associated with orogen-parallel strike slip movements) of the Cretaceous orogeny are totally different from the top to the N–NNW movements characteristic of the Tertiary orogeny.
(2) A Late Cretaceous period of extensional collapse, to be discussed below, provides a clear temporal hiatus between the two orogenies.
(3) Subduction associated with eclogite facies metamorphism took place twice in the Alps: first during the Cretaceous and then during the Tertiary. Cretaceous-aged subduction occurred before the closing of the Piemont-Liguria ocean, encompassing subduction of continental slices within the Austroalpine domain (collision due to the closing of the Hallstatt-Meliata ocean, eclogites within the Austroalpine units of Austria) and subduction of extensional allochthons situated near the active northwestern margin of Apulia (eclogites in the Sesia zone). Tertiary-aged subduction of European and Briançonnais continental crust (e.g. in the Adula nappe) is related to the closing of the Valais and Piemont-Liguria oceans as a consequence of collisions during Tertiary orogeny.

Nappe imbrication during the Trupchun phase, the principle deformation phase related to Cretaceous crustal shortening, cannot have started before about 90 Ma at the western margin of the Upper Austroalpine nappe system (Ortler unit, Figure 22-5) because of ongoing pelagic sedimentation (Figure 22-3) up to the Cenomanian or Early Turonian (Caron et al. 1982). Thrusting further to the east and along the Schlinig thrust (basal thrust of the Oetztal unit, Figure 22-5) is constrained to have initiated earlier, at around 100 Ma, by radiometric ages of synkinematic temperature-dominated metamorphism (Thöni 1986, review of age dates in Schmid & Haas 1989). This westward migration of Cretaceous orogeny is also seen on a much larger scale across Austria, e. g. from the deposition of the synorogenic chromite-bearing Rossfeldschichten in the early Cretaceous (Faupl and Tollmann 1979) and from the pre-90-Ma age of Alpine eclogite facies metamorphism in the Saualpe (Thöni & Jagoutz 1993). This supports the postulate that continental collision along the former Hallstatt-Meliata ocean initiating during the Early Cretaceous in the eastern parts of the Austroalpine units of Austria was indeed followed by westward propagation of a thrust wedge into our area of interest by Cenomanian to Early Turonian times (Thöni & Jagoutz 1993, Neubauer 1994, Froitzheim et al. 1994).
In Figure 22-3 Cretaceous orogeny is also shown to have affected the Southern Alps (pre-Adamello phase of Brack 1981 and Schönborn 1992). The exact timing of this deformation phase is ill-constrained but certainly pre-dates

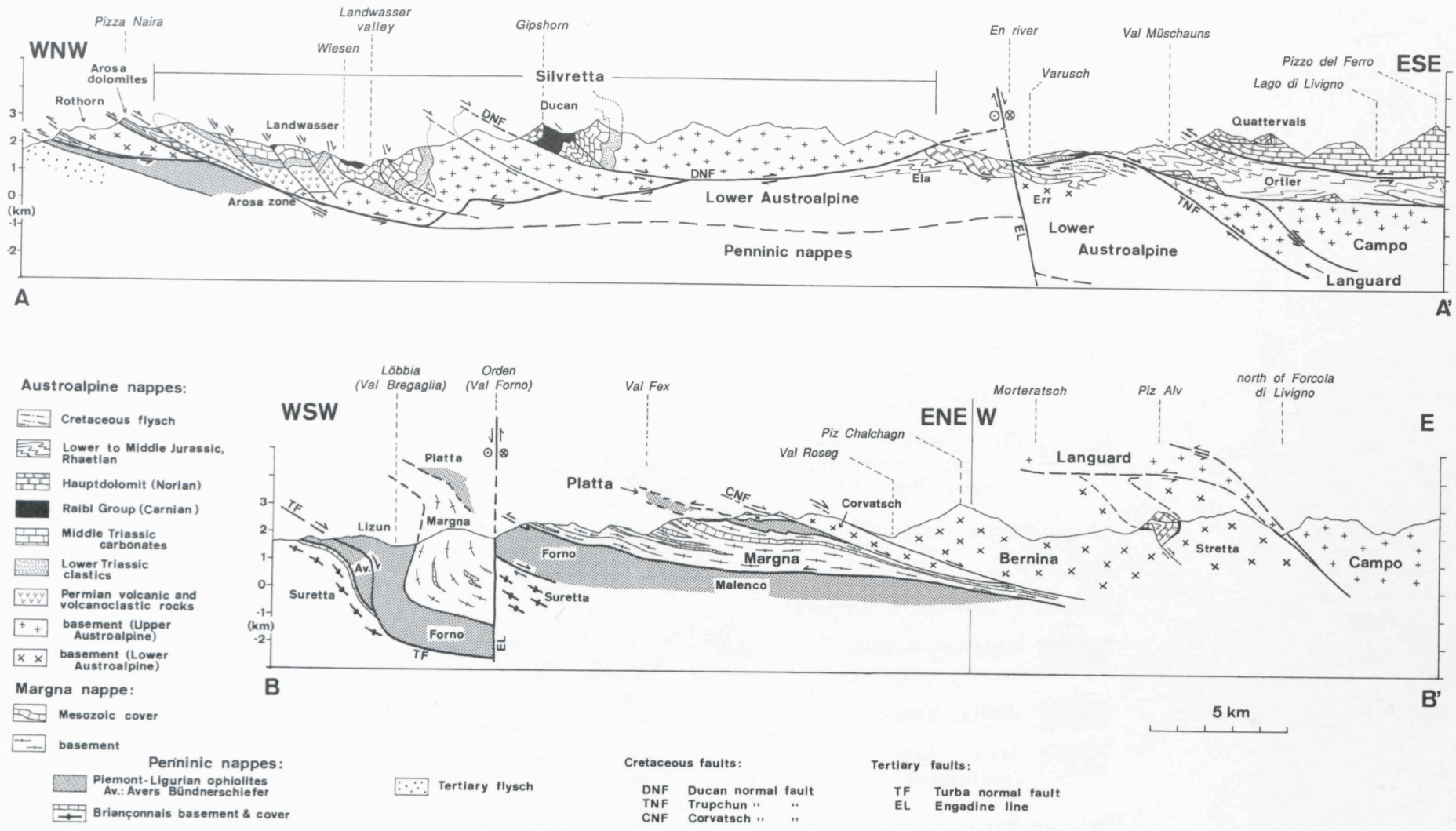

Figure 22-6
Two tectonic profiles through the Austroalpine nappes in eastern Switzerland. Profile trace indicated in Figure 22-5.

43 Ma (oldest parts of the Adamello intrusion). Assuming that flysch sedimentation in the Lombardian basin is contemporaneous with this deformation phase, and based on radiometric dating of pre-Adamello dykes crosscutting certain thrusts (Zanchi et al. 1990), a Late Cretaceous age is inferred. However, a Paleocene or Early Eocene event cannot be completely ruled out. All the top-to-the-south displacements along the Orobic thrust and parts of the displacement along the Coltignone thrust shown in Plate 22-1 are of pre-Adamello age (Schönborn 1992). This pre-Adamello N–S compression led to more than 25km of shortening and to lower greenschist facies metamorphism in the northernmost part of the Southern Alps (Orobic thrust sheet).
Activity along a precursor of the Insubric line during or immediately after Cretaceous orogeny is indicated from three lines of evidence:

(1) The kinematic and structural styles of Cretaceous deformation are totally different within the Austroalpine nappes north of the Insubric line (top-to-the-west imbrication, collision and penetrative deformation associated with metamorphism) and in the Southern Alps (top-to-the-south thrusting, foreland deformation).
(2) The Insubric line marks the limit between Cretaceous-aged metamorphic terranes to the north and the Southern Alps lacking such an overprint. Cretaceous eclogite facies metamorphism occurs in the Sesia-Dent Blanche units (Hunziker et al. 1989) and the Austroalpine units (Thöni & Jagoutz 1993), and temperature-dominated metamorphism in the Oetztal nappe (e. g. Thöni 1986). These terranes must have been at least partially exhumed by or during the Late Cretaceous and juxtaposed with the Southern Alps along this precursor of the Insubric line.
(3) The profile of Plate 22-1 directly shows a fundamental difference between the Austroalpine nappes and the Southern Alps: The former were emplaced as thin allochthonous flakes onto Penninic ophiolites in Cretaceous times, while the latter remained attached to the lower crust and upper mantle of the Apulian microcontinent, in spite of the 25km shortening of probably Cretaceous age represented by the upper crustal Orobic and Coltignone thrusts.

22.3.3 Late Cretaceous extension

Orogenic collapse behind the westward migrating Cretaceous orogenic wedge during the Ducan-Ela phase (Figure 22-3; see Froitzheim et al. 1994) led to a series of normal faults at higher tectonic levels (i. e. the normal fault at the base of the Julier nappe depicted in Plate 22-1, described by Handy et al. 1993 and several normal faults depicted in Figure 22-6, such as the Ducan, Trupchun and Corvatsch normal faults) and folding with horizontal axial planes at a lower tectonic level in the Austroalpine units of eastern Switzerland (Froitzheim 1992, Froitzheim et al. 1994). This collapse is also observed further to the east in Austria, where it is related to the formation of the 90 to 60 Ma old Gosau basins (Ratschbacher et al. 1989, Neubauer 1994). In our area of interest this extensional phase is not well dated. We place this Ducan-Ela phase somewhere between 80 Ma (end of the Trupchun phase) and 67 Ma (lower age bracket of a radiometric age determination by Tietz et al. 1993). This Ducan-Ela phase of extension appears to have migrated westward, analogous to the previously described westward migration of the Trupchun phase. Consequently, this extension is viewed as being caused by gravitational collapse of an overthickened orogenic wedge (Platt, 1986).
Exhumation and cooling of the Austroalpine units during this Ducan-Ela phase had important implications for the Tertiary orogenic evolution of the Alps. The Austroalpine units remained largely undeformed in the Tertiary and acted as an orogenic lid in the sense of Laubscher (1983); they represented a relatively rigid block characterized by friction-controlled Coulomb behaviour floating on viscously deforming Penninic units (Merle & Guillier 1989).

22.3.4 Early Tertiary convergence and subduction (65 – 50Ma)

The tectonic evolution during Tertiary orogeny is summarized in the sketches of Figure 22-7 (see also the pioneering work along the same transect by Milnes 1987, figure 3).
The earliest possible onset of thrusting in the units below the orogenic lid formed by the Austroalpine nappes and the Platta-Arosa ophiolites (Figure 22-7a, b) is locally constrained by ongoing sedimentation in the Briançonnais domain (Paleocene in the northernmost unit of the Briançonnais, the Falknis nappe; see Allemann 1957) and in the North-Penninic Bündnerschiefer (Early Eocene in the Arblatsch and Prättigau flysch; see Eiermann 1988, Nänny 1948 and Ziegler 1956).
The sketch of Figure 22-7a represents the onset of subduction of the Briançonnais domain due to complete closure of the Piemont-Liguria ocean. The formation of an accretionary wedge within the Avers Bündnerschiefer (Piemont-Liguria ocean) and northward thrusting of this wedge onto the future Suretta nappe (southernmost Briançonnais domain) is tentatively placed in the Early Paleocene (Avers phase, Figure 22-3). This allows for continued sedimentation within most of the Briançonnais domain during the Paleocene. Onset of southernmost Briançonnais domain subduction later than 65 Ma would require convergence rates higher than 1.5 cm/yr (see Table 22-1) given the width of the paleogeographical domains adopted for constructing the

time interval	amount of convergence across the Alps	convergence rate	plate tectonic reconstruction (Dewey et al. 1989)
Early Paleocene to Early Eocene (65–50 Ma)	200 km inferred from relative displacement between points a and b in Figure 22-7 116 km of thinned continental crust of the Briaçonnais domain and the Valais ocean enter the cubduction zone.	1.33 cm/a	0.22 cm/a 55 Ma
Early to Late Eocene (50–40 Ma)	150 km inferred from relative displacement between points a and b in Figure 22-7 150 km of distal European margin situated between the southern edge of the Helvetic domain and the southern tip of stable Europe enter the subduction zone.	1.5 cm/a	0.4 cm/a 51 Ma
			1.2 cm/a 38 Ma
Late Eocone to Oligocene (40–32 Ma)	45 km inferred from relative displacement between points a and c in Figure 22-7 Detachment of the Helvetic sediments and deformations within the Subpenninic nappes. Unknown amount of shortening in the vicinity of the Insubric line and in the Southern Alps: 45 km represent a minimun estimate only	at least 0.55 cm/a	
Olifocene to Early Miocene (32–19 Ma)	a total of 58 km consisting of: 33 km from relative displacement between points a and c in Figure 22-7 (including 6 km out of a total ov 21 km shortening in the Aar massif) 15 km from backthrusting along the Insubric line 10 km out of a total of 56 km post-Adamello phase shortening in the Southern Alps	0.45 cm/a	0.94 cm/a 19 Ma
Early Miocene to recent (19–0 Ma)	a total of 61 km consisting of: 15 km from shortening in the Aar massif 46 km from shortening in the Southern Alps	0.3 cm/a (0.5 cm/a if deformation stopped at 7 Ma)	0.3 cm/a 9 Ma
			0.43 cm/a 0 Ma
Total time span (65–0 Ma)	more than 514 km	more than 0.79 cm/a	average: 0.72 cm/a amount of convergence: 481 km

Table 22-1
N–S convergence along the Eastern Traverse derived from the profiles of Figures 22-7 and plate rotation parameters of Dewey et al. (1989).

sketches (see discussion above and further discussion in Chapter 14). Such high convergence rates are unrealistic in comparison with plate movement reconstructions based on the analysis of magnetic anomalies in the Atlantic (Dewey et al. 1989). Our interpretation leaves very little time for a quiescent phase between the Cretaceous and Tertiary orogenies (the often quoted "Paleocene restoration"), somewhere near the Cretaceous-Tertiary boundary (Figure 22-3).

By the end of the Early Eocene (Figure 22-7b) the entire width of the Briançonnais domain had been subducted, together with those parts of the North-Penninic Bündnerschiefer or Valais basin that are assumed to have been underlain by oceanic lithosphere. Sedimentation in parts of the North-Penninic Bündnerschiefer basin continued up to this time (Arblatsch and Ruchberg flysch). The Tambo and Suretta nappes, representing the southern parts of the Briançonnais domain continental basement, must have reached their maximum depth (corresponding to peak pressures of 10–13kb, see Baudin and Marquer 1993) no later than this time (about 50 Ma), in order to allow for subsequent heating to peak temperatures at 40–35 Ma (discussion in Chapter 14, Hurford et al. 1989). Because the onset of penetrative cleavage formation (Ferrera phase of Figure 22-3) is associated with this metamorphism it is assumed to have started near the Paleocene-Eocene boundary in the Tambo and Suretta nappes. This significantly predates the onset of the Ferrera phase deformation in the North-Penninic Bündnerschiefer (Figure 22-3). This finding is in accordance with the general trend of northward younging for the onset of penetrative cleavage formation shown in Figure 22-3.

The northern parts of the Briançonnais basement are assumed to have been permanently subducted ("subducted Briançonnais" in Figure 22-7b). At about 50 Ma, the southern tip of stable Europe, represented by the Adula nappe, is about to enter the subduction zone. Figure 22-7b represents a snapshot of the onset of final collision caused by the complete closure of the North-Penninic Bündnerschiefer realm.

The convergence rate resulting from the relative displacement (200km) of points "a" (northern edge of the orogenic lid represented by the Austroalpine nappes) and "b" (southern tip of stable Europe, i.e. the Adula nappe) in Figures 22-7a and 22-7b is 1.3 cm per year (Table 22-1). It is noteworthy that the reconstruction of Figure 22-7 implies that the northern tip of the Austroalpine nappes marked by "a" in Figure 22-7a (and corresponding to the front of the Northern Calcareous Alps in a present-day profile, see Figure 22-7g) has moved northward by a total of about 450km relative to a point attached to stable Europe presently situated below the northern edge of the Northern Calcareous Alps. This 450 km of convergence (out of a total 514 km of Tertiary N-S convergence across the Alps, Table 22-1), was accommodated by subduction and shortening within the northern foreland. Relative to stable Europe, point "a" in the sketch of Figure 22-7a would have to have been located near Pisa in Northern Italy at the onset of Tertiary convergence. This illustrates well the important point that Cretaceous orogeny took place far from the present-day position of the Austroalpine nappes at the front of the Alps, overriding the southern Molasse basin.

22.3.5 Tertiary collision (50–35 Ma)

Collision of stable Europe with the orogenic lid led to the situation in Late Eocene times depicted in Figure 22-7c. Rapid exhumation of the Adula eclogites immediately followed and the establishment of the stack of the higher Penninic nappes occurred by the Early Oligocene (Figure 22-7d).

The amount of convergence between the stages of Figures 22-7b and 22-7c (Table 22-1) is determined by the peak depth of the Adula nappe (corresponding to 27kbar reported for the Cima Lunga unit by Heinrich 1986) and the chosen subduction angle. Other important constraints on the convergence rate are offered by the interpretation of the Adula nappe as representing the southern tip of the European foreland and the Tertiary age of eclogite facies metamorphism (Figure 22-3) inferred from geochronological (Becker 1993, Gebauer et al. 1992, 1996) and structural (Partzsch et al. 1994) data. Based on these constraints the convergence amounts to 150 km, or 1.5 cm/yr. The additional 45 km of shortening inferred to have been produced between the stages illustrated in Figures 22-7c and 22-7e (indicated by the relative movement of points labelled "a" and "c", see Table 22-1 and Figure 22-7) is a minimum estimate since it does do not account for an unknown amount of retroshearing associated with the initial phases of backthrusting and vertical extrusion in the vicinity of the Insubric line.

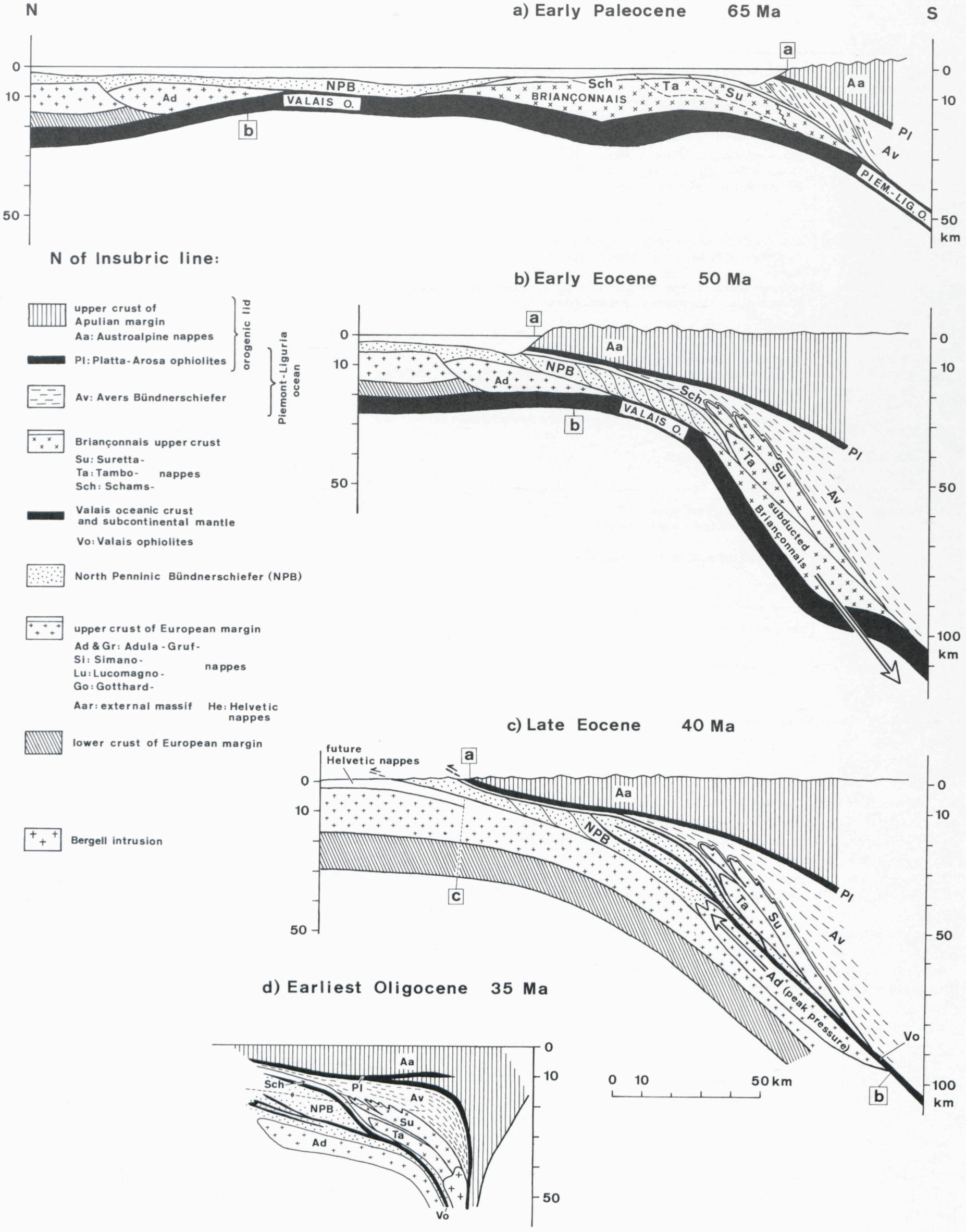

Figure 22-7
Scaled and area-balanced sketches of the kinematic evolution of the Alps from early Tertiary convergence and subduction (stages a and b) to collision (stage c) and post-collisional shortening (stages d to g).

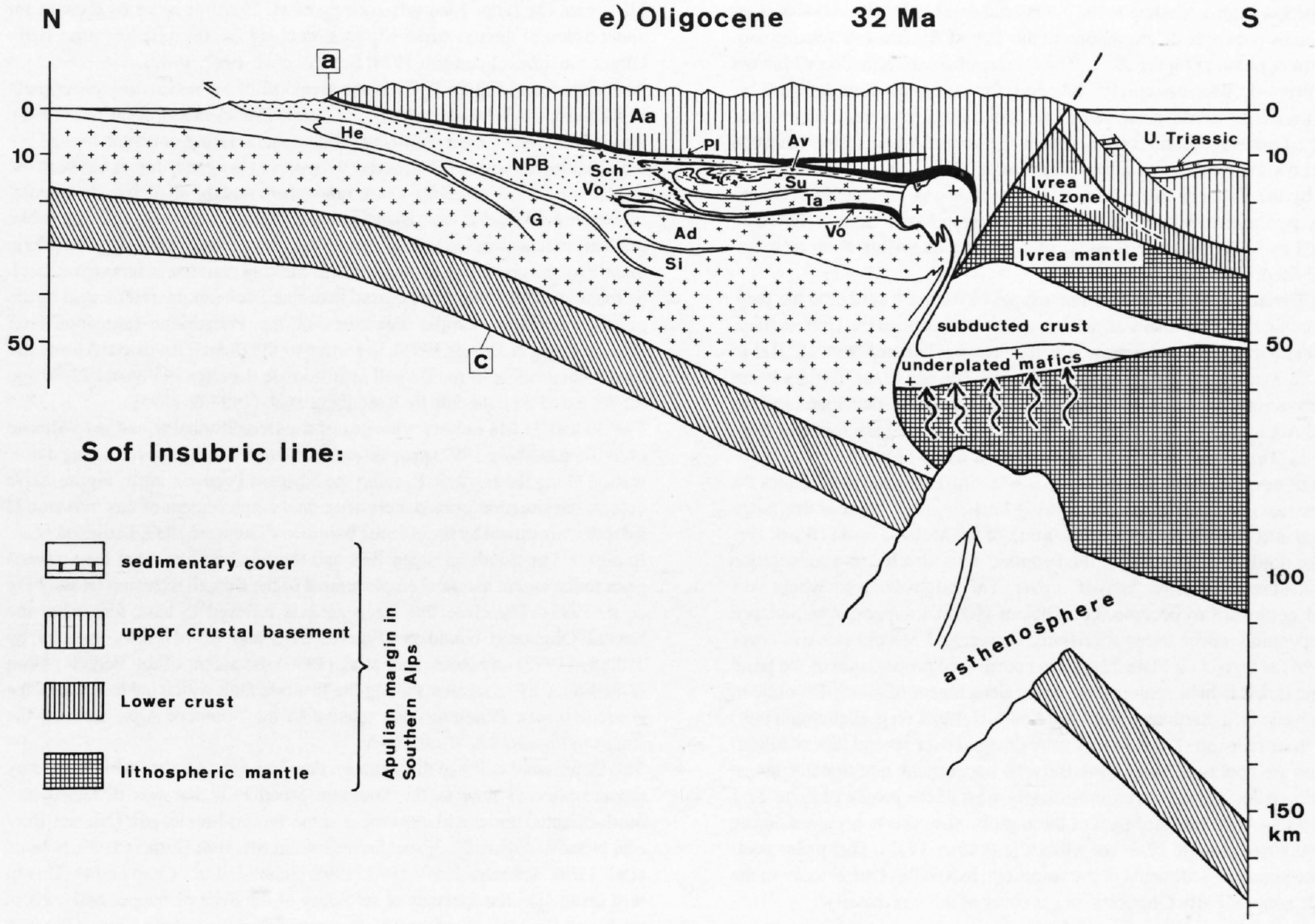

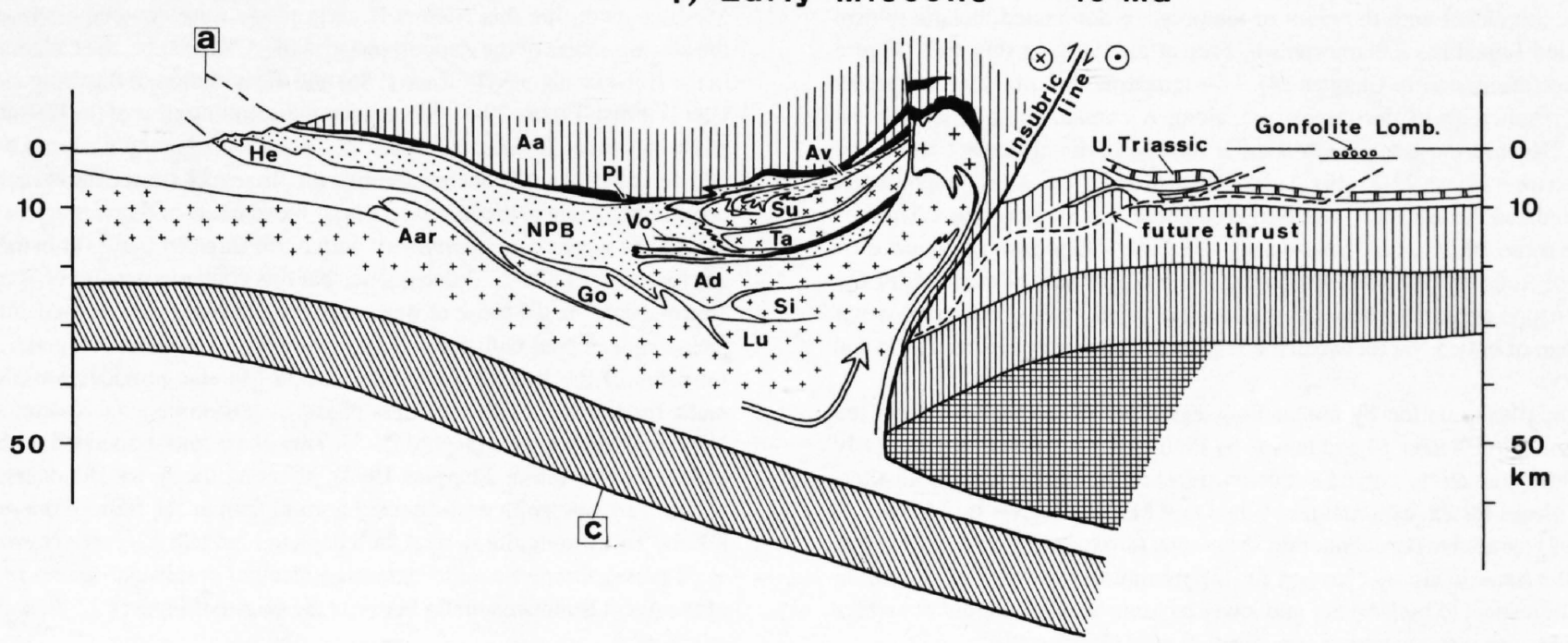

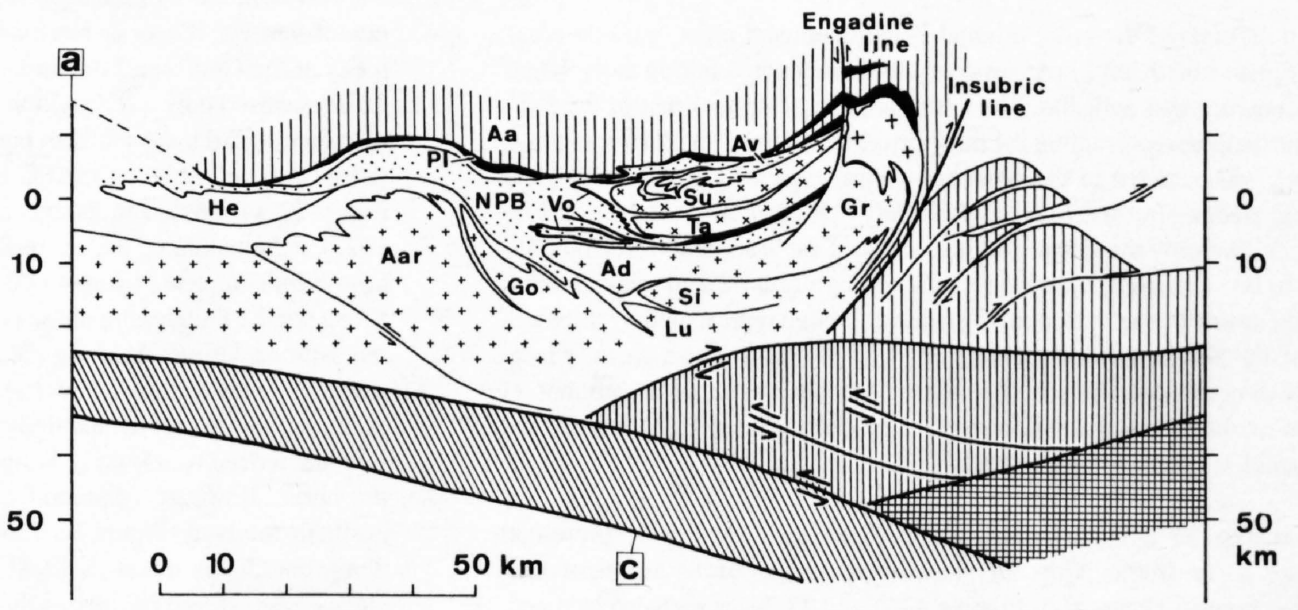

Figure 22-7 (continued)

The time span corresponding to the collisional event (50 to 35 Ma) was characterized by penetrative deformation in the Tambo, Suretta and Schams nappes (Ferrera phase of Figure 22-3). The Ferrera phase deformation within the North-Penninic Bündnerschiefer falls entirely within this time interval. Intense imbrication of Mesozoic sediments, continental basement, and mafics rocks of possibly oceanic origin within the future Adula nappe (Sorreda phase, Löw 1987) occurred under prograde conditions. This phase was followed by the Zapport phase (Löw 1987), which was characterized by extremely penetrative deformation, initially under eclogite facies conditions, followed by lower pressure metamorphic conditions arising from near isothermal decompression.

During Tertiary collision the Penninic nappes thrust northward onto the foreland, forcing the detachment of sediments that later formed the Helvetic nappes from their original substratum, i.e. the present Gotthard "massif" (D1 in Figure 22-3) at the end of the collisional stage. The age of the Tertiary cover basal unconformity (Herb 1988, Lihou 1995) in the Helvetic nappes and the internal Aar massif (Infrahelvetic units) decreases toward the foreland (Figure 22-3). This decrease may be interpreted in terms of northwestward migration of a peripheral bulge within the subducting European plate across the Helvetic realm during the Eocene. During later stages of orogeny this bulge migrated into its present-day location north of the Molasse basin (Black Forest). The northward thrusting of the Penninic units also led to a substitution of the southern Gotthard "massif" cover. The original cover, which was sheared northward to become the incipient Helvetic nappes, was replaced by Subpenninic cover slices ("Triassic, Lower, and Middle Jurassic cover slices" in the legend on Plate 22-1). This northward propagation of the basal Penninic thrust is held responsible for the detachment of North-Penninic or Ultrahelvetic (e. g. Sardona flysch) and South-Helvetic (e. g. Blattengrat unit) slivers in its footwall. These slivers were dragged over several tens of kilometers and are now found above the Helvetic nappes and, additionally, above the northern Aar massif cover immediately west of the profile of Plate 22-1 in the Glarus Alps. Emplacement of these exotic strip sheets occurred during the Pizol phase (Figure 22-3; see Milnes & Pfiffner 1977). This phase postdates the youngest sediments in the respective footwalls (Late Eocene in the Helvetic nappes, Early Oligocene in the cover of the Aar massif).

The early phases of exhumation of the Adula nappe brought the frontal parts of this unit to moderate pressures of around 6–8kb by about 35 Ma (Figure 22-7d), coincident with the onset of temperature-dominated metamorphism (so-called Lepontine metamorphism, Frey et al. 1980) in this area (Figure 22-3, see discussion in Chapter 14). This temperature-dominated metamorphism resulted from decompression along a continuous p-T loop (Löw 1987). Because the Bergell intrusion is located in direct contact above the Adula nappe (Plate 22-1) this early exhumation of the Adula nappe must have predated the intrusion. The Bergell tonalite was emplaced at a depth of merely some 20 km at its base during the Early Oligocene (pressure estimates of Reusser 1987, Davidson et al., in press). Early exhumation of the Adula nappe appears to have been extremely rapid, having occurred over a time span of only 5 Ma (between the stages represented in Figures 22-7c and 22-7d).

Such rapid exhumation by corner flow, extension or buoyancy forces (see discusssion in Chapter 14 and review by Platt 1993) is unlikely for this early phase of exhumation. Forced extrusion (recently proposed as a viable alternative model for the exhumation of the Dora Maira eclogites by Michard et al., 1993) parallel to the subduction shear zone (arrow in Figure 22-7c) seems to be the most likely mechanism for differential exhumation of the Adula nappe in respect to both higher and lower tectonic units which did not suffer eclogite facies metamorphism (see discussion in Chapter 14).

22.3.6 Post-collisional shortening (35 Ma to present)

Substantial parts of the more internal Penninic crustal units (oceanic crust, Briançonnais and distal European crust) were subducted during early stages of convergence and collision. The entire volume of upper crust in the Subpenninic nappes, representing the more proximal parts of the European crust, however, was accreted to the orogenic wedge. Excessive thickening of the orogenic wedge after the Eocene effectively "clogged" the subduction system, such that only the detached lower crust of the European foreland continued to be subducted. This led to backfolding north of, and backthrusting along the Insubric line in front of the Adriatic wedge represented by the basement of the Southern Alps (Schmid et al. 1989). This "retro-shear" meets with N-directed detachment ("pro-shear" in the sense of Beaumont et al.,1994) at the base of the Subpenninic nappes near the interface between the upper and lower crust (Figures 22-7e,f,g).

The **first step** (35 to 32 Ma) of this post-collisional shortening is represented in Figure 22-7e. In this figure the present-day portion of the Southern Alps along the transect (Plate 22-1, Figures 22-7f and 22-7g) is replaced by a profile across the Ivrea zone (after Zingg et al. 1990) in order to account for about 50km of dextral strike-slip motion along the Insubric line after Early Oligocene times (Fumasoli 1974, Schmid et al. 1987, 1989).

Also depicted in Figure 22-7e is the break-off of the subducting lower parts of the European lithosphere proposed by von Blanckenburg & Davies (1995). The subduction of light continental lithosphere during collision created extensional forces within the slab, due to opposing buoyancy forces between the deeper subducted, relatively dense lithosphere and the shallower continental lithosphere (Davies & von Blanckenburg 1995). As a result, the slab broke off. This mechanism led to heating and melting of the overriding lithospheric mantle by the upwelling asthenosphere. Melting resulted in mixing of basaltic magmas with assimilated crustal material. Such mixing is indicated by the geochemical and isotopic signatures of the Periadriatic intrusions (von Blanckenburg & Davies 1995), in particular the Bergell intrusion. Ascent and final emplacement of the Bergell intrusion are depicted in Figures 22-7d and 22-7e, based on field data by Rosenberg et al. (1994 & 1995).

The 30 and 32 Ma radiometric ages of the Bergell tonalite and granodiorite (von Blanckenburg 1992) provide excellent time constraints for dating deformation along the Insubric line and the adjacent Penninic units. Figure 22-7e depicts the situation immediately after final emplacement of this intrusion at a depth constrained by hornblende barometry (Reusser 1987, Davidson et al., in press). The Southern Steep Belt and the Insubric line must have existed prior to the ascent and final emplacement of the Bergell intrusion (Rosenberg et al. 1995). Therefore this steep zone is inferred to have formed at the Eocene-Oligocene boundary (Figures 22-3 and 22-7d). As suggested by Trümpy (1992) and Rosenberg et al. (1995) the ascent of the Bergell pluton is facilitated by movements along the Insubric fault which led to uplift of the entire southern Penninic zone relative to the Southern Alps between the stages in Figures 22-7d and 22-7e.

This differential uplift of the southern Penninic zone was probably caused by upward-directed flow in the Southern Steep Belt that was deflected into north-directed horizontal movement of the Tambo-Suretta pair (Niemet-Beverin phase of Figure 22-3, see discussions in Merle & Guillier 1989, Schmid et al. 1990, Schreurs 1990, 1993, 1995, Schmid et al., Chapter 14). This in turn resulted in the spectacular refolding of the Schams nappes and parts of the North-Penninic Bündnerschiefer around the hinge of the Niemet-Beverin fold (axial trace indicated in Figures 22-7d and 22-7e).

Movements during this Niemet-Beverin phase were contemporaneous with the closing stages of the Zapport phase in the Adula nappe, the Calanda phase in the Helvetic nappes (Pfiffner 1986) and the initiation of thrusting along the Glarus thrust (Figure 22-3). Movement of the trailing edge of the Helvetic nappes at this time, depicted in Figure 22-7e, ensured that these nappes were not affected by any significant metamorphism (these rocks now exhibit anchizonal conditions). Hence, the initial stages of movements in the vicinity of the Insubric line were contemporaneous with north-directed transport in the northern foreland. Figure 22-3 documents that this contemporaneity of "pro-" and "retro-shears" in the sense of Beaumont et al. (1994) is maintained during the later stages of post-collisional deformation throughout the Neogene.

Intrusion of the Bergell granodiorite at 30 Ma also provides a useful time mark for the end of this earliest phase of post-collisional shortening, the Niemet-Beverin phase (Figure 22-3). This phase was associated with E–W-extension (Baudin & Marquer 1993), affecting the Avers Bündnerschiefer, which were cut by an east-directed normal fault at the base of the orogenic lid (the Turba mylonite normal fault depicted in Plate 22-1; see Nievergelt et al. in press). Orogen-parallel extension resulted in substantial area reduction of the Avers Bündnerschiefer between the stages of Figures 22-7d and 22-7e.

The **second step** (32 to 19 Ma) of post-collisional shortening was dominated by backthrusting of the Central Alps over the Southern Alps along a mylonite belt associated with the Insubric line. This backthrusting, in combination with erosion, led to amazingly rapid exhumation of the Bergell area at the rate of 5mm/yr (Giger & Hurford 1989). Deposition of boulders of Bergell rocks in the Gonfolite Lombarda (mainly in the Como formation of Figure 22-3) occurred only a few million years after intrusion. Based on the cooling ages coming from the southern part of the Tambo nappe in the vicinity of this intrusion (cooling below 300°C between 21 and 25 Ma as summarized in Figure 22-3 from data in Jäger et al. 1967, Purdy & Jäger 1976, Wagner et al. 1977), exhumation of the entire Bergell area to shallow crustal depths must have been completed by about 20 Ma.

Effects of the Domleschg phase (see Chapter 14) which were contemporaneous with backthrusting along the Insubric mylonite belt (Figure 22-3) were relatively weak within the central Penninic region. The large-scale structure of this region was not substantially altered during this Domleschg phase which is characterized by a steeply S-dipping crenulation with constant vergence to the north. However, important contemporaneous movements affected the northern foreland (Figure 3). There, the main activity involved movements along the Glarus thrust (Schmid 1975) and the formation of a penetrative cleavage above and below this thrust (Calanda phase, Pfiffner 1986).

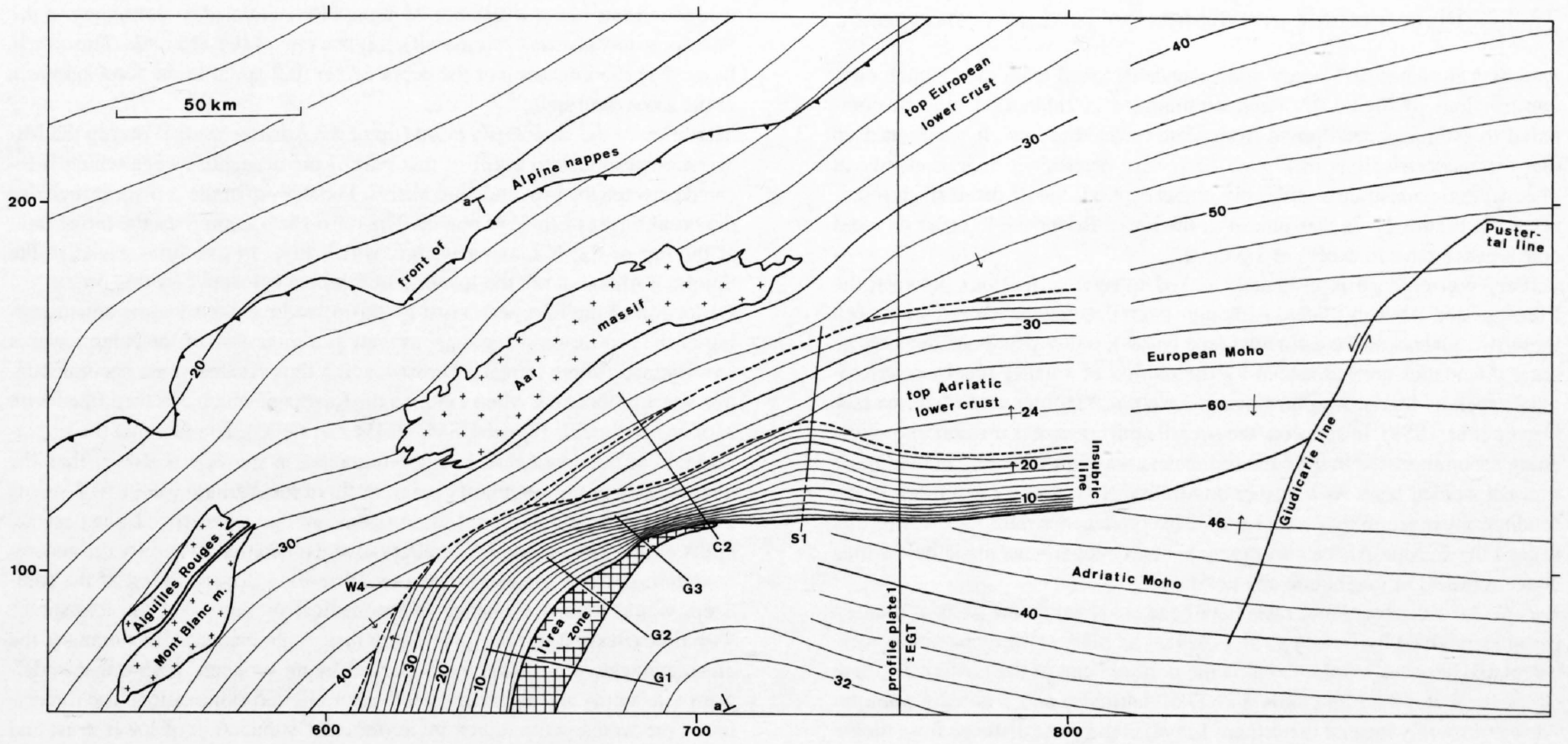

Figure 22-8

Map outlining the contours of the top of the Adriatic lower crustal wedge and its relation to the top of the European lower crust and the Insubric line, and additionally, the Adriatic and European Moho (eastern and southern part of area covered by Figure 22-8). Contour lines are given in 2 km intervals. The contours of the Insubric line are constrained by field data (Schmid et al. 1987), migrated reflection lines S1 and C2 (Valasek 1992) and 3D gravity profiles G1, G2 and G3 obtained from 3D modelling by Kissling (1980). The migrated seismic line W4 is also indicated but was not used for constraining the dip of the Insubric line. Contours of the top of the European lower crust and Moho are taken from Valasek (1992). The Adriatic Moho is contoured after data compiled by Kissling (1993) and after a seismic refraction profile by Deichmann et al. (1986). a-a: profile trace of Figure 22-9.

The leading edge of the Helvetic nappes emerged at the erosional front of the early Alps in Mid-Miocene times (Pfiffner 1986), as witnessed by Helvetic pebbles (Leupold et al. 1942) in the Upper Freshwater Molasse (OSM). The basal thrust of the Helvetic nappes (Glarus thrust in Plate 22-1) migrated towards the foreland. Displacement considerations suggest that this fault broke surface in Early Miocene times (Figure 22-7f, Pfiffner 1985). Outward migration was also true for the nappe-internal deformation (folds, thrusts, cleavage), which is attributed to the Calanda phase (Figure 22-3). This phase is of Early Oligocene age in the Helvetic nappes (Hunziker et al. 1986) and of Mid to Late Oligocene age in the internal Aar massif.

Movements at a time near the Oligocene-Miocene boundary led to the situation depicted in Figure 22-7f. These movements include: (i) dextral strike slip under brittle conditions along the Insubric line, without associated backthrusting (Schmid et al. 1989), (ii) differential uplift of the Bergell intrusion with respect to the Penninic units, caused by block rotation along the sinistral Engadine line (Schmid & Froitzheim 1993), (iii) E–W orogen-parallel extension at the eastern margin of the Lepontine dome (Forcola phase of Figure 22-3, see Chapter 14), and (iv) further movement along the Glarus thrust, leading to a second crenulation cleavage (Ruchi phase in Figure 22-3) in the area of the internal Aar massif (Pfiffner 1977, Milnes & Pfiffner 1977). Effects of contemporaneous backfolding south of the external massifs and in the northern part of the transect (Carassimo phase and formation of the Chiera synform in Figure 22-3; see Löw 1987) were relatively minor along our transect, but their importance increases rapidly further to the west. There, very intense backfolding (however of substantially younger age according to Steck & Hunziker 1994) is observed at the southern margin of the Aar massif (see Figure 22-9 and profile along the Western Traverse presented in Chapter 16). The closing stages of displacement along the Glarus thrust and the initiation of thrusting in the Molasse basin associated with shortening within the Aar massif also occurred during this second step of post-collisional deformation (Grindelwald phase in Figure 22-3; see Pfiffner et al., Chapter 13.1).

Although 33 km out of a total of 58 km shortening between the stages represented by Figures 22-7e and 22-7f took place in the northern foreland (Table 22-1), deformation in the southern part of the profile outweighted the one in the northern part during a **third step** that began in the Early Miocene (46 km out of a total of 61 km shortening, see Table 22-1). It is this final stage of post-collisional shortening that profoundly influenced the deep structure of the Alps as revealed by geophysical information, but which only led to uplift and erosion in the central part of the Alps along our transect (erosional stage of Pfiffner 1986).

According to Table 22-1 the greatest part of post-Adamello shortening in the Southern Alps occurred during this third step. It led to the impressive foreland wedge of the Southern Alps, sealed by the Messinian unconformity that formed at around 7 Ma. This post-Adamello shortening was mainly achieved by thrusting along the Milan thrust and the later out-of-sequence Lecco thrust (Plate 22-1). According to Schönborn (1992), N–S-shortening was contemporaneous and related to the displacement of the Periadriatic line by younger movements along the Giudicarie line. Retro-deformation of the post-Adamello shortening leads to a perfect alignment between the Insubric and Pustertal lines (Schönborn 1992). Together with the fact that the lower crustal volume related to this shortened upper crust is presently found at great depth north of the surface expression of the Insubric line, this is convincing evidence for a direct relationship between shortening in the Southern Alps and indentation of the Adriatic lower crustal wedge as proposed by Pfiffner (1992). Based on maps of the Moho, the Conrad discontinuity (top of the lower crust) and the top basement surface, Hitz & Pfiffner (1994) argued in favour of such a mid-crustal decoupling. Indentation of the Adriatic lower crust into the interface between the south-dipping European lower crust and the European upper crust (Subpenninic nappes) took place during this latest stage (see Figuress 7f,g and 8) and postdated final movements along the Insubric line, as already suggested by Laubscher (1990).

Shortening within the external Aar massif (Grindelwald phase of Figure 22-3) and a large part of the thrusting in the Molasse basin were contemporaneous with indentation of the Adriatic wedge (Pfiffner et al., Chapter 13.1). Outward and downward (in-sequence) propagation of thrusting also affected the Molasse basin. The depot center of this foredeep (including the Oligocene North-Helvetic Flysch deposited on the internal Aar massif) migrated outward at a rate of 0.3 cm/a in the Oligocene, slowing down to 0.2 cm/a in Miocene times (Pfiffner 1986). Thrusting in the Molasse basin and possibly folding of the Jura mountains west of our transect postdates, and in Central Switzerland actually deforms the basal thrust of the Helvetic nappes (Pfiffner et al., Chapter 13.1). Within the transect exhumation of the Aar massif from a paleo-depth of approximately 7km to about 4km beneath the paleo-landsurface occurred in the Miocene, as indicated by fission track data (see Chapter 13.1). The thrust indicated in Figure 22-7g at the base of the Aar massif delimits the boundary between deformed and undeformed European foreland.

Updoming of the Aar massif may be viewed as a crustal-scale ramp fold related to detachment at the interface between lower and upper European crust. This detachment is kinematically linked to the Adriatic lower crustal wedge. The intersection point between "pro"- and "retro-shears" in the sense of Beaumont et al. (1994) is now situated further to the north (i.e. at the northern tip of the lower crustal wedge) and at the interface between lower and upper European crust.

22.3.7 Plate tectonic constraints on Tertiary convergence

Amounts and rates of Tertiary convergence deduced from the kinematic reconstructions of Figure 22-7 and summarized in Table 22-1 may be compared to estimates determined from plate reconstructions. It is emphazised that the reconstructions in Figure 22-7 were determined independently of plate tectonic constraints with only one exception: the ill-dated stage represented in Figure 22-7a was placed in the lower Paleocene in order to avoid convergence rates in excess of 1.5 cm/a.

Tertiary convergence is ultimately linked to relative motions between the Eurasian and African plates. Although overall convergence rates between these two plates can be estimated (see below), many details of the smaller scale kinematics are influenced by the motion of smaller blocks or microplates such as Iberia, Apulia, Corsica-Sardinia, Mallorca and Menorca (see Dewey et al. 1989). In addition, the overall convergence is divided into shortening accommodated in the Mediterranean area and shortening in the Alpine transect studied here. As a further possibility, N–S directed extension in the Mediterranean realm may have resulted in convergence rates for the Alps that exceed the Europe-Africa convergence rate. Comparisons made below thus concern orders of magnitude and not detail.

Europe-Africa convergence rates have been analyzed on the basis of rotation parameters given by Dewey et al. (1989). The plate convergence rates were calculated between a point fixed on the northern end of the Eastern Traverse (Rorschach at +9.5° longitude and 47.5° lattitude) and a moving point on Africa (presently located in northern Libya) at the same distance from the rotation pole as Rorschach). Angular velocities for the various time intervals were determined using an average rotation pole (–15°/31°) determined from the data in Dewey et al. (1989). These velocities were then converted to local velocities (cm/a) and are listed in Table 22-1. The average velocity over the entire time span (65 Ma to present) is 0.72 cm/a, and very close to the estimate of 0.79 cm/a determined from our reconstructions. The total convergence between Europe (Rorschach) and Africa (northern Libya) is 480 km as estimated from the rotation parameters.

Local interval velocities of plate motion suggest much slower convergence rates (0.22–0.4 cm/a) in Paleocene times than the estimates based on our reconstruction (1.33 cm/a) . The reasons for this discrepancy are not clear, but might be due to independent motions of microcontinents such as the Briançonnais-Iberia terrane (Stampfli 1993). Rapid convergence (0.94 to 1.2 cm/a), however, is indicated for Eocene-Oligocene times by Dewey et al. (1989) data, in excellent agreement with our kinematic reconstruction. This higher convergence rate is linked to subduction and high-pressure metamorphism in the southern tip of Europe (Adula nappe). There is surprisingly good agreement of convergence rates in Miocene to recent times and also in respect to the total amount of convergence.

22.4 Discussion and conclusions

The Alpine section described in this contribution is similar in many ways to some of the numerical models of crustal scale deformation provided by Beaumont et al. (1994). The driving force in these models is provided by underthrusting of the mantle lithosphere (in our case the European lithosphere), coupled with asymmetric detachment emerging from a velocity discontinuity at a point (point "S") where two inclined step-up shear zones ("pro-shear" and "retro-shear") meet. The gently dipping pro-shears may be compared to the south-dipping thrust faults in the Helvetic and northern Penninic zone. More steeply inclined retro-shears, such as the Insubric line, develop above the subduction zone, causing relative uplift of the southern Pennine zone.

The analogy between model 5 of Beaumont et al. (1994), characterized by subduction of 1/3 of the crustal column, and the post-collisional stages depicted in Figures 22-7e-g is particularly striking. Intra-crustal detachment allows for simultaneous foreland migration to the north and south. Model M4 (Beaumont et al. 1994) illustrates the important role of denudation in amplifying the movement along the retro-shear. Erosion of a thickness of several kilometers of material is in fact known to have occurred in Late Oligocene times north of the Insubric line within a very short time span (Giger & Hurford 1989). This resulted in rapid exhumation of high grade metamorphic rocks north of the Insubric line (Figure 22-7e,f). Note that Figure 22-7f does not indicate the large amount of erosion which undoubtedly occurred, as documented by the deposition of Bergell boulders in the Gonfolite Lombarda of the Southern Alps.

In the course of Miocene and Pliocene times the singularity point "S" (Beaumont et al. 1994) between the pro- and retro-shear migrated northward (Figures 22-7f and 22-g). This corresponds to the tip of the Adriatic wedge encroaching along the top of the European lower crust, uplifting the Alpine nappe stack. Between 19 Ma (Early Miocene, Figure 22-7f) and 8 Ma (Mid Miocene: end of sedimentation in the Molasse basin) the tip of the Adriatic wedge migrated over a distance of about 38km (related to shortening in the Subalpine molasse and Aar massif), i. e. at a rate of 0.4–0.5 cm/a. This rate is faster than the migration of the depot center (0.2 cm/a) in the foreland basin in the same time span.

Migration of the singularity point (tip of the Adriatic wedge) during the Miocene corresponds to uplift of that part of the orogenic wedge which is located between the pro- and retro shears. The step-up of the pro-shear includes the basal thrust of the Aar massif. The retro-shear comprises the thrust fault at the top of the N-moving wedge, which links to the thrust faults in the Southern Alps (but not the Insubric line, which is inactive by this time).

Deflection of the European crust by thrust loading caused some downwarping of the pro-thrust shear zone, as well as a migration of the bulge towards the foreland (hinge retreat). Thrust loading thus created some accommodation space (Sinclair & Allen 1992) in the foredeep, which was then filled with Molasse sediments (upper USM, OMM and OSM). The fact that the migration rate of the depot center, or accommodation space, was slower than the advance rate of the singularity point, or tip of the Adriatic wedge (0.2 versus 0.4–0.5 cm/a), suggests that the orogenic wedge experienced a net crustal uplift in this time interval. The alternative explanation, whereby the accommodation space is created by an ever increasing downwarping of the foredeep, would require a change of mechanical properties of the lithosphere with time (flexural rigidity), for which there is no evidence. In summary, the closing stages of collision were marked by an orogenic wedge that underwent thickening and shortening, and net uplift and exhumation. The dynamics of the wedge were driven by asymmetric subduction of lower crust and lithospheric mantle.

The model of tectonic evolution depicted in Figure 22-7 has implications for the rheological properties of the lithosphere. Shallow-dipping upper crustal detachments, typically at depths of around 4-8km below the top of the basement, are characteristic of nappe formation in the Penninic zone during collision. The existence of such shallow detachment levels might be surprising, when compared to models of rheological stratification (e. g. Ord & Hobbs 1989). It is only feasible to associate shallow detachments with the onset of crystal plasticity in quartz, once additional overburden has been created by partial subduction to considerable depth, such as depicted for the Penninic nappes in Figure 22–7a-d. It is noteworthy that this detachment level coincides with the shallowest zone of reduced P-wave velocity typical for the European crust of the northern Alpine foreland (Mueller 1977, Mueller et al. 1980).

Substantial parts of the European and Briançonnais continental crust were subducted during the collisional stage of orogeny, in contrast to the findings of Ménard et al. (1991). During the post-collisional stage, however, the thickness of the European crust increased significantly, as more proximal parts of the European margin (underlying the Helvetic realm) entered the subduction zone. This led to the detachment of the entire upper and middle crust at the interface between lower and middle crust, a characteristic of post-collisional orogeny (Figures 22-7e–g). The European lower crust represented a layer of realtively high strength, thus pointing to a 2-layer rheology of the crust, with the high strength of the lower crust being controlled by the rheology of feldspar and/or mafic minerals. In fact model M9 of Beaumont et al. (1994) produced a lower crustal wedge very similar to that shown in Figure 22-7g. Interestingly, this model assumes a 2-layer rheology for the crust (wet quartz and wet feldspar rheologies according to Jaoul et al., 1984 and Shelton & Tullis, 1981). In order to arrive at the geometry of the Adriatic lower crustal wedge depicted in Figure 22-7g, some detachment must also have occurred above the Adriatic Moho, i. e. at the base of the lower crust.

Figures 22-8 and 22-9 address some of the 3D problems in the Alps. How far may the section depicted in Plate 22-1 be taken as representative of Alpine sections further to the east and the west (Western Switzerland, discussed in Chapters 12 and 16, ECORS-CROP profile of the Western Alps, Nicolas et al., 1990)? The contour map of Figure 22-8 indicates that the Adriatic lower crustal wedge depicted in Plate 22-1 underthrusts the Insubric line by some 45km in the east (measured between the intersection point with the N-dipping Insubric line and the tip of the wedge). This displacement drops to zero at a point northwest of the Ivrea zone. Hence, the Ivrea body, which is located to the southeast and underneath the moderately NW-dipping Insubric line represents a separate and shallower wedge that reaches the surface in the Ivrea zone. The contours of the Insubric line in Figure 22-8 have been determined from the profile of Plate 22-1 and from migrated sections of seismic lines S1 and C2 (after Valasek 1992).

Only north of the western edge of the Ivrea zone is a steep dip of 75° measured in the field (Schmid et al. 1987), whereas Kissling (1980) has modeled the Ivrea gravitational anomaly with a dip of 80° along profile G3 in Figure 22-8, where the contour spacing yields a dip of 75°. The dip becomes more gentle further to the southwest where 45° are measured according to field data, arrived at by contouring the intersection of the Insubric line with 2km of topography (Schmid et al., 1987). Section G 2 of Kissling (1980) yielded

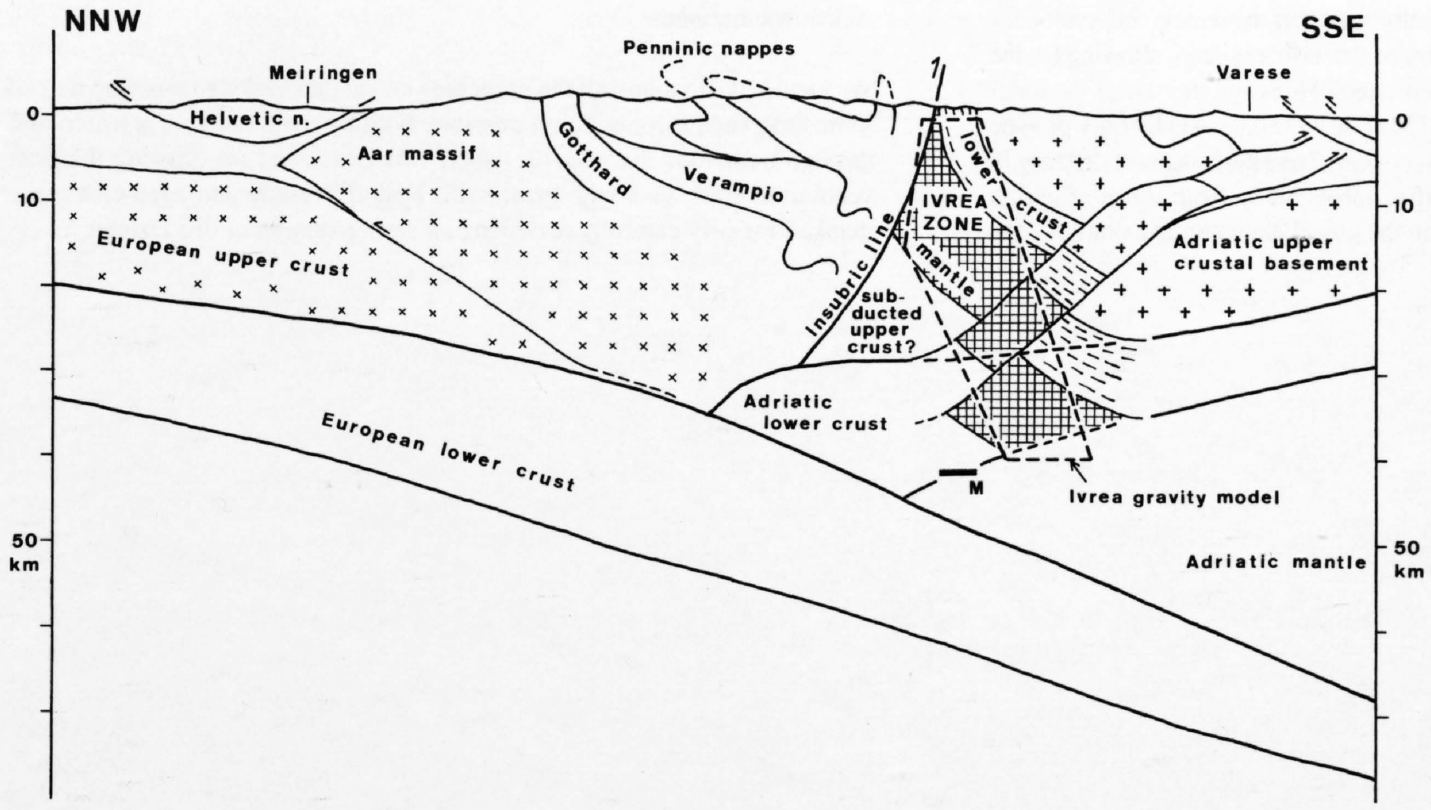

Figure 22-9
Profile west of the transect of plate 22-1 (see Figure 22-8 for location), constructed using the contours given in Figure 22-8. The position of the European Moho is taken from Valasek (1992). The Ivrea gravity model corresponds to the model of Kissling (1980, profile III). The top of the Adriatic lower crust is taken from Valasek (1992). The exact position of reflector "M" is unknown, the given approximate position is taken from Ansorge (1968).

60°, a value of 50° was assumed for constructing the contours in Figure 22-8. This angle does only slightly increase again to the southwest, where profile G1 crosses the Insubric line.

Westward decreasing indentation of the Adriatic lower crustal wedge indicates that the amount of post-Early Miocene N–S shortening within the Southern Alps (46km according to Table 22-1) also decreases towards the west. This points to the existence of a left lateral transpressive transfer zone running along the western margin of the Southern Alps (Laubscher 1991) and possibly to some counterclockwise rotation of the Southern Alps. Another left-lateral transpressive zone (the Giudicarie belt, Laubscher 1991), extending along the Giudicarie line (Figure 22-8), delimits the likely eastern termination of the Adriatic wedge. On geometrical grounds this wedge which underthrusts the Central Alps is replaced by the wedge of the Eastern Southern Alps which encompasses the entire crustal section situated south of the Tauern window (Ratschbacher et al. 1991). Note that the Giudicarie line does not appear to offset the contour lines of the European and Adriatic Moho (Figure 22-8). This is explained by the fact that the Adriatic Moho underlying the lower crustal wedge in the profile of Plate 22-1 is continuous with the Moho underlying the wedge of the eastern Southern Alps. On both sides of the Giudicarie line the Adriatic Moho overrides the uniformly S-dipping European Moho. This demonstrates the kinematic link between post-Early Miocene shortening in the Southern Alps, movements along the Giudicarie line, and north-directed indentation of the Adriatic lower crustal wedge underneath the Penninic zone (Laubscher 1990, Schönborn 1992).

The 3D problems associated with the westward termination of the Adriatic lower crustal wedge are far from solved due to incomplete seismic coverage in this area. The profile of Figure 22-9 represents an attempt to discuss some of these problems (see also Figure 11-7). In particular, a possible relationship between the Ivrea body and Adriatic lower crustal wedge is shown. Knowledge of the pre-orogenic evolution of the Ivrea zone (Schmid 1993) plays a crucial role for an improved understanding of this 3D problem. Exhumation of the Ivrea zone was related to Mesozoic passive continental margin formation near the continent-ocean transition (immediately adjacent to the Sesia extensional allochthon indicated in Figure 22-4). Alpine orogeny steepened the entire crustal section into its present-day subvertical orientation (Figure 22-9; see also Zingg et al. 1990), thereby probably exposing the ancient (Mesozoic) Moho of the Adriatic crust at the surface. This led some authors (e. g. Giese & Buness 1992) to postulate a dramatic change in the present-day topography of the Adriatic Moho near the western termination of the Ivrea zone; the northward dip of the Moho along the profile of Plate 22-1 is postulated to change into a southeasterly dip, away from the Ivrea zone and towards the west.

This direct correlation of the Paleo-Moho exposed in the Ivrea zone with the present-day Moho of the Adriatic wedge is at odds with seismic refraction data obtained along a refraction profile parallel to the Ivrea zone (Ansorge 1969). These seismic data, together with 3D gravity modelling by Kissling (1980, 1982) point to the existence of a velocity and density inversion underneath the Ivrea body and a second Adriatic Moho (labelled "M" in Figure 22-9). This second (present-day) Moho may be continuous with the north-dipping Adriatic Moho east of Figure 22-9 and beneath the transect of Plate 22-1. The cause of the density inversion below the Ivrea zone is controversial. Schmid et al. (1987) have speculated that it may be due to Cretaceous-age subduction of parts of the Sesia zone below the Ivrea body.

The contour lines of Figure 22-8 suggest that the Ivrea zone may have been underthrust by Adriatic lower crust in post-Early Miocene times. The exact geometry of the underthrust material and associated overthrust blocks within the westernmost Southern Alps is unknown and drawn schematically in Figure 22-9. This figure depicts the amount of shortening due to thrusting in this part of the Southern Alps to be substantially less (of the order of 10–20km; see also Pfiffner & Heitzmann, Chapter 11) than that further to the east (see Schumacher et al., Chapter 15, for an alternative interpretation). The geometry of the Adriatic lower crustal wedge is bound to be considerably more complex than shown in Figure 22-9.

Reconciliation of our estimate of some 500km of N-S shortening along the profile of Plate 22-1 since the Paleocene with the smaller amounts of E–W shortening recorded in the Western Alps remains a major problem, providing a challenge for future investigations. As pointed out by Laubscher (1991), large amounts of strike-slip faulting and independent motions of large blocks such as the Adriatic block were inevitable. The large amount of N–S convergence postulated along the eastern Swiss transect (Plate 22-1) indicates that much of the E–W shortening in the Western Alps must be due to an independent westward motion of the Adriatic block during the Neogene and decoupled from the Central Alps by dextral movements along the Insubric line and its precursors. There is evidence for an older and northerly directed motion in the internal zones of the Western Alps (eclogitic episode of Choukroune et al. 1986 which may have been erroneously dated as Cretaceous), suggesting that the Western Alps acted as a sinistrally transpressive belt during the Paleogene (Ricou & Siddans 1986). Only after 40 Ma did the displacement vector change into a westerly direction (Choukroune et al. 1986). Deflection of a unique west-northwest directed plate movement vector of Adria into north- and west-directed components of tectonic transport (in the Western and Central Alps, respectively) due to gravitational forces (Platt et al. 1989) is at odds with the very substantial amount of N–S convergence deduced in this study.

From the profile of Plate 22-1 the following major conclusions emerge:

1. Shortening within the Austroalpine nappes is testimony to a separate Cretaceous-age orogenic event, unrelated to the collision between Europe and Apulia that caused the closure of Penninic oceanic domains. West-directed thrusting in the Austroalpine units was related to westward propagation of a thrust wedge resulting from continental collision along the Hallstatt-Meliata ocean further to the east.

2. Considerable amounts of oceanic and continental crustal material were subducted during Tertiary orogeny, which involved some 500km of N–S convergence between Europe and Apulia. Only a very small percentage of this crustal material is preserved within the nappes depicted in the transect of Plate 22-1.

3. Post-collisional orogeny is characterized by simultaneous activity on gently dipping north-directed detachments (pro-shears) and steeply inclined south-directed detachments (retro-shears), both detachments nucleating at the interface between the lower and upper crust. This indicates a two-layer rheology of the continental crust during post-collisional orogeny.

4. Seisimic reflection and refraction information is extremely important for constraining the present-day geometry of the Alpine orogen, allowing for the reconstruction of the latest stages of orogeny. However, in view of the long-lasting history of orogeny (some 100 Ma), seismic data usually only provide a snapshot of the latest stages of this orogeny. The latest stages of orogeny in the Alps exhibit geometries that differ substantially from those of earlier stages, even given the uncertainties in the kinematic reconstructions.

Acknowledgements

We would like to thank all the numerous colleagues and students who helped in making such a compilation possible, both by their valuable research and through numerous discussions. Albert Uhr is thanked for drawing the final version of Plate 22-1 with great skill. Rudolf Trümpy and Alan Green are thanked for very carefully reviewing an earlier version of this chapter.

Plate 22-1

ALPINE CROSS SECTION ALONG THE NFP-20-EAST TRAVERSE

COMPILED BY S.M.SCHMID

Molasse basin and Helvetic zone by O.A.Pfiffner, Southern Alps by G.Schoenborn, Geophysics by ETH working group on Deep Seismic Profiling

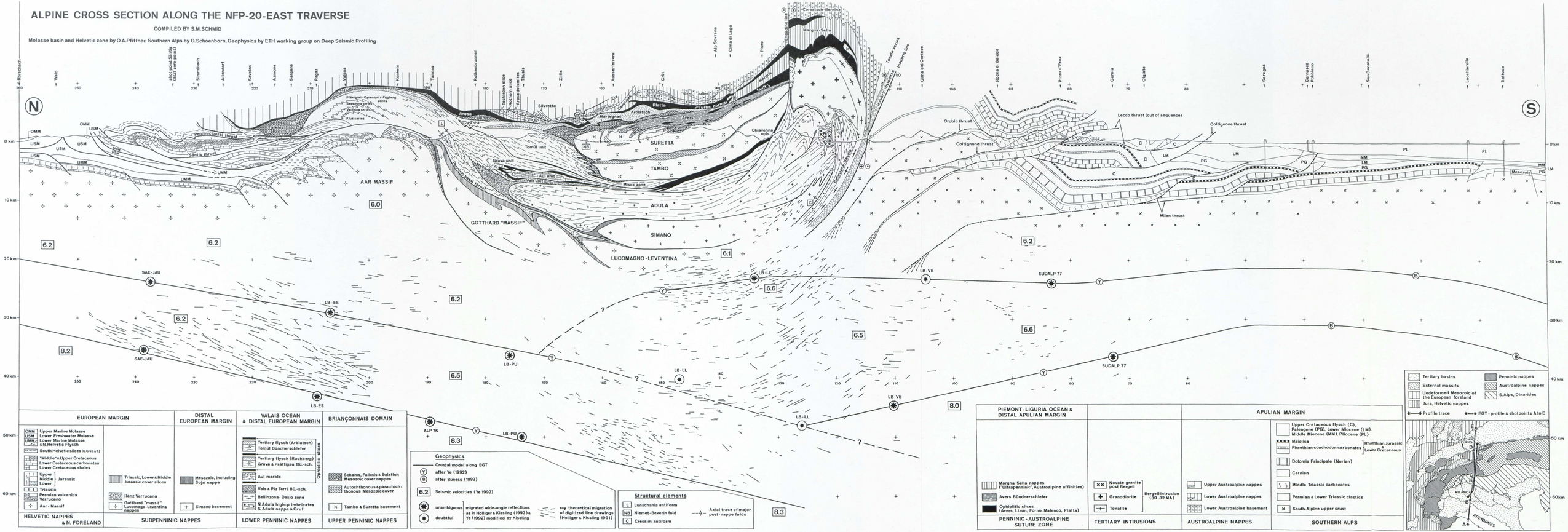

EUROPEAN MARGIN		DISTAL EUROPEAN MARGIN	VALAIS OCEAN & DISTAL EUROPEAN MARGIN	BRIANÇONNAIS DOMAIN
OMM Upper Marine Molasse USM Lower Freshwater Molasse UMM Lower Marine Molasse & N.Helvetic Flysch South Helvetic slices (L,Gnt,s,t.) "Middle" & Upper Cretaceous Lower Cretaceous carbonates Lower Cretaceous shales Upper / Middle / Lower Jurassic Triassic Permian volcanics Verrucano Aar - Massif	Triassic, Lower & Middle Jurassic cover slices Ilanz Verrucano Gotthard "massif" Lucomago-Leventina nappes	Mesozoic, including Soja nappe Simano basement	Tertiary flysch (Arblatsch) Tomül Bündnerschiefer Tertiary flysch (Ruchberg) Grava & Prättigau Bü.-sch. Aul marble Vals & Piz Terri Bü.-sch. Bellinzona - Dasio zone N.Adula high-p imbricates S.Adula nappe & Gruf Ophiolitic slices	Schams, Falknis & Sulzfluh Mesozoic cover nappes Autochthonous & parautochthonous Mesozoic cover Tambo & Suretta basement
HELVETIC NAPPES & N. FORELAND	SUBPENNINIC NAPPES		LOWER PENNINIC NAPPES	UPPER PENNINIC NAPPES

Geophysics

- Crustal model along EGT
- (Y) after Ye (1992)
- (B) after Buness (1992)
- 6.2 Seismic velocities (Ye 1992)
- unambiguous / doubtful — migrated wide-angle reflections as in Holliger & Kissling (1992) & Ye (1992) modified by Kissling
- ray theoretical migration of digitized line drawings (Holliger & Kissling 1991)

Structural elements

- L Lunschania antiform
- NB Niemet-Beverin fold
- C Cressim antiform
- Axial trace of major post-nappe folds

PIEMONT-LIGURIA OCEAN & DISTAL APULIAN MARGIN		APULIAN MARGIN	
Margna Sella nappes ("Ultrapenninic", Austroalpine affinities) Avers Bündnerschiefer Ophiolitic slices (Avers, Lizun, Forno, Malenco, Platta)	Novate granite post Bergell Granodiorite Tonalite Bergell intrusion (30-32 MA)	Upper Austroalpine nappes Lower Austroalpine nappes Lower Austroalpine basement	Upper Cretaceous flysch (C), Paleogene (PG), Lower Miocene (LM), Middle Miocene (MM), Pliocene (PL) Maiolica Rhaethian conchodon carbonates Rhaethian, Jurassic, Lower Cretaceous Dolomia Principale (Norian) Carnian Middle Triassic carbonates Permian & Lower Triassic clastics South-Alpine upper crust
PENNINIC - AUSTROALPINE SUTURE ZONE	TERTIARY INTRUSIONS	AUSTROALPINE NAPPES	SOUTHERN ALPS

- Tertiary basins
- External massifs
- Undeformed Mesozoic of the European foreland
- Jura, Helvetic nappes
- Penninic nappes
- Austroalpine nappes
- S.Alps, Dinarides
- Profile trace
- EGT - profile & shotpoints A to E

23 A 3D tectonic model of the Central Alps based on an integrated interpretation of seismic refraction and NRP 20 reflection data

P. Valasek & St. Mueller

Contents

23.1 Introduction

The Alps represent a relatively young continental collision zone (Fig. 23-1a) involving the convergence of the Adriatic promontory of the African plate and the European plate. Recently, several international communities have focused their investigations of this orogenic belt on the acquisition of deep crustal seismic reflection profiles. The Swiss National Research Program NRP 20 stands out as a leader in these efforts with the initiation of a campaign in the mid 1980's to acquire both refraction and reflection profiles across the Alps as part of the Swiss contribution to the "European Geo-Traverse" project (cf. Frei et al., 1989; Blundell et al., 1992). The initial success of this program propelled continued seismic data acquisition which ultimately led to a series of deep crustal traverses distributed across the Alps (Fig. 23-1b). These data represent a valuable link between the existing refraction data sets (cf. Egloff, 1979) and provide detailed images of key crustal features which are vital to understanding the geodynamic processes governing this prominent collisional zone.

The new reflection profiles together with contemporary and earlier wide-angle (WA) reflection/refraction profiles form a largely-spaced grid of two-dimensional (2D) seismic coverage across the Alps (Figures 23-1a and 23-1b). This collisional zone is unquestionably a three-dimensional (3D) orogenic belt both on the large scale, for example the arc of the Western Alps, and on smaller scales such as the cylindrical geometry of the exposed thrust sheets. Because of this complex tectonic environment, a considerable amount of the recorded wavefield is reflected off of structures located out-side the vertical planes of the 2D surveys. Subsequent processing of this "side swipe" data using 2D approaches produces distorted and incomplete images which generally underestimate the true subsurface locations beneath the profiles. Moreover, analysis and interpretations made without considering the 3D variations further compound these errors. In particular, integrated methods which involve combining local seismic images to obtain unified acoustic images are strongly affected by the 3D nature of the subsurface structures sampled by the profiles. This problem is frequently encountered during the construction of regional Alpine seismic transects where significant lateral projections of the individual profiles are required (cf. Frei et al., 1989; Holliger 1991; Holliger & Kissling, 1991; Valasek, 1992). In these cases variations in the 3D layer geometries throughout the crust produce distorted representations regardless of the chosen projection bearing.

The only way to properly carry out an integrated interpretation of the Alpine data is to use an approach which addresses the influence of 3D layer geometries. In this study an initial 3D crustal model of the Central Alps was constructed by uniting the 2D subsurface findings obtained from the network of reflection and refraction data with surface geology. One method of carrying this out involves map migration of the unmigrated reflection data using velocities derived from the refraction data (ex. Reilly, 1991). Another approach used in this study is to use both the depth-migrated reflection data and the refraction-based models to directly form a 3D model. While this approach has the advantage of using both the velocity and structural information derived from the refraction data, it has the potential for introducing distortions based on the 2D depth migrations and refraction modeling. A subsequent analysis of potential geometric errors introduced by constructing a 3D model directly from 2D depth profiles was carried out using ray tracing. By simulating the 2D grid of seismic profiles using normal-incidence ray tracing, the degree to which the 3D effects influence the 2D measurements could be quantified. This analysis revealed that while distortions are introduced, they are insignificant when considering the large-scale crustal features of the Alpine orogen. The resulting 3D model of the Central Alps that has recently been complemented to also include the transition to the Eastern Alps (Pfiffner & Hitz, Chapter 9 and Hitz, 1995) yields an initial representation of the main tectonic elements associated with this collisional zone.

23.2 Development of a 3D Alpine Model

Model Resolution

The network of 2D seismic reflection data crossing the Swiss Alps has a limited 3D subsurface resolving capability because of the large average spacing (>25 km) between adjacent profiles (Figure 23-1b). To minimize the spatial aliasing which is developed under these conditions, a generalization of the locally detailed 2D profiles was required. Despite the complexity of the Alpine tectonic units which is exhibited in outcrop, an initial interpretation of the seismic data revealed that a consistent large-scale reflection pattern could be recognized on most of the seismic images which cross the central Alpine axis. This regionally correlatable reflectivity was interpreted as outlining an orogenic belt formed by the convergence of two three-layered crustal plates (see also discussion by Pfiffner & Hitz, Chapter 9 and Schmid et al., Chapter 22). In this view, the collisional zone involving the European and Adriatic plates (Figure 23-2a) is represented by an uppermost crustal boundary (B) outlining several tectonic units, such as the imbricated Alpine nappe sequences, the interface separating the upper and lower crust (C1, C2) and the crust/mantle boundary (M1, M2).

Uppermost Crustal Boundary (B)

This comprehensive boundary spans both the European and Adriatic crustal plates and outlines the dominant deformational features of the shallow crust across the Alps. Within the fold belt it serves to distinguish the highly allochthonous upper crustal flakes (ex. Helvetic, Penninic and Austroalpine nappes) from the primarily autochthonous and the slightly allochthonous margins (e. g. Aar & Gotthard massifs and the Orobic basement) of the European and Adriatic plates. For a typical N–S section across the Alps (Figure 23-2a), this boundary defines the base of the Molasse over which the Helvetic nappes have been displaced, the top of the external massifs, the base of the Penninic and Austroalpine nappes, the Insubric Line and the transition from basement to sediments within the Southern Alps. In areas where these units are juxtaposed against each other, they are treated together as a combined layer. This occurs primarily at the foreland margin where the Helvetic nappes are thrust on top of the Molasse and in the western Swiss Alps where various configurations involving the Helvetic, Penninic and Austroalpine nappes are present (e. g. Escher, 1993). The allochthonous Gotthard "massif" which is considered to have originated from an intermediate position between the European and Penninic basements is classified here together with the external massifs (Pfiffner et al., 1990a and Chapter 13.1). Furthermore, the "Ivrea body" is not uniquely distinguished because of insufficient subsurface sampling. Only one of the seismic reflection profiles actually crosses this exposed high-density body just at its northeasternmost edge. Its northern boundary is, however, approximated by the Insubric Line which was shown by gravity modeling to truncate this proposed southeast-dipping slab of mantle material (Kissling, 1984).

The reflectivity interpreted to define the uppermost crustal interface (B) varies considerably as one would expect with such a broad definition. In the relatively undisturbed northern margin of the Alps, a thin layer of autochthonous sediments (primarily Mesozoic carbonates) separates the basement from the Molasse which is recognized on the seismic profiles by a rather sharp sequence of reflections (cf. Stäuble & Pfiffner, 1990). A similar reflection signature is recognized from data which image the South-Alpine basement/cover contact. Within the Alpine fold belt, the intensely sheared crystalline nappes are either in direct contact with the underlying basement, which may be strongly deformed, or in contact with thin zones of deformed cover sediments associated with either or both units. All of these possible situations generally led to a more multicyclic reflection pattern compared with

a)

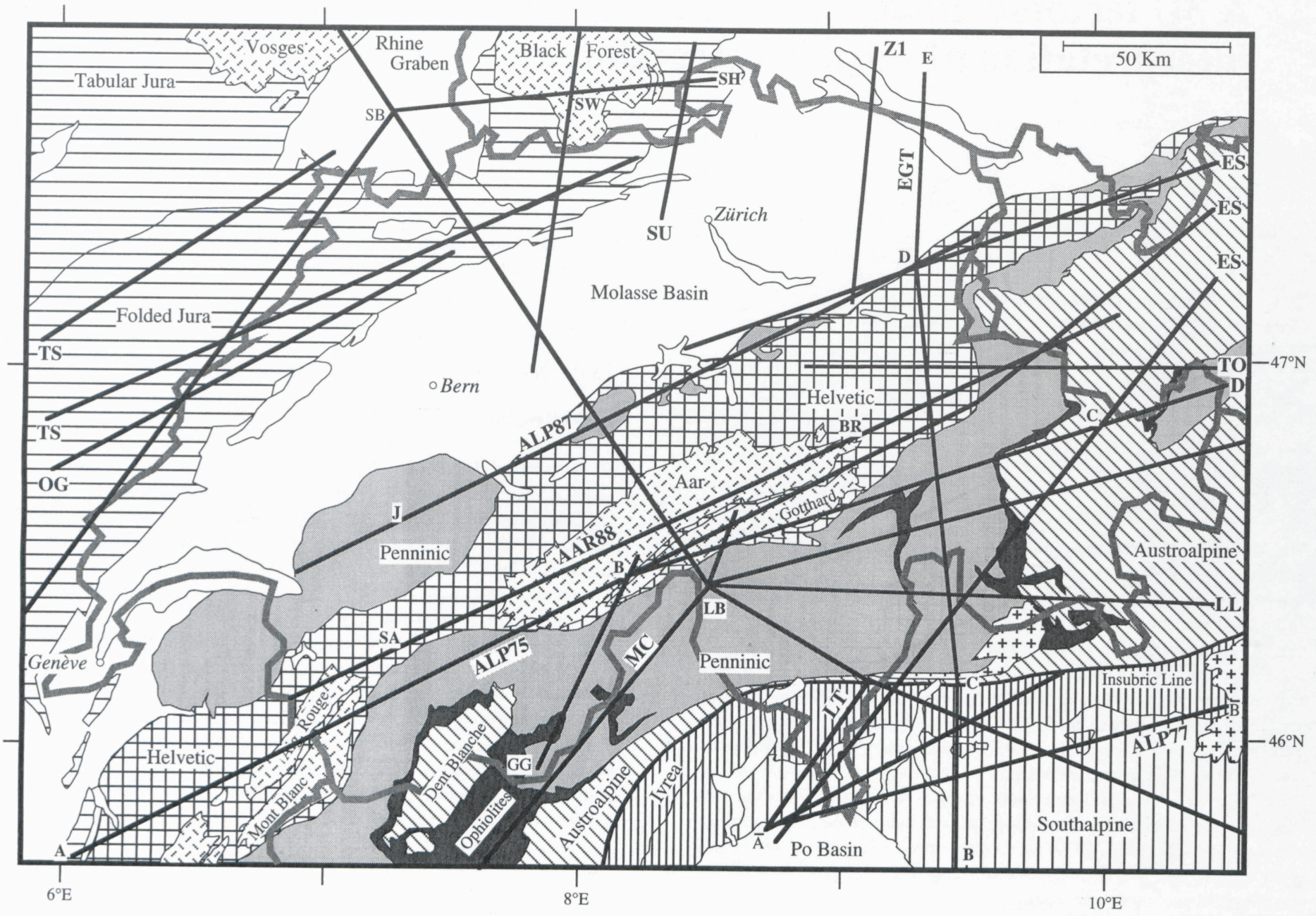

Figure 23-1a
Tectonic sketch map of Switzerland with the location of the network of seismic refraction profiles: ***ALP87*** *= Alpennordrand Profile;* ***AAR 88*** *= Aar Massif Profile;* ***ALP75*** *= Alpine Longitudinal Profile;* ***ALP77*** *= Southern Alps Profile;* ***EGT*** *= European Geotraverse.*
Supplementary and older shotpoints and profiles: A, B, C, D on ***ALP75****; Ā, B̄ on* ***ALP77****;* ***ES:*** *Eschenlohe; GG: Gornergrat; LB: Lago Bianco; LL: Lago Lagorai; LT: Lentate/Varese;* ***MC:*** *Mt. Cenis;* ***OG:*** *Orgelet; SB: Steinbrunn; TO: Osttirol; TS: Tournus; J: Jaunpass; SA: Saviese; BR: Brigels;* ***SW:*** *Black Forest;* ***SU:*** *Sulz;* ***SH:*** *Schaffhausen;* ***Z1:*** *Hohenzollerngraben.*

the sharp reflection character observed in the foreland or hinterland. This reflection pattern can be explained by the interference of wavefields reflected off of the thin alternating layers with differing compositions and/or deformational (i. e. mylonitic fabrics) characteristics (Pfiffner et al., 1991; Valasek et al., 1991).

"Conrad" Interface (C1/C2)

This boundary defines the top of the European (C1) and Adriatic (C2) lower crustal layers. Typically, the lower crust is identified by a significant increase in the P-wave velocity which is interpreted to indicate a transition from basic or intermediate compositions to more mafic constituents and has historically been termed the "Conrad" discontinuity. In the Alps, the velocity increase is significantly less dramatic which has implications for the petrologic make-up and rheologic behavior of the lower crust. The seismic signature of the lower crust varies considerably on the Alpine profiles from sharp reflection bands to the base or top of broader, more diffuse reflection zones and, in some cases, particularly beneath the central axis, its trace is significantly reduced (see also discussion by Pfiffner & Hitz, Chapter 9 and Pfiffner & Heitzmann, Chapter 11). The upper and middle crust exhibit different degrees of reflectivity across and along the tectonic strike of the Alps. Generally, a faint reflection zone beneath the Alpine foreland at 5 to 6 s may be evidence for the upper to middle crustal transition or, alternatively, it may represent a low-velocity zone identified on refraction profiles (Mueller, 1977; Mueller et al., 1980; Ye, 1992; Ye et al., 1995). Further south across the central Alpine axis, more chaotic reflections associated with the intensive deformation of the external massifs can usually be recognized above the lower crust. The generally layered reflection nature of the lower crust itself also implies internal structuring possibly related to the intermixing of mafic with less mafic material or zones of concentrated ductile deformation.

"Mohorovičić" Interface (M1/M2)

This boundary (abbreviated "Moho") marks the crust/mantle transition for the European (M1) and Adriatic (M2) lithospheric plates. The European "Moho" is usually defined by the base of a pronounced 1 to 2 s thick zone of reflectivity beneath the Alpine foreland at 9 to 13 s two-way time (TWT) and by weaker discontinuous events further south beneath the central axis which extend down beyond 20 s. The subsurface evidence for the Adriatic "Moho" is largely derived from the regional refraction data since only a few reflection profiles provide convincing evidence. An increase in P-wave velocity from values of 6.5 km/s to 7.9–8.1 km/s is typically indicated from these refraction/wide-angle reflection profiles to mark these crust/mantle boundaries (cf. Mueller et al., 1980).

Detailed Crustal Pattern

During the past decades details of the crustal structure beneath the Molasse Basin in the northern Alpine foreland together with the Eastern and Southern Traverses across the Swiss Alps have been surveyed more thoroughly by various geophysical methods. An interpretation of the seismic refraction and wide-angle reflection results combined with near-vertical seismic reflection data along the same profiles has made it possible to image consistent crustal features along a lithospheric cross section through the Central Alps. Based on both reliable travel-time and amplitude information this joint inversion procedure led to an unambiguous identification of low-velocity zones and velocity-depth gradients. The depth ranges of decreased velocity are apparently associated with increase electrical conductivity and appear as zones of lowered mechanical strength (cf. Figure 23-2b) which favour detachment at various levels in the upper and lower crust (Mueller, 1990). In particular, during the continuing collisional process which has formed the Alps and their north-

b)

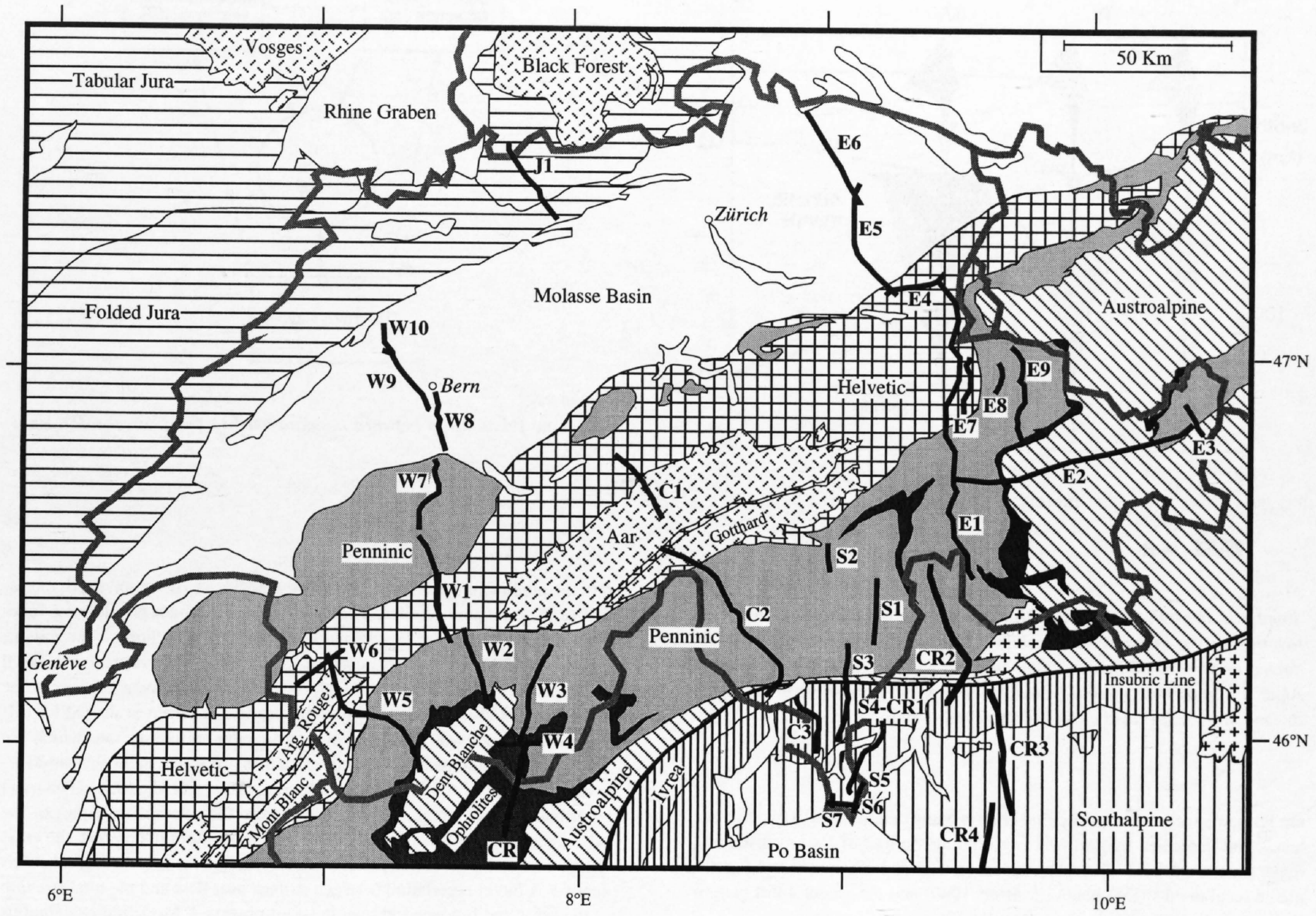

Figure 23-1b

*Tectonic sketch map of Switzerland with the location of seismic reflection lines: Eastern Traverse: **(E6; E5; E4)**; **E1** (86NFET). Southern Traverse: **S1** (88NFS1); **S3** (88NFS3); **S4** (88NFS4); **CR1, CR2, CR3, CR4** (88CROP01, 88CROP02, 88CROP03, 88CROP04); **S5** (88NFS5); **S6** (88NFS6). Central Traverse: **C1** (90NFC1); **C2** (90FNC2); **C3** (90NFC3). Western Traverse: **W10; W9; W8; W7, W1** (87NFW1); **W2** (87NFW2); **W3** (87NFW3); **W4** (87NFW4); **CR** (87CROP03).*

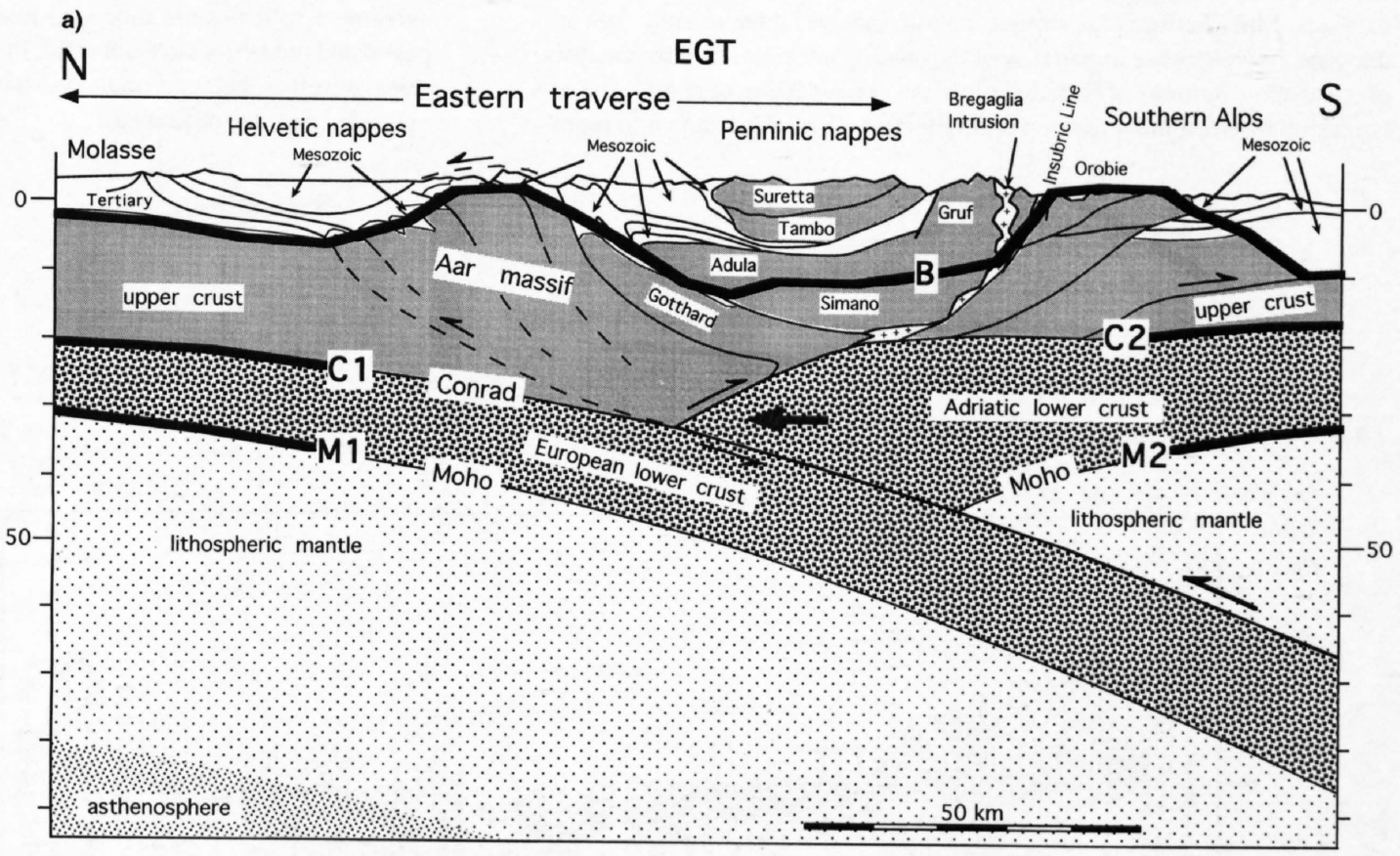

Figure 23-2a
*Generalized description of the three-layered crustal structure interpreted in this study from the network of NRP20 Alpine seismic reflection lines. Refer to the text for a discussion of each of the following modeled crustal boundaries: uppermost crustal boundary (**B**), European Conrad (**C1**), European Moho (**M1**), Adriatic Conrad (**C2**) and Adriatic Moho (**M2**). Cross section is adapted from Pfiffner (Figure 9-8b).*

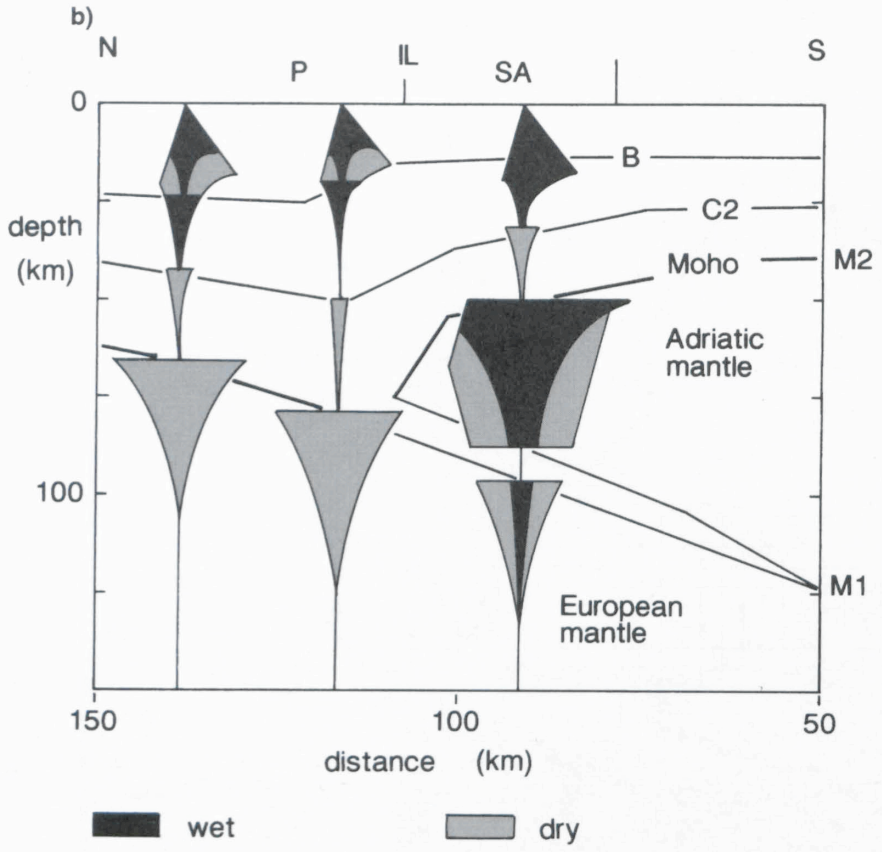

Figure 23-2b
Simplified strength profiles for the Central Alps, assuming a petrological layering of the lithosphere. The European lower crustal material is subducted to depth (P = Penninic domain; Il = Insubric Line; SA = Southern Alps; B = uppermost crustal boundary). Black and grey refers to a wet and dry rheology, respectively (after Okaya et al., 1996).

ern foreland, the southward dipping crust is being delaminated at two to three levels and deformed by northward protruding wedges of lower crustal and upper mantle material. This mechanism can explain both the observed earthquake focal depths (Deichmann & Baer, 1990) and the recent uplift pattern (Geiger et al., 1993; Kahle et al., Chapter 19).

Model Constraints

The construction of a 3D model of the Alps was based on data compiled from refraction-derived velocity models, the depth-migrated reflection data and on a regional map of the top of the basement compiled primarily from extensive surface mapping (Pfiffner et al. 1990a and Chapters 9 and 13.1). Figure 23-3 shows schematically the basic relationships between these three constraining data sets. Links between the surface measurements and the seismic data are drawn to emphasize the importance of the outcrop information in the analysis of the shallow portions of both the refraction and reflection data sets. The relationship between the refraction and reflection data sets is shown to represent the application of refraction-derived velocities to drive the depth migration of the reflection profiles. The calculation of strength profiles as a function of depth along the European Geotraverse (EGT) through the eastern Swiss Alps yields additional constraints on the large-scale vertical and lateral mechanical structure through the Alpine continent-continent collision zone (cf. Figure 23-2b). A variety of strength profiles has been evaluated for different assumptions on petrological stratification and strain rate which are based on temperature-depth functions derived from transient thermo-kinematic modeling of the Neo-Alpine orogeny (Okaya et al., 1996). The main contribution to the total strength results from the upper-mantle part of the lithosphere that is primarily controlled by temperature. In contrast, the crustal contribution is essentially determined by variations in petrological stratification. A direct correlation between surface heat flow and the total strength of the crust and lithospheric mantle is not observed. Modeling calculations have demonstrated that in tectonically active areas a transient thermal model utilizing a detailed knowledge of the deep structure and petrology is necessary to evaluate lithospheric strength envelopes. In the collision zone proper strain rate exerts a significant control on the lower part of the mechanically strong crust, whereas outside the collision zone this effect is less pronounced. The cut-off depth of seismicity along the cross section (cf. Deichmann & Baer, 1990), which correlates largely with the deeper-reaching portion of the mechanically strong crust, deviates from the 300–400°C isotherm. The inferred effective elastic thickness for the Molasse Basin north of the Alps is in agreement with flexural modeling results, while for the Southern Alps the postulated predictions are not valid. In the following sections, these relationships as well as their contribution to the development of the 3D Alpine model presented here are described.

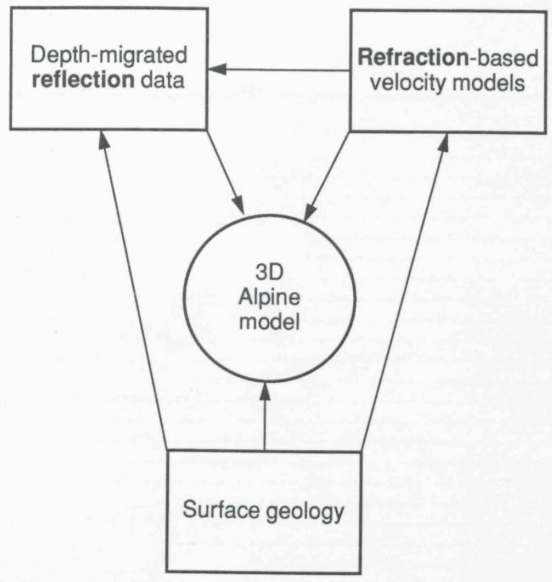

Figure 23-3
Schematic relationship between the data used to constrain the 3D Alpine model.

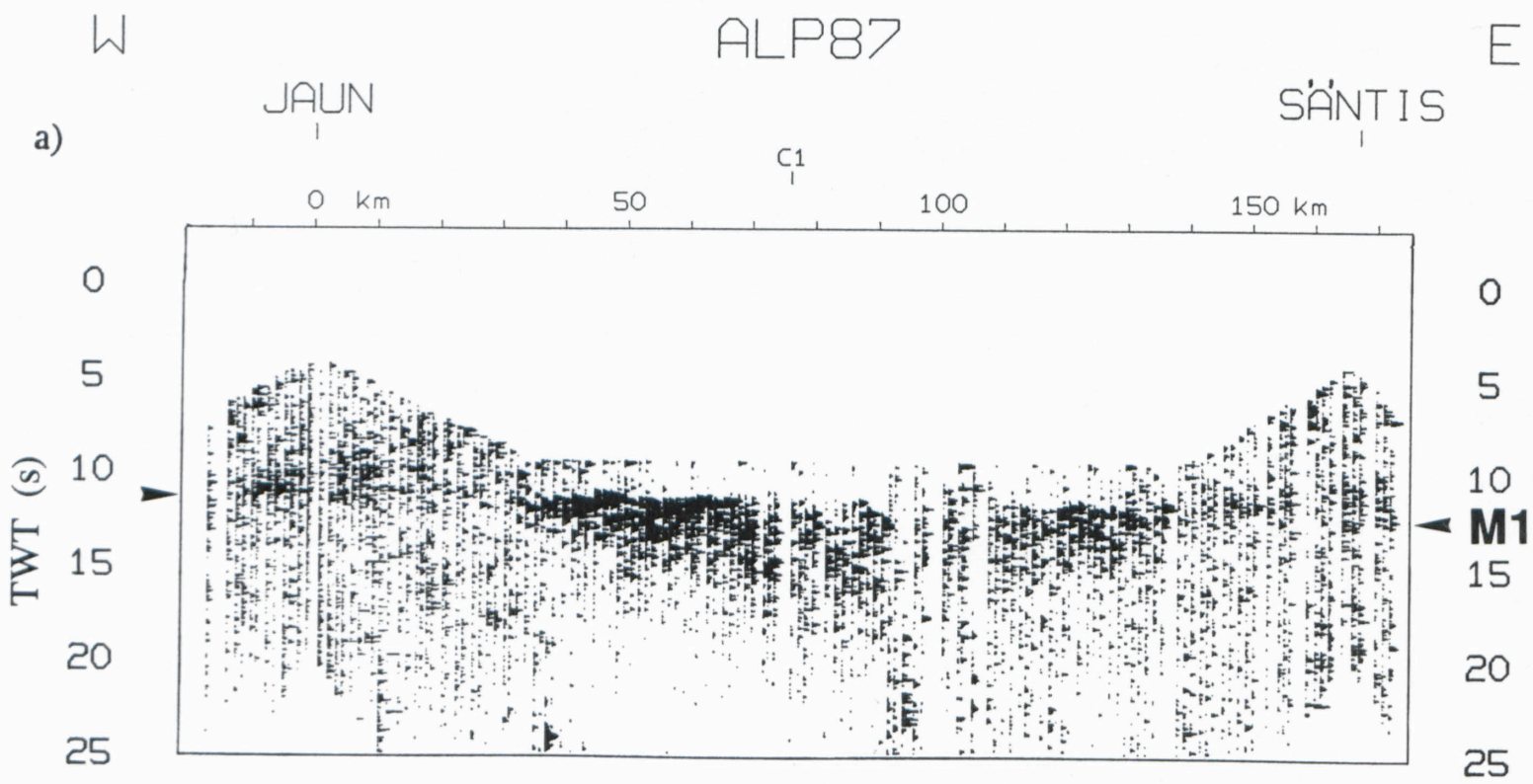

Figure 23-4
Normal-incidence representations of the Alpine refraction/wide-angle reflection profiles. These sections can be compared with the corresponding 2D velocity structures shown in Figures 23-5a to d.
*a) West-East reversed profile ALP87 comprised of data recorded from shot points JAUN (**J**) in the west and SÄNTIS (**S=D**) near the eastern end of the line.*

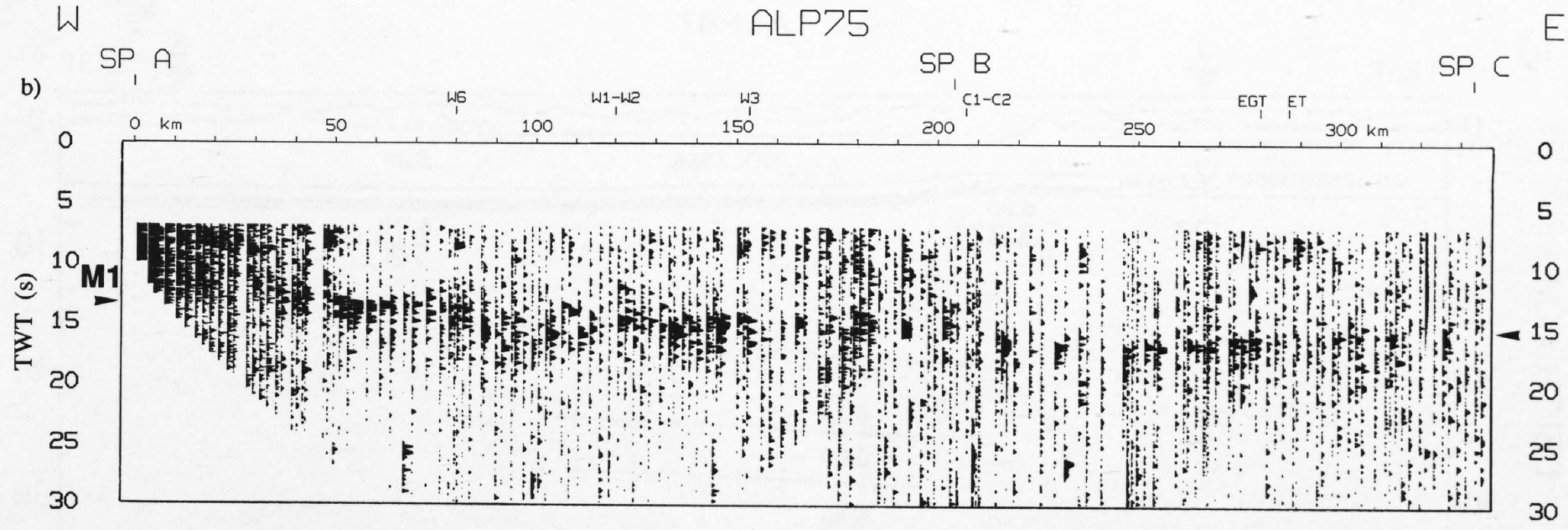

*b) West-East reversed profile ALP75 obtained from three shot points (**A**,**B**,**C**) along the entire central axis of the Swiss Alps.*

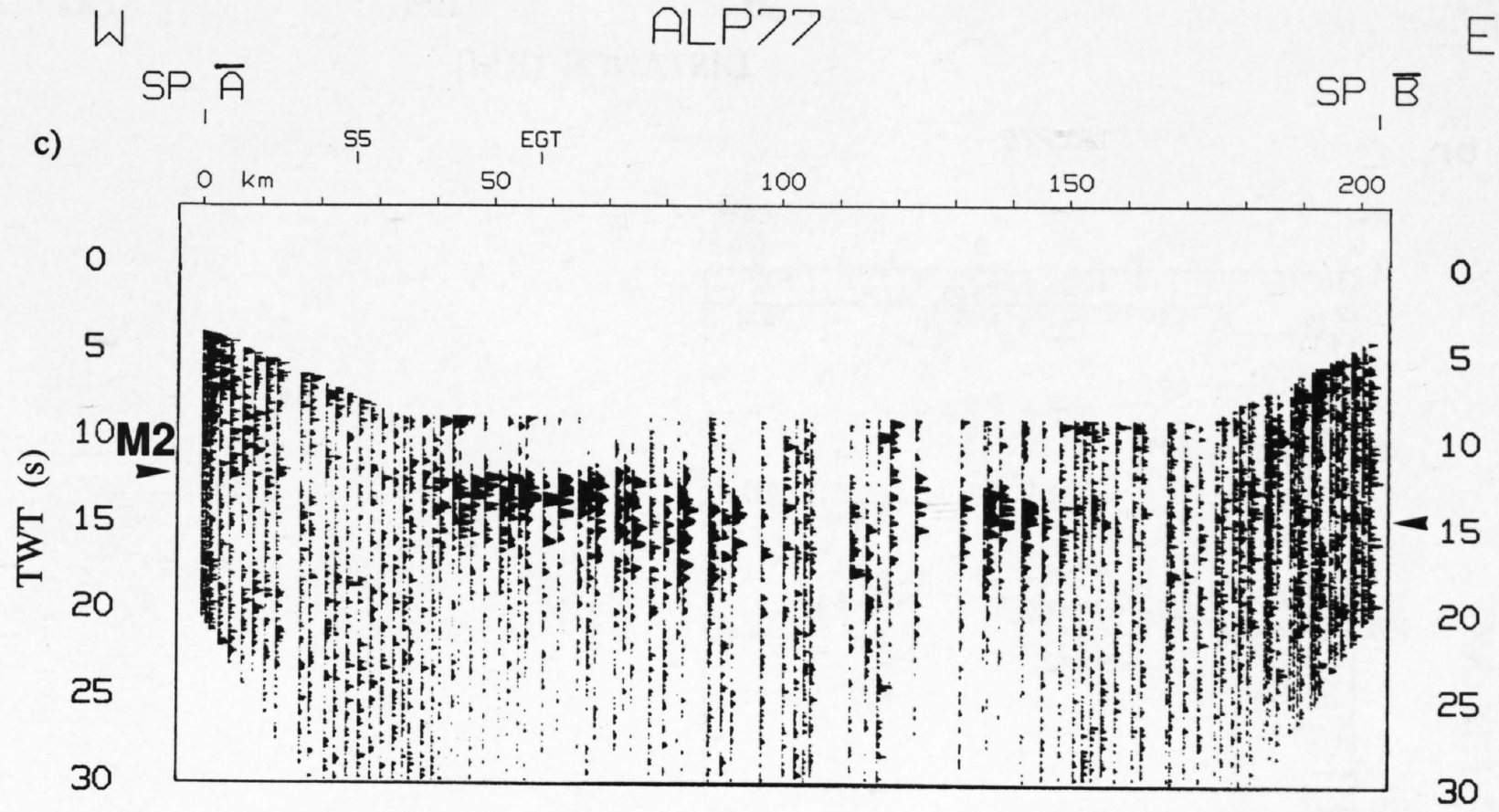

*c) West-East reversed profile ALP77 recorded across the Southern Alps from shot point (**Ā**) in the west and (**B̄**) in the east.*

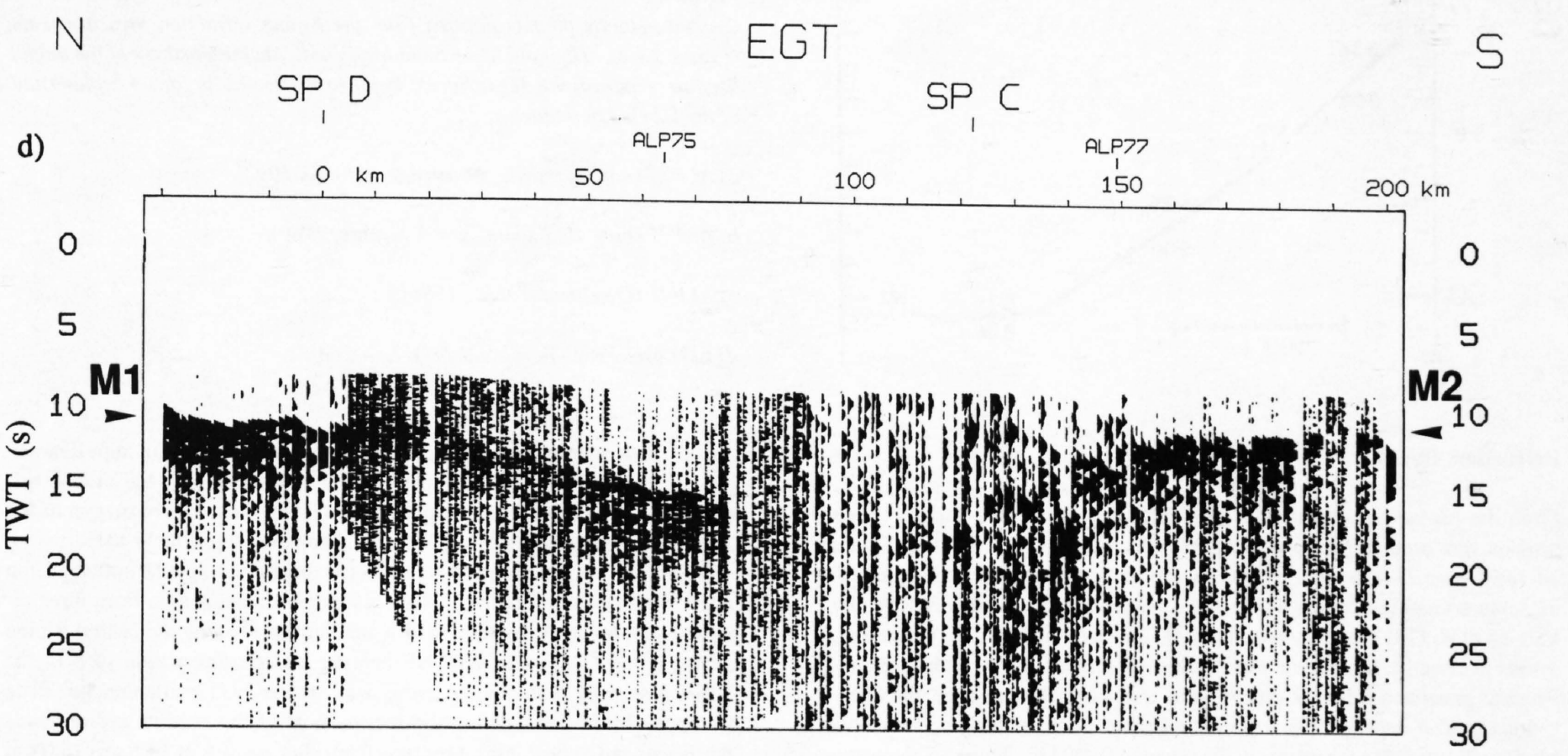

*d) Reversed profile EGT recorded across the eastern Swiss Alps from shot points (**D** & **C**) with shot points **E** and **B** extending the profile to the north and south, respectively. Refer to Figure 23-2a for an explanation of the labeled boundaries.*

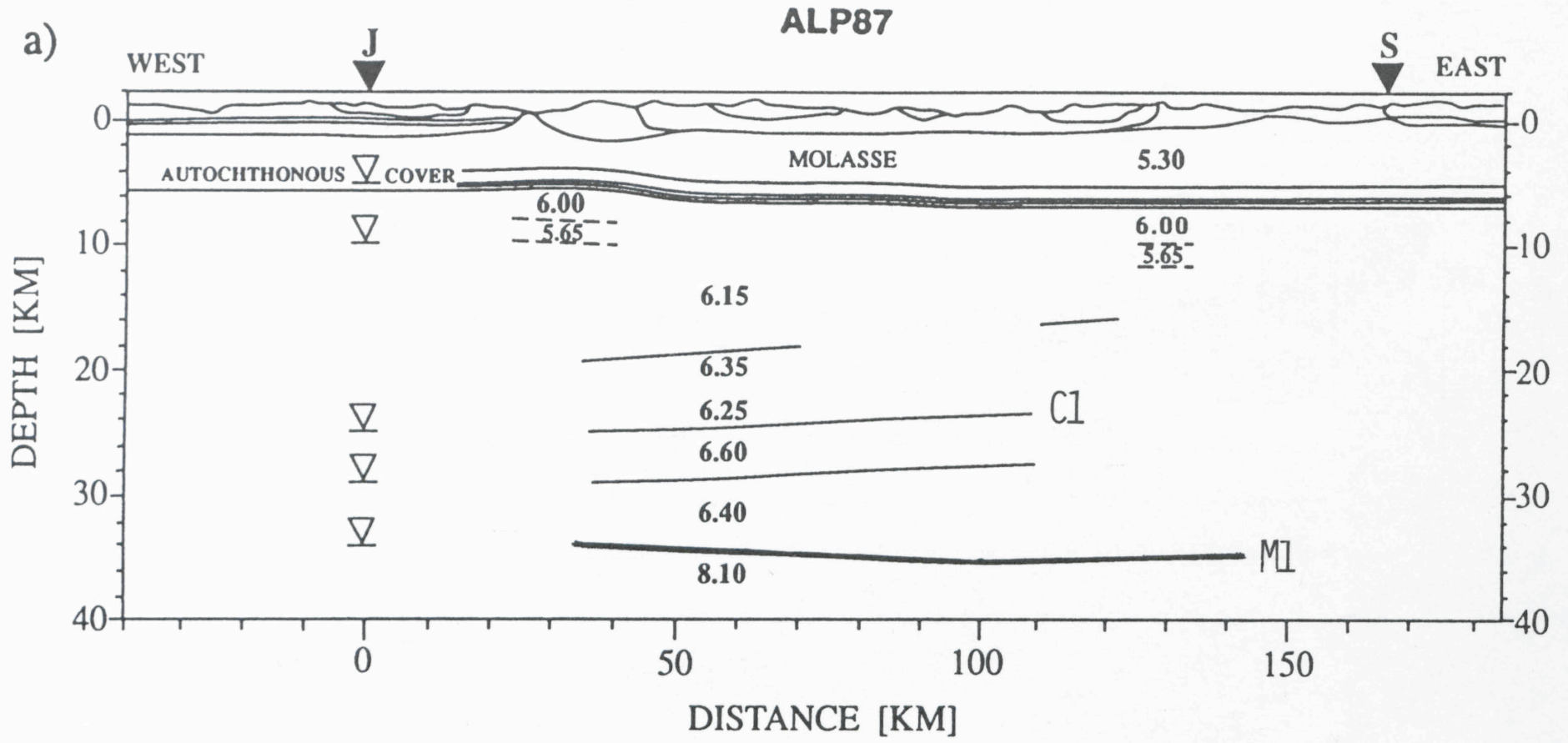

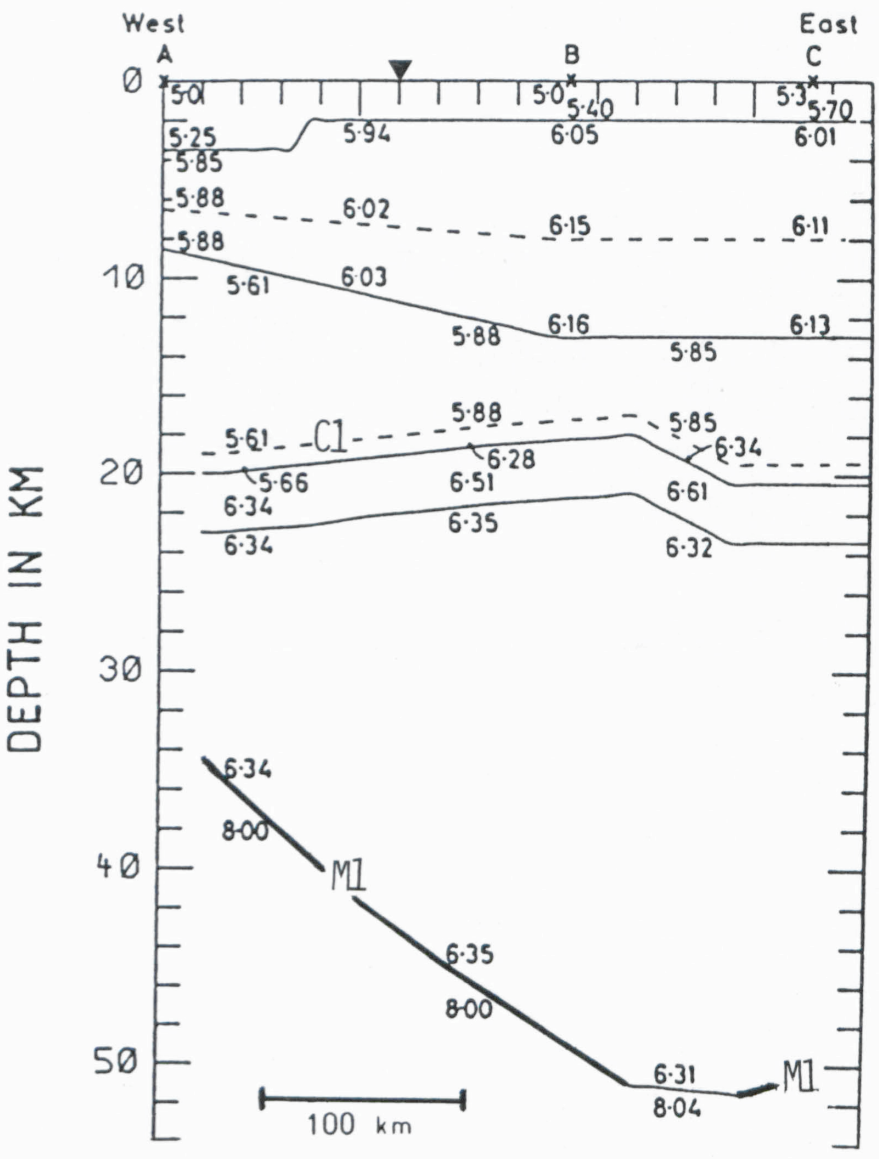

Figure 23-5
Crustal velocity models derived from the Alpine refraction measurements (Figure 23-4). The bold layer boundaries indicate the portions of the model used to constrain the 3D surfaces. Refer to Figure 23-2a for an explanation of the labeled boundaries.

a) ALP87 (note 2:1 scale; Maurer & Ansorge, 1992);

b) ALP75 (note 10:1 scale, Yan & Mechie, 1989);

c) ALP77 (Deichmann et al., 1986);

d) EGT (Ye, 1992; Ye et al., 1995).

Refraction Data

From the Alpine refraction/wide-angle reflection data base, a total of four profiles was used in this study (ALP 87, ALP 75, ALP 77 & EGT, Figure 23-1a). Figure 23-4 shows the conversion of these refraction/wide-angle profiles into normal-incidence (NI) sections following a procedure described by Valasek et al. (1991) and in Valasek (1992 and section 3.4). This processing results in effective representations of the PmP phase (i.e. the wide-angle reflection) generated from the crust/mantle transition. Furthermore, the application of offset-dependent bandpass filtering reveals previously undetectable Moho reflections at near offsets in the range of 0–20 km. These sections visually confirm and represent the general outline of the detailed velocity models determined from rigorous 2D modeling approaches (see Figure 23-5).
Figure 23-4a shows the section obtained from the refraction line ALP 87 (Maurer & Ansorge, 1992) which was recorded in the Helvetic domain along the northern margin of the Alps (Figure 23-1a). This profile contains data obtained from two shots roughly positioned at opposite ends of the SW-NE oriented line. In general, the European Moho along the northern margin of the Alps is rather structureless with a gradual apparent dip from W to E.
The normal-incidence section for the refraction/wide-angle reflection profile ALP 75 is shown in Figure 23-4b. This profile contains data from three reversed shot points A, B and C which are distributed along the central Alpine axis (Figure 23-1a). The SW–NE bearing line crosses a total of 5 of the NRP 20 seismic reflections lines as well as the EGT refraction line. The European Moho (M1) is imaged across most of the section with a gentle northeastward apparent dip observed from shot point A at 13.5 s to 15.0 s at shot point B. East of shot point B the dip increases to the observed maximum traveltime of 16 s at a distance of 235 km, then begins to gradually rise to 15 s at shot point C.
Figure 23-4c shows the normal-incidence section for ALP77 recorded across

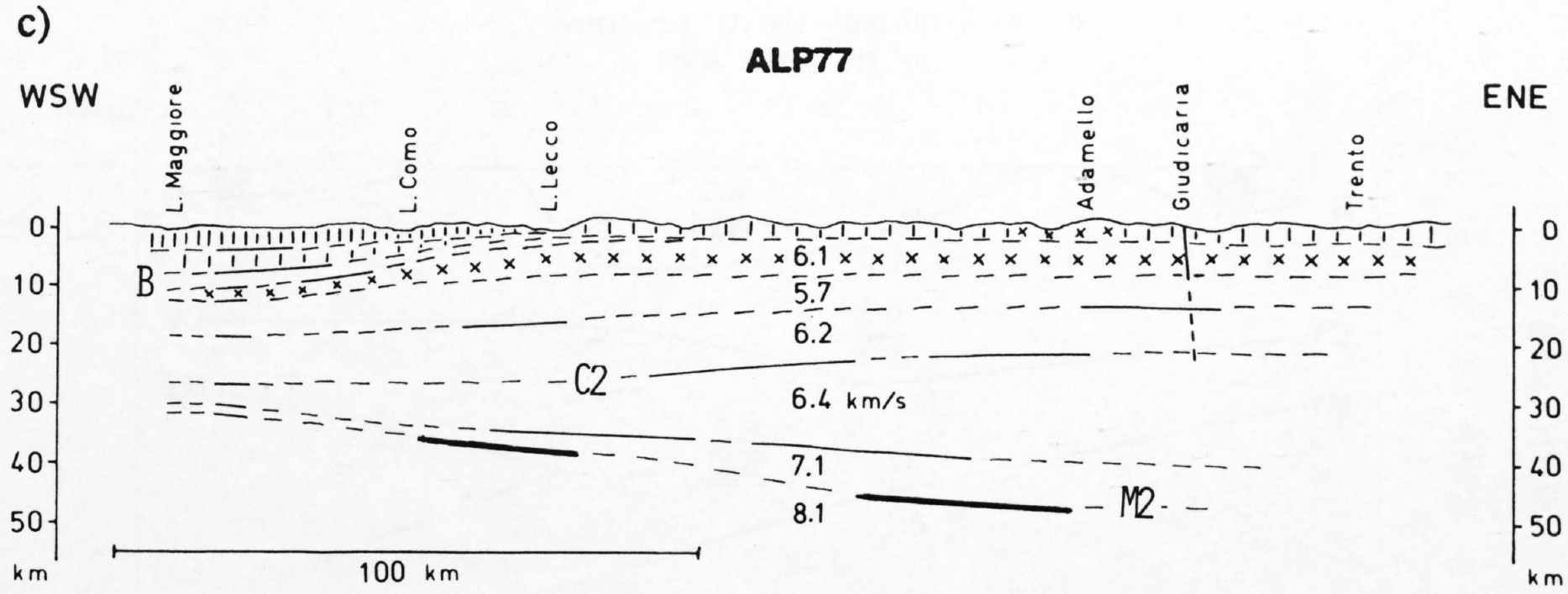

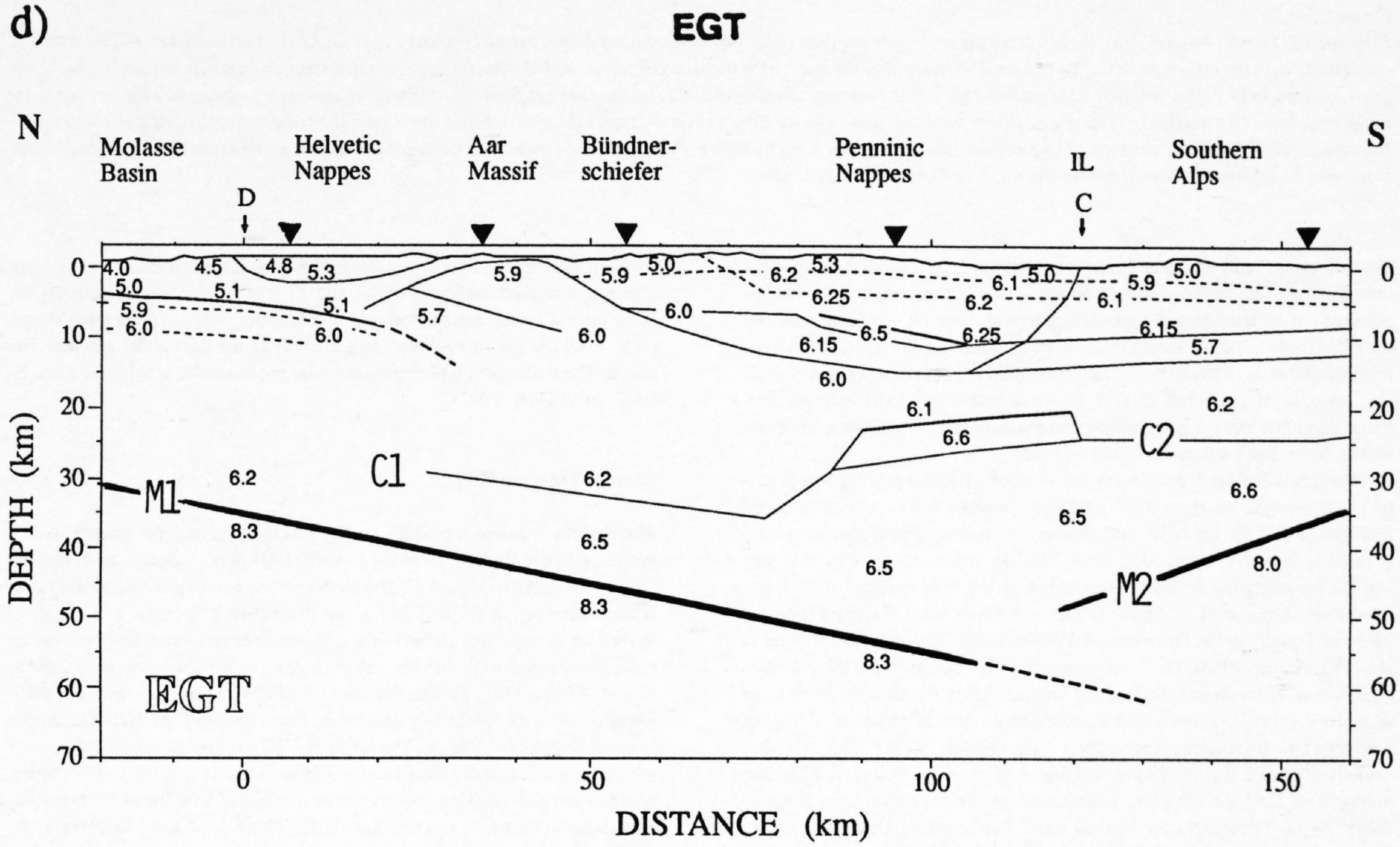

the Southern Alps (Deichmann et al., 1986). The wide-angle reflection (M2) on this profile is associated with the Adriatic Moho which reveals a crustal thickening from west to east. On the western end of the profile the crust/mantle boundary is faintly recognized at 12 s and on the eastern end at 14.5 s.

All three of the strike-parallel profiles described above are crossed by the north-south trending EGT refraction line (Ye, 1992; Ye et al., 1995) which is shown in Figure 23-4d. This section is comprised of data from the reversed shot points D and C and is extended north and south by shot points E and B, respectively (Figure 23-1a). The profile stretches from the northern margin of the Molasse Basin across the Alps and ends in the Po Basin. At distances of 0 to 90 km the line parallels the adjacent NRP 20 reflection line E1 (see Figure 23-1b). This section clearly illustrates the opposing dips of the European (M1) and Adriatic (M2) crustal plates. The southern extension of the European crust beneath the base of the Adriatic crust is supported by weaker south-dipping reflections at a distance of 110 to 150 km (cf. Valasek et al., 1991).

Figures 23-5 show the detailed 2D velocity models derived from these four profiles using forward modeling techniques (Maurer & Ansorge, 1992; Yan & Mechie, 1989; Deichmann et al., 1986; Ye 1992; Ye et al., 1995). The bold portions of the layer boundaries represent the data which were extracted from the refraction models and used in the construction of the 3D surfaces. The model depths obtained from these profiles were primarily restricted to those defining the crust/mantle boundaries (M1 and M2) which were well resolved by these measurements. Additional control for the upper two boundaries (B and C2) was extracted only for the Southern Alps profile ALP 77 and Figure 23-5c. On this profile the bold portions of the interfaces represent the areas of the model which were determined by Deichmann et al. (1986) to be well constrained.

Reflection Data

A representative portion of the NRP 20 seismic database consisting of 14 sections was selected for use in this study. These data were processed using conventional deep-crustal techniques (cf. Valasek et al., 1990) and were subsequently converted into a line-drawing format using a new automatic technique developed by Valasek (1992; see Valasek & Frei, Chapter 4). These unmigrated data were then interpreted by identifying the reflective bounda-

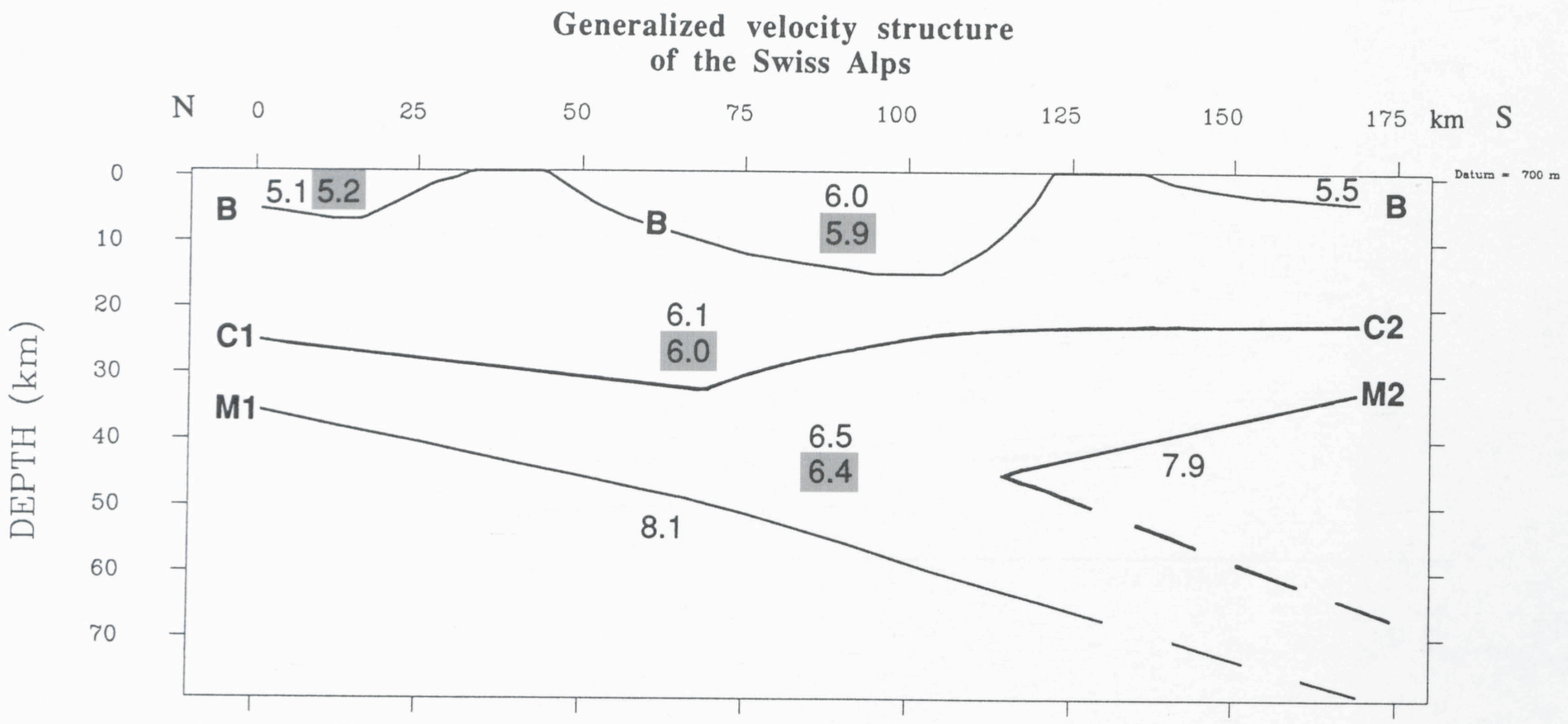

Figure 23-6

Schematic 2D model summarizing the results of the smoothed analysis of the refraction-based velocity models across the Swiss Alps. A three-layer velocity structure compatible with the reflection data was obtained by averaging the interval velocities associated with the finer-scale crustal heterogeneities. At this scale, the Alpine crust appears to be rather uniform with the most significant velocity variations outlining the changes from crystalline to dominantly sedimentary lithologies in the uppermost layer (B), particularly for the northern foreland. The velocity values assessed from the western Swiss Alps (grey-shaded values) showed a slight decrease from those found further to the east. The procedure used to tie this velocity information to the reflection data for migration is discussed in the text. Labeled boundaries are: B: uppermost crustal boundary; C1, C2: Conrad; M1, M2: Moho.

ries associated with the three-layered crustal structure outlined above. This interpretation was based primarily on the seismic images except for the uppermost crustal boundary (B) where outcrop information was used to extend the reflectivity to the surface. On some of the sections, however, unambiguous identification of even this greatly simplified crustal structuring was difficult because of poor data quality. In these situations, local extrapolation based on higher-quality neighboring images was used to facilitate a complete and uniform depth migration of the sections.

To obtain detailed depth profiles, the network of reflection profiles was depth-migrated using a ray-theoretical approach (Warner, 1987) implemented by Holliger (1991) for the NRP 20 database. The four-step procedure involved in this application is outlined in Table 23-1. To arrive at a velocity structure suitable for migrating the NRP 20 seismic data, the velocity-depth models derived from the network of Alpine refraction profiles were evaluated (Figures 23-5 and Egloff, 1979; Thouvenot & Perrier, 1980; Brändli, 1981; Miller et al., 1982; Noack, 1984). The level of information obtained from these studies is, however, more than sufficient for characterizing the desired three-layer crustal velocity distribution, and in most cases a certain degree of averaging was required to simplify the models (see Valasek, 1992). The resulting smoothed three-layer velocity distributions (Figure 23-6) were tied to the unmigrated 2D time structure interpreted on the reflection data (step 2, Table 23-1). These velocity bounds were then depth-migrated to provide the required subsurface velocity model for the actual depth migration of the reflection data. The 2D extrapolation of the generalized 1D velocity-depth functions resulted in changes in the average 1D crustal velocity of ± 0.1 km/s which is considered to be within the margin of accuracy of the original measurements.

Table 23-1

Four-step procedure for depth migration

Step 1:	Smooth the refraction-based velocity models (3-layer crustal configuration).
Step 2:	Define 2D velocity-time models by associating the generalized 3-layer velocity distribution to the unmigrated NRP 20 reflection sections.
Step 3:	Depth-migrate the 2D velocity-time models (Holliger, 1990)
Step 4:	Depth-migrate the NRP 20 reflection section using the resulting 2 D velocity-depth models (Holliger, 1990).

In the following section, two representative depth-migrated reflection profiles are described. In Figures 23-7 and 23-8 velocity contours defining the three crustal layers are shaded and in addition, circles representing depth-picks used for the subsequent construction of the 3D model are superimposed. The entire set of 14 depth-migrated profiles used in this study can be found in Valasek (1992).

Eastern Traverse (E1)

The Eastern Traverse (86 NFET or E1) was the first major Alpine reflection profile recorded by NRP 20 along a nearly 100 km NS transect traversing the eastern Swiss Alps (Figure 23-1b). In the northern part of the depth-migrated E1 seismic section (Figure 23-7), the distinctive reflections at a depth of around 6 km were interpreted as the uppermost crustal boundary (B) and are most likely associated with the autochthonous sedimentary cover of the Aar massif (Pfiffner et al., 1990b; Stäuble et al., 1993). Above this interface, shallower continuous reflectivity defines the basal thrust of the Helvetic nappes over the Subalpine Molasse. The boundary (B) rises southward to the surface where the Aar massif outcrops in the Vättis "window". In the south, the imbricated stack of Penninic nappes can be associated with the observed prominent reflectivity which extends down to their base at 14 km where boundary (B) is defined. This interpretation is based on projections made from surface exposures to the west which dip eastward beneath the seismic profile (Pfiffner et al., 1990b; 1991).

With the exception of a few isolated bands of subhorizontal reflections, the upper and middle crust beneath the Aar massif and northward into the foreland shows little coherent structuring. The top of the lower crust of the European plate (C1) is identified by the south-dipping reflections beginning at a depth of 24 km in the north. The base of the European crustal plate (M1) is clearly marked by the bottom of a high-amplitude reflective zone occurring at a depth of 36 km in the north and dipping southward. Both of these boundaries continue to plunge southward to just beneath the Penninic domain where their quality abruptly diminishes. This phenomenon is a characteristic feature of the Alpine profiles and will be addressed in more detail later. Toward the southern end of the profile, the continuation of the European crust is cautiously recognized by faint traces of south-dipping reflections masked by the more dominant north-dipping events. At a higher position on the southern end of the profile, the top of the Adriatic lower crust (C2) is marked by the north-dipping reflections between depths of 20 to 25 km. The deeper north-dipping events below depths of 25 km are associated with deformation resulting from the convergence of the north-dipping Adriatic crust into the European crust, whereas the subhorizontal reflections are interpreted as defining the base of

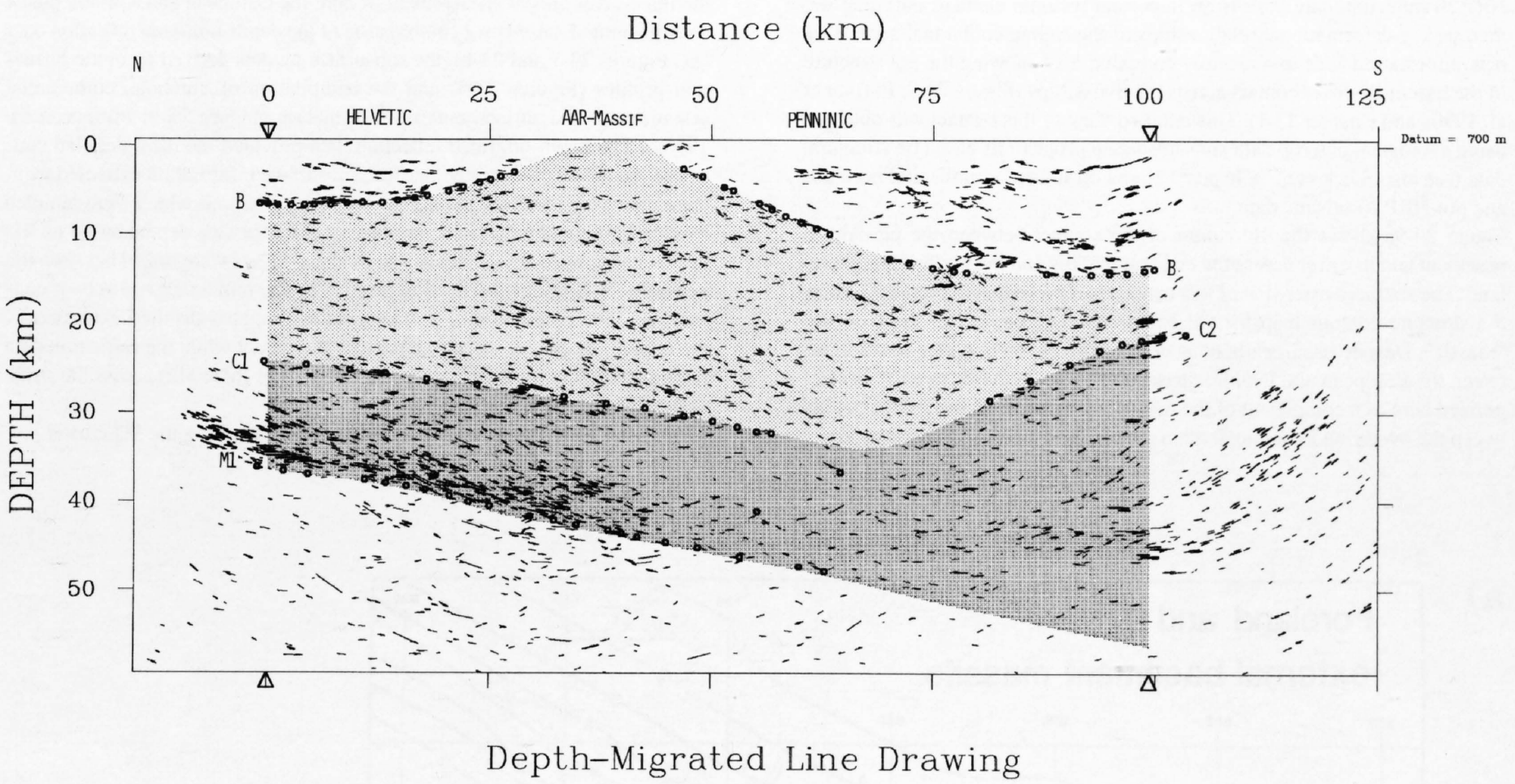

Figure 23-7
Depth migration of line E1 (86NFET) recorded across the eastern Swiss Alps (Figure 23-1b). The shaded areas represent the velocity bounds (step 3, Table 23-1) used for depth-migrating the data. The circles represent depth-picks used to constrain the 3D Alpine model. Labeled boundaries are: B: uppermost crustal boundary; C1, C2: Conrad; M1: European Moho.

the Adriatic crustal plate (M2). This latter assessment is somewhat tenuous; however, it is strengthened by observations made on adjacent profiles, including the EGT refraction/wide-angle reflection data (Figure 23-4d).

Western Traverse (W3)

Figure 23-8 shows the depth migration of line W3 recorded in the western Swiss Alps along a profile extending from the Rhone valley southward to a position near the base of the Matterhorn (Figure 23-1b). The top of the external Aar massif (B) projects down from the surface outcrops in the north to join with the base of the south-dipping series of high-amplitude reflections which reach down to depths of around 18 km. The top of the European lower crust (C1) was identified by a concentration of south-dipping reflections similar to those recognized on an adjacent profile (W2) located to the northwest. In contrast, the top of the Adriatic lower crust (C2) was interpreted to follow the more subhorizontal reflections trending across the section at a depth of 24 km which are truncated by reflections from the European lower crust in the north. The European Moho (M1) is clearly defined in the north at a depth of 45 km and may be cautiously extended down to depths greater than 50 km further to the south. The Adriatic Moho (M2) is interpreted on this section by the presence of the subhorizontal reflections at a depth of around 36 km in the middle of the section.

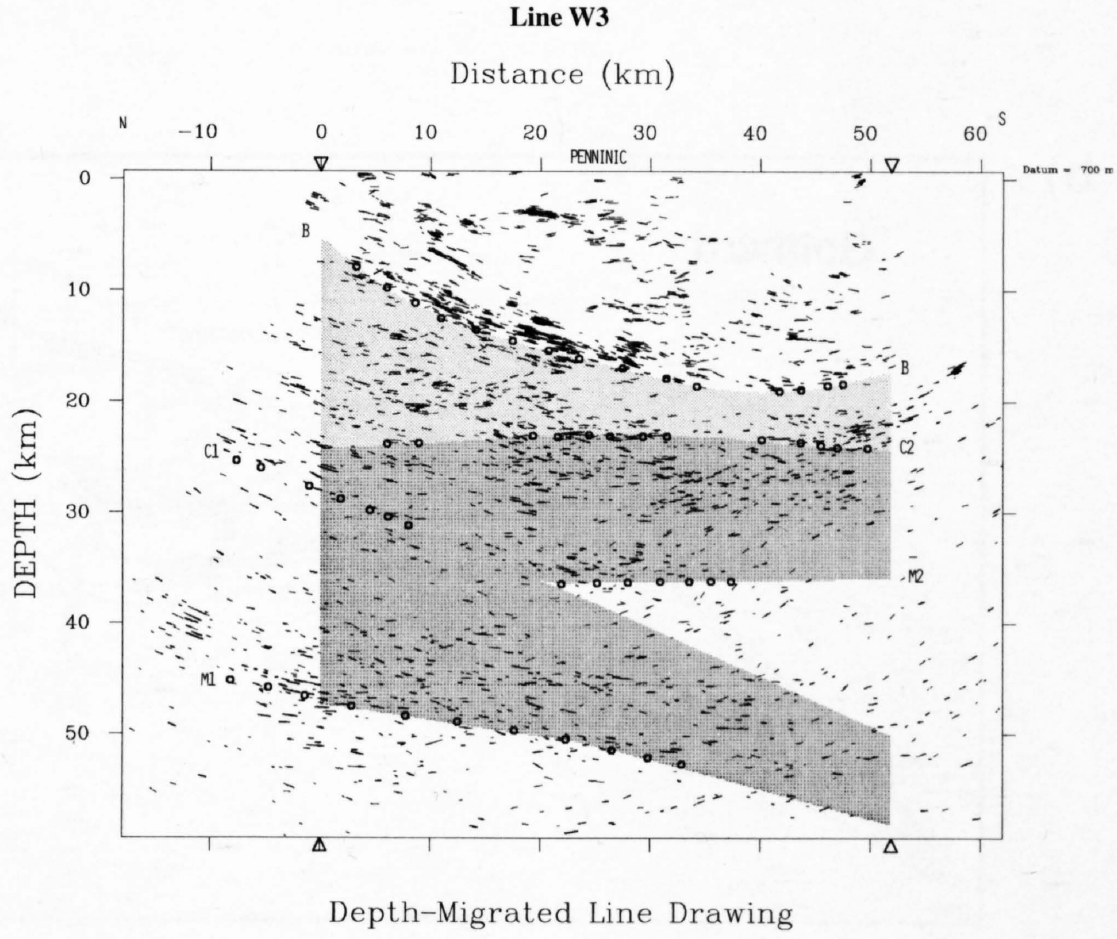

Figure 23-8
Depth migration of line W3 (87NFW3) recorded across the western Swiss Alps (Figure 23-1b). The shaded areas represent the velocity bounds (step 3, Table 23-1) used for depth-migrating the data. The circles represent depth-picks used to constrain the 3D Alpine model. Labeled boundaries are: B: uppermost crustal boundary; C1, C2: Conrad; M1, M2: Moho.

The subsurface nature of the uppermost crustal boundary (B) defined by the NRP 20 reflection data base is an important tectonic element outlining numerous key deformational relationships of the Alpine collisional zone. This new information adds to a recently compiled map showing the 3D structure of the basement-cover contact across the Swiss Alps (Figure 23-9; Pfiffner et al. 1990a and Chapter 13.1). This detailed view of this contact was obtained using geological outcrop data and subsurface projections based on structural data (see also Steck et al., Chapter 12) and on limited commercial borehole and pre-NRP 20 seismic data.

Figure 23-9a shows the 3D nature of the contact between the pre-Alpine basement and its cover across the external massifs and the north-Alpine foreland. The southern extension of this contact is represented in Figure 23-9b by the structure-contour map for the basement-cover contact of the Gotthard "massif". Despite its allochthonous origin from an intermediate position between the European and Penninic basements, the Gotthard "massif" is categorized here as a component of the pre-Alpine basement with its contact between the overlying Penninic domain defining the modeled boundary (B).

23.3 Model Construction

To construct a 3D model of the Central Alpine subsurface, surfaces defining the three-layer crustal arrangement of both the European and Adriatic plates were generated, based on a combination of the depth-migrated reflection data (ex. Figures 23-7 and 23-8), the subsurface models derived from the refraction profiles (Figures 23-5) and the compilation of borehole, commercial seismic data and surface outcrop information (Figure 23-9; Pfiffner et al. 1990a). The depth-migrated reflection data provided the most detailed control of the modeled layer geometries. Subsurface information extracted from these data were restricted to only the boundary positions which were sampled by clearly-defined reflections; in other words, interface depths based on 2D interpolation were not included. The modeled layers were linked between the generally N–S oriented reflection profiles by the remaining two sets of constraints. The compilation of surface geology enabled detailed extension of the uppermost crustal surface (B) across the model while the refraction data provided the link for the crust/mantle boundaries (M1, M2) across the strike of the Central Alps.

The "SierraTM" software package was used for creating the 3D crustal lay-

a)

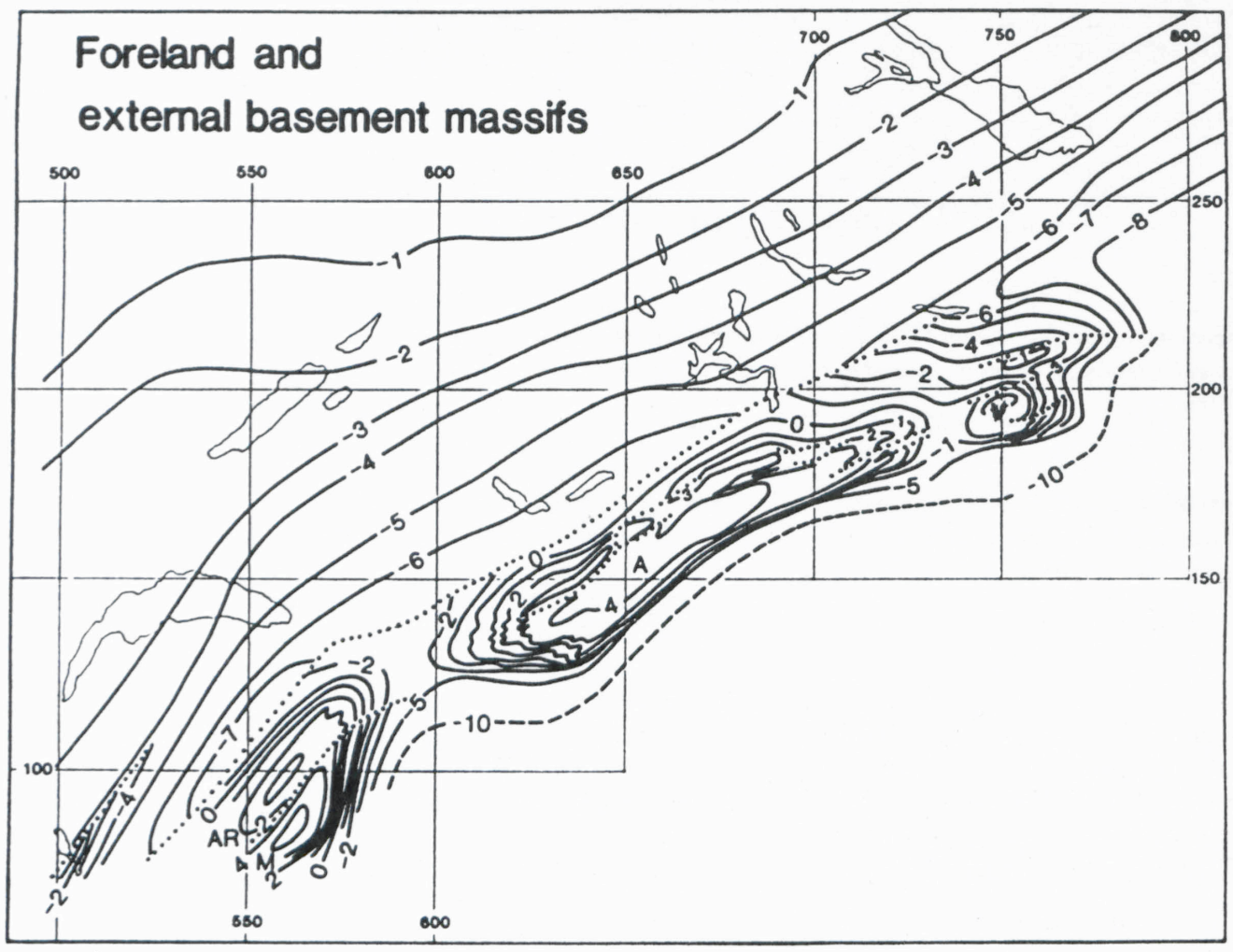

b)

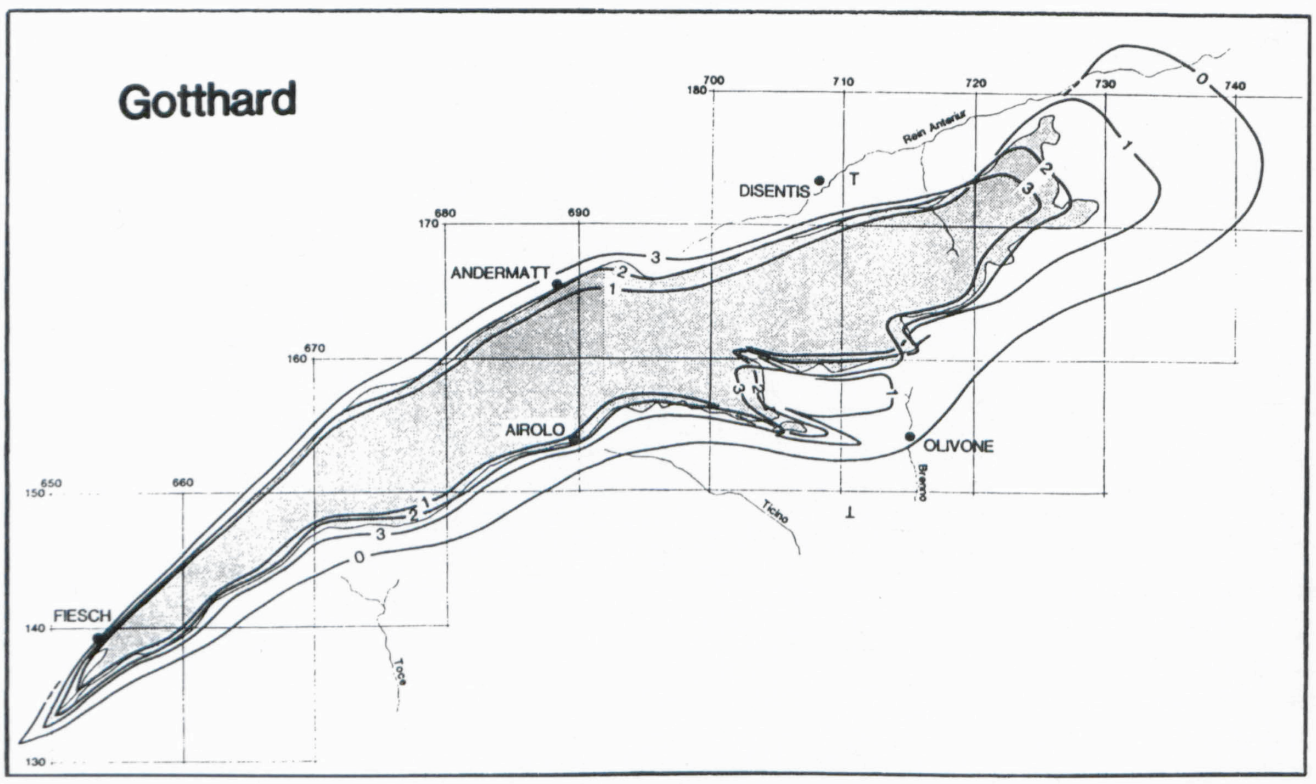

Figure 23-9
Structure contour maps for the basement-cover contact (adapted from Pfiffner et al. 1990a). Contour interval = 1 km. Gridlines with numbers correspond to the Swiss National km-Grid System.

a) North-Alpine foreland and the external basement massifs. Depth data from the foreland are based on both borehole and commercial seismic data. ***A****: Aar massif,* ***AR****: Aiguilles Rouges massif,* ***M****: Mont Blanc massif,* ***V****: Vättis window. Dotted lines mark the change from an upper to a lower contoured surface.*

b) Gotthard "massif". The grey shading represents the surface outcrop of the "massif".

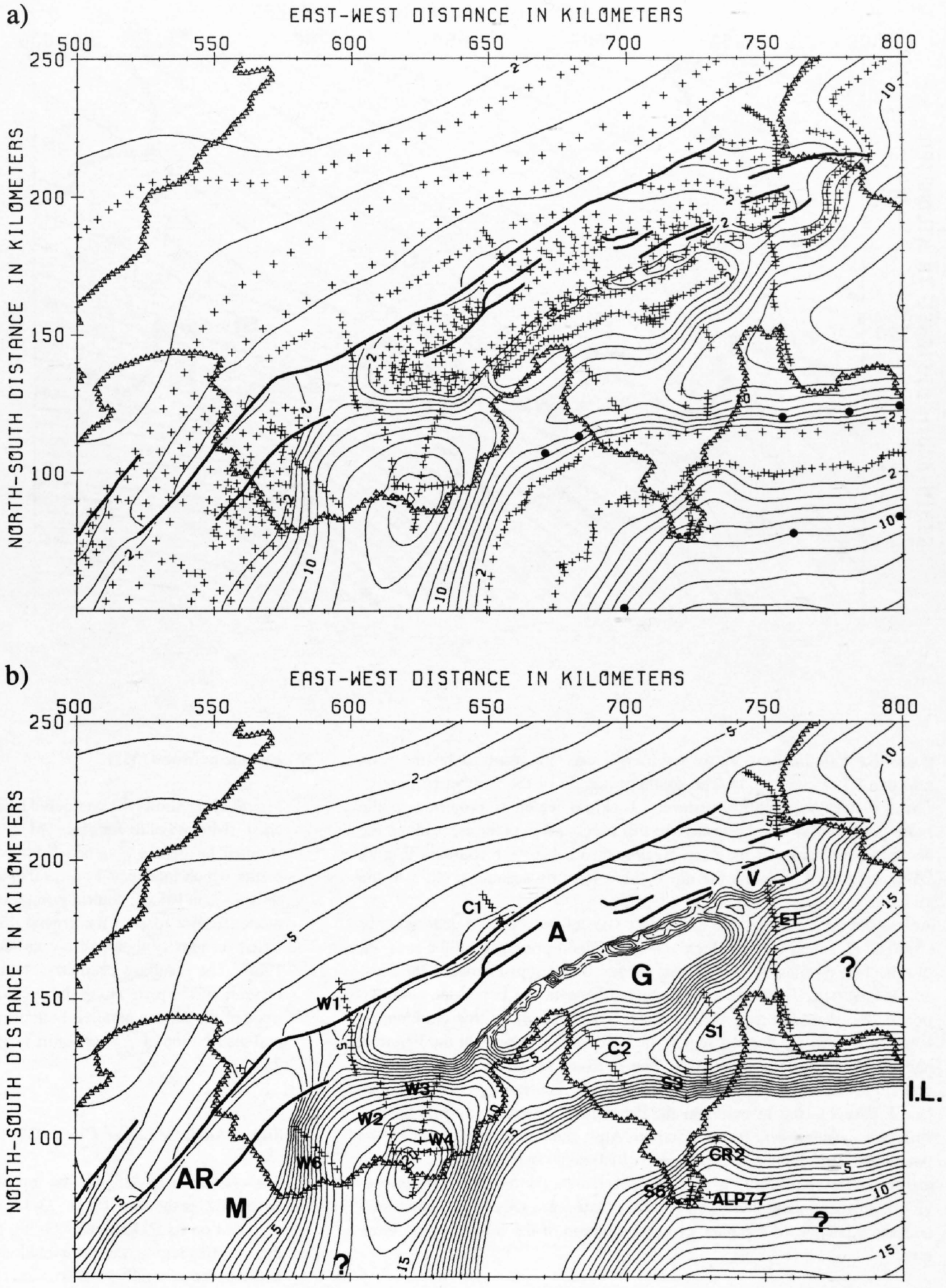

Figure 23-10
a) Structure contour map of the boundary (B) constrained by seismic data and the structure contour maps of Figures 23-9a and 9b. Contours above the top of the model (0 m) were not drawn, however, the information was used to define the near-surface gradients for gridding the surface. The dark circles represent artificial depths used to maintain the estimated geometry of the layer.
b) The same surface shown in a) with only the depth points plotted which were extracted from the seismic data. Refer to Figure 23-9a for an explanation of the labeled units.

ers and for the subsequent synthetic modeling using asymptotic ray tracing. This software package requires that the modeled layers extend across a rectangular grid. For this reason, the model dimensions were set to encompass all of the Alpine seismic profiles used in this study and to include a peripheral buffer of approximately 50 km. It is noteworthy to point out that the top of the model at z=0 m actually represents the seismic datum of 700 m above mean sea level (msl) and that layer depths are defined as positive values below this datum. Thus, a model depth of 50 km represents a subsurface position of 49.3 km below msl.

The 3D interfaces for the three crustal layers were defined by extrapolation between the data points onto a 2x2 km grid using an inverse interpolation method. In areas with a low number of data points, the computed contours sometimes failed to adequately match the data values and artificial points had to be added to control the interpolation. The locations where this situation occurred are pointed out in the upcoming description of each of the crustal surfaces.

Uppermost Crustal Boundary (B)

Figures 23-10 show the contour map of the uppermost crustal boundary (B). The first layer above is by far the most constrained because of the additional information obtained from Figures 23-9. Along the SE margin of the gently dipping foreland, the basement depths extracted from the migrated NRP 20 profiles agreed well with those determined from the commercial seismic profiles. The distinctive highs distributed in an "en échelon" pattern along the Central Alpine axis define the chain of external basement massifs. The covered basement link between the Aiguilles Rouges and the Aar massifs in the Rawil axial depression is imaged on line W1 (Figure 23-10b) as an arched continuation with a vertical offset towards the north corresponding well with the northern limit of the exposed massifs. The narrow NE–SW trending low between the Aar and Gotthard massifs is occupied by cover remnants and in the east by additional basement slivers (e. g. Tavetsch massif, Pfiffner et al., 1990a). The reflection profile (90NFC1 or C1, see Figure 23-1b) which crosses this zone was unable to provide any further control, in part because of its low fold, but more likely because of the steepness of the structures. Likewise, the detailed structuring of the easternmost

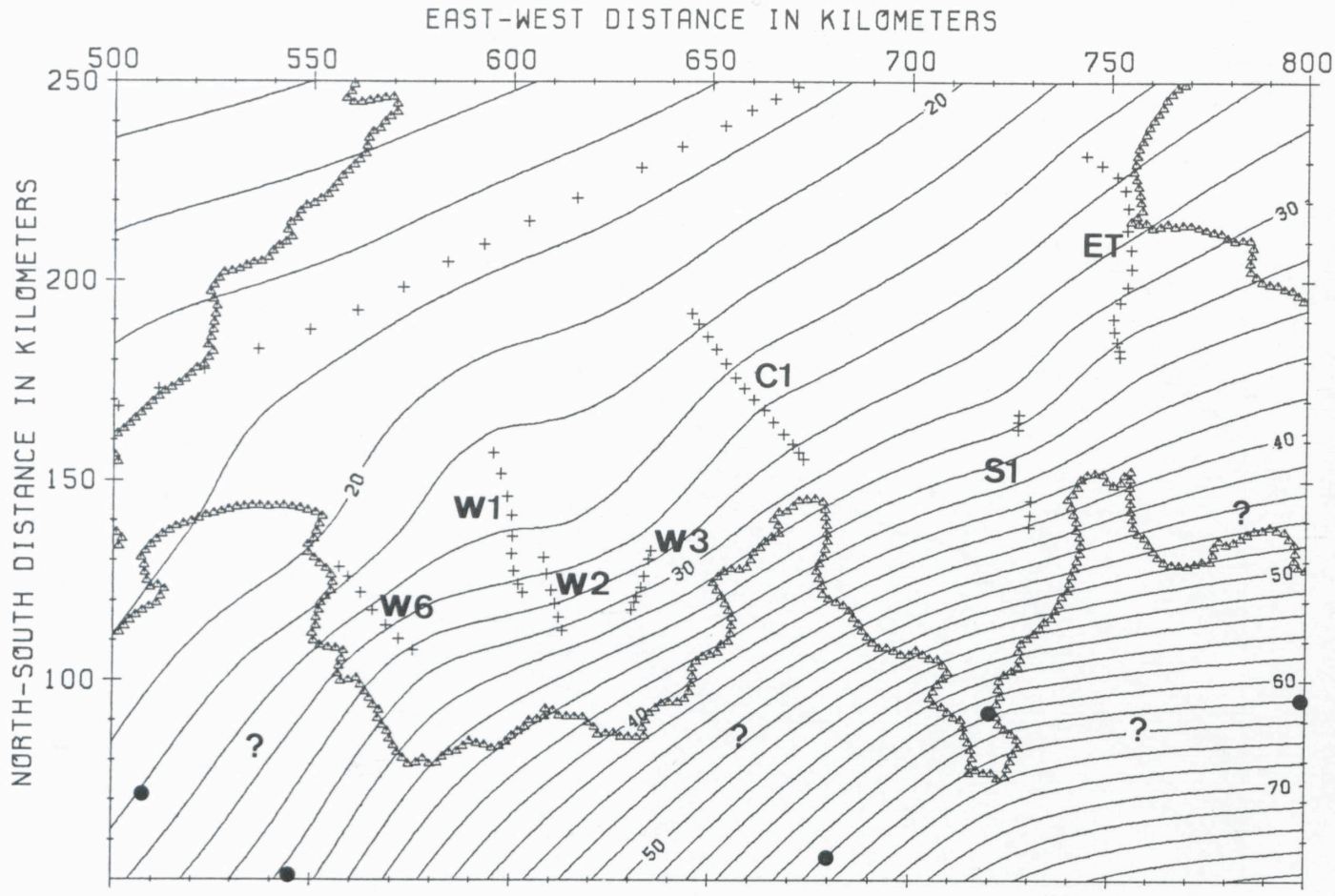

Figure 23-11
*Structure contour map representing the European Conrad (**C1**). The surface was constrained using only the depth-migrated seismic reflection profiles. Support for the lateral, albeit highly variable, continuation of the lower crust between the reflection lines is found on nearly all of the crossing strike-oriented refraction lines. The NE–SW trending series of points across the NW corner of the model represents artificial depths used to maintain a constant layer thickness along strike. Contour interval = 2 km.*

dome-like culmination (Vättis "window") was not resolved by the seismic line E1 (Figure 23-7). The southern margin of the Gotthard "massif" forms a steep to slightly overturned backfold which is projected to dip more gradually in the subsurface. In this case, and in other areas along the south-eastern flanks of the massifs, projected subsurface contours (Figure 23-9) were used to define the dip if there were no seismic profiles in the vicinity.

Across the Penninic domain, the surface (B) defines a curved depression or "trough" (Figure 23-10b) which was determined primarily by the network of reflection profiles. A swell in this surface is developed between the Eastern and Western Traverses and is situated beneath the Lepontine culmination of the Penninic nappes. The steep SW flank off of this culmination leads down into the deepest region of this depression beneath the Penninic nappes of the western Swiss Alps. The southern boundary of the Penninic domain is defined by the Insubric Line which required five control points (see Figure 23-10a) to maintain the dip defined primarily by line S1 and surface measurements. In the Southern Alps, the subsurface extent of the boundary (B) is defined as the basement/sediment contact by both reflection and refraction results only within a restricted area. For the most part, this region is unconstrained and three control points were required to preserve a consistent basinward dip parallel to the outcrop of the South-Alpine basement.

Top of European Lower Crust (C1)

The surface defining the top of the European lower crust (Conrad interface C1) is displayed in Figure 23-11. This second layer boundary is based only on the depth-migrated reflection data, and thus required a considerable amount of extrapolation. The results for the refraction profiles were excluded because the weak and variable reflectivity associated with this boundary led to inconsistent lower crustal depths (ex. compare Thouvenot et al., 1990, Miller et al., 1982, and Yan & Mechie, 1989). The resulting reflection-based lower crustal depths closely match the pronounced lower crustal reflectivity observed on the ECORS-CROP profile which was recorded across the Western French-Italian Alps (cf. Nicolas et al., 1990b).

In addition to the reflection-based data, a series of control points were required to stabilize the contouring out to the model borders. The depth values of the artificial points were chosen to preserve a constant lower crustal thickness (~14 km) along the strike of the Alps. These artificial points are located primarily across the NW corner of the model along a NE–SW linear trend. Across the SE corner of the model there were no data points to establish this thickness, and a thinning of the lower crust to 10 km along the contour +62 km was assumed. The resulting lower crustal surface has an overall southeastward dip with a shape which reflects the arcuate distribution of the exposed tectonic units (Figures 23-1a and 23-1b).

European Moho (M1)

Figure 23-12 shows the contoured interface defining the base of the European crust (Mohorovičić interface M1). This third layer boundary was constrained by depths obtained from both reflection and refraction measurements which intersected each other in several locations. In addition to the seismic data values, control points were added along the NW corner of the model from a map of the crustal thickness across Switzerland which was based on gravity data and on earlier refraction results (cf. Mueller et al., 1980). The resulting geometry of the European crust reveals a distinctive bending of the plate along the southern margin of the foreland. The overall trend of the surface parallels both the top of the lower crust (C1) and the general distribution of tectonic units exposed on the surface (Figures 23-1a and 23-1b).

Top of Adriatic Lower Crust (C2)

The contour map defining the top of the Adriatic lower crust (Conrad interface C2) is shown in Figure 23-13. With the exception of the refraction data recorded on ALP77 (Figure 23-5c), the surface is defined by the reflection data. In this region, the extrapolation of the modeled second layer boundary between the generally N–S oriented reflection profiles is strengthened by the prominent wide-angle reflection observed on the refraction line LB-LL (Figure 23-1a) which was associated with a high-velocity layer (6.6 km/s) at depths appropriate for the Adriatic lower crust (Egloff, 1979). Control points were required on the northern edge of the layer to maintain the dip defined by the data values. A single point near the south-western edge of the model was used to provide a constant lower crustal thickness. The general shape of the lower crust outlines a rather featureless subhorizontal layer in the south which bulges slightly upward before plunging steeply northward toward the foreland where it is truncated by the European lower crust (interface C1, Figure 23-11). Furthermore, the trend of this plunging surface roughly mimics the surface expression of the Insubric Line (Figures 23-1a and 23-1b).

Adriatic Moho (M2)

Figure 23-14 shows the surface defining the base of the Adriatic crust (Mohorovičić interface M2). In the Southern Alps, both refraction and reflection data constrain the surface, whereas in the western Swiss Alps, only two reflection lines provide subsurface depths. Control points were required at the leading edge of the surface to continue the dip defined by the data points far enough outward to intersect with the European lower crustal surface (C1) which cuts both the top of the Adriatic lower crust (C2) and the M2 interface (cf. Figure 23-2a). An additional artificial point was added along the southern

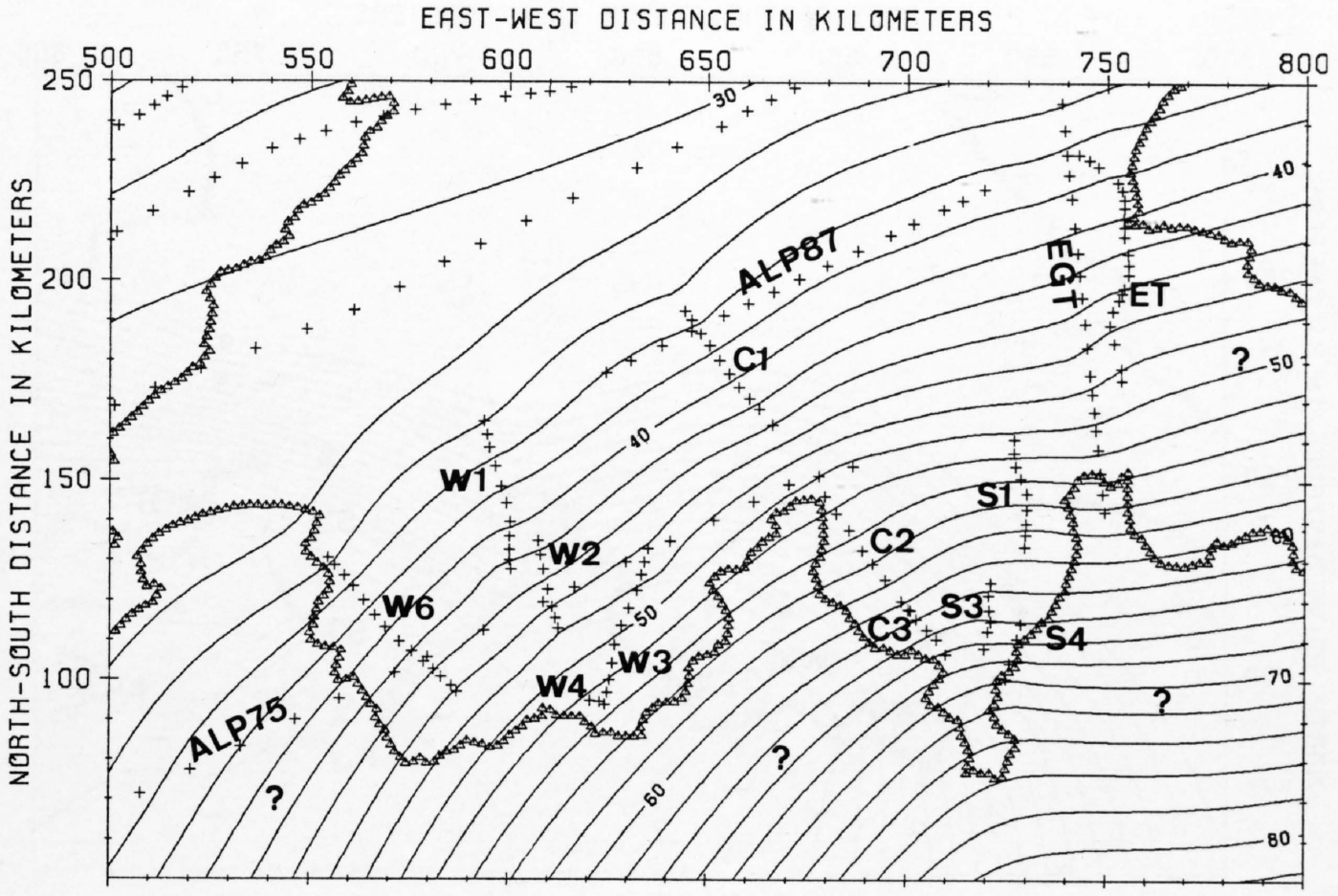

Figure 23-12
*Structure contour map of the European Moho (**M1**). Both refraction- and reflection-derived depths were used to constrain this surface. The three sets of NE–SW trending points across the NW corner of the model represent depths obtained from the map of crustal thicknesses compiled by Mueller et al., 1980. Contour interval = 2 km.*

edge of the model to preserve the N–S strike defined by the line W3. The overall trend of the Adriatic crustal base roughly parallels the Insubric Line; however, because of the low number of data points, this result has to be considered with caution.

Combined 3D Model

The surfaces defining the European and Adriatic crustal plates were combined together to form a 3D model of the Alpine collisional zone. Figure 23-15 shows the resulting 3D configuration beginning at the base with the south to southeastward plunging European Moho (M1) and Conrad interface (C1), followed by the north to northwestward dipping Adriatic Moho (M2) and Conrad interface (C2) which are truncated by the European Conrad interface (C1) and ending with the uppermost crustal boundary (B). The refraction-based generalized velocities (Figure 23-6) used for depth-migrating the reflection data were associated to the surfaces and are displayed in this perspective view.
As mentioned earlier, the "Ivrea body" was not explicitly incorporated into this model of the Central Alps because of a lack of seismic coverage. The geophysical profiles which cross the Ivrea zone providing seismic refraction (Berckhemer, 1968; Ansorge, 1968; Ansorge et al., 1979) and gravity data (Kissling, 1984) indicate that this structure dips steeply to the SE and eventually flattens out at mid-crustal levels beneath the Po Basin. If this anomalous structure had been included in the model, it would have appeared as an imbrication of the Adriatic lower crust and mantle rising steeply above the modeled Adriatic wedge in the SE corner of Figure 23-15.

23.4 Model Verification

The 3D Central Alpine model shown in Figure 23-15 was constructed primarily from subsurface information obtained from 2D analysis of a network of seismic data. This method has the advantage that the true spatial locations of all of the observations were used (i. e. no assumptions about projections were required); however, as mentioned before, these 2D results themselves were not analyzed to account for the contribution of 3D layer geometries. Seismic measurements obtained along 2D lines such as the networks of Alpine reflection and refraction profiles provide only a 2D sampling of a 3D wavefield. For this type of data, 2D methods of analysis are valid only in cases of a horizontally stratified media or in areas where the lines were recorded along the dip direction of a sequence of tilted, planar layers. In all other situations a portion of the recorded wavefield originates from outside the plane of the survey and these "side-swipe" components cannot be properly handled by 2D approaches alone. In general, without considering 3D effects, layer depths are underestimated.

Forward Modeling

To evaluate the degree to which 3D effects influence the reflection data recorded across the Swiss Alps, synthetic seismic data were generated by normal-incidence ray tracing to compare with the observed data. The position of the synthetic reflection points with respect to the 2D plane of the seismic profiles reveals the horizontal magnitudes of the 3D effects while the vertical components can be assessed by comparing the synthetic seismic sections with the observed unmigrated data.
For all of the reflection profiles, synthetic normal-incidence sections were generated and compared with the unmigrated reflection profiles. The resulting simulations revealed that the magnitude of out-of-plane distortions were greatest for the Moho surfaces M1 and M2 with negligible effects encountered for the top of the lower crustal interfaces (C1 and C2) and only localized effects observed for the uppermost crustal layer (B). These results can be viewed in Figures 23-16 and 23-17 for the Eastern (E1) and Western (W3) Traverses, respectively, which show the unmigrated data together with their interpretations (shaded) and the calculated traveltimes of the synthetic sections (circles). The temporal differences between the observed and synthetic times give a quantitative measure of the vertical distortion for each modeled interface. Inspection of these results reveals that the match for both the upper crustal and lower crustal interfaces was quite close indicating that 3D problems were not too severe. One notable exception for (B) occurs along line E1 where a mis-tie of nearly 500 ms occurs within the Penninic domain at distances between 65 and 75 km (Figure 23-16). This suggests that the reflection data do not support the projected subsurface extent of the Gotthard massif shown in Figure 23-9b. Instead, a slightly steeper plunge than is currently modeled would better satisfy the observed data. This point is discussed in detail by Pfiffner & Hitz, Chapter 9 and Hitz (1995).
The influence of 3D layer geometries was more severe for the deepest layers defining the crust/mantle boundaries M1 and M2 for the European and Adriatic crustal plates, respectively. Along the line E1 (Figure 23-16), the synthetic data for M1 match quite closely beneath the foreland but the fit degrades further to the south. In the western Swiss Alps (Figure 23-17), a nearly constant offset ranging from 300 to 400 ms can be recognized for the synthetic data of both crustal plates (M1 and M2). The nature of these mis-ties can be more readily assessed in a map view of the actual ray paths traced down to the European Moho M1 (Figure 23-18). This display reveals that for all of the profiles excluding lines W6, C1, C2 and S1, the synthetic responses generated from the European Moho originated from out-of-plane positions. This occurred primarily because of the oblique orientation of these lines to the local planar trend of the modeled surface. As can be seen, line W3 is quite oblique to the local strike of the surface resulting in ray paths originating from locations offset more than 10 km away from the seismic profile. In contrast, line E1 only shows significant out-of-plane rays in the middle portion where the line changes orientation with respect to the local strike of the modeled surface.

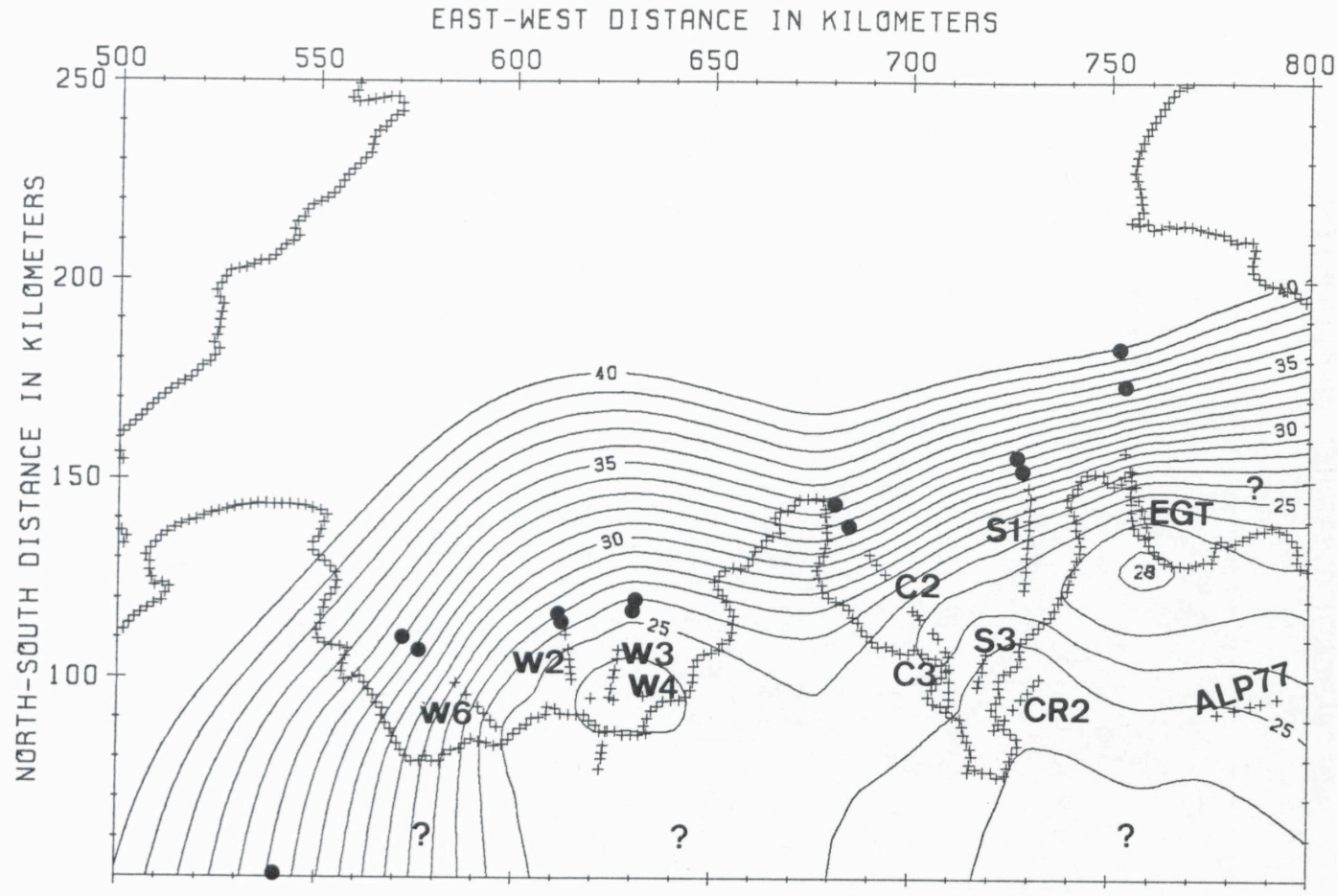

Figure 23-13
*Structure contour map of the Adriatic Conrad interface (**C2**). This layer was constrained primarily by the depth-migrated reflection data with the exception of the refraction-based depths obtained from ALP77 (Figure 23-5c) in the Southern Alps. Contours were drawn only out to positions just beyond the artificial points (filled circles) used to maintain the data-defined dip. In the subsequent insertion of this layer into the 3D model, some of the frontal contours shown are cut by the top of the European lower crust (Figure 23-11). Contour interval = 1 km.*

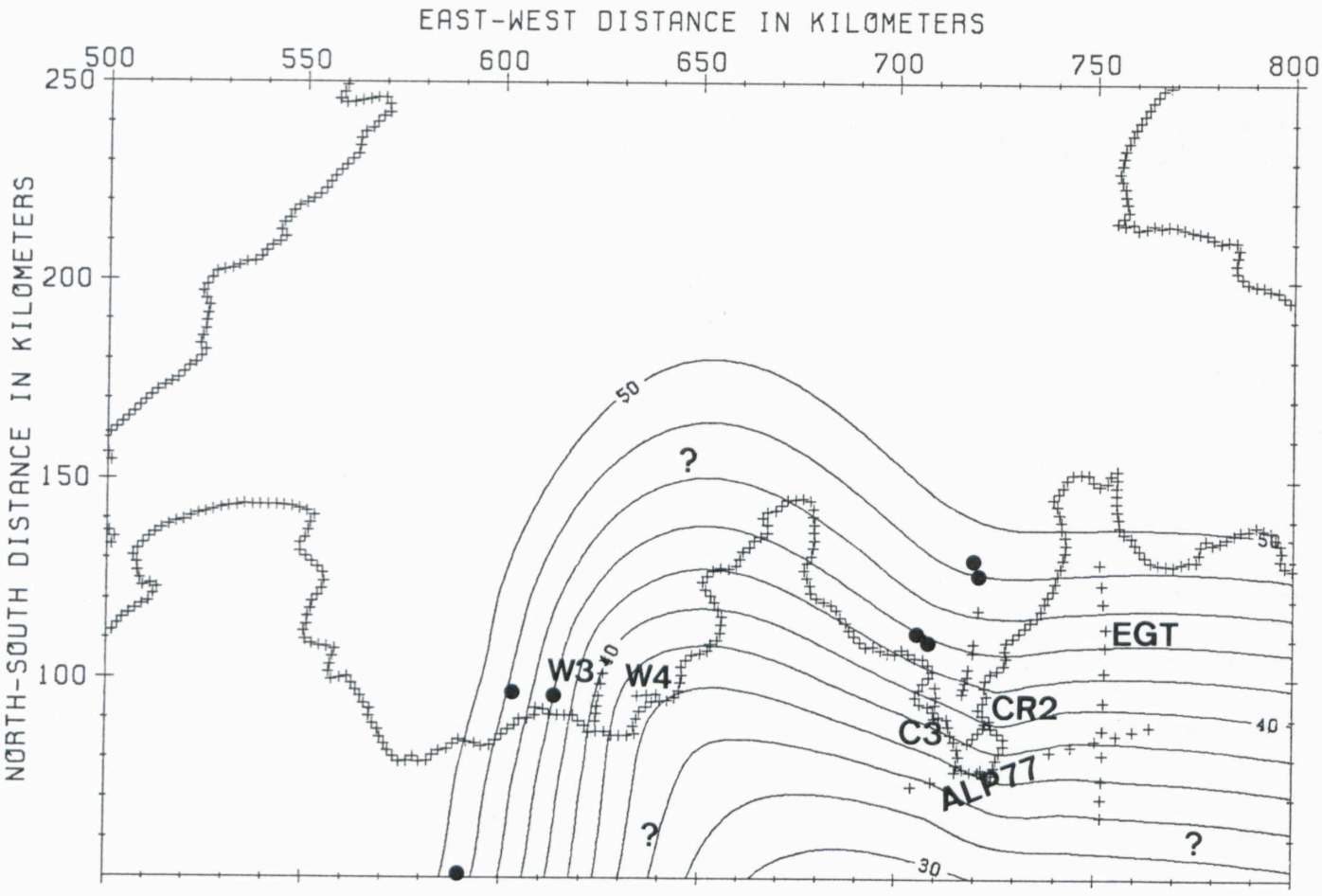

Figure 23-14
*Structure contour map of the Adriatic Moho (**M2**). Both reflection and refraction depths combine to define the subsurface geometry of this layer in the SE corner of the model, whereas only two reflection profiles constrain the surface in the western Swiss Alps. The discussion of the artificial control points and the restricted contouring given in the caption of Figure 23-13 also applies to this layer. Contour interval = 2 km. Note that the Adriatic mantle indentation is quite well outlined.*

Summary of 3D effects

Table 23-2 summarizes the 3D effects for all of the modeled layers. The maximum perpendicular offsets of the modeled ray paths were measured from the map views of each surface (cf. Figure 23-18), whereas the maximum depth distortions were obtained by depth-converting the time differences between the synthetic and observed normal-incidence reflections (ex. Figures 23-16 and 23-17). The implications of these errors introduced by constructing a 3D model using data analyzed with 2D methods depend on the desired resolution. For the objective of defining the general relationships between the main crustal boundaries, the errors are insignificant. While a lateral displacement of around 10 km seems large, the actual vertical distortion beneath the profile is less than the grid size used for generating the model. In fact, the average depth distortion caused by out-of-plane effects is well below the maximum value of 2 km which is not large enough to alter the present overall geometry of the 3D Alpine crustal model with layer thicknesses averaging around 15 km. Further refinements by iterative adjustment to obtain a best-fit model would, however, serve to enable more quantitative assessments of the finer-scale crustal structuring.

Table 23-2

Maximum perpendicular offset of modeled out-of-plane ray paths:

Basement/nappe boundary (B)	10 km
Upper/lower crustal boundary (C1/C2)	5 km
Crust/mantle boundary (M1/M2)	12 km

Maximum depth distortions caused by out-of-plane reflections:

Basement/nappe boundary (B)	-1 km
Upper/lower crustal boundary (C1/C2)	-1 km
Crust/mantle boundary (M1/M2)	-2 km

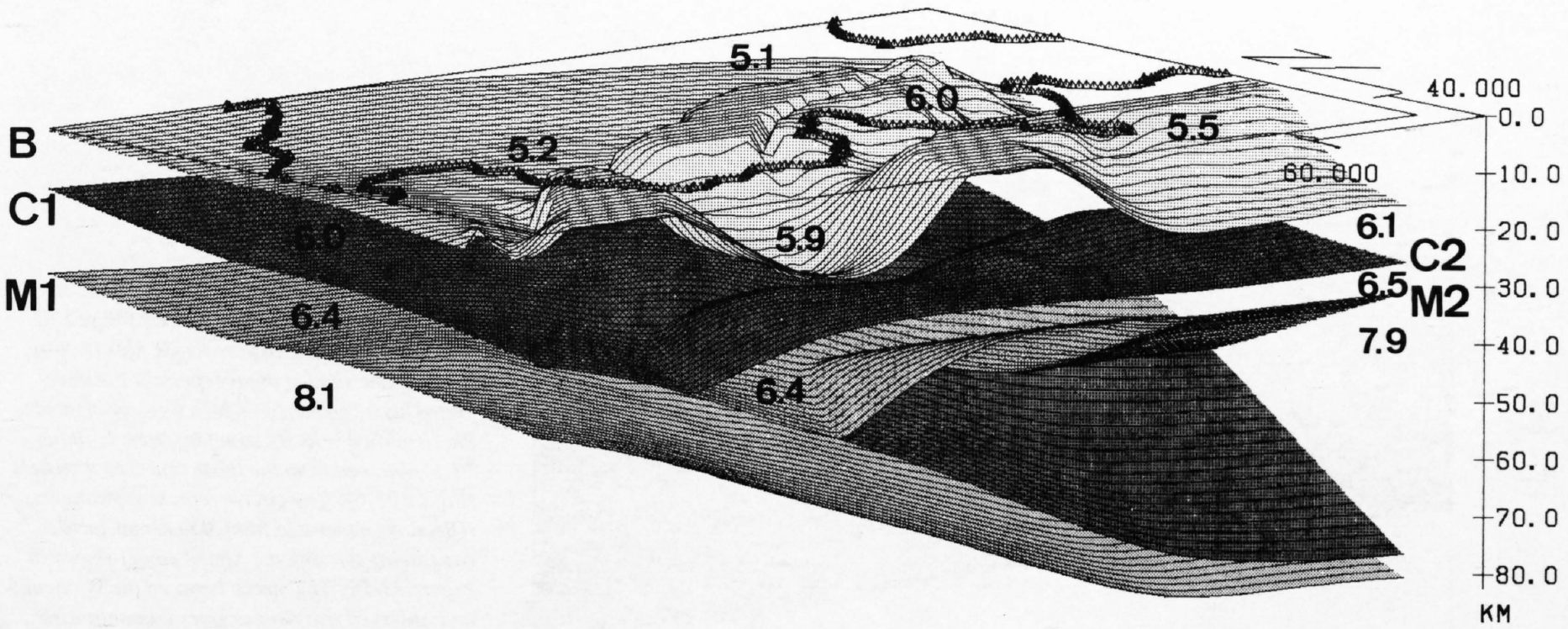

Figure 23-15
Perspective view of the Alpine crustal model showing the general velocity distribution derived from refraction measurements (view is to the NE; vertical exaggeration = 1.5). These velocities are the same values which were used to depth-migrate the reflection profiles. Labeled boundaries are: B: uppermost crustal boundary; C1, C2: Conrad; M1, M2 Moho.

23.5 Discussion

The large spacing between the network of Alpine seismic profiles made it necessary to evaluate the data on a similarly large scale. This simplification led to interpreting a three-layered crustal structuring of both the European and Adriatic crustal plates defined by their respective upper/lower crustal (C1/C2) and crust/mantle (M1/M2) boundaries and an uppermost crustal boundary (B) defining the base of the main allochthonous Alpine tectonic units. While this represents a gross generalization of the complex Alpine subsurface, the overall geometry and interrelationship of this simplified crustal layering provides important constraints for understanding the main geodynamical processes involved in the Alpine orogeny.
The resulting initial 3D model represents a snapshot of the present crustal arrangement, and thus, the important dimension of time is absent. The observed reflectivity used to constrain the 3D model actually represents the culmination of a protracted history of polyphase deformation. Furthermore, this initial 3D approximation must be viewed as a somewhat "blurred" image of the subsurface because of the amount of interpolation which was required to produce even this greatly simplified model and because of the bias introduced by a dominance of N–S oriented seismic profiles. Because of this, there is potential that more localized features have been smoothed, particularly those exhibiting variability along the Alpine axis. Notably absent from this model is the "Ivrea body" which was excluded because of a lack of subsurface constraints from seismic data. Nevertheless, some fundamental aspects of the tectonic evolution can be obtained from this initial representation of the Alpine subsurface which appears to primarily document the late collisional phase of deformation. In the following evaluation, the implications of the 3D Central Alpine crustal model are discussed primarily in terms of this Neo-Alpine tectonic activity.

Crustal Wedging and Neo-Alpine Crustal Deformation

The wedging of the Adriatic lower crust into the European crust has long been suspected to play a major role in Neogene deformation of the Alps (cf. Pavoni, 1961; Mueller, 1977; Kahle et al., 1980; Miller et al., 1982; Mueller, 1989). This prediction was based primarily on the observed geometric relationship of anomalous high- and low-velocity zones developed within the middle crust beneath the internal zones of the Alps (Mueller, 1977) and on gravity modeling, as well as on the recent tectonic stress field developed within the Alpine crust (Pavoni, 1961). Interpretations of the more recent seismic data including both seismic refraction (Ye & Ansorge, 1990a; 1990b; Ye, 1992) and reflection data (cf. Frei et al., 1989; 1990; Pfiffner et al., 1988; 1990b; Pfiffner, 1990) and their combined synthesis (Mueller, 1989; 1990; ETH Working Group on Deep Seismic Profiling, 1991; Valasek et al., 1991) have all found additional support for this type of mechanism. The improved resolution obtained from these data has defined a wedge of the Adriatic lower crust driven into the European middle crust which has promoted both the subduction of the European lower crust and the thickening of the upper crust. This appears to be the response to continued oblique convergence following the closure of the oceanic basins and troughs separating the European and African margins (Eo-Alpine orogeny) and the formation of a continuous orogenic belt in the late Eocene (Meso-Alpine orogeny).
In this study, the integrated interpretation of the network of deep crustal Alpine seismic profiles provides a 3D view of this style of Neo-Alpine deformation (Figure 23-19). The initial 3D model of the Alps reveals a wedge of Adriatic lower crust (C2, Figure 23-20) extending from the eastern to the western Central Alps above the subducting European lower crust (C1, Figure 23-20). The lower crustal wedge was defined primarily by reflectivity occurring at depths of around 20 km beneath the internal zone of the Alps. These reflections dip towards the external margins where they merge with south- to southeastward-dipping reflections from the European lower crust. The orientation of the Adriatic wedge is suggestive of a NW transport direction which matches the estimated average convergence angle between the Adriatic microplate and European platform based on plate reconstructions (cf. Dewey et al., 1973). Its arcuate shape is expressed on the surface by the distribution of tectonic units as well as by their subsurface geometry (Figure 23-21). This general trend is also exhibited by the 3D shape of the surfaces defining both the top of the European and Adriatic lower crust (Figure 23-20) and the crust/mantle boundary (see Figure 23-12). The arcuate nature of the Alpine chain is most likely related to the counterclockwise rotation of the Adriatic microplate during the Alpine orogeny (Lowrie & Alvarez, 1975; Heller et al., 1989; Platt et al., 1989). This rotation imparted a westward dextral translation of the Adriatic promontory along the Insubric Line which eventually led its indentation into the Western Alps (Neo-Alpine orogeny) and the creation of the large-scale bending of the Alpine chain in this region (cf. Rod, 1979).
The top of the Adriatic wedge is associated with a general increase in velocity of 0.4 km/s which also characterizes the top European lower crust (see Figure 23-6). Recent gravity modeling shows that an anomalous mid-crustal body positioned beneath the axial zone of the Alps with a density equivalent to the lower crust (2.95 g/cm^3) satisfies the observed shorter wavelength components of the Bouguer gravity anomaly (Holliger & Kissling, 1992). The existence of an aseismic zone at depths greater than 15-20 km across the axial zone of the Alps (Roth, 1990; Deichmann & Baer, 1990, Pavoni et al., Chapter 18) seems to support a more ductile rheology (Sibson, 1982; Meissner & Strehlau, 1982). The top part of the Adriatic lower crust and lithosperic mantle are, however, characterized by an increase in strength (Okaya et al., 1996) which would correspond to the proposed wedges of the Adriatic lower crust and upper mantle (cf. Figure 23-2b). Furthermore, the arcuate shape of the Adriatic wedge and the other modeled layers conform to the current fan-like regional stress pattern derived from an analysis of focal mechanisms within the Alps and adjacent regions (Pavoni, 1977; Mueller, 1984; Pavoni & Roth, 1990).
The European crust responded to the late-collisional wedging of the Adriatic lower crust by delaminating and subducting at the top of the lower crust and brittle decoupling and stacking in the upper crust. Figure 23-22 schematically summarizes these key relationships across a north-south transect through the eastern Swiss Alps. In the following, these different mechanical responses are discussed in relation to the present 3D structural arrangement of the Alps.

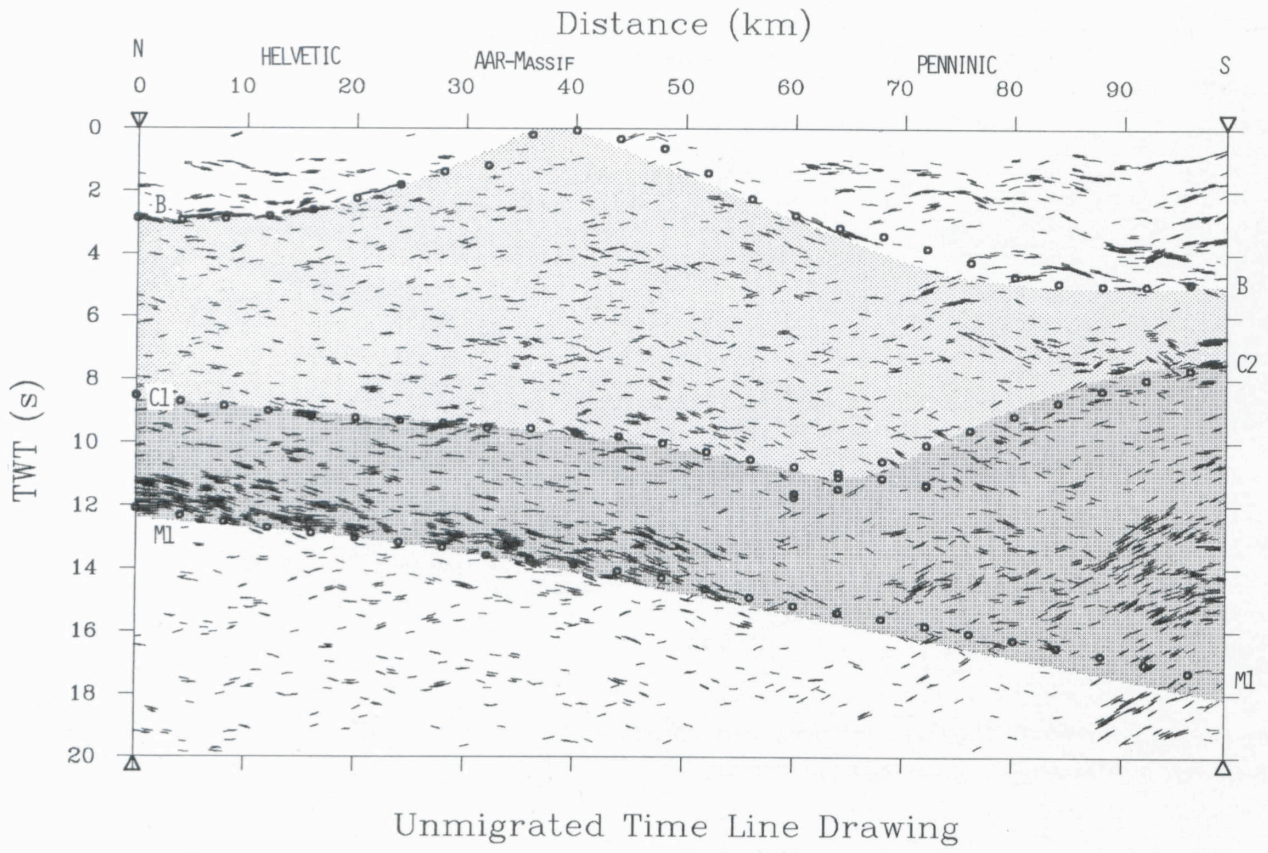

Figure 23-16
Unmigrated time section of line E1 (86NFET) recorded across the eastern Swiss Alps (Figure 23-1b). The shaded areas represent the interpreted layer boundaries which were associated to the simplified velocity structure (step 2, Table 23-1) obtained from the refraction-based models (Figure 23-6). The circles represent synthetic reflections generated from 3D normal-incidence ray tracing through the Alpine model shown in Figure 23-15. The match between the synthetic and observed traveltimes gives a quantitative estimate of the degree to which 3D layer geometries influence the 2D seismic profile. Labeled boundaries are: B: uppermost crustal boundary; C1, C2: Conrad; M1: European Moho.

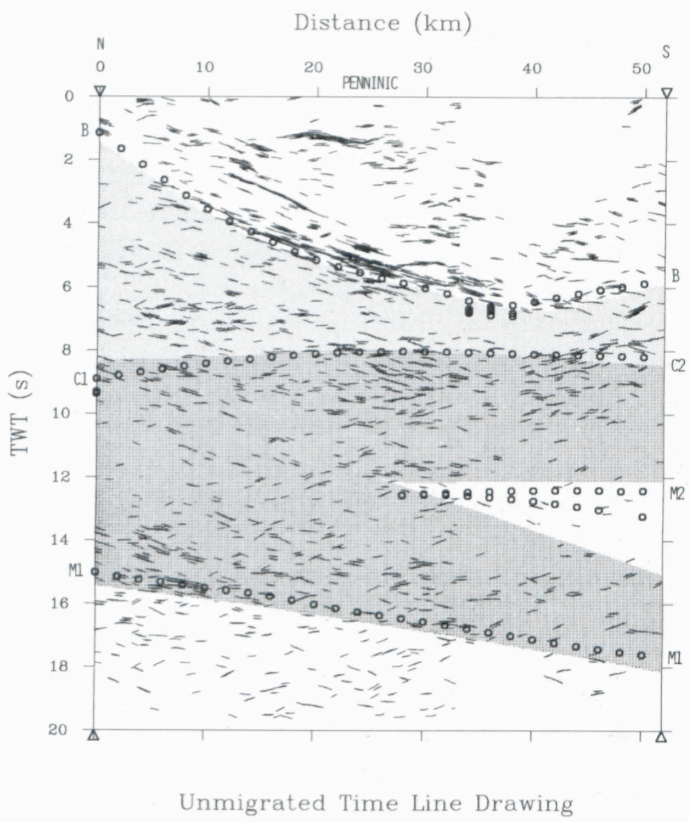

Figure 23-17
Unmigrated time section of line W3 (87NFW3) recorded across the western Swiss Alps (Figure 23-1b). The shaded areas represent the interpreted layer boundaries which were associated to the simplified velocity structure (step 2, Table 23-1) obtained from the refraction-based models (Figure 23-6). The circles represent synthetic reflections generated from 3D normal-incidence ray tracing through the Alpine model shown in Figure 23-15. The match between the synthetic and observed traveltimes gives a quantitative estimate of the degree to which 3D layer geometries influence the 2D seismic profile. Labeled boundaries are: B: uppermost crustal boundary; C1, C2: Conrad; M1, M2: Moho.

Upper crustal thickening by flake tectonics

The recent thickening of the upper crust across the Alpine axis can be attributed to the dynamics associated with the wedging of the Adriatic plate (Figures 23-19, 23-20 and 23-22). This appears to be generally occurring in a symmetric, fan-like geometry with both south- and north-vergent thrusting centered above the top of the wedge (Pfiffner et al., 1990b). The divergent relationship defined by the north-dipping Adriatic wedge and the shallower, south-dipping thrusting is a common feature observed in compressional belts and has been described as "flake tectonics" (Oxburgh, 1972), "wedge tectonics" (Price, 1981; 1986) and more recently as "crocodile tectonics" (Meissner, 1989) based on the observed "jaw-like" relationships between the wedge and thrust geometries. Contemporaneous dextral strike-slip motion has accompanied this north- and south-directed thrusting primarily along the Insubric Line (cf. Laubscher, 1983; 1984; Schmid et al., 1987; 1989). This style of deformation cannot be readily addressed in a model which is biased in the N–S direction, however, this dextral motion has played an important role in the crustal thickening process and may be responsible for exposing deep-seated blueschist-facies and eclogitic slivers (e. g. the Monte Rosa nappe) along brachyanticlinal structures during the late stages of collision (cf. Laubscher, 1991).

South-vergent thrusting

The NW-directed convergence between the European and Adriatic plates has been partitioned into both N–S thrusting and E–W strike-slip faulting (cf. Lacassin, 1989). A significant component of the partitioned south-directed backthrusting appears to be dominantly focused along the "southern steep belt" and the Insubric Line (Milnes, 1974; Heitzmann, 1987; Schmid et al., 1987; 1989; Bernoulli et al., 1990). Across the southern Swiss Alps, reflections associated with this mylonitic belt were recognized to merge or sole into the reflectivity outlining the Adriatic wedge (cf. line S1 in Figure 23-10b; Bernoulli et al., 1990). In the western Swiss Alps, the profiles do not extend far enough southward to cross the Insubric Line, however, reflections potentially associated with the steep belt encompassing the overturned Monte Rosa nappe and Sesia zone are observed to sole into the Adriatic lower crustal reflections (Figure 23-8, distance = 50–60 km, depth = 15–20 km). This implies a genetic relationship between the deformation developed along the wedge and the south-vergent crustal shortening which has occurred in the upper crust. Backthrusting is also documented in the Southern Alps which may be represented by the north-dipping shallow reflections observed throughout this region (Bernoulli et al., 1990).

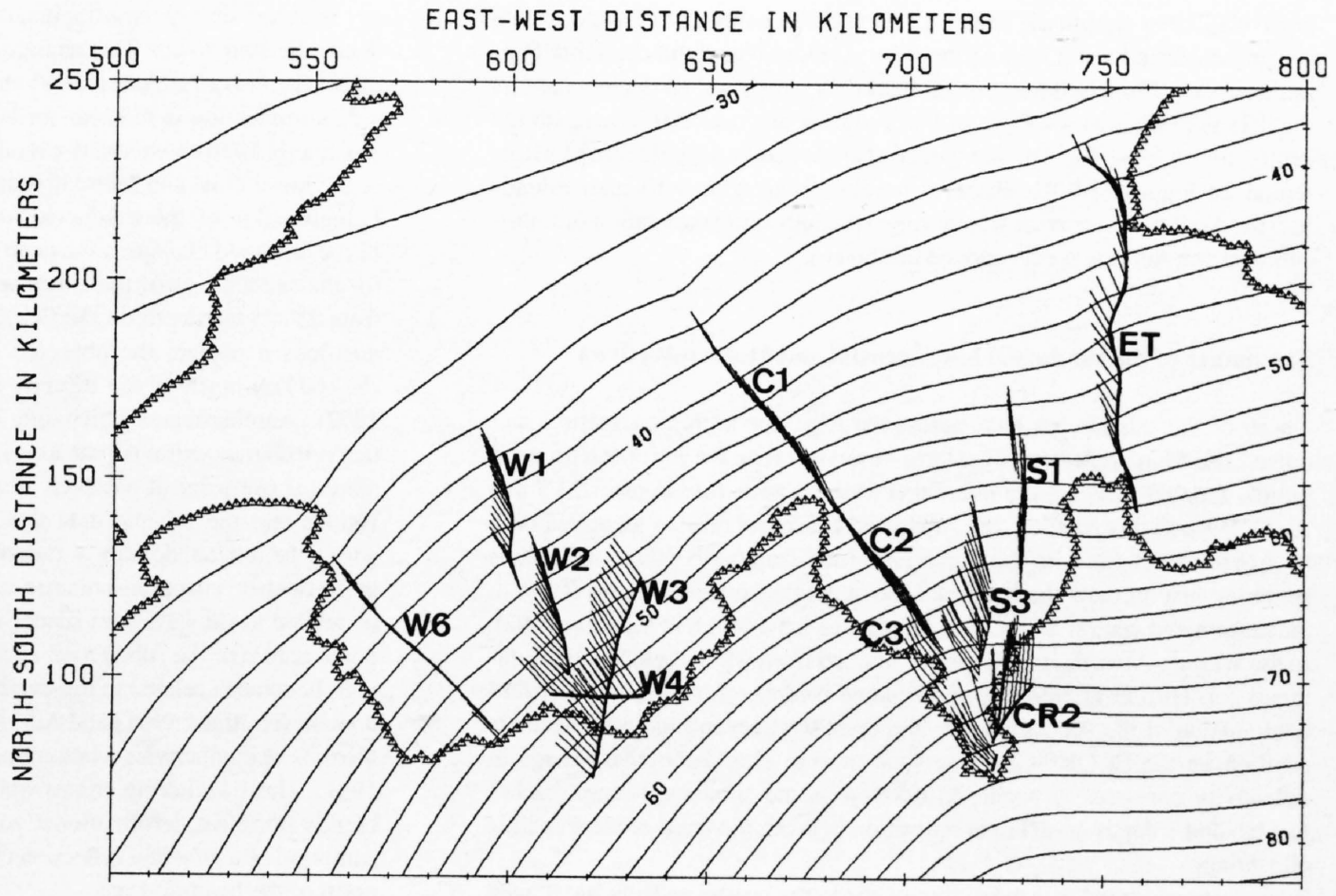

Figure 23-18
*Contour map of the European Moho (**M1**) surface with normal-incidence ray paths displayed in map view. Most of the simulated reflectivity off this modeled surface originates from out-of-the-plane locations. Contour interval = 2 km.*

North-vergent thrusting

The northward-directed response of the upper crust to the ongoing late-collisional Adriatic wedging is documented by the continued uplift of the internal (Penninic) zone of the Alps. The 3D trend of the basal Penninic thrusting is indicated by the steep slope which curves around the internal side of the exposed massifs (PF in Figure 23-21). This feature was constrained by both surface projections (Figures 23-9a and 9b) and by prominent south-dipping reflections observed on seismic profiles in both the eastern (Figure 23-7) and western Swiss Alps (Figure 23-8). Deeper detachments associated with the displacement of the external massifs may be represented by weaker subhorizontal reflections seen beneath the boundary (B). On both the eastern (Figure 23-7) and the Western Traverses (Figure 23-8) these types of reflections can be recognized north of the Adriatic wedge between depths of 10 to 15 km.

Analogous occurrences of deep-seated thrust faulting can be observed in outcrops of the Penninic nappes (Pfiffner et al., 1990a). This earlier deformation developed during the Late Eocene to Early Oligocene (Meso-Alpine orogeny) when these basement-cored nappes were buried at depths in excess of 30 km by the Austroalpine nappes (Frey et al., 1980; Hurford et al., 1989; see also discussion by Schmid et al., Chapters 14 and 22). Additional evidence for mid-crustal detachments can be found from the presence of at least two low-velocity zones beneath the Alps; one of which coincides with the subhorizontal reflections observed between depths of 10 and 15 km (e. g. Mueller et al., 1980). On the more recent EGT refraction profile, Ye (1992) and Ye et al. (1995) have modeled a second, shallower low-velocity zone beneath the Aar massif (Figure 23-5d). Mueller (1977; 1989) has proposed that these features represent zones of weakness which serve as decoupling horizons. He based this on the correlation of earthquake foci near their boundaries and suggested that both the low velocities and the earthquakes are most likely related to the presence of overpressured fluids in zones of pervasive granitic intrusions. These fluids may have originated from high-grade metamorphic reactions (e. g. devolatilization of micas; Hall, 1986) which have been trapped during subsequent cooling (Pfiffner et al., 1988). Mylonitic shear zones developed along these detachments may also contribute to the decrease in P-wave velocity and may also promote the reflective nature of these boundaries. In this view, the dynamics associated with the wedging of the Adriatic lower crust appears to take advantage of this rheologic structuring by using the zones of reduced shear strength as detachment planes. This leads to both a significant thickening of the crust by large-scale overthrusting of basement slices in the axial zone as well as to the propagation of stresses outward to deform the external regions (i. e. the Folded Jura Mountains and the fold and thrust belt beneath the Po Basin, Figures 23-22a and 22b).

In addition to the overthrusting, crustal shortening associated with the external massifs is enhanced by folding which is largely facilitated by ramp anticlines with overturned limbs (Pfiffner, 1985; Pfiffner et al., 1990b; Stäuble & Pfiffner, 1991). It is difficult to find direct seismic evidence for these features on the profiles largely because of their unfavorable steep orientations. However, through detailed modeling of the fold and thrust geometry, Stäuble & Pfiffner (1991) have shown that diffracted phases can account for the observed imbricated nature of the reflections associated with the proposed folded and faulted contact between the Aar massif and the sub-Alpine Molasse (see Figure 23-7).

Current uplift rates across the Alps document the ongoing deformation associated with the late collisional indentation of the Adriatic wedge (see discussion by Kahle et al. in Chapter 19). Gubler et al. (1981) have measured a distinctive pattern of maximum uplift rates from repeated first-order leveling which appears to be confined across the internal (Penninic) zone of the Alps (Figure 23-21). In addition, significant lateral variations in uplift rates are observed (Gubler et al., 1981) which attests to the variable dynamics involved in this flake-style of crustal thickening. From these results it appears that the entire Penninic allochthon has been uplifted in a vertical escape (Mueller, 1990) or "pop-up" fashion with both north- and south-vergent components of thrusting (Figure 23-22b; Merle et al., 1989; Pfiffner et al., 1990b; Pfiffner, 1990, 1992).

Lower crustal delamination and subduction

The wedging of the Adriatic lower crust appears to propagate along the transition from the European middle to lower crust which has responded by delaminating and subducting into the upper mantle (Figures 23-19, 23-20 and 23-22). This subduction geometry is defined by the shape of the European Moho (see Figure 23-12) which has been flexed downward by the continued loading of the thickened upper crust. The crust/mantle boundary is documented by the reflection data to reach depths exceeding 60 km beneath the overriding Adriatic microplate. The transport of lower crustal material into the upper mantle is supported by evidence of a dense, high-velocity lithospheric slab descending southward beneath the Alps and reaching into the asthenosphere (Panza & Mueller, 1979; Mueller, 1984; Mueller & Panza,1986; Spakman, 1986; 1990; Mueller, 1989). The ongoing crustal deformation may, in part, be enhanced by the resulting gravitational instability developed between the dense, eclogitized slab and the lighter asthenosphere as has been proposed for the Himalayas (Bird, 1978). The continual subduction of the mafic lower crust has the effect of pushing the bulk crustal composition towards a more intermediate level which may explain the relatively low average crustal velocity in the central part of the Alps (6.1–6.2 km/s).

Figure 23-23 shows an isopac map of the European lower crust determined from the 3D model. The main feature of this map is the thickening of the lower crust concentrated beneath the central Swiss Alps. This indicates that a significant amount of lower crust is stacked-up prior to being subducted into the upper mantle. In Figure 23-7, north-dipping reflections can be seen within the European lower crust which may be a manifestation of this stacking process. As will be discussed below, this localized thickening of the lower

crust may have significant influence on the shallower detachment system causing enhanced uplift of both the external massifs and the overlying Penninic nappes. The maximum crustal thickness which can be documented by the data is reached at the front of the wedge at just over 50 km beneath the central Swiss Alps. The Adriatic wedge also appears to have thickened in this region. In Figure 23-7 the observed north-dipping reflectivity also extends into the Adriatic lower crust which suggests southward propagation of imbrication as the Adriatic wedge moved northward.

The nature of the subducted lower crustal and Moho reflectivity

On all of the seismic transects across the Alps, the highly energetic lower crustal and Moho reflection signatures observed along the European foreland rapidly fade out beneath the internal (Penninic) zone (see Figures 23-7 and 23-8). Beyond this position, the subducted European crust is identified only by sparse reflections with the exception of the stronger bands of reflections resuming just north of the Insubric Line at depths between 50 and 60 km in the eastern and central Swiss Alps (cf. figures 8.5 and 8.8 in Valasek, 1992). In the Western Alps, deep reflections obtained from wide-angle fan measurements (cf. Hirn et al., 1989) provide some evidence for the southeastward continuation of the subducted foreland crust well beyond its last detectable position on the ECORS-CROP seismic profile. This distinctive change in reflectivity consistently begins to develop as the subducted crust reaches just beyond a depth of 40 km at a position beneath the front of the Penninic allochthon.

It has been proposed that the fading of the lower crustal reflectivity at deep levels of the Alps is the result of the chemical transformation of gabbros into denser eclogites which have P-wave velocities comparable to or exceeding upper mantle peridotites (Butler, 1986; Butler et al., 1986; Bois et al., 1989; Laubscher, 1988 and 1990). This phase change occurs over a rather large pressure interval (400–500 MPa) and the equilibrium curves defining the P-T conditions where this transition begins to occur depends largely on the bulk composition of the lower crust (e.g. 1.0–1.4 GPa and 600 – 800°C for intermediate to mafic constituents; cf. Green & Ringwood, 1972). Modeling of heat flow measurements along the EGT reveals an anomalously high temperature gradient developed across the Alps (e. g. Rybach et al., 1980; Pasquale et al., 1990). These results suggest that the appropriate conditions for the gabbro-eclogite transformation in the Alps are reached at depths of 40 km where the lower crust is subjected to temperatures in excess of 700°C and pressures greater than 1 GPa. Given this situation, the laminated lower crust of the European foreland may be altered to a more diffuse and irregular density structure during the eclogitization of the lower crust as it is subducted to depths beyond 40 km. This change from a laminated sequence of first-order discontinuities to a more gradational density structure would result in a significant reduction in the near-vertical incident seismic response (e. g. Braile & Chiang, 1986) which may explain the observed change in the reflectivity of the lower crust and Moho beneath the internal zone of the Alps.

Eclogitization of the subducted lower crust may be responsible for some of the observed change in the deep reflectivity; however, it does not account for the sudden loss of the entire sequence of lower crustal reflectivity (e.g. from 25–38 km depth on the ECORS-CROP profile, Nicolas et al., 1990b), nor does it explain the observed re-appearance of the deeper reflectivity (50–60 km) north of the Insubric Line (cf. figures 8.5 and 8.8 in Valasek, 1992). Another factor which may explain these latter reflection characteristics across the central Alpine axis is the onset of a strong Neo-Alpine deformational overprint. It has been clearly established from both surface observations and the seismic data that the crust becomes more heterogeneous within the internal domain of the Alps. In this situation, the consistent change in the deeper reflection signature at the front of the Penninic allochthon may be related to (a) wavefront scattering generated from the complex deformational nature of the subduction zone (Pfiffner et al., 1988) and/or (b) scattering phenomena related to the overlying complex structuring in the Penninic domain (Holliger, 1991) and Adriatic indenter (Pfiffner et al., 1990b) which disrupts the otherwise continuous wave fronts (Carbonell & Smithson, 1991). These scattering effects would be expected to diminish further south of this intensive deformational zone which may explain the observed resumption of a coherent reflection response defining the subduction zone just north of the Insubric Line.

3D Nature of the Uppermost Crustal Boundary (B)

The combination of the seismic data with well-known geologic structures exposed on the surface led to an initial approximation of the 3D geometry separating the uppermost crustal boundary (B) which outlines several key Alpine units. The resulting surface (Figures 23-19 and 23-21) outlines the distinctive arcuate trough occupied by the Penninic nappes. This allochthon was denudated by both north- and south-vergent thrusting as described in the previous section (Figure 23-22b).

The boundary (B) serves to separate an earlier episode of deformation which developed during the initial collision of the European and Adriatic plates (Meso-Alpine orogeny) from the more recent phase of late-collisional crustal shortening (Neo-Alpine orogeny). In the Penninic complex, the entire stack

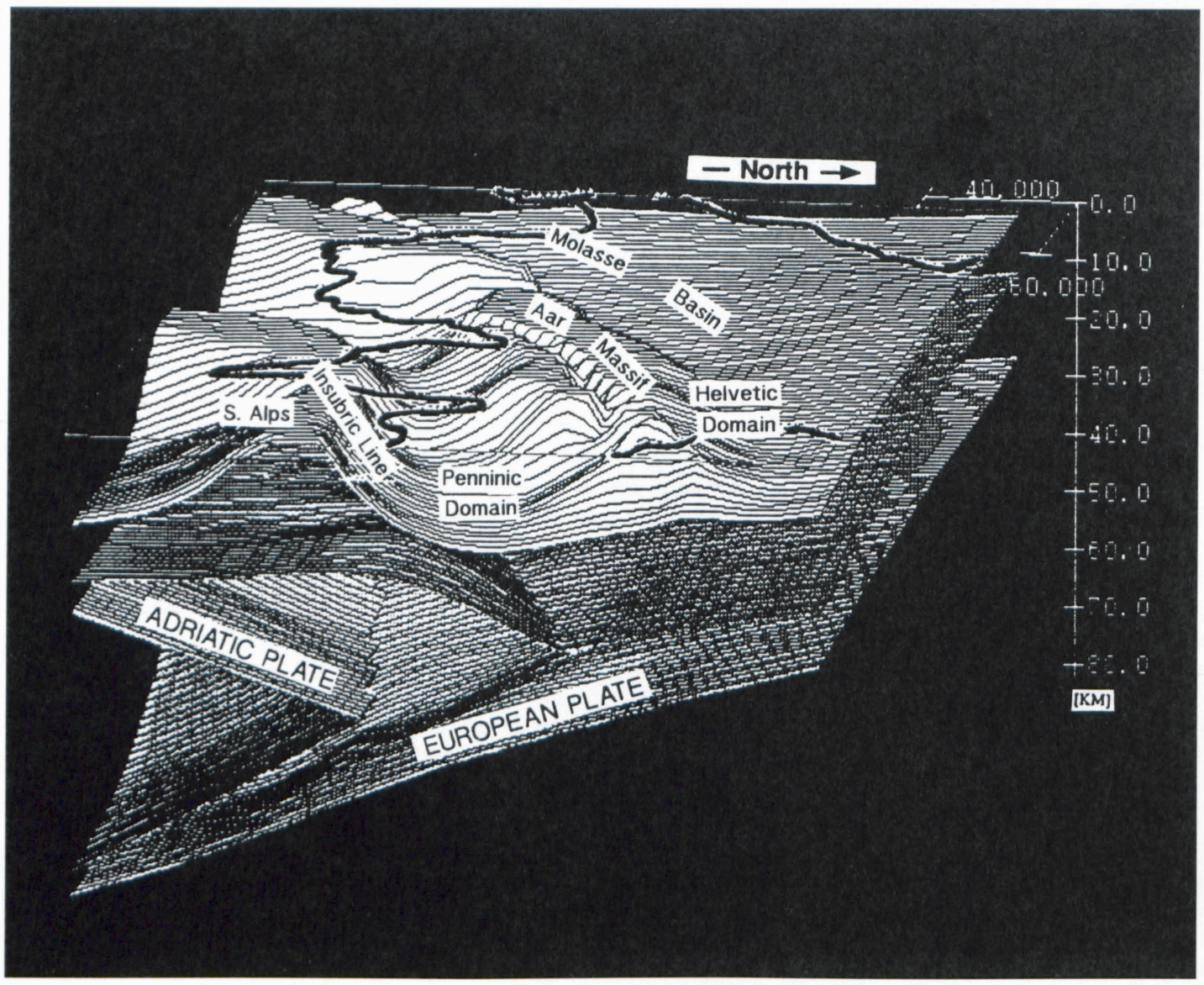

Figure 23-19
The initial 3D tectonic model of the Alps revealing the late-collisional wedging of the Adriatic plate (lower crust and uppermost mantle) into the subducting European plate (lower crust and uppermost mantle). The base of the Penninic nappes defines a deep trough bounded by the Insubric Line in the south and the external massifs in the north. These steep flanks define a bivergent system of folds and thrusts propagated by the continued driving force of the two Adriatic wedges below (cf. Figure 23-2a). View is from the east toward the southwest (vertical exaggeration = 1.5).

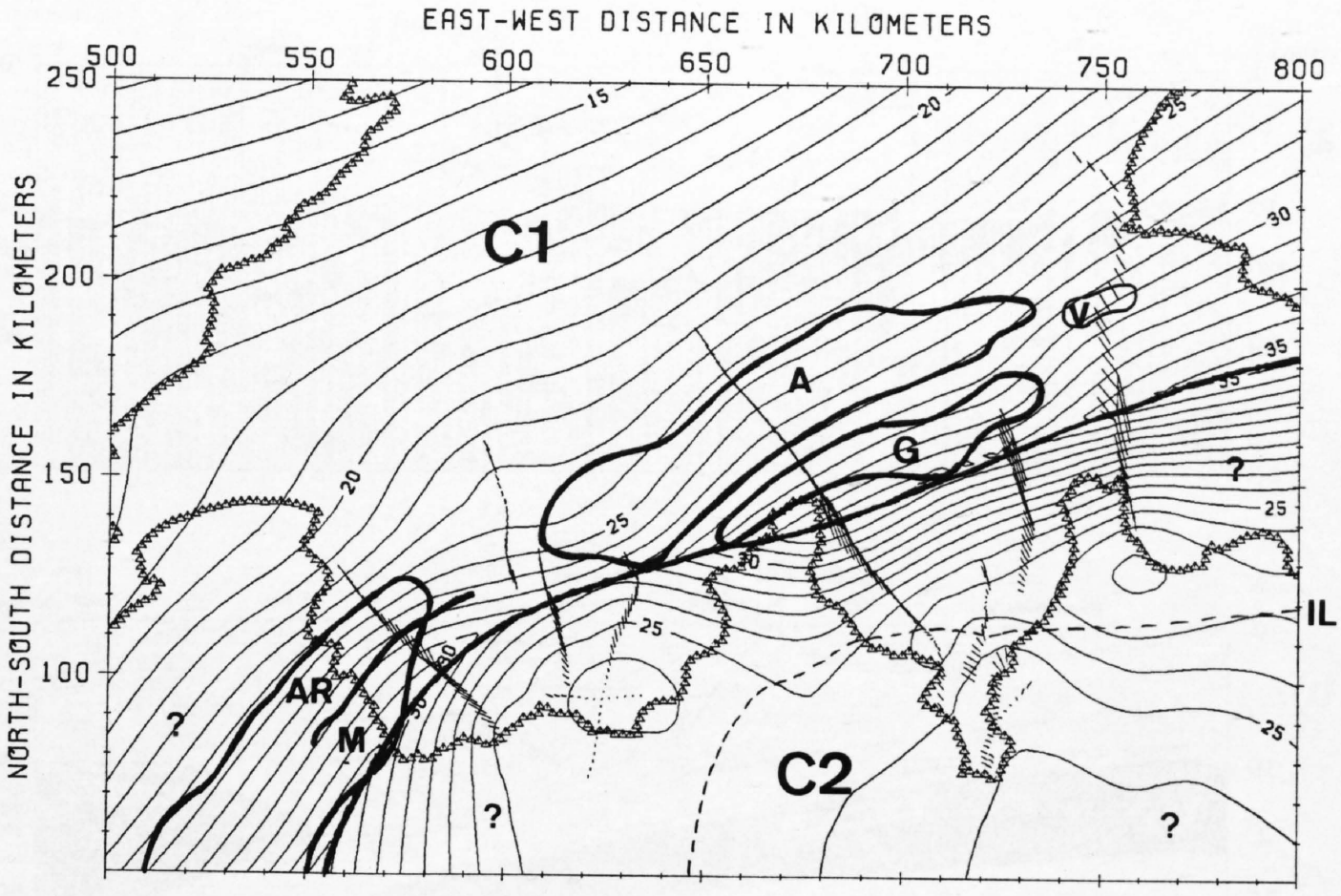

Figure 23-20
*Contour map showing the position of the top of the Adriatic lower crustal wedge (**C2**) and its northwestern limit (thick solid line) with respect to the top of the subducting European lower crust (**C1**). The outline of the external massifs and the Insubric Line (dashed) is also superimposed on this map. Contour interval = 1 km. Refer to Figure 23-21 for an explanation of the labeled units.*

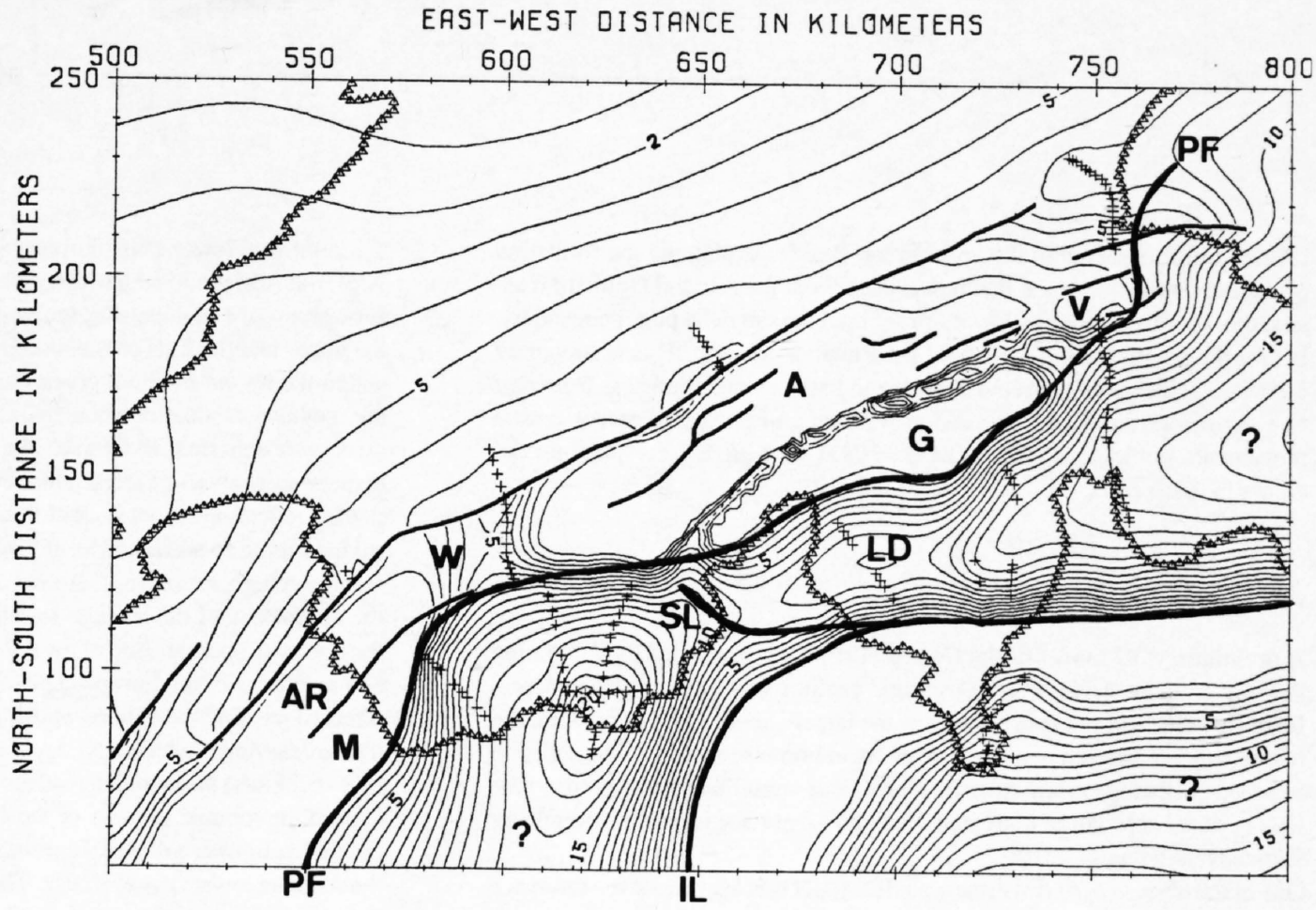

Figure 23-21
*Contour map of the boundary (**B**). **AR**: Aiguilles Rouge massif, **M**: Mont Blanc massif, **W**: Rawil axial depression, **A**: Aar massif, **G**: Gotthard "massif", **V**: Vättis window, **LD**: Lepontine dome, **SL**: Simplon Line, **PF**: Penninic Front, **IL**: Insubric Line (cf. Figures 23-9 and 23-10).*

of imbricated nappes appears to react rigidly as one interlocked unit in response to the more recent Neo-Alpine deformation; thus the subsurface extent of this boundary represents a major component of late-collisional structural modification.

The Lepontine Dome – a consequence of an overthickened lower crust?

The Lepontine dome occupies the central part of the Penninic complex and exposes the deepest nappes in the region. This culmination actually consists of two subdomes, the Toce in the west and the Ticino in the east, separated on the surface by the shallow, N–S trending Maggia synform (Merle et al., 1989). The Ticino dome consists of the granitic gneisses of the Leventina nappe and is flanked on the east by a plunging sequence of nappes. These thrust sheets dip around 25°E and consist of the successively higher nappes, Simano, Adula, Tambo and Suretta, which can be associated with reflections recorded on line E1 (see Figure 23-7, upper right corner, and Pfiffner et al., 1990b). The Toce dome is comprised of the Verampio nappe and its western flank is defined by the Simplon normal fault which dips between 25–30°SW (Mancktelow, 1985). Merle et al. (1989) propose that these differential culminations are the result of a polyphase deformational history involving dextral shearing and backthrusting along the north-dipping Insubric Line, backfolding along the northern boundary and lateral extensional escape along their margins (i. e. along the Simplon normal fault).

The 3D expression of the Lepontine dome is marked by an elongate high within the Penninic "trough" (Figures 23-19 and 23-21). The transition from this high to the base of the Penninic nappes of the western Alps is defined by a steep 30°SW slope which begins to plunge in the vicinity of the surface of the Simplon line, whereas in the east, the surface dips 24°E which is similar to the estimated dip prior to becoming more gradual at 10°E further east beneath line S1. Thus, the subsurface geometry of the boundary (B) obtained from the seismic data appears to corroborate well with the surface data. Furthermore, the location of the thickening of the European lower crust (Figure 23-23) coincides with this elongated doming as well as with the culminations of the external massifs to the north. This suggests that there may be a correlation between the excessive buildup of lower crust and the apparent in-

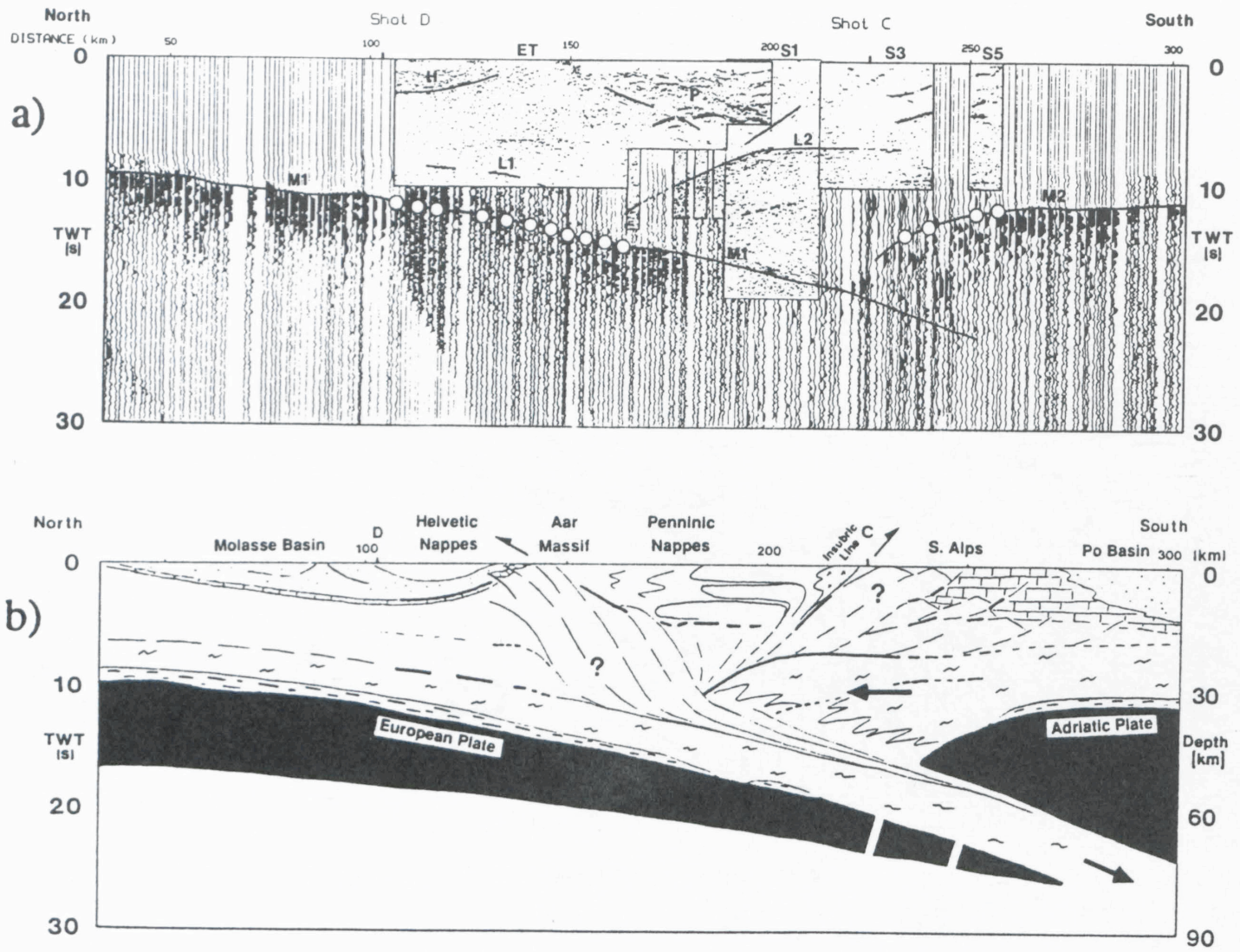

Figure 23-22
*a) Composite north-south section based on NMO corrected wide-angle and normal-incidence reflection data across the eastern Swiss Alps (ET = E1) with a correlation of the main crustal boundaries (L1 = **C1**, **M1**; L2 = **C2**, **M2**). **H**: Helvetic domain, **P**: Penninic domain. The white circles represent the superposition of the crust-mantle boundaries (**M1** and **M2**) obtained from the two different data sets. The distance scale is measured from EGT shot point E in the north (cf. Figure 23-1a).*
b) Schematic cross section along the Swiss segment of the European Geotraverse (EGT) illustrating the bivergent asymmetric thickening of the Alpine crust in response to the late-collisional wedging of the Adriatic lower crust and uppermost mantle above the subducting European crust and uppermost mantle (adapted from Valasek et al., 1991).

creased uplift observed in the upper crust. Besides explaining the formation of the Lepontine dome and the high exposures of the Aar and Gotthard massifs, this lateral variation in lower crustal thickness may, in part, be responsible for the neighboring axial low of the Rawil depression. This is supported by the coincidence of the rapid decrease in lower crustal thickness from east to west across the Rawil depression with measurements of recent crustal movements in the Alps (Gubler et al., 1981) showing a corresponding decrease in uplift rates.

23.6 Conclusions

A preliminary 3D model of the Central Alps was constructed by combining the results of the network of 2D seismic profiles with surface observations. Because of the low resolving power of the largely-spaced grid of profiles, the model was generalized to a three-layer crustal representation of the collision between the European and Adriatic plates. This simplified model outlines the lower crust and Moho of both plates and the subsurface nature of several key Alpine tectonic units.

One of the objectives of constructing a 3D model was to evaluate the influence of 3D effects on the 2D Alpine seismic profiles. To carry this out, the velocity model determined from the wide-angle reflection/refraction analysis, and subsequently used to depth-migrate the automatic line drawings of reflection elements, was incorporated into the three-layer Alpine model. Synthetic normal-incidence seismic profiles were then generated from the initial Alpine model and compared directly to the observed unmigrated seismic data. While the ray-path distribution demonstrated that out-of-plane reflectivity would be commonly encountered on the actual data, the direct comparison of the synthetic and observed data indicated that the large-scale characteristics of the collisional zone are adequately imaged and processed on the 2D profiles.

The initial 3D model of the Central Alps (Figure 23-19) supports the proposed Neo-Alpine, late-collisional mechanism involving the northwestward indentation of the Adriatic microplate into the subducting European plate (Laubscher, 1988; Mueller, 1989; 1990; Pfiffner et al., 1990b; Frei et al., 1989; 1990; ETH Working Group on Deep Seismic Profiling, 1991). Following the formation of a continuous orogenic belt in the Eocene, continued plate convergence led to the wedging of the Adriatic lower crust between the middle and lower crust of the European plate and the displacement of the European lower crust into the upper mantle. The symmetrical thickening of the Alpine crust which reaches outward into the external foredeeps appears to be genetically linked to this wedging process.

Across the northern margin of the Alps the reflection data consistently revealed a uniform south to southeastward plunge of the European Moho and the laminated lower crust. Further south beneath the internal domain of the Alps, the Adriatic indenter interrupts this regular trend by splitting apart the European crust and causing the lower crust to delaminate and subduct into the upper mantle. This crustal configuration in the eastern Swiss Alps is also supported by the Bouguer gravity anomaly (Holliger & Kissling, 1992) and the modeled subduction geometry corroborates with evidence of a subsiding dense lithospheric root beneath the Alps based on a regional surface-wave dispersion analysis of teleseismic events (Panza & Mueller, 1979). The degraded reflection response of the subducted lower crust in this region is attributed more to wavefield scattering (Pfiffner et al., 1990b; Holliger, 1991) than to eclogitization (e.g. Butler, 1986; Laubscher, 1988; 1990) based on the abruptness of this change in reflectivity developed consistently beneath the complex internal zone of the Alps. The continual displacement of the mafic lower crust of the European plate into the upper Alpine mantle has had the effect of pushing the bulk composition of the Alpine crust towards a more intermediate range which may explain the rather low average crustal velocity (6.1–6.2 km/s) measured across the Alps.

Within the internal domain of the Alps, consistent north- to northwest-dipping reflections at a depth of approximately 20 km were modeled as outlining the Adriatic lower crustal wedge. The large-scale east-to-west bending of this feature conforms to the arc of the Central to Western Alps which is expressed by the exposed tectonic units. This arcuate shape is most likely related to the average NW-directed motion of the Adriatic microplate (e.g. Dewey et al., 1973) with a counterclockwise rotation superimposed (e.g. Lowrie & Alvarez, 1975). This resulted in an oblique convergence which imparted both a significant east-west as well as a north-south component of deformation throughout the course of the Alpine orogeny. The position of the "Ivrea body" above the modeled Adriatic wedge suggests that this pre-orogenic, crustal-scale imbrication was emplaced at a shallow crustal level and carried northward within the overriding Adriatic plate during the course of the Alpine orogeny (cf. Schmid et al., 1987). The influence of pre-existing, crustal-scale dislocations appears to have been more extensive in the Western Alps compared to the Central Alps based on the multiple mantle wedges interpreted on the ECORS-CROP deep crustal profile (cf. Nicolas et al., 1990a and 1990b). Because of a lack of direct seismic evidence of the subsurface geometry of these features, they could not be included in this model of the Central Alps.

The upper crust of the Alps has reacted to the wedging of the Adriatic plate by forming a divergent system of folds and thrusts which has led to a considerable amount of crustal thickening. At the center of this system is the highly-deformed Penninic nappe complex which occupies the large, trough-like depression trending across the 3D Alpine model. This earlier-formed thrust complex has responded as a large-scale, rigidly-interlocked "pop-up" struc-

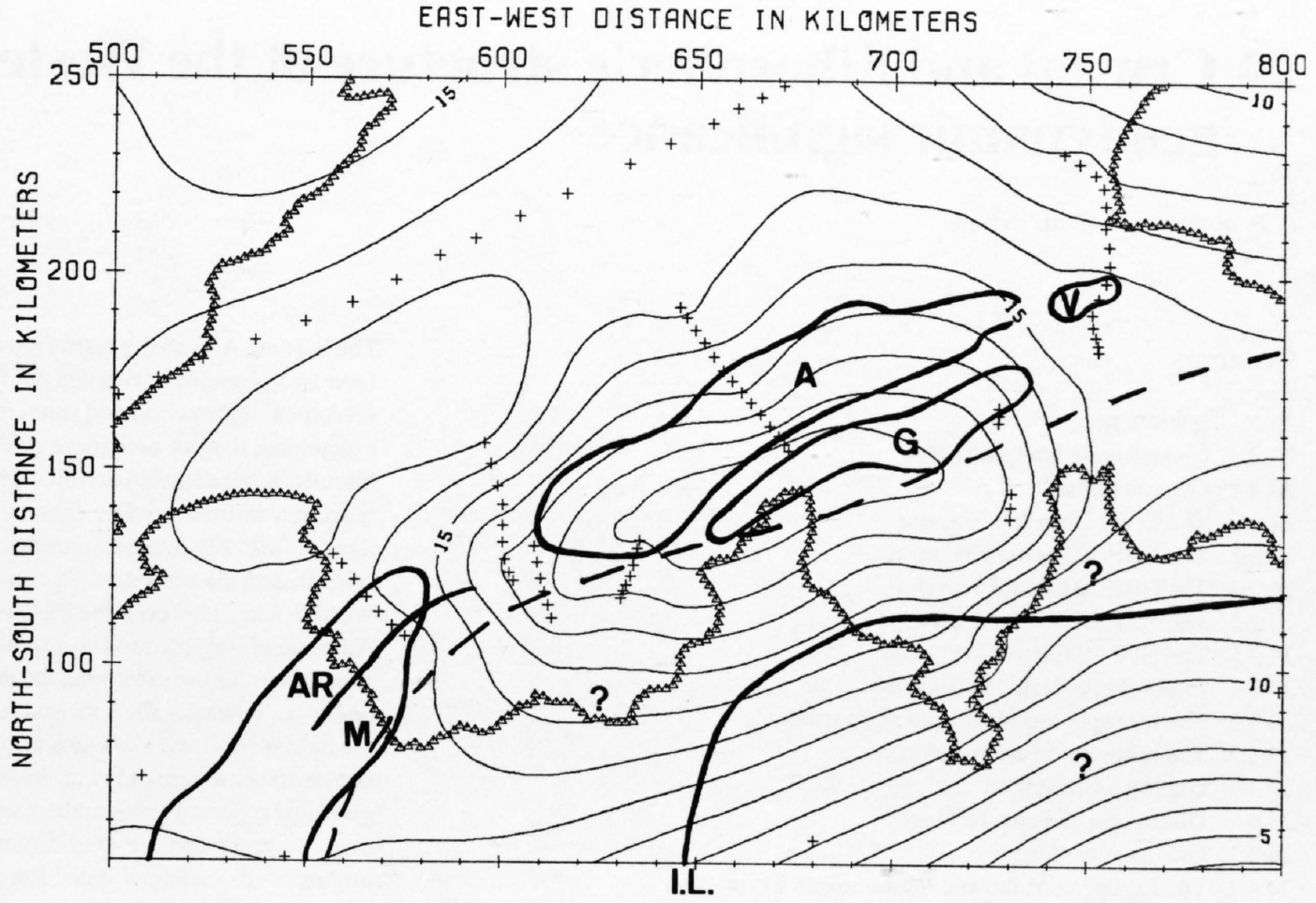

Figure 23-23
Isopach map of the European lower crust between C1 and M1. A distinctive thickening is developed beneath the central Swiss Alps and south of the external Aar (A) and Gotthard massifs (G) which are superimposed. Also shown is the trace of the northernmost extent of the Adriatic lower crustal wedge (thick dashed line). The thicknesses outside of the region encompassed by the seismic profiles are unconstrained (I.L. = Insubric Line). Contour interval = 1 km. Refer to Figure 23-21 for an explanation of the labeled units.

ture to the underlying wedging deformation with displacements extending outward to more external regions in the north and south (e.g. Pfiffner et al., 1990b; see Schmid et al., Chapters 14 and 22). The uplift of the external massifs, which form the prominent culminations in front of the Penninic trough, is a recent manifestation of the north to northwestward component of this displacement. Recent geodetic measurements (Gubler et al., 1981) reveal maximum uplift rates concentrated within the internal zone of the Alps which attests to the continued late-collisional response of the upper crust to the wedge-related stresses. During the early stages of this late-collisional deformation, south-vergent thrusting, backfolding and dextral strike-slip motion were all concentrated near the Insubric Line which defines the southern limit of the modeled Penninic allochthon. More recently, the tectonic stresses have been transferred externally which has led to the development of major backthrusts within the Southern Alps. Along the Alpine axis, the axial culminations of the Aar and Gotthard external massifs and the Lepontine dome in the Penninic domain appear to be associated with an anomalous increase in the thickness of the European lower crust developed in front of the encroaching Adriatic wedge.

The initial 3D crustal model of the Central Alps outlines and explains several important features of this collisional zone. The asymmetric subduction complex provides an efficient means of removing the excess mass of crust built up during plate convergence, and the large-scale wedging of the Adriatic lower crust establishes a viable mechanism for producing the symmetric thickening of the Alpine crust which radiates outward into the external foredeeps of the Molasse and Po Basins. Despite the unsurpassed efforts in imaging the deep structures of a continental collision zone, these integrated results provide only a general 3D tectonic framework of the Central Alps. Many important questions surrounding more specific relationships between the tectonic units and structures remain to be refined by further data and more detailed studies.

23.7 Summary

A synoptic (integrated) interpretation of the network of deep crustal seismic profiles across the Central Alps has led to the development of an initial three-dimensional (3D) tectonic model of this collisional zone. The extensive seismic data base used to constrain the 3D model was primarily comprized of a grid of refraction and reflection profiles acquired through the National Research Program NRP 20. The unified interpretation of these data centered around the observation of a consistent crustal-scale reflection pattern on a majority of the NRP 20 profiles crossing the Alpine axis. This regionally correlatable distribution of reflectivity was interpreted as outlining an orogenic belt involving the collision of the European and Adriatic plates subdivided into three crustal layers: an uppermost crustal layer distinguishing several key tectonic units, and the upper and lower crust extending to the crust/mantle boundary. A 3D model of the Alps depicting the variation of these three layers across the Central Alps was developed based on the refraction-based velocity models and the depth-migrated reflection profiles. A subseqent analysis of potential geometric errors introduced by constructing a 3D model directly from 2D depth profiles was carried out by normal-incidence ray tracing. This investigation revealed that while distortions are introduced, they are insignificant when considering the large-scale crustal features of the Alpine orogen. From this initial 3D model of the Central Alps, several fundamental tectonic relationships can be drawn. Namely, the resulting 3D configuration of the Central Alps depicts a wedge of the Adriatic lower crust and a wedge of the Adriatic upper mantle penetrating into the European plate. The European crust appears to have responded to these stresses by delamination and subduction of its lower crust into the upper mantle. At shallower levels, the crust is thickened by massive overthrusting in response to the late-collisional dynamics of the underlying Adriatic wedges. The rigidly interlocked Penninic allochthon occupies an arcuate trough across the internal zone of the Alps and appears to be displaced upward in a vertical-escape fashion with thrusts radiating outward toward more external regions in both the north and south. The initial 3D crustal model of the Central Alps outlines a late-collisional tectonic framework which accounts for the observed Neo-Alpine uplift and shortening, and the corresponding subduction of the European lower crust.

Acknowledgements

The authors would like to thank the numerous colleagues and students who helped throughout the various stages of this program. In particular, Peter Finckh is acknowledged for his work in data acquisition and establishing the data processing center at the ETH. The cooperative efforts together with CROP-Italia were instrumental in extending our observations across key areas of the Alps. The project benefited considerably from assistance of Scott Smithson and other collaborators from the University of Wyoming who were supported by US National Science Foundation grants EAR-8300659 and EAR-8419154. Critical comments by Scott Smithson, Adrian Pfiffner and Peter Heitzmann and the two reviewers Rolf Meissner and Gérard Stampfli helped substantially to improve this paper. Contribution No. 890 ETH-Geophysics, Zürich, Switzerland.

24 Crustal and lithospheric structure of the Western Alps: geodynamic significance

R. H. Marchant & G. M. Stampfli

Contents

24.1 Introduction

The first part of this chapter presents a comparison of the various deep seismic traverses shot through the Western Alps at a crustal-scale. The second part concentrates on a lithospheric-scale interpretation of some of these traverses, based on tomographic images and gravity modelling. One of the points is to highlight similarities and differences which occur along the arc of the Western Alps and to relate these to the geodynamic evolution of this mountain belt. Thus this chapter is closely related to Chapter 17 (Stampfli & Marchant) which presents a broad review of the geodynamic evolution of the Western Alps.

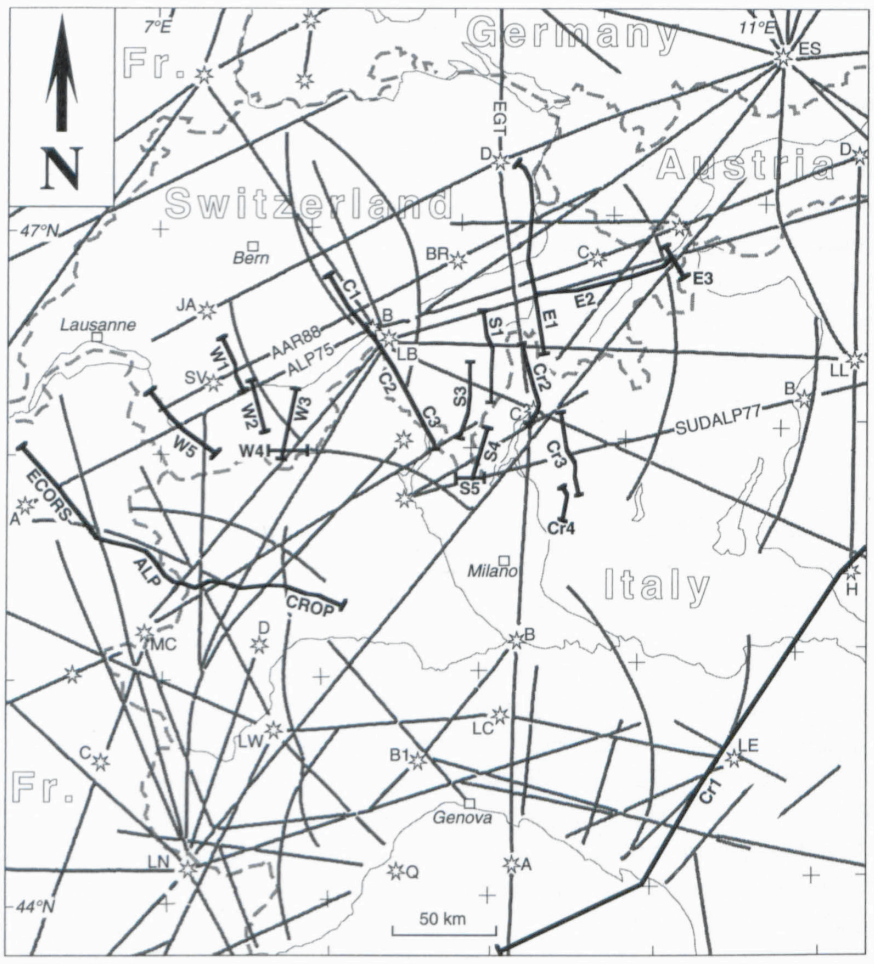

Figure 24-1
Location map of the deep-seismic reflections profiles (thick black lines) and the refraction lines (finer lines; stars = main shots) shot in the Western Alps (modified from Giese & Buness 1992).

The Western Alps are by far the most extensively studied orogen in the world. Over two centuries of detailed field work has provided an impressive sum of geological information and furthermore this mountain belt is covered by an exceptional density of seismic profiles (see Figure 24-1): several thousands kilometres of refraction-seismology and about a thousand kilometres of deep reflection-seismic profiles shot by French (ECORS), Italian (CROP) and Swiss (NRP 20) research groups. This exceptional density of crustal-scale seismic data allows a detailed comparison of structures along the arc of the Western Alps. However, the great number of published interpretations of the Alpine deep-seismic profiles makes a direct comparison of these rather awkward. Even for the same line, the proposed interpretations can differ considerably, so much for the concepts (tectonic style, implications on the geodynamic evolution, etc.) so much also for graphical reasons. Therefore we have chosen to show here only our preferred interpretations, drawn with the same graphical style and at the same scale to facilitate a direct comparison between them. In particular, we used different patterns to highlight the geodynamic origins of the structural units: European, Valais, Briançonnais, Piemont and Adriatic. We would also like to point out that this contribution is not an official synthesis of the NRP 20 project and the reader is referred to the other chapters of this volume for alternative interpretations.

The approach behind our interpretations was the following: first we interpreted the nappe-system, in particular in the Penninic domain along the Western and Eastern Traverses (Marchant 1993). It then became less equivocal to understand deeper structures at a crustal-scale, not only along these two traverses, but also along the other deep seismic profiles surveying the Western Alps. As these profiles are separated only by a few tens of kilometres (for location, see Figure 24-1), it is most likely that their interpretation will show striking similarities. Therefore the results of the interpretation of one individual traverse helped us to understand the structures of neighbouring profiles. Furthermore we made sure that our interpretations are consistent with the gravity field and with tomographical models at a lithospheric-scale, as well as with the overall geodynamic evolution (Stampfli & Marchant, Chapter 17).

24.2 Crustal-scale interpretation

24.2.1 General remarks

Five crustal-scale interpretations are presented here, starting in the west with the Ecors-Crop Alp traverse and then going progressively to the east with the NRP 20 traverses: the Western, Central, Southern and finally the Eastern Traverse. As detailed interpretations of the nappe-system along most of these profiles can be found throughout this volume, our comments will focus mainly on crustal-scale features. Furthermore, as most of this contribution is a summary of a Ph.D. thesis (Marchant 1993), the reader is referred to this work for additional information.

The quality of data available along these profiles varies; for example, thanks to the European GeoTraverse, there exists a far denser network of refraction seismology data along the Eastern Traverse, as compared to the other traverses. Furthermore, only the Ecors-Crop Alp Traverse crosses the whole Alpine belt, therefore a few assumptions have to be made when extending the other profiles.

24.2.2 The Ecors-Crop Alp Traverse

The Ecors-Crop Alp deep seismic traverse was shot in 1986 and 1987 (Bayer et al. 1987) and as this profile is not described elsewhere in this book, we will comment it in more detail than for any of the other profiles. This traverse starts in the Bresse graben and finishes in the Po plain (for location, see Figures 24-1 and 24-2). It has the advantage of being a continuous profile made up of 6 individual near-vertical-reflection seismic lines (Damotte et al. 1990) completed by a wide-angle reflection seismic survey (ECORS-CROP Deep Seismic Sounding Group 1989a & 1989b; Thouvenot et al. 1990). The wide-angle reflections (Thouvenot et al. 1990; Sénéchal 1991) are plotted in Figure 24-3a by projecting them onto a depth-migrated section of the near-vertical

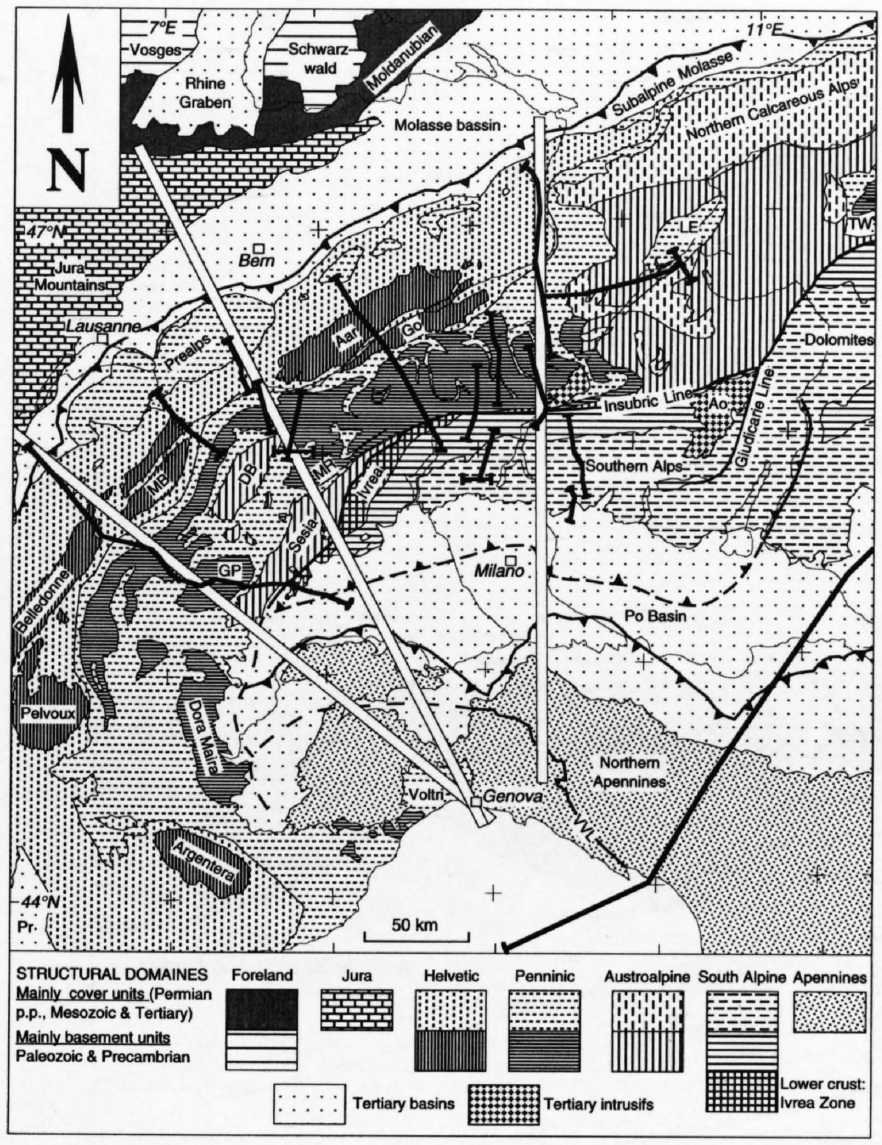

Figure 24-2
Tectonic map (modified from Berthelsen et al. 1992), with location of the deep seismic profiles (black lines) shot in the Western Alps and location of the three lithospheric cross-sections (white lines) of Figure 24-9. Ao = Adamello intrusions; DB = Dent Blanche nappe; Go = Gotthard massif; GP = Grand Paradis massif; LE = Lower Engadine window; MB = Mont Blanc massif; MR = Monte Rosa nappe; Pr = Provence basin; TW = Tauern window; VVL = Villalvernia–Varzi–Levanto line.

reflection survey (Sénéchal & Thouvenot 1991). Unfortunately part of this wide-angle survey is located 50 km south of the deep seismic profile (Figure 24-1) and as these data were recorded using a fan layout, depths and velocities cannot be determined accurately. However this survey (Figure 24-3a) clearly images an east-dipping European Moho, which reaches a depth of 50 km below the Penninic thrust. A high-velocity body is found at mid-crustal level in the Penninic domain (the "Briançonnais" reflection) and another sharp velocity discontinuity at 15 km below the Sesia zone (the "Sesia-Lanzo" reflection). Just south of the Insubric line, the Adriatic Moho is interpreted to show a staircase-like structure tending towards an upwards flexure, thus bringing the Adriatic Moho very close to the surface.

Along the External Alps, the near-vertical seismic section (Figure 24-3a) shows a good reflectivity in its upper part, a rather transparent upper-crust and a highly reflective lower-crust. In the Penninic domain, the upper half of the crust is very reflective down to the depth corresponding to the wide-angle "Briançonnais" reflection, which according to the ECORS-CROP Deep Seismic Sounding Group (1989b) could act as a mask preventing the seismic energy from penetrating deeper. The Austroalpine domain is transparent down to the "Sesia-Lanzo" reflection, which is not surprising as the Austroalpine main structures at the surface are sub-vertical in this area. East of the Insubric line, the Adriatic crust generally shows good reflectivity. Additional seismic information can also be gained by consulting the coherency-weighted migrated section of Mugnier & Marthelot (1991).
Up to now over a dozen different interpretations have been published (Bayer et al. 1987; Guellec et al. 1989, 1990a & 1990b; Mugnier et al. 1989 & 1990; Bois & Ecors Scientific Party 1990; Polino et al. 1990; Tardy et al. 1990; Butler 1990a; Nicolas et al. 1990a & 1990b; Mugnier & Marthelot 1991; Ricou & Dauteuil 1991). Some of these interpretations are very different, in particular in the Penninic domain. This is partly due to the fact that most of these interpretations were established before any good migrated sections were available.
The interpretation of the Ecors-Crop Alp Traverse (Figure 24-3b) presented here ranges from the Molasse basin to the Po plain. In the external Alps, this interpretation differs from previous ones (Guellec et al. 1989, 1990a & 1990b; Mugnier et al. 1989 & 1990) mainly by a more pronounced allochthony of the Bornes and Aravis nappes. Epard (1990) has shown that these nappes are equivalent to the Morcles nappe and that they find their homeland on the Internal Belledonne massif and not on the External Belledonne massif. Another difference with Roure et al. (1989) and Mugnier et al. (1990) is that the Roselend nappe is not regarded as Ultrahelvetic (as indicated on some tectonic maps) but as an equivalent of the Wildhorn nappe s.l. (J.-L. Epard pers. comm.), which should find its homeland at depth towards the east. The paleogeographic position of the Wildhorn rim-basin north of the European margin shoulder (Stampfli 1993; Stampfli & Marchant Chapter 17) implies the subduction of the whole European margin s.str. (at least 100 km of thinned crust).

The internal Alps along this traverse do not lend themselves to detailed interpretation, as shown by the extremely varied interpretations published up to now. Probably the main reason for this is the difficulty in projecting surface geology at depths greater than 5 km. This is due, in part, to the shallow valleys and the relatively weak axial plunges when compared to the Central Alps. Therefore the interpretation of Figure 24-3b is partly based on a extrapolation of the structures observed along the Swiss Western traverse, located 50 km to the NE, in an area where the control from surface geology is much better. The interpretation of the Western Traverse (Du Bois et al. 1990; Marchant 1993; Marchant et al. 1993; Steck et al., Chapter 12) has underlined the importance of backfolding, not only for the Southern Steep Belt but also for the external crystalline massifs. Geochronological data (Hunziker et al. 1992; Steck & Hunziker 1994) clearly show that the Southern Steep Belt's backfolds (formed around 30 to 18 Ma) preceded the external crystalline massifs backfolding (around 12 Ma). This last folding event is thought to be expressed on the deep seismic profiles by a bunch of north-dipping reflections situated at a depth of 15 to 20 km on the W5 line and 11 to 18 km on the W2 line (Steck et al., Chapter 12). Similar reflections are found on the Ecors-Crop Alp line at a depth of 15 to 22 km and various interpretations have been proposed. By analogy with the Swiss Western Traverse, these north-dipping reflections are interpreted here as the overturned limb of a large-scale backfold of the Belledonne massif.
The Valais suture zone, underlined by high-amplitude reflections due to contrasting lithologies, can easily be followed from the surface down to a depth of about 15 km under Val d'Isère. In that area many superposed reflections show opposite dips. This could be caused by 3-D effects due to a change of 60° in the orientation of the seismic line (see Figure 24-1). From there on, this strong-reflectivity strip continues nearly horizontally to the east up to beneath Noasca, where it becomes more transparent, suggesting the presence of basement units which could belong to the European margin. These units, as well as those situated above them, are affected by the large-scale backfold system of the Alpine Root zone.
The Briançonnais and Piemont units are nearly impossible to project to depths greater than a few kilometres (Deville 1990; Deville et al. 1992). Therefore the extrapolation presented here is ill constrained. Our interpretation was guided by analogies with the interpretation of the nearby NRP 20 Western profiles (see Steck et al., Chapter 12); we tried to attribute the strong reflections either to ophiolitic slivers or marble/crystalline contacts (which can also yield high-amplitude reflections) and the transparent areas to basement nappes.

At a depth of 15 km under the Sesia zone, a very strong 15 km long reflection appears nearly horizontal at the same location as the "Sesia-Lanzo" reflection detected by the wide-angle shot D (Thouvenot et al. 1990). Such a high-amplitude reflection could well be caused by the contact between the Sesia zone and the Lanzo lherzolites. This intensively refolded contact outcrops 20 km south of the seismic line and shows a northward dip (Spalla et al. 1983). Being of the same lithology as the Ivrea mantle body (a part of the Adriatic upper-mantle), the Lanzo lherzolites and serpentinites will not produce any significant reflectivity along the Insubric line. Nearly vertical at the surface, the Insubric line at depth could dip either towards the east or the west (Tardy et al. 1990). All the other deep seismic lines crossing the Insubric line have shown that this accident has a listric shape dipping towards the N or NW and flattening out at a depth of 30 to 40 km. Therefore this accident is prolonged here towards the west and down to a depth of 30 km to match a few west-dipping reflections truncated by the strong reflections associated with the top of a high-velocity body (called "mantle slice" in Figure 24-3b). The presence of this high-velocity and dense body, detected by the wide-angle survey (ECORS-CROP Deep Seismic Sounding Group 1989b), is also implied by gravity data (Bayer et al. 1989). Although its velocity and density cannot be determined precisely, it corresponds most probably to a sliver of upper-mantle (Nicolas et al. 1990a).
As mentioned above, this mantle slice could act as a mask preventing the seismic energy from penetrating deeper, which could provide a good explanation for the absence in Figure 24-3a of any significant reflection below a depth of 30 km under the Penninic domain. Nevertheless the coherency-weighted migration of Mugnier & Marthelot (1991) in this area shows a few

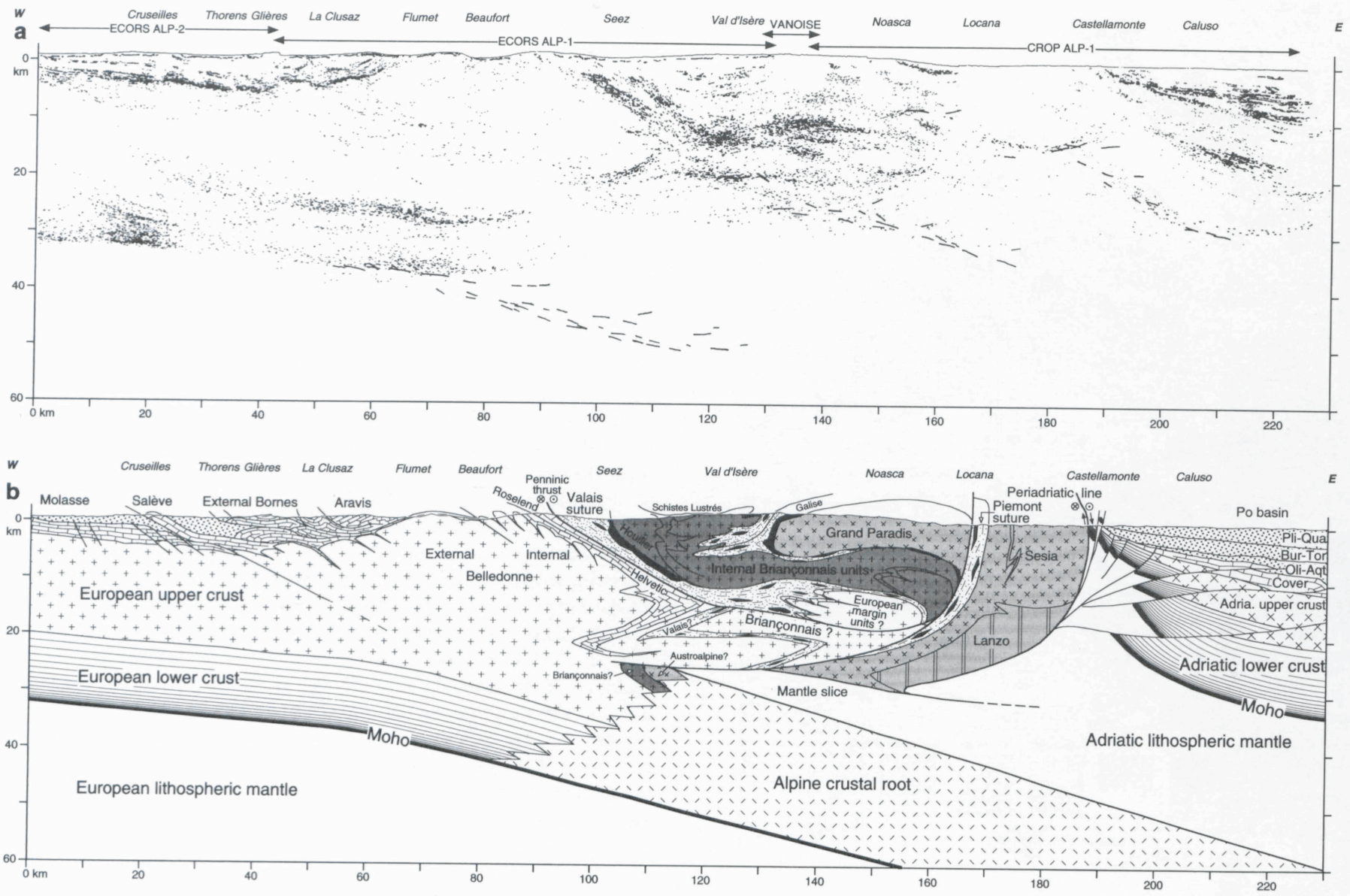

Figure 24-3
The Ecors-Crop Alp Traverse.
a) Depth-migrated section (after Sénéchal & Thouvenot 1991) with projections of the migrated wide-angle data (thicker and longer reflections; after Thouvenot et al. 1990; Sénéchal 1991).
b) Crustal-scale interpretation.

slightly-east-dipping reflections, more or less parallel to the trend of the European Moho. These reflections are interpreted here (Figure 24-3b) as due to the Alpine Crustal root (the crustal material subducted during the continental collision). This material therefore corresponds to European crust, to the Briançonnais and Austroalpine terranes and to the Valais and Piemont suture zones. The Alpine Root zone is thus in an overturned position above the "mantle slice" and below it is refolded back into a normal position, similar to the crustal-scale interpretation of the Swiss Western Traverse (Marchant 1993; Marchant et al. 1993; Steck et al., Chapter 12).

On the eastern side of the Insubric line, the Adriatic Moho is clearly defined both on the vertical and wide-angle migrated sections (Figure 24-3a). From a depth of around 30 km at the end of the line, the Adriatic Moho bends upwards up to a depth of about 20 km near the Insubric line. From there onwards the Moho discontinuity is segmented by a series of west-dipping reverse faults, showing an asymmetric flower structure. Locally the Adriatic upper-mantle even reaches the surface, as witnessed by the peridotitic outcrops near Castelmonte.

A detailed interpretation of the Po plain part of the Ecors-Crop Alp line is published by Roure et al. (1990) on the basis of a conventional migrated section on which unfortunately the Adriatic Moho is hardly visible. Down to a depth of 10 km the interpretation shown here (Figure 24-3b) is very similar to theirs, with a rather transparent Plio-Quaternary sequence overlying the Messinian erosional event underlined by a strong reflection. Under this reflection, one finds relatively undeformed Burdigalian to Tortonian deposits yielding well stratified reflections. Near the eastern end of the section, the contact between the Burdigalian unconformity and the Oligo-Aquitanian Gonfolitic Group can be calibrated by exploration wells (Roure et al. 1990). The Mesozoic and Paleogene sediments, whose thickness varies between 0 and nearly 5 km (Roure et al. 1990), could correspond to the stratified reflections found at a depth of 7 to 10 km near the end of the line. They overlie a rather thick transparent zone which becomes suddenly highly reflective at a depth between 12 and 17 km. Roure et al. (1990) have interpreted these as Mesozoic sediments, implying a reduction of the Adriatic crust to a thickness of just a few kilometres, which is most unlikely. We prefer the interpretation relating these reflections to the transition from the upper- to lower Adriatic crust.

24.2.3 The NRP 20 Western Traverse

This traverse is discussed in more detail by Steck et al. (Chapter 12) and is composed of 5 individual lines (W1–W5; Figure 24-4) scattered in an area covering the Prealps to the Insubric line (for location, see Figure 24-1 and 24-2; for an extensive introduction to the geology of this area, see Escher et al. Chapter 16). They do not form a continuous line but rather a network of complementary and intersecting profiles, which has the advantage of constraining the interpretation thanks to some 3-D information. Nevertheless, this traverse has two disadvantages: it does not image the southern side of the Insubric line and it is poorly surveyed by refraction data. In the external Helvetic zone, the Western Traverse intersects three longitudinal refraction profiles (see Figure 24-1). In the Penninic Alps, the traverse runs parallel to the Brig-Sesto refraction profile compiled by Ansorge et al. (1979); it is situated 40 km to the NE of the deep seismic profiles. This refraction model is rather old and would need to be reinterpreted taking into account possible 3-D effects. However it shows a high-velocity body at 29–37 km below the Monte Rosa nappe and some curious velocities for the Ivrea mantle body (5 km/s), that might be due to serpentinization, a process which can drastically reduce the velocity of peridotitic material.

Crustal-scale interpretations of the individual NRP 20 Western profiles (W1–W5) can be found in Marchant (1993), Marchant et al. (1993), Steck et al. (Chapter 12) and Pfiffner et al. (Chapter 13.1). On the basis of these individual interpretations we have drawn a synthetic geological cross-section along the Western Traverse. This synthetic profile starts in the Molasse basin, follows the W1 and W2 lines, intersects the W3 and W4 lines at Zermatt, and then continues down to the Po plain, where it nearly reaches the eastern end of the Ecors-Crop Alp traverse (for location, see map in Figure 24-1 & 24-2). The structures of the Molasse basin and the Prealps are based on surface-geology projections; Pfiffner et al. present in Chapter 8 interpretations of this area based on industry seismic lines. The structure of the external basement massifs is also discussed by Pfiffner et al. in Chapter 13.1. The reader is referred to the above mentioned publications for a detailed account on the interpretation of the individual profiles on which this synthetic section is based. As this synthetic cross-section (Figure 24-4d) approximately follows the Rawil–Valpelline axial depression, it is possible here to project with confidence surface-geology down to considerable depths (eg. Escher et al., Chap-

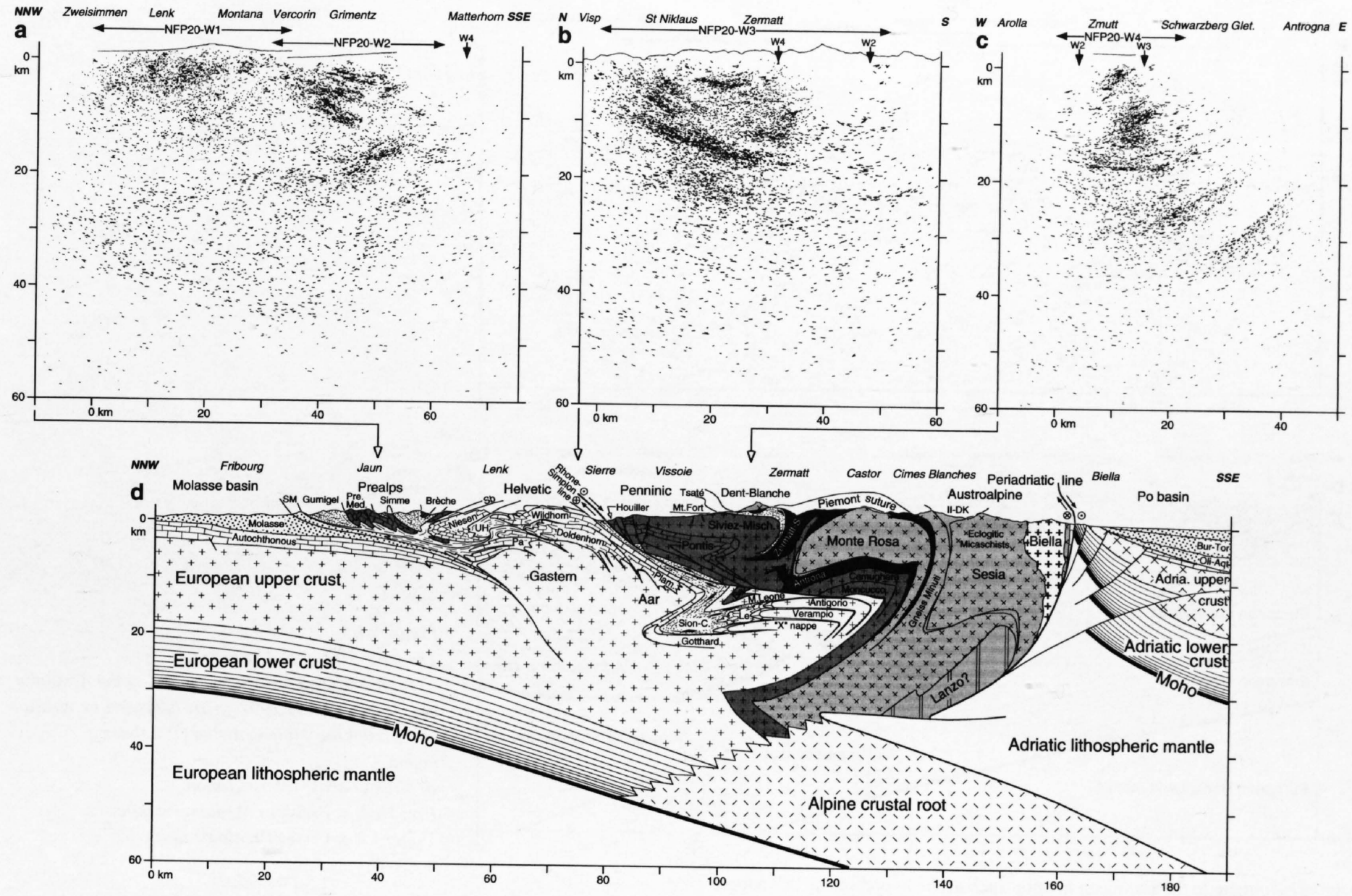

Figure 24-4
The NRP-20 Western Traverse.
a–c) Combined (Vibroseis and dynamite data) depth-migrated sections of the W1–W2, W3 and W4 profiles (Marchant 1993).
d) Crustal-scale interpretation along a synthetic cross section of the Western Traverse, for location, see fig. 24-2. Be = Berisal unit (Pontis nappe); II-DK = 2nd Diorite Kinzigite unit; Le = Lebendun nappe; Pa = Parautochthonous cover units; Pre. Med. = Préalpes Médianes nappe; SM = Subalpine Molasse; UH = Ultra-helvetic nappes; "X" = hypothetical nappe.

ter 16). Already in 1916, Argand used this information to extrapolate the nappe structure in this region down to depths of about 20 km. In this sense, the nappe-system along our synthetic cross-section is much better constrained than along the Ecors-Crop Alp Traverse. However, this is not the case for deeper structures, such as the "mantle slice", where one lacks detailed geophysical information on its geometry. Its existence here is indicated by the presence of a high velocity zone (6.8 km/s) detected by refraction seismology (Ansorge et al. 1979). In particular, the European lower-crust and Moho can be seen on the stacked sections of the dynamite data ?(Valasek 1992? and Plates 12-3 and 12-5) to subduct smoothly down to depths of around 50 km beneath the Penninic and Austroalpine nappes. The associated reflectivity then peters out, which is possibly due to eclogitization processes. The deep structures near the Insubric line are based on a projection of the interpretation of the W4 profile (Marchant 1993; Marchant et al. 1993; Steck et al. Chapter 12) which images an area situated 20 km to the NE of our cross-section. If the Austroalpine domain seems very large here, this is due to the obliquity of the synthetic section with regard to the Sesia zone. It is quite probable that at depth this zone gives way to the Lanzo peridotites, in the same way as on the Ecors-Crop Alp Traverse (Escher et al., Chapter 16). The structure of the Adriatic plate is based on our interpretation of the Ecors-Crop Alp profile which is situated less than 20 km from this cross-section.

24.2.4 The NRP 20 Central Traverse

This traverse is discussed by Pfiffner & Heitzmann in Chapter 11 and comprises three individual deep seismic lines (C1–C3) constituting a nearly continuous line from the front of the external Alps to the Southern Alps (for location, see Figures 24-1 and 24-2). The seismic section of Figure 24-5a is a combination of a section from Valasek (1992, figure 7.7) and a depth-migration of a line-drawing from a preliminary stacked section (P. Lehner pers. comm.) which has the advantage of outlining the main reflections (thicker and longer lines). As this data was acquired using single-fold dynamite shots, the first few seconds of the data yield little information. More detailed Vibroseis sections of the near-surface can be found in this volume in the contribution of Pfiffner & Heitzmann (Chapter 11). This traverse is very close to the "Swiss Geotraverse", a compilation of refraction data along a profile starting near Basel and finishing near Chiasso (Mueller et al. 1980). This profile provides for the Penninic domain the following velocity data: below some rather low-velocity layers (5.3 to 6.3 km/s), a high-velocity layer (6.7 km/s) appears at a depth of around 30 km, overlying a thick low-velocity zone (5.9 km/s), which at a depth of 45 km gives way to a thin layer yielding a velocity of 6.6 km/s typical of the lower-crust. Additional refraction data can be found on strike lines which intersect the northern part of this profile (Baumannn 1995; Maurer & Ansorge 1992).

Our interpretation of the Central Traverse (Figure 24-5b) is based mainly on the dynamite data as the Vibroseis data has a rather low signal to noise ratio. Additional information regarding this traverse can be found in Chapter 11 (Pfiffner & Heitzmann). Our interpretation (Figure 24-5b) starts in the Subalpine Molasse and then crosses a klippe of Penninic nappes. These units, not imaged on the seismic section, are projected from surface geology. At a depth of 8 km under Meiringen, some nearly horizontal reflections mark the contact between the Aar and Gastern massif. At a depth of 15 km under the same locality, a strip of south-dipping reflections probably underline the frontal thrust of the external crystalline massifs on the autochthonous European crust (a contrasting interpretation with regard to these reflections is discussed by Pfiffner et al., Chapter 13.1, and Pfiffner & Heitzmann, Chapter 11). Further to the SE, the structures become more sub-vertical and therefore units such as the Urseren zone and the Gotthard "massif" are not imaged. In the Val Bedretto an antiform-backfold affects all units, putting them in an overturned position with a dip of 70° to the NW (e.g. Probst 1980). From surface-geology data it is not possible to calibrate the amplitude of the synform-backfold which brings these units back into a normal position.

Further to the SE, the Antigorio nappe is doubled by a series of backfolds with an axis nearly parallel to the seismic line (Huber 1981; Steck 1990). Under this nappe, a transparent zone can be related to the Verampio nappe. Its base is underlined by a strong south-dipping reflection, probably due to a strip of metasediments separating the Verampio nappe from other basement

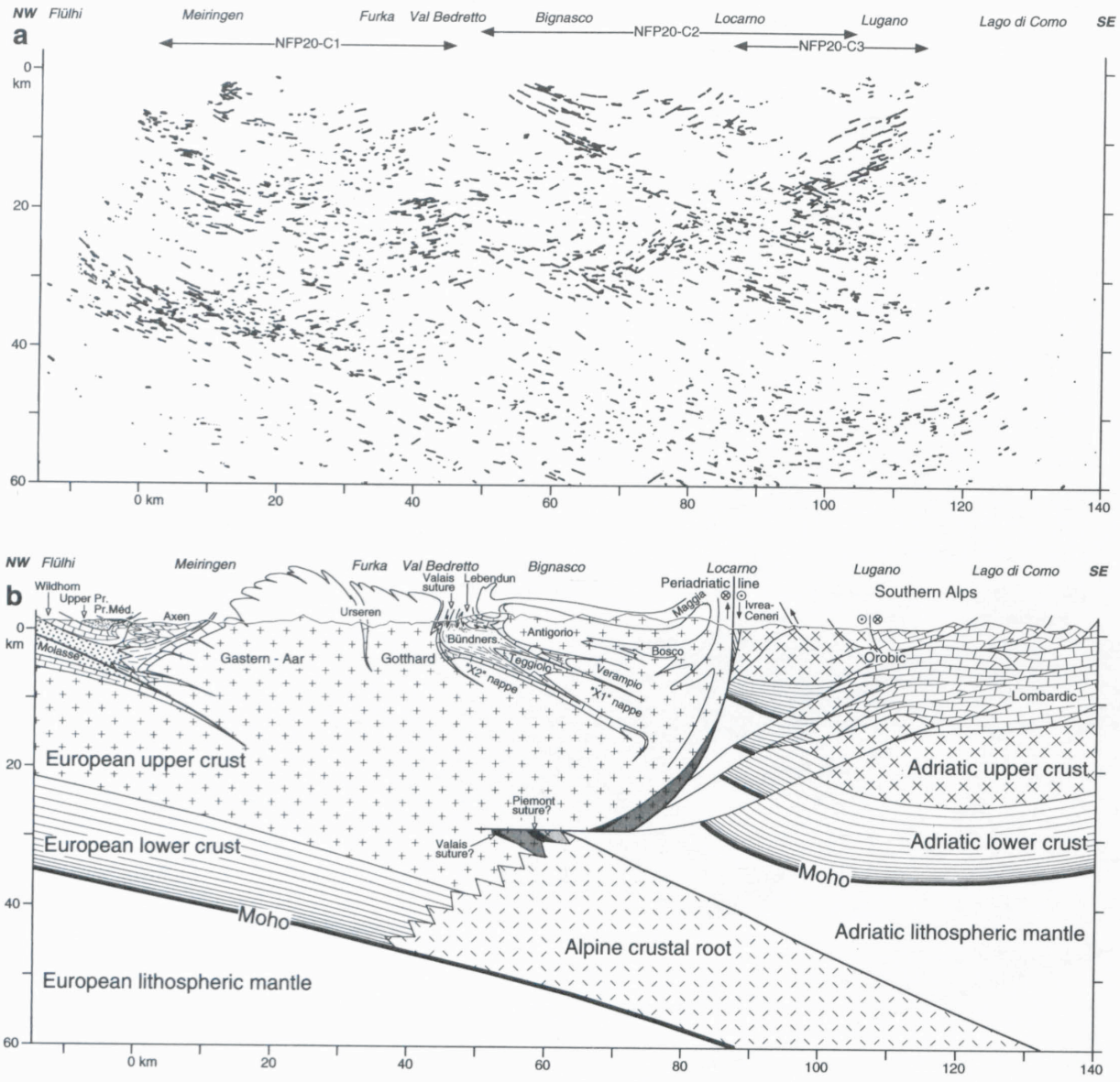

Figure 24-5
The NRP-20 Central Traverse.
a) Depth-migrated section overlaying the dynamite data (after Valasek 1992, figure 8.7) with a migration of a preliminary line-drawing (P. Lehner pers. comm.).
b) Crustal-scale interpretation.
Pre. Med. = Préalpes Médianes nappe;
Upper Pr. = Upper Prealpine units.

units belonging to the European margin, such as the hypothetical "X" nappe. Just north of the Insubric line, the Southern Steep Belt could be refolded at a depth of 10 km as the presence of some sub-horizontal reflections suggest. Such a structure can be expected, as the backfolding of the Southern Steep Belt shows at the surface an "en échelon" pattern of backfolds (Steck 1990, figure 4).

The Insubric line and the Southern Steep Belt, vertical at surface, can be traced down to a depth of 30 km along a set of high-amplitude reflections showing a listric shape oriented towards the NW. At depths around 30 km beneath Bignasco some strong reflections seem to outline a similar (though smaller) structure to the "mantle slice" observed on the Ecors-Crop Alp traverse. Its position coincides with the high-velocity layer detected by refraction seismology (see above). As on all the other Alpine profiles, the European lower crust and the Moho discontinuity are subducted towards the SE, accompanied by metamorphosed parts of the Briançonnais and Austroalpine terranes and relics from the Valais and Piemont oceans (the Alpine Crustal root), which would correspond well to the low-velocity layer detected on the refraction profile.

The reflections situated under the Southern Alps correspond extremely well to the structures predicted from surface geology on the cross-sections of Schumacher (1990 and Chapter 10). In particular the north-dipping reflections below Lugano highlight the basement thrusts typical of this part of the Southern Alps (for additional information see Schumacher, Chapter 10). Beneath Como, refraction data locate the Adriatic Moho at the depth of 34 km. From there onwards to the NW, we follow it upwards as a kind of staircase coinciding with the high-amplitude reflections reaching a depth of 22 km below Locarno. In contrast, other authors (Valasek 1992, figure 8.8; Pfiffner & Heitzmann, Chapter 11; Schumacher, Chapter 10) have interpreted the Adriatic Moho as a NW-plunging surface, reaching a depth of 45 km below Locarno. We believe such an interpretation to be rather unlikely as their Moho does not correspond to any significant reflections.

24.2.5 The NRP 20 Southern Traverse

This traverse is described in more detail by Schumacher in Chapter 10 and is composed of several individual lines surveying the Penninic domain and the Southern Alps in Ticino. Only an interpretation of the S1 line (for location, see Figures 24-1 and 24-2) is presented here on the basis of a depth-migration (Figure 24-6a) processed by Valasek (1992). This line is a crucial profile because it images the structures related to the Insubric line. Several very similar interpretations have been published for this line (Frei et al. 1989; Bernoulli et al. 1990; Bernoulli & Bertotti 1991; Heitzmann et al. 1991) but always on the basis of unmigrated data. A stacked section showing such steeply dipping

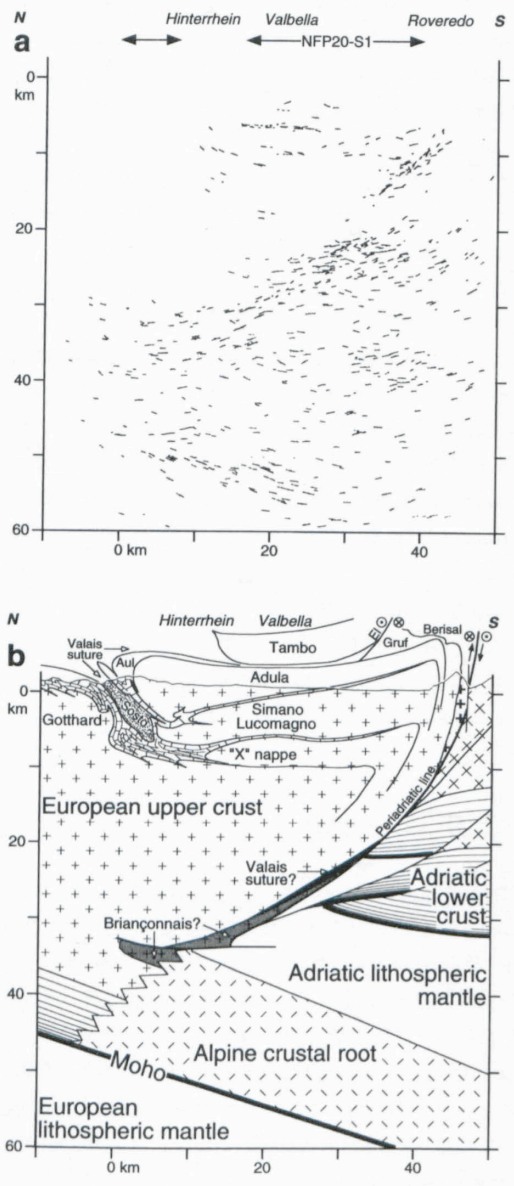

Figure 24-6
The NFP-20 S1 profile.
a) Depth-migrated section (after Valasek 1992, fig. B16)
b) Crustal-scale interpretation of the S1 profile.
EL = Engadine line.

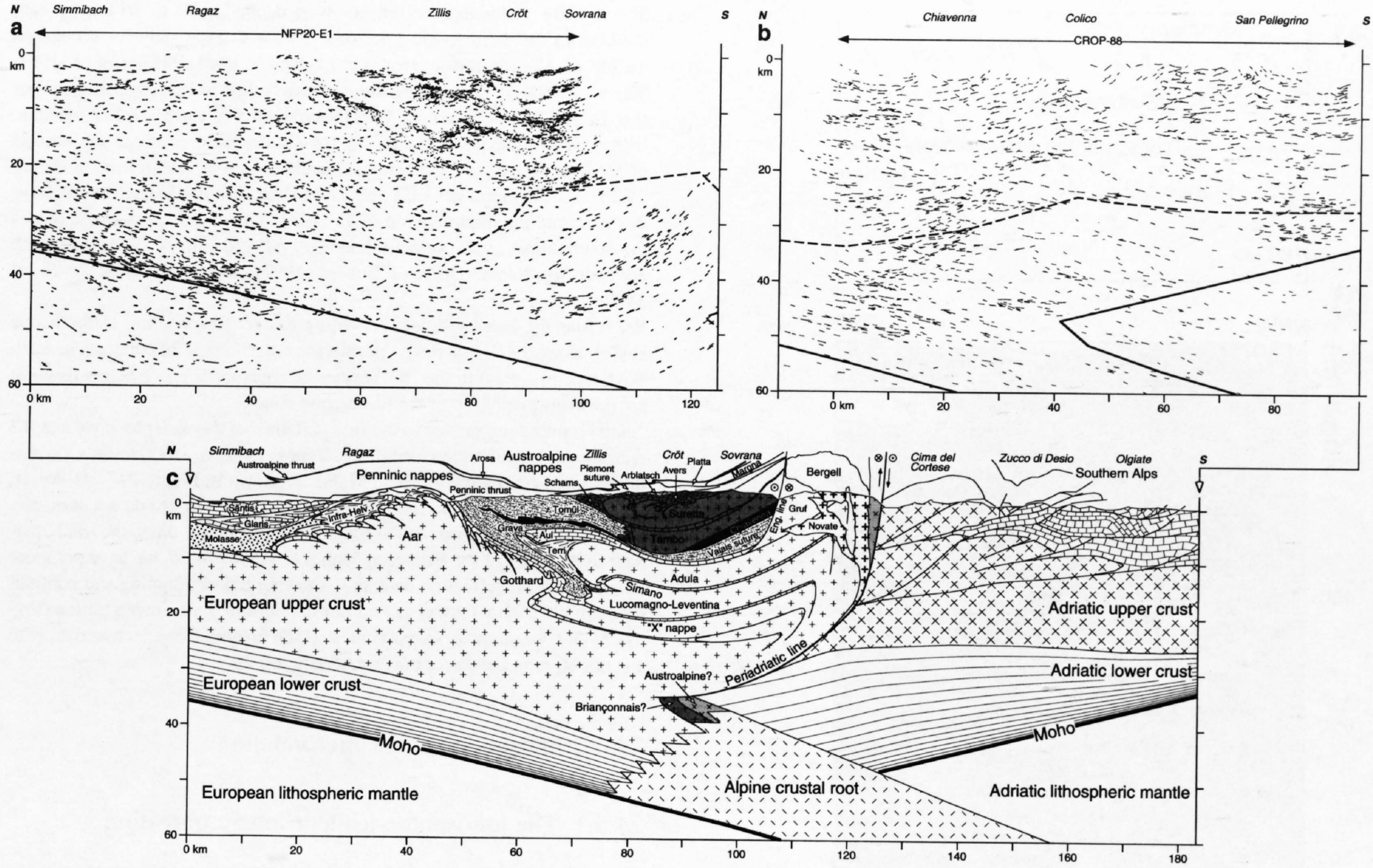

Figure 24-7
The NRP-20 Eastern Traverse.
a) Depth-migrated section of the E1 profile (after Valasek 1992, figure B9) with an overlay of the migration of the Vibroseis data in the Penninic domain (Marchant 1993, figure 6-19). The thick line corresponds to the European Moho and the dashed line to the Conrad discontinuity as determined by the modelling of the EGT refraction data by Ye (1992).
b) Depth-migrated section of a line-drawing (Cernobori & Nicolich 1994) of the CROP-88-2, -3 and -4 lines. The thick line corresponds to the European and Adriatic Moho and the dashed line to the Conrad discontinuity as determined by the modelling of the EGT refraction data by Buness (1992).
c) Crustal-scale interpretation (Southern Alps after Schönborn 1992, figure 61).

reflections can induce significant interpretation mistakes; migration will change considerably the position and dip of the reflections. Furthermore the Southern Traverse has been most often interpreted by combining it with the Eastern Traverse (Holliger 1990; Ansorge et al. 1991; Valasek et al. 1991; Valasek 1992). Such a combination, a horizontal projection of the Southern traverse onto the Eastern Traverse can be misleading and therefore each line needs to be interpreted separately, as has been done by Schumacher (Chapter 10)

Hardly any reflections image the near-surface structures of the northern end of the line, but in this region surface geology can be projected down to a depth of a few kilometres (Probst 1980), showing a slightly backfolded Gotthard "massif" (Figure 24-6b). As proposed by Frei et al. (1989), the strong and horizontal reflections at a depth of 7 km below Valbella are very likely to correspond to the base of the Simano-Lucomagno nappe. The contact of this nappe with the Adula nappe is not imaged on the seismic section as it lies too close to the surface. Two nearly horizontal reflections packages at a depth of 10 and 12 km beneath Hinterrhein and Valbella suggest the possibility of the presence of one or two extra basement nappes ("X" in Figure 24-6b), unknown at the surface (Bernoulli et al. 1990).

The Southern Steep Belt and the Insubric line can be followed northwards down to a depth of 35 km; they are underlined by a highly reflective band, which corresponds well to the contrasting lithology of the Southern Steep Belt. The European Moho is well defined here, even down to a depth of 60 km. The Adriatic Moho, located at a depth of about 30 km, a few km south of the line by refraction data, is not clearly imaged on the reflection seismic section (Figure 24-6b). The migrated section does not show a north-dipping Adriatic Moho as the stacked section would suggest, but rather a slightly south-dipping and fragmented Moho outlined by a strip of reflections situated at a depth of 28 to 30 km. The profile is located about 20 km to the east of the end of the Ivrea mantle body, therefore probably only a little Adriatic upper mantle material is uplifted by reverse faults as was the case with the previous traverses.

24.2.6 The NRP 20 Eastern Traverse

This traverse follows closely the European GeoTraverse (EGT, Blundell et al. 1992) and results from seismic refraction modelling are shown in Figure 24-7. From the Helvetic nappes to the Periadriatic line, this traverse is covered by the NRP 20 E1 profile (Figure 24-7a). The CROP-88-02, -03 & -04 deep seismic profiles (Montrasio & Sciesa 1994) image the area from the Penninic nappes down nearly to the Po plain. Numerous interpretations have been proposed for the E1 profile (see ref. in Marchant 1993, p. 52); Pfiffner & Hitz present in Chapter 9 detailed interpretations of this profile and of the E2 to E9 lines, which cover the area east of the E1 profile.

One of the differences with the interpretation of the NRP 20 E1 from Pfiffner & Hitz (Chapter 9) and Schmid et al. (Chapter 22), is that we believe the southern side of the external crystalline massifs to be slightly backfolded (Figure 24-7c), as proposed also by Schmid (1992) and Montrasio et al. (1994), who followed interpretation C of Pfiffner et al. (1990b). In Figure 24-7c, two sets of north-dipping reflections can be seen at depths around 15 km in the area below Zillis: slightly to the north and slightly to the south of this locality. The latter most probably correspond to the front of the Simano nappe, as shown by 3-D seismic modelling (Litak et al. 1991 & 1993). We interpret the more northern reflections as the overturned limb of the Gotthard "massif", which is restored in a normal position below the "X" nappe. Along this profile, the amplitude of the backfolding of the southern side of the external crystalline massifs is smaller than on the profiles further to the west, which agrees well with the Tertiary geodynamic evolution proposed by Stampfli & Marchant (Chapter 17).

Even though, thanks to the EGT, geophysical data is abundant along this traverse, the interpretation of the Periadriatic line and the Adriatic indenter has yielded many different solutions. This is mainly due to the fact that the Periadriatic line is near-vertical at the surface, thus it is not imaged by reflection seismology. However, assuming a listric shape for this structure as seen on the previous profiles, its extension at depth could correspond to any of the north-dipping reflections situated at depths between 20 and 40 km beneath

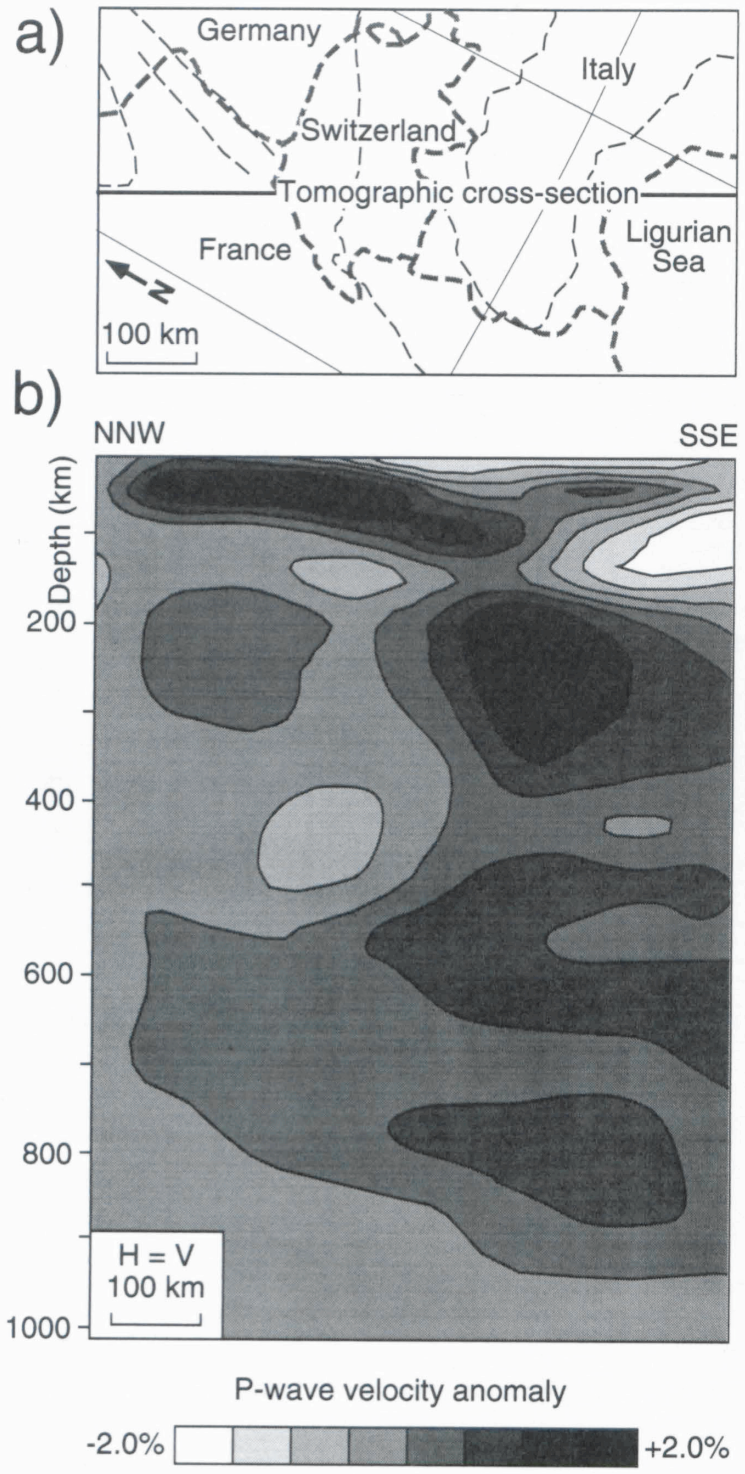

Figure 24-8
Tomographic cross-section (W. Spakman pers. comm) along the NRP-20 Western Traverse from the EUR89B model (Spakman et al. 1993).
a) Geographic map; the central line corresponds to the location of the cross-section.
b) Tomographic cross-section.
c) Interpretation.

Sovrana. By attributing the reflections at depths of 20 to 30 km beneath Sovrana to the Periadriatic line, one defines a large indenter composed mainly of Adriatic lower crust (i.e. Laubscher 1990; Pfiffner et al. 1991; Schmid 1992). By considering the Periadriatic line to be deeper and steeper (i.e. Butler 1990b; Marchant 1993), one defines a much smaller indenter. Unfortunately gravity modelling is not discriminant: compare the models of Holliger & Kissling (1992) and Marchant (1993; shown here in Figure 24-15). Furthermore, the EGT refraction data does not help either to solve this problem: the interpretation of Ye (1992) shown in Figure 24-7a, places the lower-upper crust velocity-boundary at a depth of 20 km beneath Sovrana; the interpretation of Buness (1992), shown in Figure 24-7b, at 35 km.

We favour the latter solution: according to our interpretation of the nappe system along the S1 and the E1 profile, the reflections at 20 km depth beneath Sovrana correspond to the "X" nappe, thus one needs space below this unit for the overturned limb of the Alpine root zone.

Another ambiguity related to the interpretation of this indenter concerns the Adriatic Moho: refraction modelling (Buness 1992; Ye 1992) reveals a north-dipping and continuous Adriatic Moho, as shown in Figure 24-7. However, in this area, the CROP-88 reflection profiles (Figure 24-7b) do not show any north-dipping reflections: on the contrary, all reflections dip to the south, parallel to the trend of the European Moho. In Figure 24-7c, we have put more emphasis on the refraction data, thus showing a north-dipping and continuous Adriatic Moho. Further on, for our lithospheric scale interpretation (Figure 24-9c), we show an interpretation which favours the reflection data with a south-dipping but discontinuous Adriatic Moho.

24.3 Lithospheric-scale interpretation

24.3.1 The lithosphere-asthenosphere transition

Three lithospheric cross-sections of the Western Alps are presented here: one in the area surveyed by the Ecors-Crop Alp deep seismic profile, the second corresponding to the NRP 20 Western Traverse and the third following the European GeoTraverse, which coincides with the NRP 20 Eastern Traverse (for location see Figure 24-2). They are an update of those published by Stampfli (1993, figures 2 and 3) and one of their purposes is to serve as a starting point for mass-balancing of the Western Alps (Stampfli & Marchant, Chapter 17). These lithospheric-scale cross-sections are based on a wide range of geological and geophysical data such as deep seismic profiles, refraction seismology, tomography, etc. In order to see if these cross-sections are consistent with the gravity field, some gravimetrical modelling was carried out as well.

Since the 1970's, many different methods have been used to try to determine the depth of the lithosphere-asthenosphere transition in the Alps. These include seismic methods (e.g. Panza & Mueller 1978; Spakman 1986a, 1986b, 1990a & 1990b; Babuska et al. 1990; Cattaneo & Eva 1990; Guyoton 1991; Viel et al. 1991; Spakman et al. 1993), gravity modelling (Schwendener & Mueller 1985)?, thermal studies (Pasquale et al. 1990; Cermak et al. 1992) or a combination of several methods (Suhadolc et al. 1990; Blundell 1992).

Until recently the lithospheric structure of the Alps was often regarded as a symmetrical and vertical subduction ("Verschluckung") of both the European and Adriatic plates (i.e. Laubscher 1975; Panza & Mueller 1978). Thanks to relatively high-resolution methods such as the recent tomographical studies, the symmetrical "Verschluckung" concept gave way to a basically asymmetrical lithospheric structure, showing a substantial subduction of the European continent under the Adriatic plate (Stampfli 1993). This highlights the astonishing cross-section drawn by Argand in 1924, which is in fact very similar to those one would actually build on the basis of recent geophysical data. Argand's cross-section shows a very substantial south-vergent subduction of the European plate under the Adriatic micro-continent, which first overthrusted the European plate before acting at depth as an indenter, causing the large-scale backfolding and backthrusting affecting the southern part of the Alps (the Insubric phase of Argand 1911).

Depending on the method and the data base used to determine the depth of this boundary, the results vary considerably in absolute value but nevertheless nearly all show the presence of an asymmetrical south-dipping Alpine lithospheric root. Kissling (1993) presents a critical review of the various approaches used for determining this transition and comes to the conclusion that the most reliable results come from the tomographic studies of Cattaneo & Eva (1990) and Spakman (1990b). Since then, a more refined tomographic model of the European-Mediterranean region has been published by Spakman et al. (1993) and a cross-section through this model is shown in Figure 24-8. This tomographic image follows the NRP 20 Western Traverse and

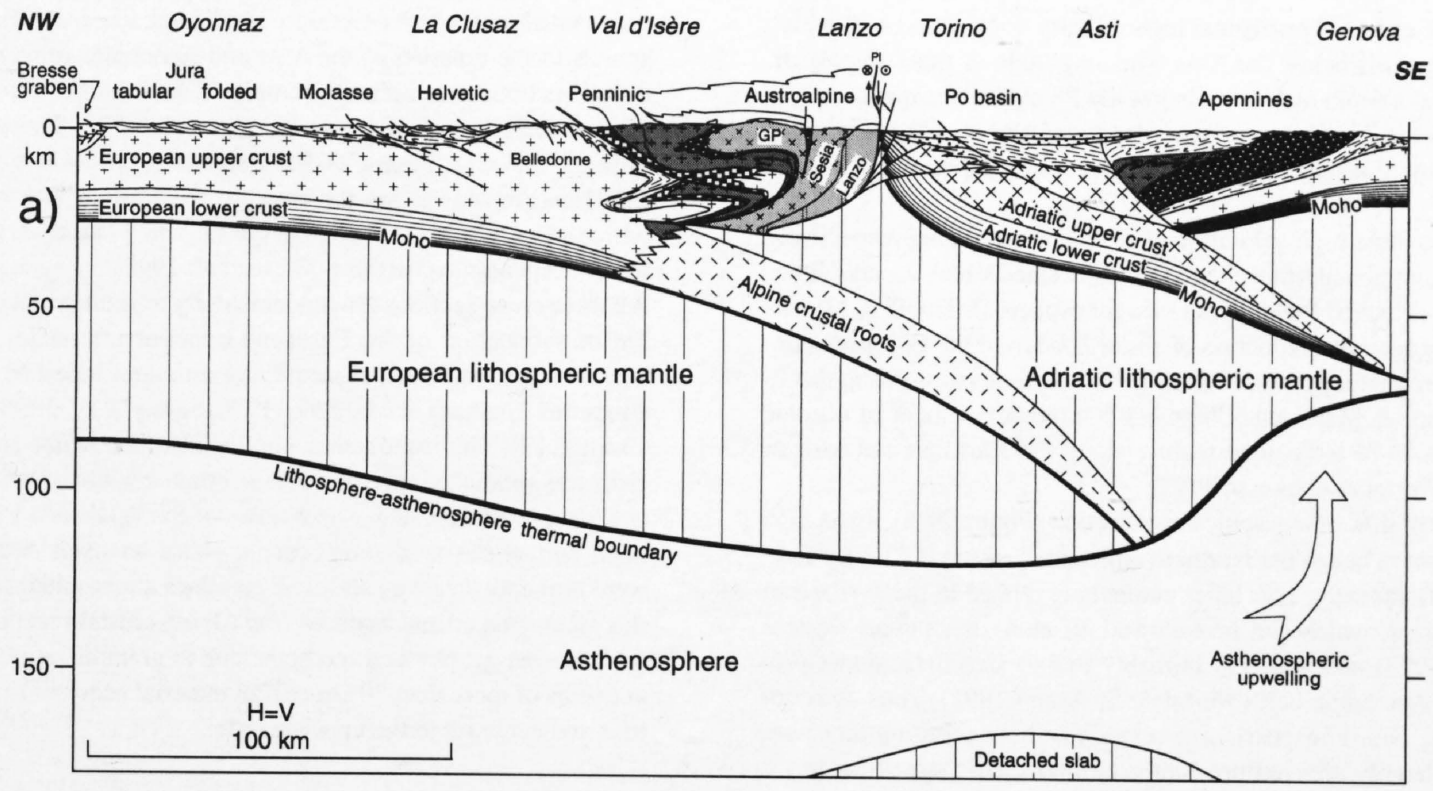

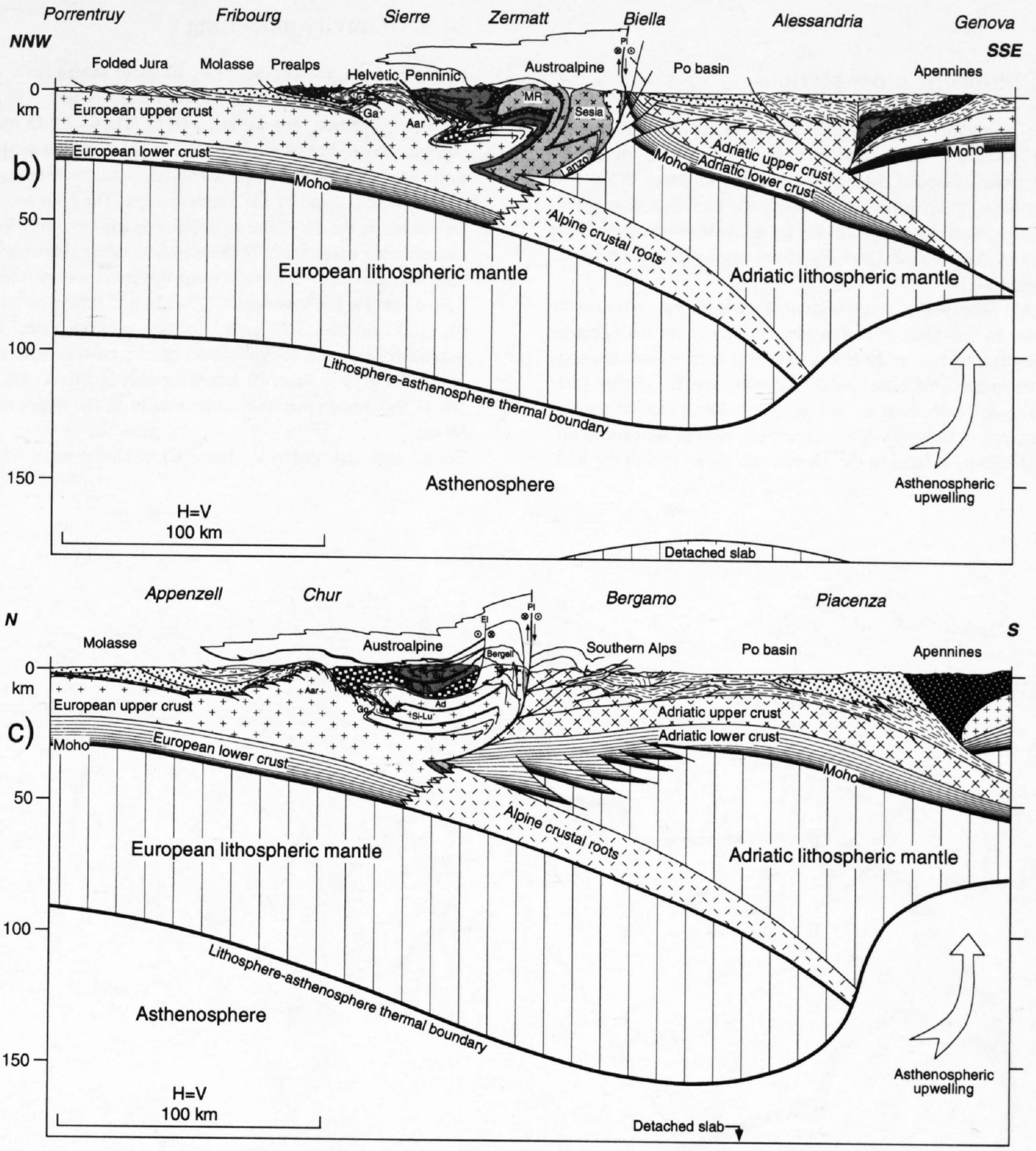

Figure 24-9
Lithospheric cross-sections along
a) the Ecors-Crop Alp Traverse,
b) the NRP-20 Western Traverse and c) the NRP-20 Eastern Traverse. For location, see Figure 24-2.
Ad = Adula nappe; EL = Engadine line; Ga = Gastern massif; Go = Gotthard "massif"; GP = Grand Paradis massif; Lu = Lucomagno nappe; MR = Monte Rosa nappe; Pl = Periadriatic line; Si = Simano nappe; Tb = Tambo nappe.

shows at its NNW end a subhorizontal high velocity body (thus cold) which starts to dip southwards below the Alps. The amplitude of this anomaly diminishes sharply at a depth of 155 km below the Po plain, to reappear deeper down in a near-vertical position between depths of 180 to 400 km. A third high velocity anomaly, weaker and more diffuse, is situated between 500 and 900 km depth.

We interpret these three high velocity bodies as corresponding respectively to the European continental lithosphere, to the detached Valais oceanic lithosphere and to the detached Piemont oceanic lithosphere (Stampfli & Marchant 1995). This significant subduction of about 200 km of the European continental lithosphere perfectly matches estimates based on palinspastic reconstructions (Stampfli & Marchant, Chapter 17). Slab detachment of oceanic lithosphere seems to be a frequent feature along the Eurasian and African plate boundary (Wortel & Spakman 1992).

Near the SSE end of this tomographic cross-section (Figure 24-8), a thin high velocity body appears below the Northern Apennines, overlying a very low-velocity (thus hot) anomaly. This latter anomaly is related to the Tyrrhenian asthenospheric diapir which can be followed all along the Italian western coast (Stampfli 1993) and which is probably due to slab detachment processes along the Apenninic belt (Wortel & Spakman 1992). Thus asthenospheric upwelling, sub-lithospheric assimilation and oceanisation processes must have considerably affected pre-Neogene lithospheric structures in the area near Genova.

24.3.2 The lithospheric cross-sections

Three lithospheric-scale cross-sections are presented in Figure 24-9. All start on the European hinterland and are oriented perpendicular to the Alpine strike. Due to the arched shape of the Alpine belt, they all finish in the area of Genova after crossing the Northern Apennines, and therefore their southern ends show a rather similar structure. In the areas where the cross-sections are not constrained by deep seismic lines, the Moho depth was taken from the map shown in Figure 24-10.

The Ecors-Crop Alp lithospheric cross-section (Figure 24-9a) starts on the Western side of the Bresse Graben and heads for Genova on the Ligurian coast. As it does not exactly follow the Ecors-Crop Alp deep seismic traverse, a few features close to the surface are slightly different from the crustal-scale interpretation of Figure 24-3b, such as the Lanzo unit which reaches the surface along this transect. In Italy this cross-section encounters two crustal discontinuities, which can be related to the Monferrato thrust and to the VVL line (Villalvernia-Varzi-Levanto line, Laubscher 1988). This area corresponds to the junction of the Alps and Apennines orogenic systems and its deep structures are extremely complex ("the Ligurian knot"), as shown by interpretation of refraction data (Biella et al. 1993). The southern end of the Western Traverse (Figure 24-9b) also crosses these two crustal discontinuities. However this is not the case for the Eastern Traverse (Figure 24-9c), where a few tens of kilometres of the Adriatic plate seem to be subducted below the Apenninic crust (e.g. Giese et al. 1992).

All three cross-sections are fundamentally asymmetrical and show about 150 km of subduction of the European upper-mantle under the Adriatic plate, which corresponds well to shortening estimates based on palinspastic reconstructions (Stampfli & Marthaler 1990; Stampfli 1993; Stampfli & Marchant, Chapter 17). This subduction implies also that a fair amount of European crust was subducted together with a certain amount of Briançonnais and Austroalpine crust as well as some relics of the Valais and Piemont oceans. The main part of the subducted oceanic plates involved in the Alpine collision were probably detached and sank into the asthenosphere. An exact amount of this subducted crustal material (the Alpine crustal root) cannot be estimated with present geophysical methods: due to granulitization and eclogitization, at depths of more than 50 km crustal material acquires similar seismic velocities and densities to the upper-mantle.

24.3.3 Gravity modelling

In order to test the compatibility of these lithospheric cross-sections with the gravity field, four gravity models were constructed across the Western Alps (for location, see Figure 24-11). These 2.5-D models (2-D models with the possibility of introducing limited lateral extensions) are a first step towards a 3-D model, which would be more consistent with reality because of the arched shape of the Western Alps. They start in the Molasse Basin and finish in the Po Plain; to avoid side effects, these profiles were in fact considerably extended at both ends. A standard lithospheric model was used with densities of 2.75 g/cm^3 for the upper-crust (down to a depth of 20 km); 2.90 g/cm^3 for the lower-crust (20–32 km); 3.25 g/cm^3 for the upper-mantle (32–120 km) and 3.20 g/cm^3 for the asthenosphere. Due to progressive granulitization and eclogitization of the crustal material when subducted at depths greater than 40 km, a density gradient was introduced, which brings this material to the same density as the upper-mantle at a depth of 80 km.

For the area surveyed by the Ecors-Crop Alp Traverse, several gravity models

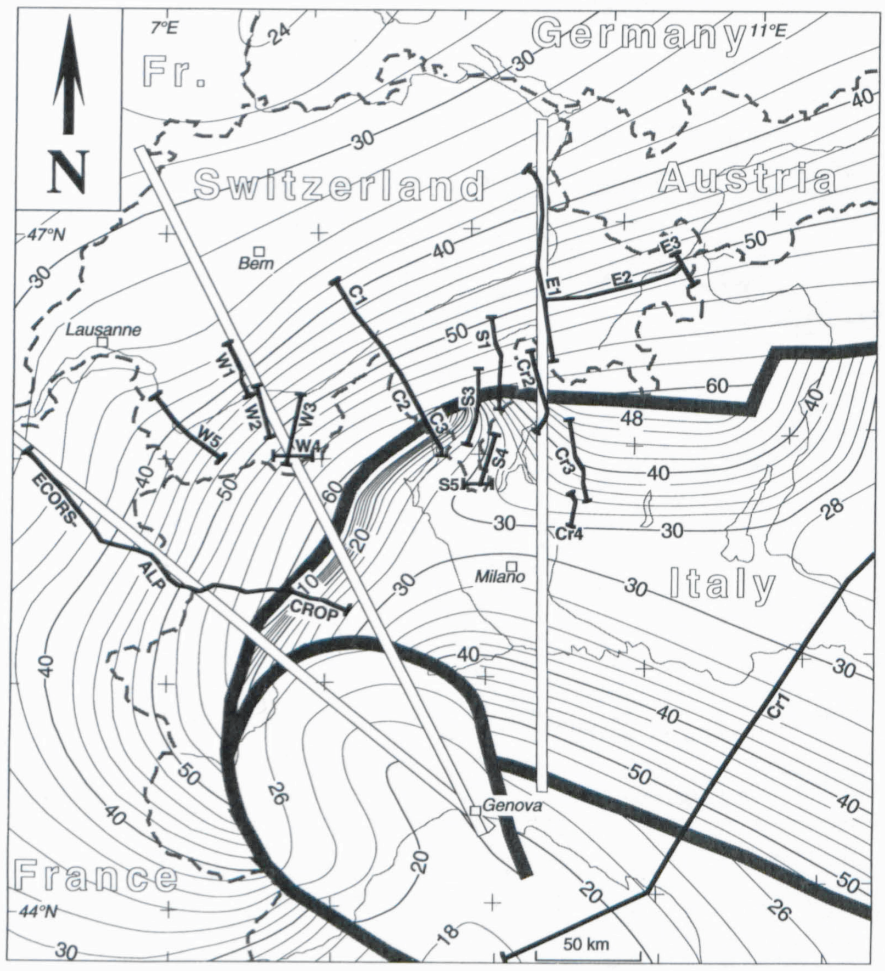

Figure 24-10
Map of the Moho discontinuity depth in kilometres (modified from Giese & Buness 1992) on the basis of data from Scarascia & Cassinis (1992), Biella et al. (1993), Kissling (1993) and Mussacchio et al. (1993). Black lines = deep seismic profiles shot in the Western Alps; white lines = location of the three lithospheric cross-sections of Figure 24-9.

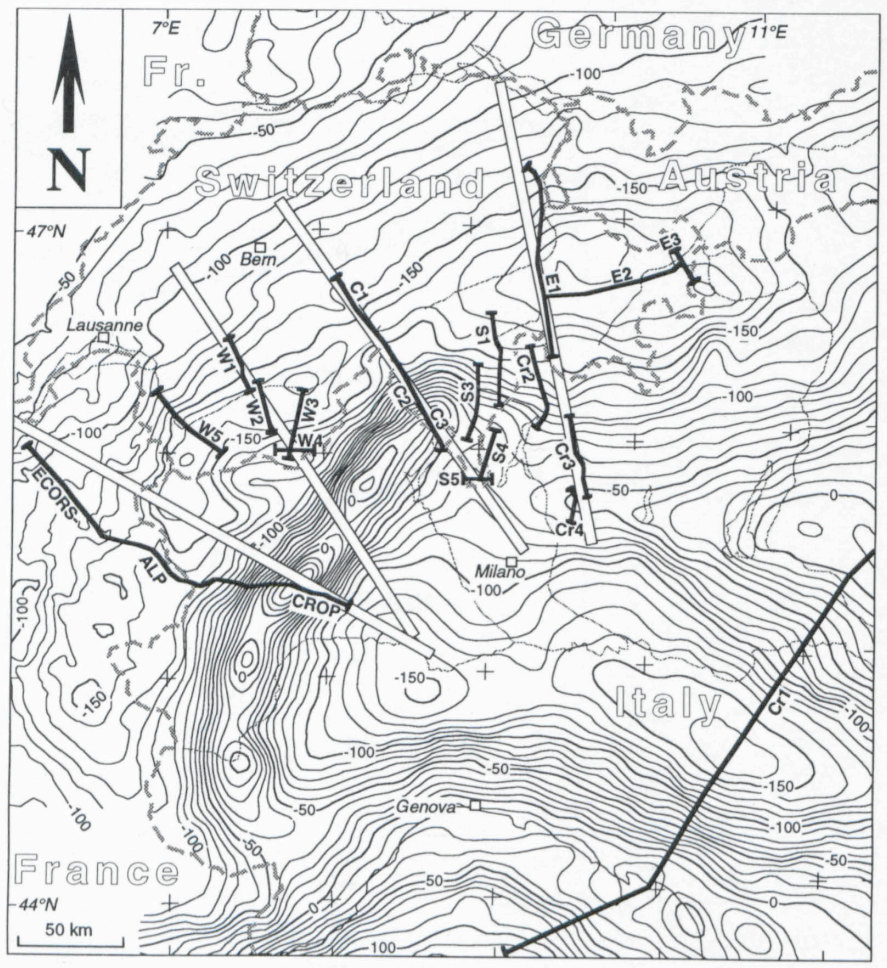

Figure 24-11
Map of the Bouguer anomaly in the Western Alps for a reference density of 2.67 g/cm^3; after Rey et al. (1990) and Klingelé et al. (1992). Black lines = deep seismic profiles shot in the Western Alps; white lines = location of the four gravity models of Figures 24-12 to 24-15.

(Berckhemer 1968; Kissling 1980; Ménard & Thouvenot 1984; Bayer et al. 1989; Rey et al. 1990) have been published showing different solutions for the Ivrea anomaly. According to Ménard & Thouvenot (1984), this anomaly is caused by several distinct upper-mantle units; on the basis of our interpretation of the deep seismic profile, we come to the same conclusion, but with a different geometry than proposed by these authors. In our gravity model (Figure 24-12), the Ivrea anomaly is caused by the following bodies (see also Figure 24-3b): the "mantle slice", the Adriatic indenter, the Lanzo peridotites and the lower-crust of the Ivrea zone. However, due to serpentinization of peridotites, the gravity method cannot determine the exact amount of upper-mantle involved in this complex structure. Nevertheless, the lithospheric cross-section along the Ecors-Crop Alp of Figure 24-3b fits the gravity data as shown by the gravity model in Figure 24-20, which follows the same profile as the model from Bayer et al. (1989, figure 4). The low density Molasse and Po Basins were introduced in the model, but not the dense ophiolitic bodies. The latter are probably responsible for the slight differences between the observed and calculated anomalies within the Alps. This gravity model is quite similar to the models published by Bayer et al. (1989, figure 4) or Rey et al. (1990, figure 8c), even though the upper mantle was not taken into account in their models.

The Western gravity profile (Figure 24-13) approximately follows the cross-section of Figure 24-4d. Its southern end joins the eastern extension of the Ecors-Crop Alp deep seismic line. The low density Molasse and Po Basins were introduced in the model as well as the high density ophiolitic bodies in the Penninic Alps. Hardly any modifications of the initial model, based on the seismic interpretation (Figure 24-4d), were necessary to get an excellent fit between the calculated and observed Bouguer anomaly. A major upwards flexure of the Adriatic crust just south of the Insubric line is necessary to bring the high density Adriatic upper-mantle close to the surface in order to match the Ivrea gravity anomaly. The near-surface ophiolitic bodies play a significant role for second order anomalies.

Gravity modelling was also carried out along the Central Traverse (Figure 24-14) which crosses the northern end of the Ivrea gravity anomaly (Figure 24-11). This model, based on the deep seismic interpretation of Figure 24-5b, is similar to the Western Traverse, but for the Adriatic plate which shows a more pinched-out lower-crust (the Ivrea zone) and a thicker upper-crust, consistent with surface observations. The slight mismatch between the observed and calculated anomaly occurring near the transition from the Helvetic to the Penninic domain could be due to heterogeneities in the external crystalline massifs and/or to some ophiolitic relics of the Valais ocean.

The Eastern gravity model (Figure 24-15) follows the same profile as the one Schwendener & Mueller (1990) used for their model showing an elliptical high density body in the upper-mantle under the Po plain. This profile is almost coincident with the crustal-scale interpretation of Figure 24-7c, which follows the EGT and the E1 deep seismic profile. Other gravity models for this area have been published by Cassinis et al. (1990) and Holliger & Kissling (1992). The relatively low density (2.70 g/cm^3) Tertiary granitic intrusions near Morbegno are represented on the model. The strong positive Bouguer anomaly on the southern end of the model is not due to the Ivrea mantle body but to a significant flexure of the Adriatic crust, squeezed between the Southern Alps and the Northern Apennines. The intensity of this anomaly increases towards the east (see Figure 24-11). Thus this section shows a very different configuration of the Adriatic plate against the Insubric line in comparison with the two previous cross-sections. The Adriatic Moho is here bending downwards against the European plate. This switch from an Adriatic Moho going upwards, over a distance of 200 km from Cuneo to Locarno, to an Adriatic Moho going downwards along the EGT must occur rather rapidly, over a distance of less than 50 km, as shown by the Bouguer anomaly map (Figure 24-11) or by the 3-D gravity model from Kissling (1980).

24.4 Discussion and conclusions

24.4.1 Gravity modelling

When calibrated by seismic interpretations, gravity modelling becomes a more powerful interpretation tool, as the infinite number of possible density models is strongly reduced. Nevertheless the solutions offered by this gravity modelling must be considered only as rough approximations:

- Although limited lateral extensions were introduced for some bodies (i.e. the Ivrea mantle body), such a 2.5-D modelling is not as precise as a true 3-D gravity modelling.
- The control on densities, although constrained by the seismic interpretations, is not perfect, in particular for the uplifted Ivrea upper mantle which can be affected by serpentinization.
- The depth of the lithosphere-asthenosphere transition is approximate and the Earth curvature was not introduced on the gravity models. However these two facts have little influence on the crustal structures, as their effects correspond to low-amplitude anomalies with a very long wavelength.

Nevertheless gravity modelling can help to determine the plausibility of different seismic interpretations. For instance, the crustal-scale interpretations of Valasek (1992) along the NRP 20 Western and Central Traverses are incompatible with the gravity data (Marchant 1993). They show a larger indenter made of Adriatic lower-crust which would cause a gravity anomaly 80 mgl smaller than the observed anomaly above the indenter. Furthermore such a model lacks a high-density body capable of causing the very strong Ivrea positive anomaly.

24.4.2 The European Moho and the European lower crust

With hardly any exception, all the deep seismic profiles shot in the Western Alps show a European lower crust becoming increasingly reflective towards the Moho, which is usually well defined. These features can be seen at normal depths below the Molasse Basin: the Conrad discontinuity at around 20 km and the Moho around 30 km. Further to the SE, they are smoothly subducted below the Alpine edifice in contrast to the European upper-crust which is strongly affected by the Alpine deformation (nappe formation and post-nappe deformation). This process is usually referred in the literature as crustal delamination. The European lower crust and Moho can be traced down to depths of around 50 km below the Penninic Alps, where their strong reflectivity tends to peter out. Nevertheless on the basis of tomographic models (e.g. Spakman et al. 1993), it can be deduced that the European lithosphere, including a considerable amount of crustal material, is subducted much further than what can be seen on most of the seismic sections. This fact is further corroborated by the deep seismic lines shot by CROP in the Italian Central and Southern Alps, which show a reappearance of reflections corresponding to the subducted European crust (Figure 24-7b). These reflections extend 40 km south of the Insubric line down to depths of over 60 km. Therefore the disappearance of the reflectivity of the European lowermost crust and Moho below the Penninic Alps is probably due to several reasons: in part to acquisition parameters (they are seen on the CROP lines but not on the NRP 20 lines), in part to the complex geology of the Penninic Alps which could diffuse the seismic energy and also in part to eclogitization processes which might render acoustic contrasts at such depths too small to be detected seismically (for discussion of this problem, see Valasek 1992; Marchant 1993). Thus, even if not visible on the seismic sections, we believe that the European lower crust, together with the Alpine crustal root follows the European upper mantle deep below the Po Plain.

24.4.3 The Alpine crustal root: subducted continental crust

The Southern Steep Belt, the strongly metamorphosed and near-vertical units outcropping just north of the Insubric line, are often referred to in the literature as the Alpine root zone. As the Southern Steep Belt is an overturned position due to the Insubric backfolding phase, an important synform-backfold must exist at depth to bring the Alpine root zone back into a normal position. From thereon, the Alpine root zone is subducted, together with the European crust, below the Adriatic plate. We call this subducted crustal material the Alpine crustal root.

The Alpine crustal root comprises units originating from the European plate, the Briançonnais and Austroalpine terranes as well as relics from the Valais and Piemont oceans. Mass-balancing at a lithospheric-scale based on geodynamic reconstructions (Marchant & Stampfli 1996; Stampfli & Marchant, Chapter 17) requires that a considerable amount of continental crustal material has been subducted together with the European upper-mantle. A very small part of it has been brought back to the surface as shown by the presence of coesite in the Dora Maira massif (Chopin 1984), indicating an Eoalpine subduction of part of the Austroalpine crust down to at least a 100 km. The volume of the Alpine crustal root shown on our lithospheric-scale cross-sections (Figure 24-9) is close to a minimum estimate; a maximum estimate would be nearly double. With reflection and refraction seismology as well as gravity methods, it is almost impossible to determine this volume, as the velocity and density contrasts between peridotites and eclogitic rocks is too small.

However, in the Pyrenees, Pous et al. (1994) have carried out magnetotelluric soundings along the ECORS-Pyrenees deep reflection seismic profile. This survey has revealed a high resistivity zone following the subducted Iberic

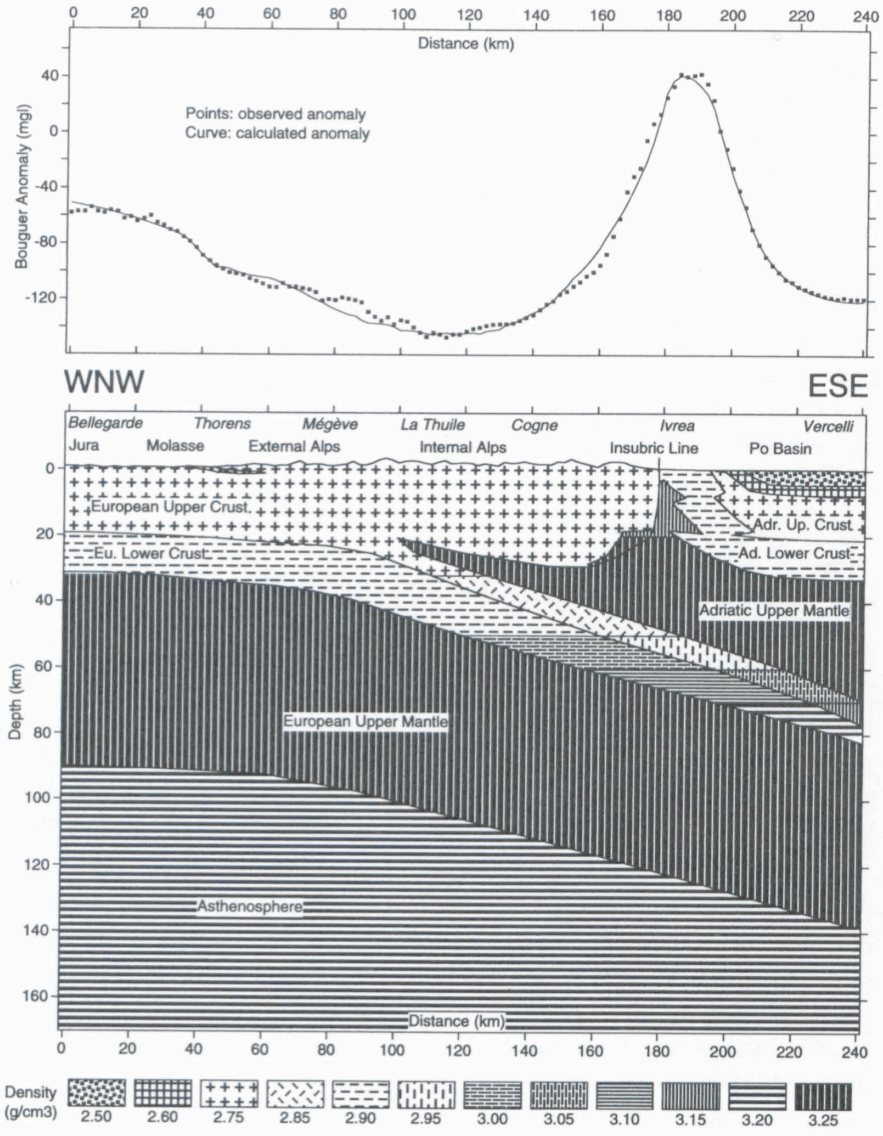

Figure 24-12
2.5-D gravity model along the Ecors-Crop Alp Traverse; for location see Figure 24-11.

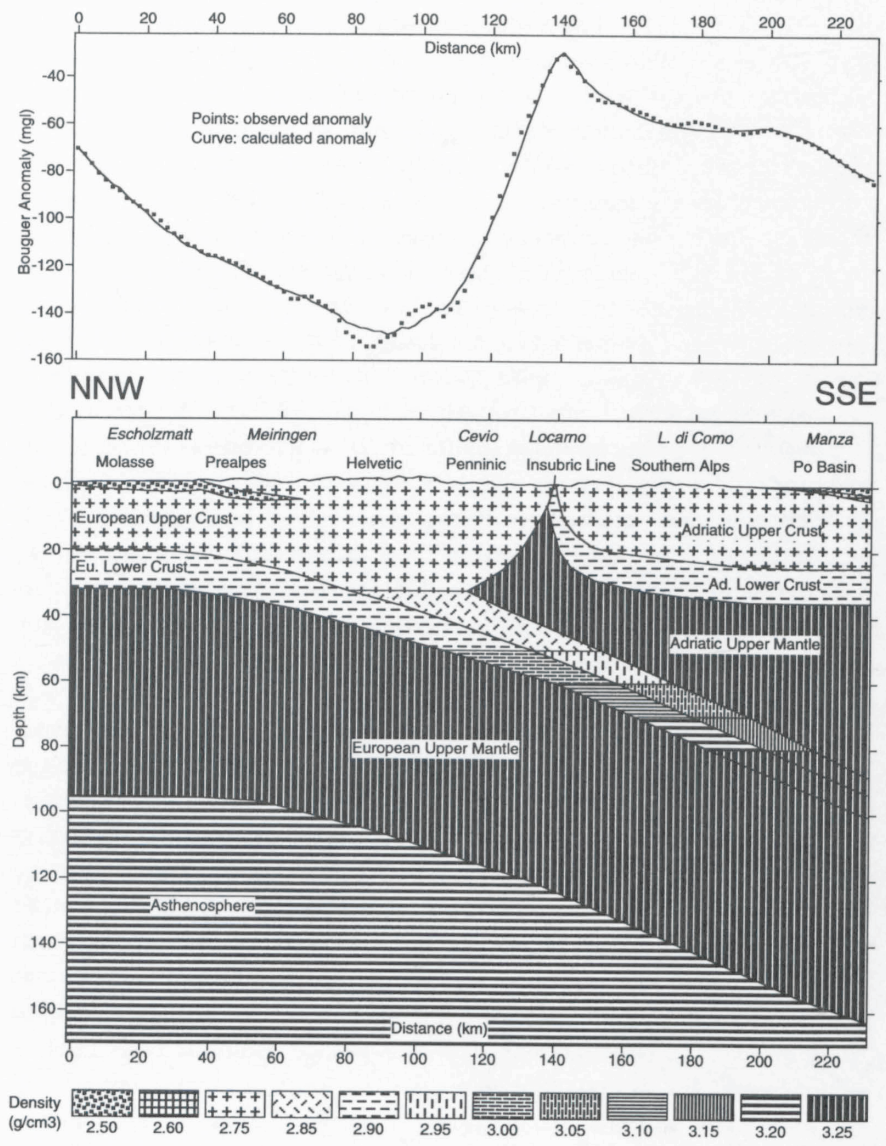

Figure 24-14
2.5-D gravity model along the NRP-20 Central Traverse; for location see Figure 24-11.

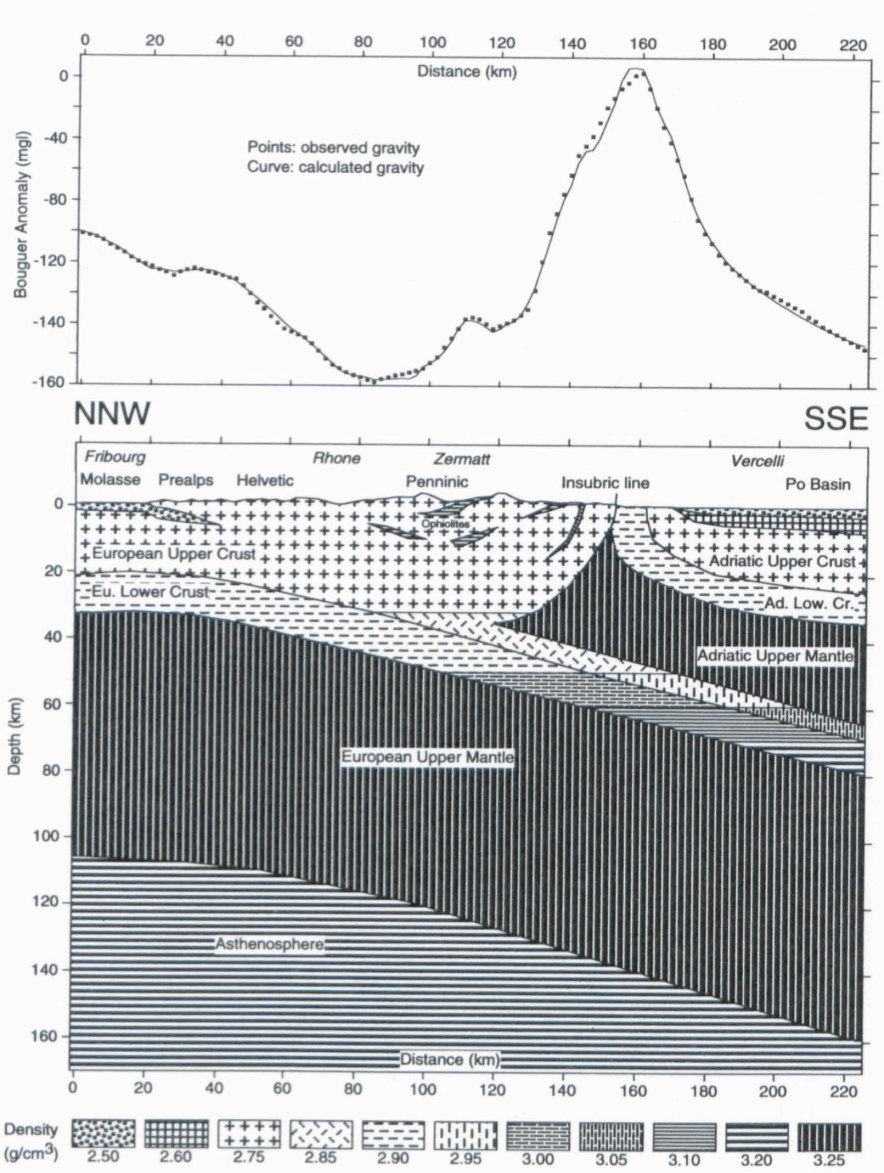

Figure 24-13
2.5-D gravity model along the NRP-20 Western Traverse; for location see Figure 24-11.

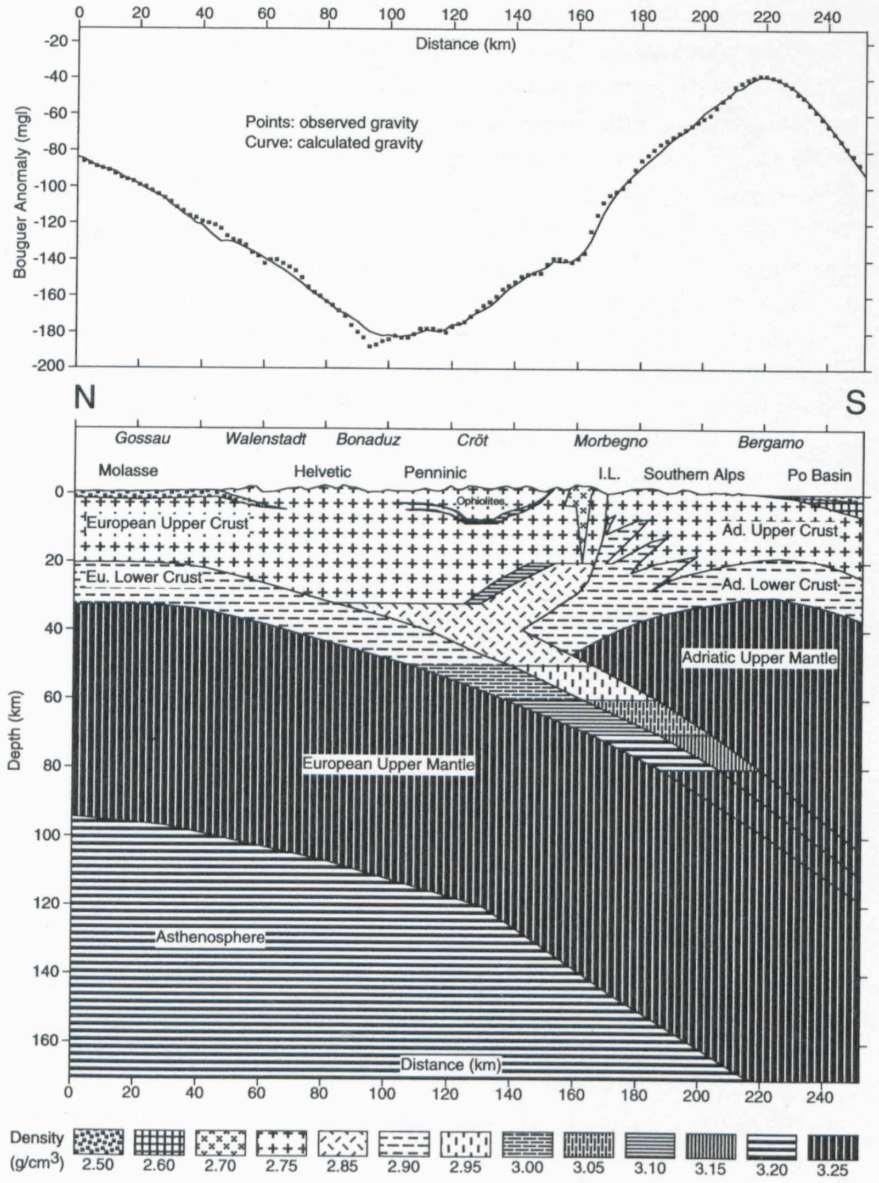

Figure 24-15
2.5-D gravity model along the NRP-20 Eastern Traverse; for location see Figure 24-11.

plate from a depth of 30 to 80 km, whereas the reflectivity of the Iberic crust stops short at a depth of 60 km. These authors favour an interpretation of this high resistivity zone as related to melts originating from the subducted crustal material. Therefore magnetotelluric soundings, not yet carried out at such a depth in the Western Alps, could be a method for estimating the volume of the Alpine crustal root.

Most plate-tectonic models never show any substantial subduction of continental lithosphere and continental crust. However an increasing number of studies of the deep structures of orogens reveal that this phenomena could be more widespread than usually thought of. Roecker (1982) on the basis of earthquake studies estimates that continental crust has been subducted to depths of at least 150 km below the Hindu-Kush range. From geological and geophysical evidences, Burtman & Molnar (1993) can follow continental crust down to depths of 150, if not even 200 km, below the Pamir range. There the length of the subducted continental lithosphere must be at least 250 to 300 km, thus nearly the double of our estimates for the Western Alps. Analogue models of the Himalayas (Chemenda et al 1995) have produced subduction of continental crust down to depths of 200–300 km.

From a very different approach, mineralogical data and comparative planetology, Anderson (1989) comes to the conclusion that much of the Earth's crust could be buried in the mantle. Although the relative amount of continental versus oceanic subduction seems presently difficult to assess, we believe that subduction of continental crust could well be an important process.

24.4.4 The Adriatic Moho

Of all the deep seismic profiles shot in the Western Alps, only the Ecors-Crop Alp Traverse images the Adriatic Moho rather clearly (Figure 24-3a). All published interpretations show a similar interpretation: at the eastern end of this profile, below the Po Plain, the Moho is located at a depth of about 30 km; further towards the west, it first shallows up gently to about 20 km depth and then it is fragmented by a series of reverse faults, showing a kind of staircase structure, finally bringing the Adriatic upper mantle to the surface near Castelmonte. This structure of the Adriatic plate is most important because it clearly shows that the top of the Ivrea mantle body corresponds to the Adriatic Moho, a feature that previously was not clearly established on the basis of gravity and refraction data (Kissling 1984).

All along the Ivrea gravity anomaly, from Cuneo to Locarno, the structure of the Adriatic Moho stays similar, as no substantial change in the gravity field is observed (Figure 24-11). However, east of Locarno, the Ivrea gravity anomaly ends abruptly, implying a drastic change in the configuration of the Adriatic plate. East of Locarno, the EGT refraction data (e.g. Buness 1992; Ye 1992) shows an Adriatic Moho dipping northwards below the outcrop of the Insubric line. About 50 km further east, the ZE refraction fan (Mussacchio et al. 1993) reveals a similar configuration. Stampfli & Marchant (Chapter 17) have related this change in the shape of the Adriatic Moho (going upwards along the Ivrea anomaly and downwards further east) to inherited rift structures.

In contrast to the smooth European Moho, the Adriatic Moho (Figure 24-10) is fragmented into a number of small pieces (Scarascia & Cassinis 1992). However the seismic coverage is insufficient (and sometimes the interpretations are contradictory) to draw a precise map of all the observed Moho discontinuities. Therefore our map of the Adriatic Moho (Figure 24-10) could be even more complex. If some of these discontinuities can be directly related to the Alpine orogeny (e.g. the staircase structure along the Ivrea anomaly), others could well be reactivated Permo-Mesozoic rift structures (e.g. the Lecco line; Giussani 1994).

24.4.5 The Adriatic indenter

Already in 1916, Argand had postulated, on the basis of his understanding of the structural geology in the Penninic Alps, the presence of an Adriatic indenter at depth which he held responsible for the backfolding phases. His hypothesis has been fully confirmed by the deep-seismic surveys in the Western Alps. However an important change in the composition of this indenter occurs near Locarno. West of Locarno, along the Ivrea gravity anomaly, the Adriatic indenter consists mainly of upper-mantle, while east of Locarno it consists mainly of lower crust; this difference finds its origin in the geodynamic evolution of the Adriatic plate as discussed by Stampfli & Marchant (Chapter 17). From the Alpine lithospheric rheology (Cloetingh & Banda 1992) it can be inferred that the lower crust is rather unlikely to act as a rigid indenter. However at the time the main indentation took place (around 30 to 18 Ma; Marchant 1993; Steck & Hunziker 1994), the Adriatic plate was situated at least 60 km to the east of its present position. Thus it was in fact the upper mantle (i.e. the present day Ivrea body) which indented the merging Alps east of Locarno. Due to the dextral movement along the Insubric line, the Adriatic lower-crust was subsequently able to creep into the gap made by the rigid, upper mantle indenter (Marchant 1993; Stampfli & Marchant, Chapter 17).

24.4.6 Backfolding and backthrusting

One of the most impressive feature of the Alps is the large scale backfolding which affects the whole nappe system. If some of these backfolds can be calibrated on the basis of surface-geology, such as the dekakilometric Vanzone antiform (Figure 24-4d), this is not the case for the backfolding affecting the southern side of the external crystalline massifs. The deep seismic profiles revealed that its amplitude is larger than previously estimated.

Structural geology and geochronological data show that the backfolding, which started at around 35 Ma, took place mainly during two distinct phases (Steck & Hunziker 1994): 30 to 18 Ma and 11 to 3 Ma. These two phases are related to rifting and oceanisation processes in the Western Mediterranean: the opening of the Algero-Provencal and Tyrrhenian basins respectively (Marchant 1993; Stampfli & Marchant, Chapter 17). The backthrusting in the Southern Alps was much less substantial where the rigid upper mantle indenter (i.e. the Ivrea body) was present. This rigid indenter transmitted the compressional stress at a mid-crustal level, and therefore the surface expression of this indentation can be found much further to the NE (e. g. the Jura Mountains) than where the indenter is composed mainly of ductile lower crust.

24.4.7 Mid-crustal deformation accommodation

We have seen above some of the consequences of crustal delamination and of the indentation processes. A combined effect of these two processes gave rise to the large scale "dome-and-basin" structure affecting the whole Western Alps (see also Hitz & Pfiffner 1994; Pfiffner & Hitz, Chapter 9). The map of the European Moho (Figure 24-10) reveals a rather smooth surface devoid of the large scale dome-and-basin structures, as observed at the surface (e.g. the Rawil-Valpelline depression, the Lepontine culmination, etc.). An important outcome of these observations is that this dome-and-basin structure must be directly linked to deformations occurring at a mid-crustal level, thus induced by the Adriatic indenter and the backfolding it produced. Thus the domes appeared most probably where the rigid indenter was large and the backfolding substantial. Furthermore, it can shown that the Lepontine dome, appearing at around 30 Ma, migrated westward together with the dextral movement of the Adriatic indenter along the Insubric line, to locate itself in the Simplon area at around 20 Ma (Marchant 1993; Steck & Hunziker 1994; Stampfli & Marchant, Chapter 17).

A consequence of this is that a simple horizontal projection of neighbouring deep seismic lines in order to produce a synthetic seismic section (e. g. Holliger 1990) can be misleading: the nappe system needs to be projected along the axial trend, which is not the case for deeper structures such as the European Moho. Thus each profile needs to be interpreted separately.

24.4.8 Concluding remarks

The deep seismic profiles shot in the Western Alps have allowed for a renewed understanding of this mountain belt. In particular we tried to show (see also Stampfli & Marchant, Chapter 17) the intimate relation between lithospheric scale processes and their surface expression in structural geology and sedimentology. This global approach has brought many new stimulating ideas on the Alpine orogenesis, but nevertheless several of the latter are still working hypothesis and additional data (geophysical as well as geological) should be collected to test their validity. In particular, we hope that some new deep seismic lines will be shot in a near future in Maritimes Alps, the Northern Apennines and the Eastern Alps in order to gain a more global understanding of the whole Alpine belt.

Acknowledgements

The authors are profoundly indebted to a great number of colleagues from the University of Lausanne for sharing their knowledge on various topics and for providing us with often unpublished information. We would like to thank W. Spakman and R. Wortel (Utrecht) for stimulating discussions on the interpretation of tomographic models. This contribution has much benefited from the reviews by E. Kissling, R. Meissner, A. Pfiffner and an anonymous reviewer. Last but not least we are deeply obliged to P. Lehner, the head of the NRP 20 program, for making this fascinating journey through the deep structures of the Alps possible.

25 The lithosphere-asthenosphere system of the Alps

St. Mueller

Contents

25.1 Introduction

Since the beginning of this century Austrian and Swiss geologists suspected that the Alps had been formed by continental collision; they postulated that the observed shortening of the upper crust must be accompanied by some kind of subduction mechanism of mantle material (for a summary, see Mueller, 1989). It had rather early been recognized that geological observations in mountain belts permit only a very limited insight into their deeper structure and the associated processes. The brilliant intuition of the Alpine geologists at that time, therefore, deserves our highest admiration. The models proposed were mostly rough sketches which have now led to a completely new picture of the deep structure in orogenic systems.

Several sets of recently acquired geophysical data can only be explained if the Alpine arc is indeed a deep-reaching continent-continent collision structure situated at the northernmost tip of the Adriatic promontory. This spur-like microplate has moved with the African plate since the Early Mesozoic, thereby eventually creating the spectacular mountain range of the Alps. New seismological and gravimetric data have shown that the continuing collision process must have led to a considerable shortening and asymmetric thickening of the Alpine crust indicating a much deeper-reaching structural anomaly involving the entire lithosphere-asthenosphere system. The still ongoing geodynamic processes in the Mediterranean-Alpine region are primarily governed by the relative movement of the African lithospheric plate against the Eurasian plate, resulting in a predominantly compressional regime along the zone of contact.

In this chapter an attempt is made to outline the deeper structure and dynamics of the Alps, as well as their past and recent evolution, i.e. more precisely during the time period of the past 35 Ma. As was to be expected, the emerging image revealed a strongly developed heterogeneity which – at this stage – had to be simplified in order to obtain a geodynamic model consistent with the presently available geophysical and geodetic data. Future studies will have to improve the regional resolution considerably with the aim to eventually produce a three-dimensional image of the crust and uppermost mantle beneath the Alps.

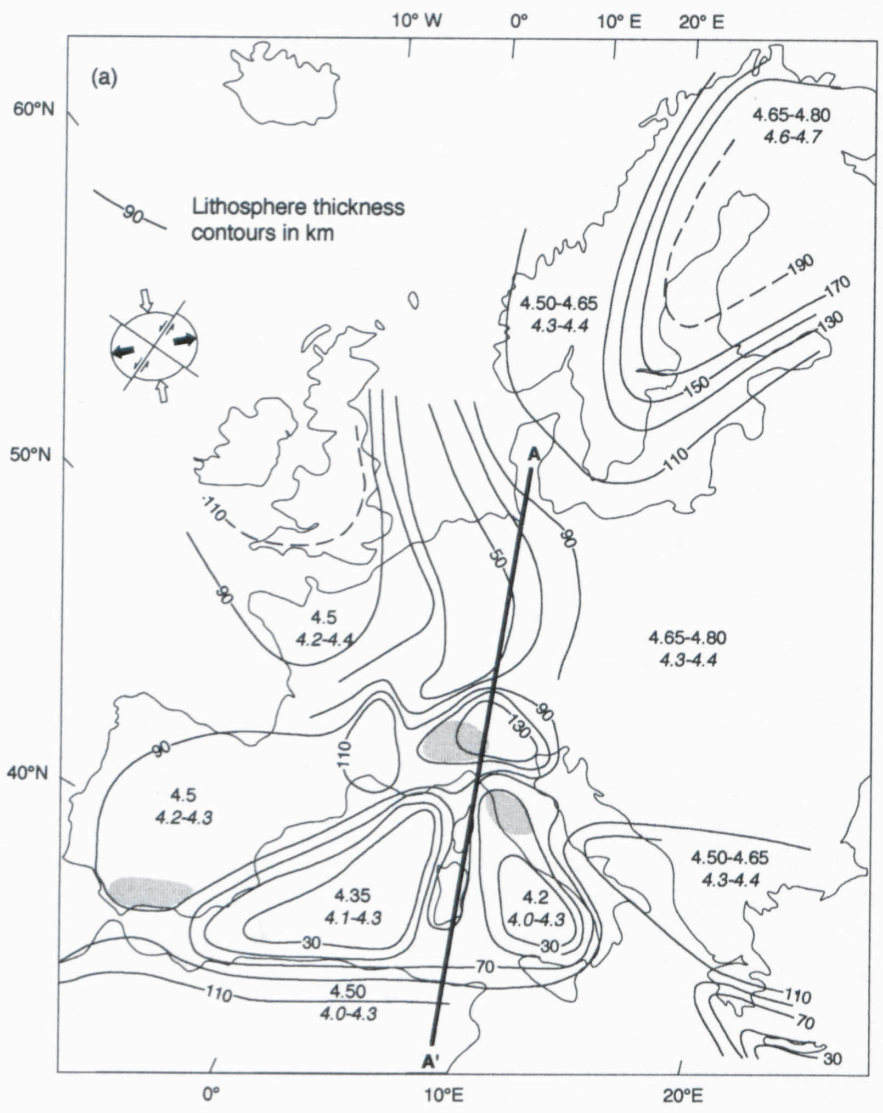

Figure 25-1a
Contour map of lithospheric thickness (in km) in the European-Mediterranean region, deduced from the regional dispersion analysis of seismic surface waves (after Panza, 1985). Representative shear-wave velocities are given for the mantle lithosphere (row of upper numbers) and for the asthenosphere (row of lower numbers). The three shaded areas outline the presence of "lithospheric roots" to depths of about 220 to 240 km. Also indicated is a simplified seismotectonic scheme for central and northwestern Europe (after Ahorner, 1975).

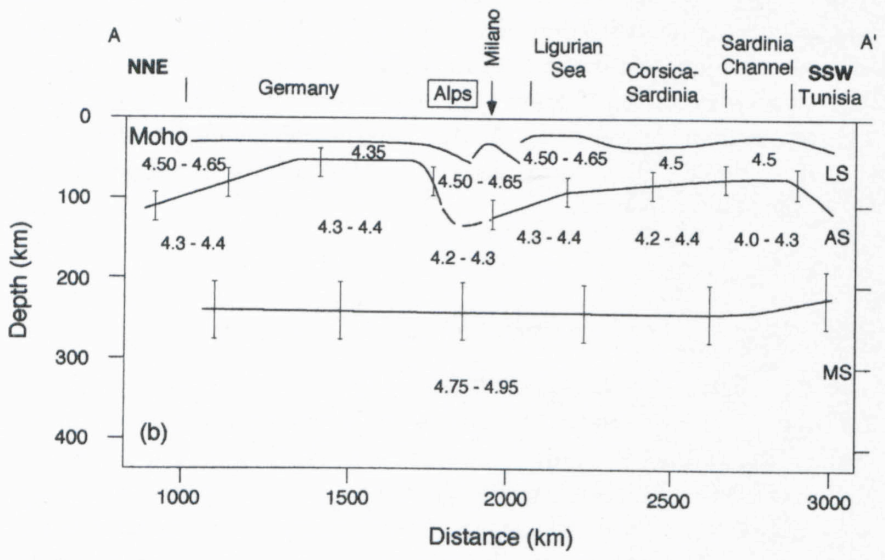

Figure 25-1b
Cross section through the lithosphere-asthenosphere system from Denmark (A) to southern Tunisia (A') along the "European Geotraverse (EGT)" with representative shear-wave velocities (in km/s) for that profile. Beneath the crust-mantle boundary ("Moho"), the vertical bars indicate the uncertainty in depth above and below the lithosphere (LS)-asthenosphere (AS) boundary and the asthenosphere (AS)-mesosphere (MS) transition zone. Under the southern Alps the lithosphere penetrates into the asthenosphere forming a clear "lithospheric root" (after Suhadolc et al., 1990).

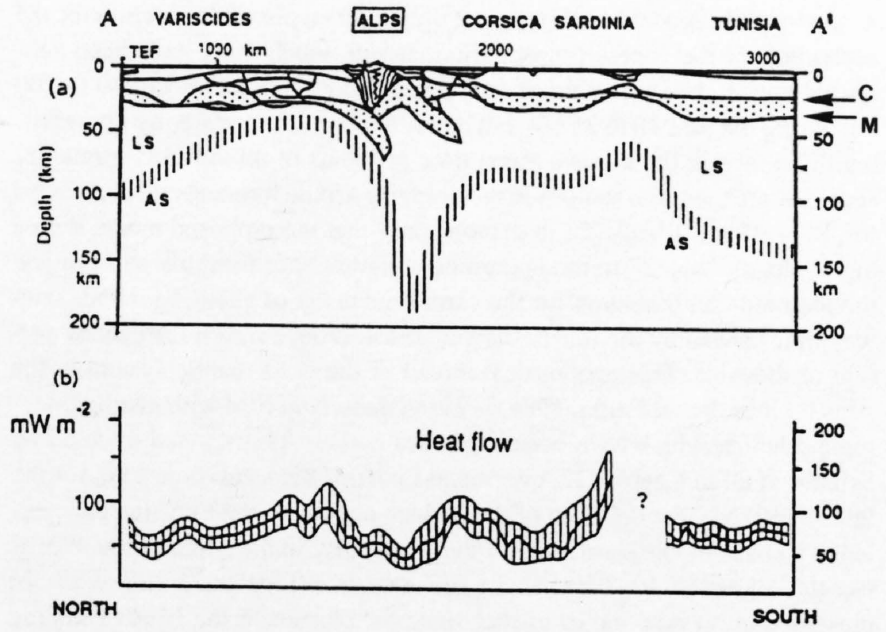

Figure 25-2
Lithospheric cross section along the EGT.
a) Detailed cross section A-A' (see Figure 25-1a) from Denmark to Tunisia (after Blundell, 1990). Upper and lower crust (stippled) are decoupled at the Conrad (C) discontinuity. Also shown is the crust-mantle boundary (M). LS = Lithosphere and AS = Asthenosphere, with both "the crustal and lithospheric roots".
b) Along the same profile (A-A') are also shown heat flow data (after Della Vedova et al., 1995) illustrating the lowered heat flow values beneath the Alps caused by "the cold lithospheric root".

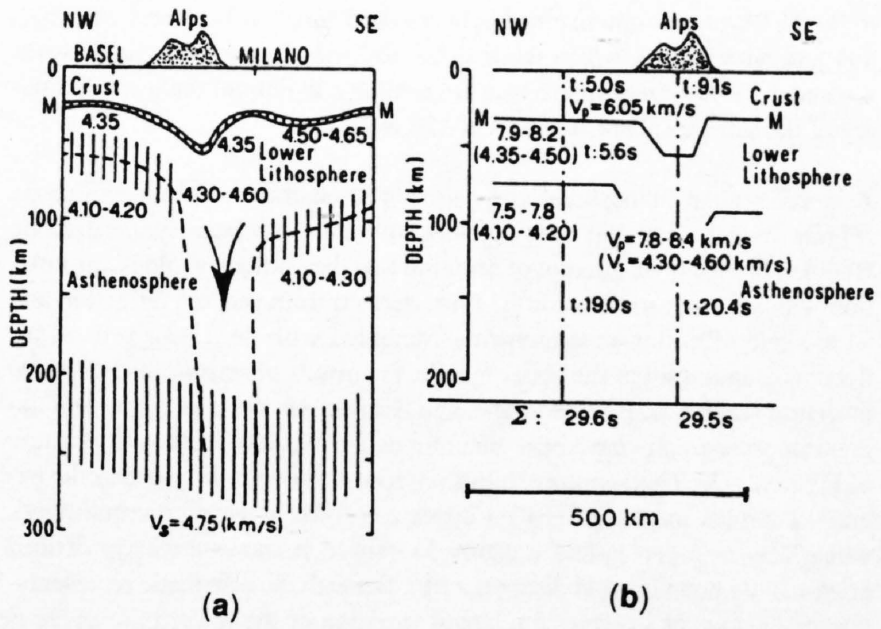

Figure 25-3
Deep structure of the Alps
a) Deep-reaching crust-mantle cross section through the Central Alps from the southern Rhinegraben (near Basel) to the Po Basin (southeast of Milano) derived from the simultaneous inversion of regional surface-wave dispersion data (after Panza & Mueller, 1978). The numbers represent shear-wave (S) velocities Vs (in km/s). Vertical "fence hachures" indicate the range of uncertainty of the base of the crust (M), the lower lithosphere and the asthenosphere. Note the nearly vertical lithospheric slab penetrating into the asthenosphere, i.e. forming a "lithospheric root".
b) Schematic crust-mantle section across the Central Alps (cf. Figure 25-3a). The one-way travel times of compressional (P) waves propagating vertically upwards with a velocity Vp from the base of the asthenosphere to the surface corroborate the hypothesis that the time delay caused by the Alpine low-velocity "crustal root" must have been compensated by the underlying high-velocity "lithospheric root" (after Baer, 1980). In the model a ratio Vp/Vs of 1.82 has been assumed.

25.2 Crust-mantle structure

25.2.1 Regionalized seismic surface-wave dispersion analysis

During the past three decades a relatively dense network of long-period seismometers has been recording teleseismic events at observatories spread across the European-Mediterranean region. Suitable station combinations permitted the measurements of fundamental mode phase velocities of Rayleigh waves from various azimuths in a wide frequency range across this station array. Since the observed phase velocity dispersion is caused primarily by the geometric and physical properties of the lithosphere-asthenosphere system, an analysis of the well-defined frequency-dependent dispersion can be used to determine the average thickness and shear-wave velocity of the mantle lithosphere provided that the average properties of the crustal structure are known.
Most of the European-Mediterranean region is sufficiently well covered by phase velocity "profiles", which provide the basis for a uniform "hedgehog" inversion of the dispersion observations. In order to apply this procedure properly it must be verified that a representative regionalization of the phase velocity dispersion for seismic surface waves can be realized from the available observational data (Panza et al., 1980). In this "hedgehog" inversion process a systematic search in a multidimensional parameter space is carried out which allows to identify models that fall within the limited range of solutions compatible with the unavoidable observational uncertainties.
The result of the regionalized inversion procedure is shown in Figure 25-1a, which depicts a schematic map of the lithosphere-asthenosphere system for most parts of the European-Mediterranean area (Panza, 1985). When interpreting this map, it is important to realize that it represents only an approximate solution to the inverse problem and is subject to inherent uncertainties (e.g. 15 to 20 km in lithosphere thickness) due to the limited resolution of long-period surface waves. Noteworthy with respect to the thickness and average shear-wave structure of the lithosphere are the following regional features:

1) Significant deviations from the "normal" lithospheric thickness of about 90 km in central and western Europe are, for instance, found in the Balearic and Tyrrhenian basins of the Western Mediterranean Sea where the lithosphere thins to 30 km or even less.

2) Another conspicuous lithospheric feature is a roughly north-south oriented asthenospheric upwarp which is associated with the so-called "Central European Rift System". It reaches from the North Sea to the Western Alps with an average lithospheric thickness of about 50 km and markedly lowered shear-wave velocities.

3) Striking also is the "tongue-like" structure which extends from North Africa through the Ionian Sea into the Adriatic Sea. This "spur" of thick lithosphere is best outlined by the European-African plate boundary as defined by the recent seismicity (see Figures 25-6a and 25-6b) and the deformed margins on the north and south side of the former Tethys (cf. Channell & Horvath, 1976), and shows clearly that the Adriatic region is part of Africa. There the upwarped crust-mantle boundary dips both, under the Apennine peninsula and the Dalmatian coastal range. It, therefore, has been suggested that the Adriatic (or Apulian) "microplate" is a promontory of the African plate which reaches all the way into the Alpine arc.

4) Of particular interest are the Alps, where the lithosphere thickness increases to 130 km, attaining even somewhat greater values beneath the Swiss Alps. "Lithospheric roots" (shaded areas in Figure 25-1a) are found under mountain belts in zones of continent-continent collision, such as the Alps (Panza & Mueller, 1978), the Ligurian-Tuscan region in central Italy (Panza et al., 1982) and the Betic Cordillera in southern Spain.
The primary large-scale stress field caused by the lithospheric plate collision also radiates into central and northwestern Europe (cf. Ahorner, 1975) as indicated by the small inset in the upper left part of Figure 25-1a. Both, the seismicity distribution and the seismotectonic stress pattern (Figures 25-6a and 6b) illustrate that the Adriatic promontory of the African plate acts as an oblique "indenter" (cf. Tapponier & Molnar, 1976), which has penetrated far into the European domain of the Eurasian plate, thus providing an explanation of why the collision structure of the Alps is at this particular location.

A north-south cross section (A-A') through the lithosphere-asthenosphere system (Figure 25-1b) which coincides with the central and southern segments of the "European Geotraverse (EGT)" from the Danish-German border to North Africa (Blundell et al., 1992) depicts the shear-wave velocity distribution in the uppermost mantle. The change in lithospheric structure from the southern margin of the Fennoscandian Shield (110 km contour of lithospheric thickness, in the upper right-hand corner of Figure 25-1a) across the "Central European Rift System" (50 km contour of lithospheric thickness in the center part of Figure 25-1a) in Germany, to the Alps, the Ligurian Sea, the island chain of Corsica and Sardinia, and finally across the Sardinia Channel to Tunisia emerges clearly from this figure. Values of S-wave veloc-

ity in the lower lithosphere range between 4.65 and 4.35 km/s and are generally around 4.5 km/s, whilst those in the asthenosphere mostly lie between 4.4 and 4.2 km/s. Only sparse data are available to delimit the lower boundary of the asthenosphere at depths of 220 to 240 km.

A more detailed lithospheric cross-section of central and southern Europe (Figure 25-2a) – but still on a continental scale – has been synthesized by Blundell (1990) in an attempt of bringing together surface geology information with structure models for the crust derived from seismic refraction and wide-angle reflection measurements combined with deep near-vertical reflection soundings. For the upper mantle, the results of seismic surface-wave inversion studies, of P-wave long-range seismic refraction profiling and delay time tomography have been incorporated in the composite cross section of Figure 25-2a. This section exhibits intracrustal boundaries, such as the laterally complex interface between upper and lower crust (C discontinuity), which acts as a decoupling horizon. Moreover, it shows a clearly defined crust-mantle boundary (M discontinuity). Beneath the schematic representation of the crustal structure the lateral variation of the lower lithosphere is displayed in Figure 25-2a with the lithosphere-asthenosphere transition indicated by the vertical "fence" hachure which also provides a measure of the uncertainty in depth. The lower limit of the asthenosphere (not shown), i.e. where it blends with the underlying mantle mesosphere, has been mapped in the depth range of 210 to 250 km based on seismic surface- and body-wave studies (Panza et al., 1980).

The cross section in Figure 25-2a illustrates convincingly that the large-scale tectonic processes apparently affect the entire lithosphere-asthenosphere system. Due to the continental plate collision in the inner Alpine arc the quasi-rigid lithosphere reacts by an apparent thickening which is caused by the formation of a high-velocity, high-density, cold and slowly subsiding "lithospheric root", thus creating a steeply dipping mantle subduction zone. It is this evidence which demonstrates that the actual plate boundary between Africa and Eurasia is characterized by deep-reaching structural features in the Alpine area as shown for the first time by Panza & Mueller (1978) and as subsequently postulated for a hidden subducted slab off the northern coast of Africa (Mueller, 1989). The deep-reaching "lithospheric root" beneath the Southern Alps and the Po Plain is associated with lowered heat flow (Figure 25-2b), while the rift structures of the Rhinegraben, the Ligurian Sea and the Sardinia Channel show conspicuously higher heat flow values (cf. Della Vedova et al., 1995).

As already indicated in Figure 25-1b, the existence of a high-velocity "root" within the upper mantle under the Alps had been deduced from the regional dispersion of Rayleigh waves in a somewhat schematic way. In the sketchy cross-section of the lithosphere-asthenosphere system (Figure 25-3a) the hatched markings show the range of uncertainty for the bottom of the crust (M), of the lower lithosphere and of the asthenosphere along a profile from Basel to Milano, which roughly coincides with the "Swiss Geotraverse" (Rybach et al., 1980). The center part is characterized by a high-velocity "slab" of subducted lower lithosphere penetrating into the asthenosphere to depths of 150 to 220 km (Panza & Mueller, 1978). It should be noted that the near-vertical subducting "slab" is not symmetrical with respect to the central zone and the crustal root of the Alps, but appears to be somewhat displaced southeastwards (see Figure 25-3a), i.e. towards the inner side of the Alpine arc.

A crust-mantle model of this type not only offers a plausible solution for the deposition of the excess lithospheric material which must have been subducted during the shortening of the Alpine lithosphere by about 240 to 200 km during the past 40 to 35 Ma, but it also explains the apparently non-existing difference in the P-wave travel time residuals of teleseismic events observed at seismograph stations in the northern Alpine foreland and in the Alps (cf. Baer, 1980). Figure 25-3b demonstrates that the proposed model with a high-velocity "block" in the uppermost mantle under the Alps will provide the required compensation for the extra time delay of about 4 seconds one-way time caused by the much "slower" crustal root beneath the central portion of the Alps. This geophysical model of the crust-mantle system in the Alps (cf. Mueller & Panza, 1986) is in satisfactory accord with geologic-tectonic schemes which have been suggested earlier. As discussed in detail by Schmid et al. in Chapter 22, ever since Eocene/Oligocene times, i.e. for the last 38 (±2) Ma, the collision of the African plate with the Eurasian plate has led to a considerable shortening of the lithosphere in the Alpine zone of contact (cf. Figure 25-10). The geophysical evidence (Figures 25-3a and 25-3b) presented up to now indicates that since the closure of the North Penninic Ocean with the associated subduction and the continuing collision process, relatively dense and cool lithospheric material has been pushed into the upper mantle to a depth of about 200–220 km.

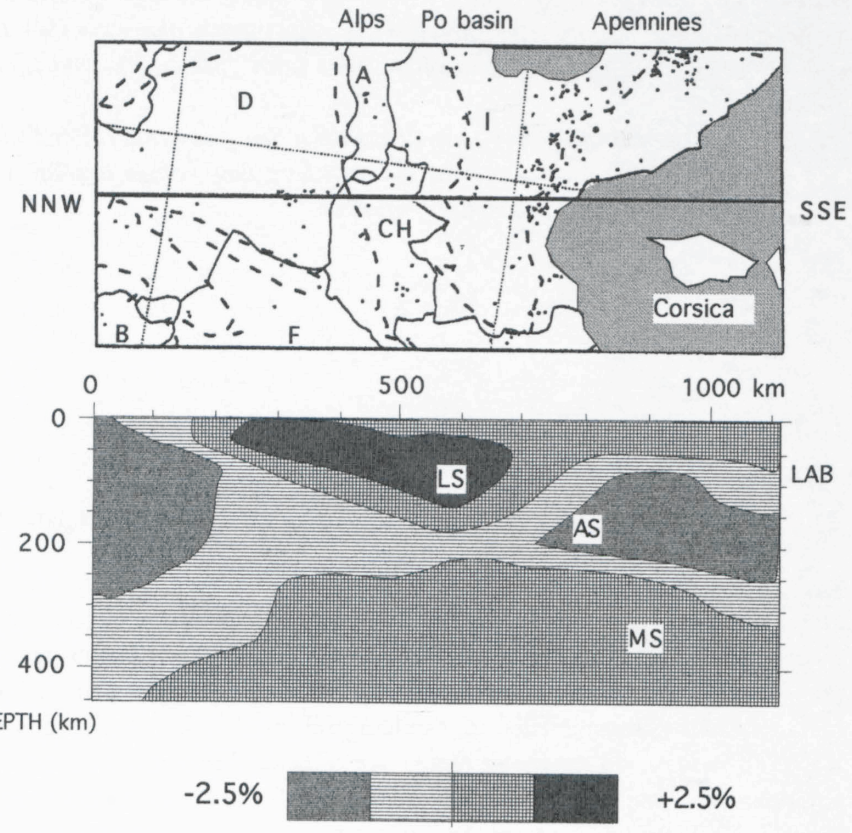

Figure 25-4b
P-wave tomographic image of the upper mantle structure beneath the Alpine segment of the EGT (after Spakman, 1990b). Square-hatching marks depth zones of higher velocity (LS and MS), while horizontal ruling denotes areas of lowered velocity (AS). Abbreviations: A = Austria, D = Germany, I = Italy, CH = Switzerland, B = Belgium, F = France. - LS = Lithosphere, AS = Asthenosphere, MS = Mesosphere.

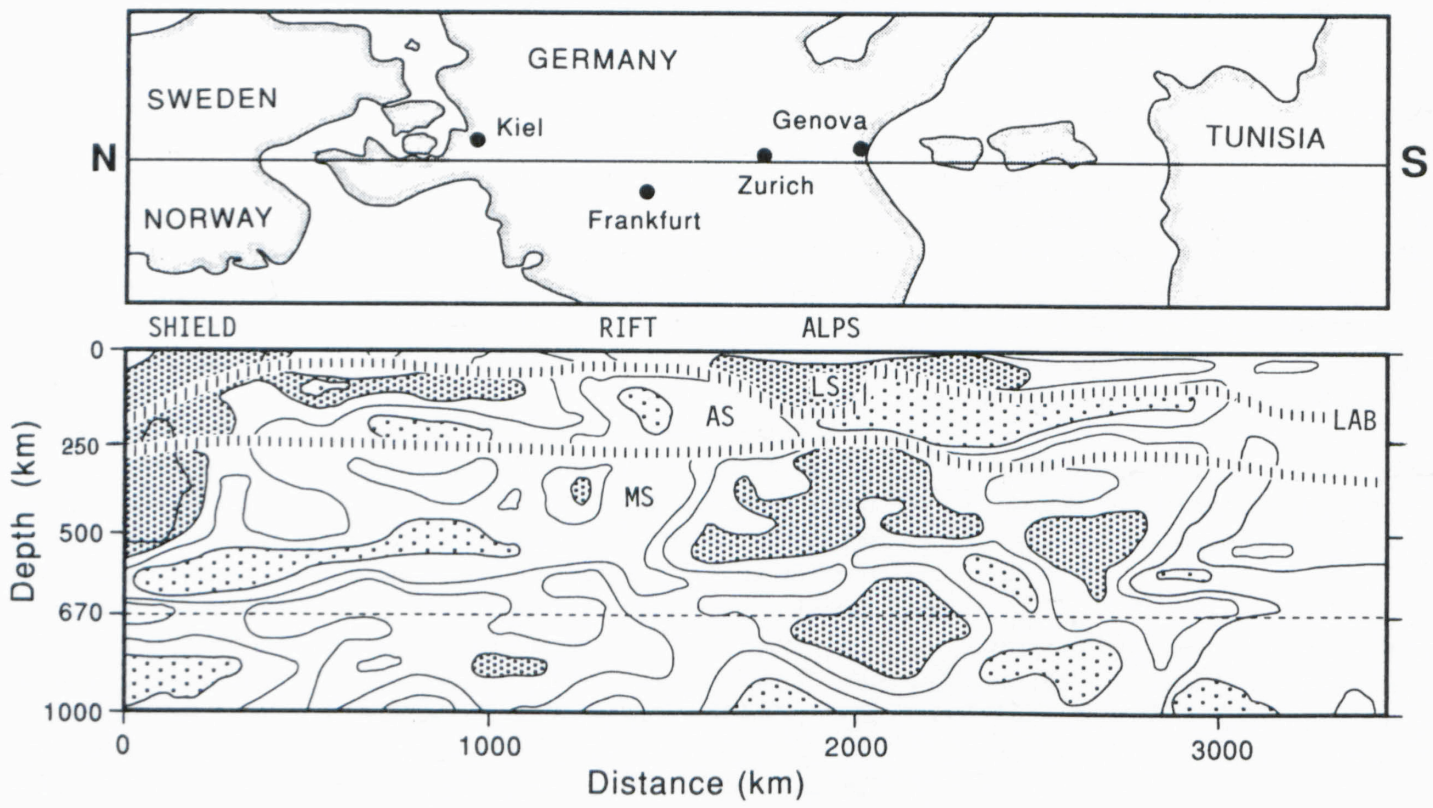

Figure 25-4a
Seismic tomography cross section of the crust and upper mantle along the EGT from the Oslo fjord to southern Tunisia. The darker shading refers to areas of higher P-wave velocity (Vp) relative to a standard Earth model (after Spakman, 1990a; Spakman et al., 1993). Superimposed by vertical hachures is an interpretation of the upper (LAB) and lower (AS/MS) boundaries of the asthenosphere (AS). The 670 km discontinuity is also marked by a weakly dashed line, while the 400 km transition zone can not easily be discerned.

25.2.2 Body-wave delay time tomography

In the preceding paragraph it has already been mentioned that large-scale delay time tomography can provide a better insight into the lateral heterogeneity of the seismic P-wave velocity field. The results obtained by Spakman (1986, 1988, 1990a, 1990b) in this context are of particular significance. In Figure 25-4a the asymmetric "lithosphere root" with a thinned asthenosphere underneath the Alps can clearly be seen (see also Spakman et al., 1993). There is an obvious correspondence with the crust-mantle cross-sections of Figures 25-1b and 25-2a which are primarily based on the S-wave velocity field derived from regional seismic surface-wave dispersion results. However, all these sections show only minor fluctuations of the lower boundary of the asthenosphere. The dashed line in Figure 25-4a indicates the approximate depth range of the 670 km transition zone (or "discontinuity"), but is also subject to lateral heterogeneity. The 400 km transition is not distinctly expressed in this EGT mantle section which would indicate that the generally invoked olivine-spinel phase change is heavily affected by the deep-reaching processes in the mantle and is, therefore, less clearly defined.

Selected tomographic images of the upper mantle structure beneath the Alps at an enlarged scale have been presented by Spakman (1990b). The cross-section which coincides with the Alpine segment of the EGT is displayed in Figure 25-4b. Cross-hatching outlines depth regions characterized by positive velocity anomalies, while horizontal ruling denotes negative velocity anomalies expressed by percentage variations referred to the Jeffreys-Bullen mantle velocity model. The feature dominating the section in its upper part is the clearly visible asymmetric "lithospheric root" which extends from the French-German border (near Karlsruhe) in the north all the way to the Northern Apennines and the Ligurian coast. A low-velocity asthenosphere of varying thickness – with its "undisturbed" lower boundary at 220–250 km – separates the deeper mantle anomalies from the overlying lithosphere, where the tomographic results compare surprizingly well with the inferences made from surface-wave dispersion studies (see e.g. Panza et al., 1980; Panza, 1985; Suhadolc et al., 1990). The Alpine "lithospheric root" dips towards the south-southeast reaching its maximum depth of 150–170 km under the Po plain. In the Gulf of Genova it borders on the asthenospheric updoming associated with the active rifting in the Ligurian Sea, while in the north it fades out towards the contact with the deep-reaching thickening of the asthenosphere beneath the "Central European Rift System" (see Figures 25-1a, 25-4a and 25-4b). The two depth sections in Figure 25-4 thus point to a decoupling between the lithosphere and the asthenosphere at varying depth levels – similar to the detachment at the Conrad (C) discontinuity within the crust (cf. Fig. 25-2a).

25.3 Dynamic processes

25.3.1 Integrated geodynamic modelling

So far it has been demonstrated that it is possible to construct gross lithosphere-asthenosphere models based on seismic surface-wave dispersion and body-wave tomography results which are representative for particular regions in the European-Mediterranean area. If – in addition – sufficiently dense and reliable gravimetric data are available they will impose one more stringent condition on the validity of the models. Time-dependent observational data, such as uplift and subsidence rates or the results of near-surface horizontal stress measurements, can provide further useful constraints. A quantitative description of these dynamic quantities would require a non-linear relation between displacement rate and stress. If it is assumed that the components of the stress tensor depend linearly on the displacement rates, then the problem can be reduced to the solution of the Navier-Stokes equation for a linear viscous, incompressible and horizontally layered Newtonian medium which utilizes a matrix formulation developed by Werner (1985; see also Gudmundsson, 1989).

Geodynamic model calculations involving the density and viscosity structure on the one hand, and the displacement rate ("velocity") and stress fields on the other, were carried out for a two-dimensional profile running from southwestern Germany to the northern Tyrrhenian Sea (Gudmundsson, 1989), crossing the Swiss Alps along the Eastern Traverse (see Pfiffner & Hitz, Chapter 9) to the Po Plain and the northwestern Apennines. The model satisfies the deep structure models (Figure 25-5a), their associated gravity anomalies (Figure 25-5b) as well as the observed uplift and subsidence rates (Figure 25-5c), particularly along the Alpine segment (Werner, 1985). For this profile five types of "load" must be taken into account: (1) the topographic load, (2) the density contrast between the crustal rocks and the sediments in the Molasse and Po Basins as well as the water layer in the northern Tyrrhenian Sea, (3) the variable crustal thickness (see e.g. Mueller et al., 1980; Valasek et al., 1991) with a density contrast between crust and uppermost mantle of 380 kg/m^3, (4) the "lithospheric root" (Panza & Mueller, 1978; Baer, 1980) characterized by relatively high seismic velocities and densities, and (5) the horizontal forces due to the present external plate-tectonic activity.

The density distribution of a reasonable model must (without the topographic load) satisfy the observed Bouguer gravity anomalies (Schwendener & Mueller, 1990). Figure 25-5b demonstrates the good agreement between the observed and calculated gravity anomalies (Gudmundsson, 1989). They show large negative values under the Alps and Apennines, interrupted by a relative "high" which is primarily due to the dense "lithospheric root" under the southern margin of the Alps. The residual gravity anomaly is the remaining anomaly after the "stripping" of all crustal effects – in other words, it exhibits the mantle portion of the anomaly.

Early in this century the Swiss Federal Office of Topography began to build up a highly precise first-order levelling network (1905-1927). A subsequent repeat measurement was completed in 1991. These levellings provide the basis for a determination of significant vertical movements between the northern Alpine foreland and the Alps (see also Kahle et al., Chapter 19). No direct connections to the coastal areas of the North Sea and the Ligurian Sea could be established up to now. For this reason only relative vertical movements have been determined so far which exceed their standard deviation by a factor of four and should therefore be regarded as highly significant. These results and preliminary geophysical interpretations have been published by Gubler et al. (1981) and Geiger et al. (1986, 1993) and are also discussed by Kahle et al. in Chapter 19.

The observed uplift rates relative to an arbitrarily fixed point of reference (Aarburg) reach values of up to 1.0–1.5 mm/a. Along the European Geotraverse (EGT) and the NRP 20 Eastern Traverse the maximum uplift in the Alps is presently located around Chur, while to the north and south the uplift rates decrease rather rapidly as shown in Figure 25-5c. Below the Po Plain the crust-mantle boundary rises to less than 30 km depth and then drops again to 45 km depth forming a crustal root beneath the Northern Apennines which should cause isostatic uplift. On the contrary, the Po Basin has been subsiding for the past 65 Ma at varying rates reaching values of up to 3.0 mm/a. At present the average rate of subsidence is 0.5 mm/a. This obvious discrepancy can only be eliminated if a dense "lithospheric root" under the Southern Alps and the Po Basin is introduced (cf. Figure 25-5a). Geodynamic modelling by Werner (1985) has demonstrated that a lithospheric "block" with a positive density contrast penetrating into the asthenosphere can explain the presently observed uplift rates.

The results of geodynamic modelling as formulated by Gudmundsson (1989) and Muttoni & Gudmundsson (1995) depend obviously to a large degree on the definition of a realistic reference model for the lithosphere-asthenosphere system. The geometry of the model chosen and its density contrast compared to the reference model together with the viscosity-depth distribution (Figure 25-5a) determine the gravity anomaly (Figure 25-5b), the uplift and subsidence rates (Figure 25-5c) as well as the stress field (Figure 25-5d). Due to the presence of the "lithospheric root" in the Alpine arc the global stress field in this region is significantly modified (Mueller, 1984). A strong compressive regime has been postulated to dominate the upper part of the Alpine crust as observed by Pavoni (1975) based on focal mechanism studies of earthquakes (cf. Figure 25-7a). Model calculations by Gudmundsson (1989) on a more detailed scale have revealed that in the central part of the Alps the shallow compressional region should be interrupted by a zone of extension (cf. Figure 25-5d) which has actually been observed (Figure 25-8b; after Maurer, 1995). It is caused by the local influence of the less dense "crustal root". The isostatic uplift (cf. Figure 25-5c) leads to north- and south-vergent reverse faulting (i.e. "positive flower structures") as illustrated by the sketch in Figure 25-2a and the model in Figure 25-8a (after Bott, 1990).

After many trial and error iterations the following characteristics have been found for the most plausible model (Gudmundsson 1989) satisfying the observed gravity anomaly as well as the uplift rates in the Alps and the subsidence rates in the Po basin:

– A density contrast at the crust-mantle boundary of + 380 kg/m^3 appears as most reasonable.

– The "lithospheric root" reaches to a depth of about 240 km, is about 120 km wide and has a density contrast of + 60 kg/m^3 compared to the surrounding asthenosphere.

– The viscosity of the crust has been assumed to be 10^{23} Pa·s with a slight decrease for the lower lithosphere, and $5 \cdot 10^{20}$ Pa·s for the asthenosphere and the "lithospheric root" increasing to 10^{21} Pa·s underneath in the mantle mesosphere (Figure 25-5a).

25.3.2 Recent seismicity and seismotectonics

Based on the recent seismicity (Figure 25-6a) as compiled by Waniek et al. (1982) a sufficiently large number of earthquake focal mechanism solutions is now available which permits to describe the seismotectonic stress pattern in the Mediterranean-Alpine region (Udias, 1982; Mueller, 1989). Several

Figure 25-5
Geodynamic model of the Alps along the line of the EGT prepared by Gudmundsson (1989) to predict the Bouguer gravity anomalies, the rates of uplift or subsidence and horizontal stress variations.

a)

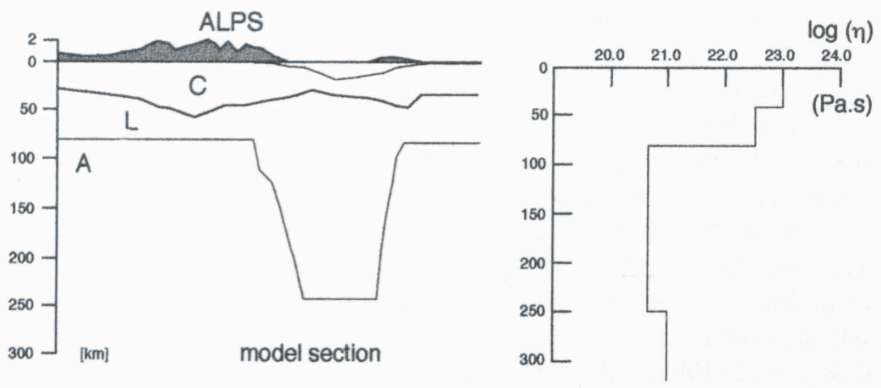

b)

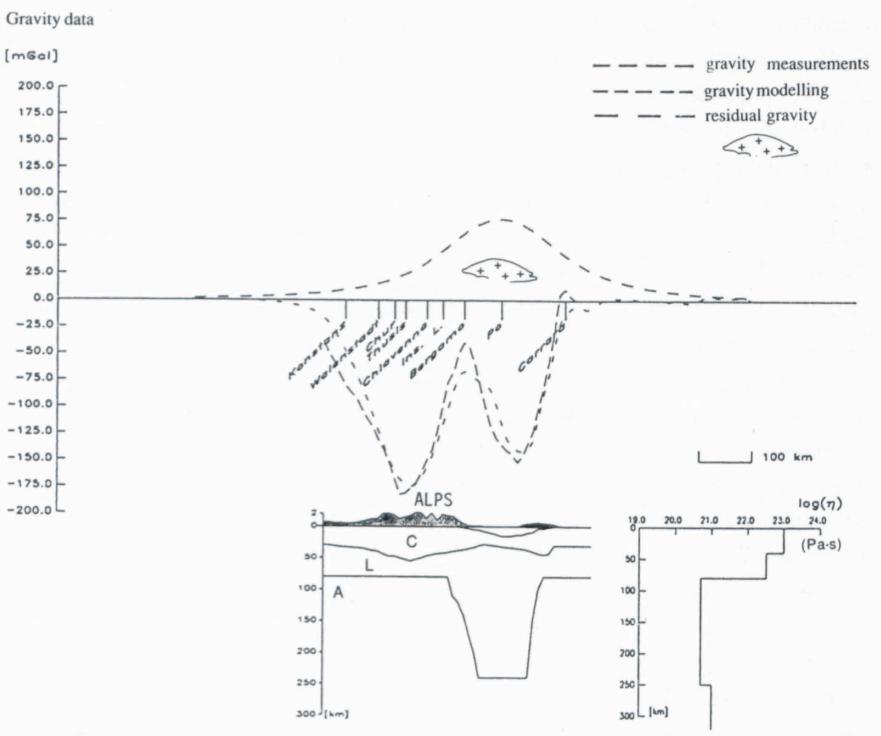

c)

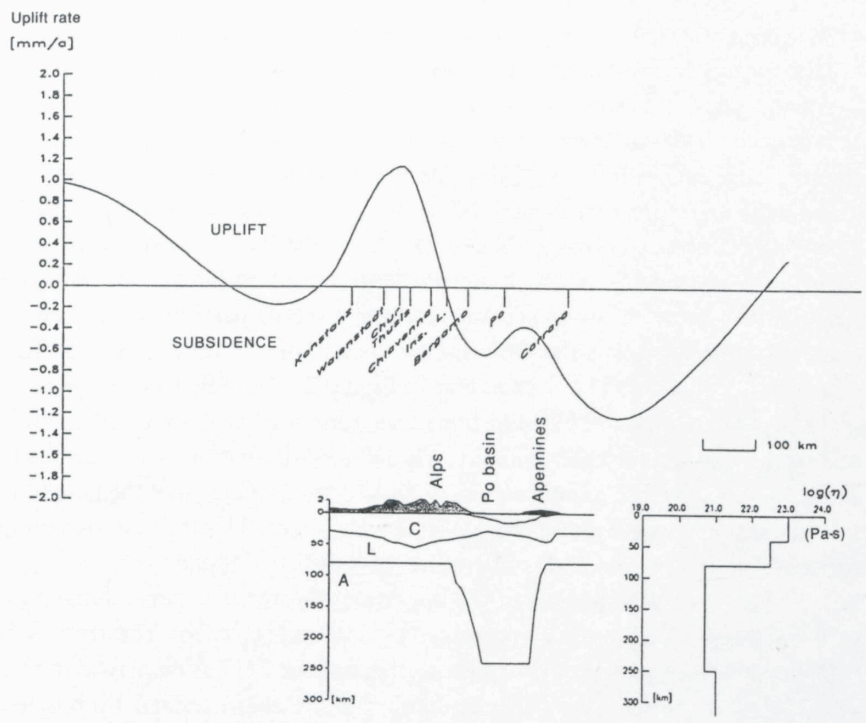

d)

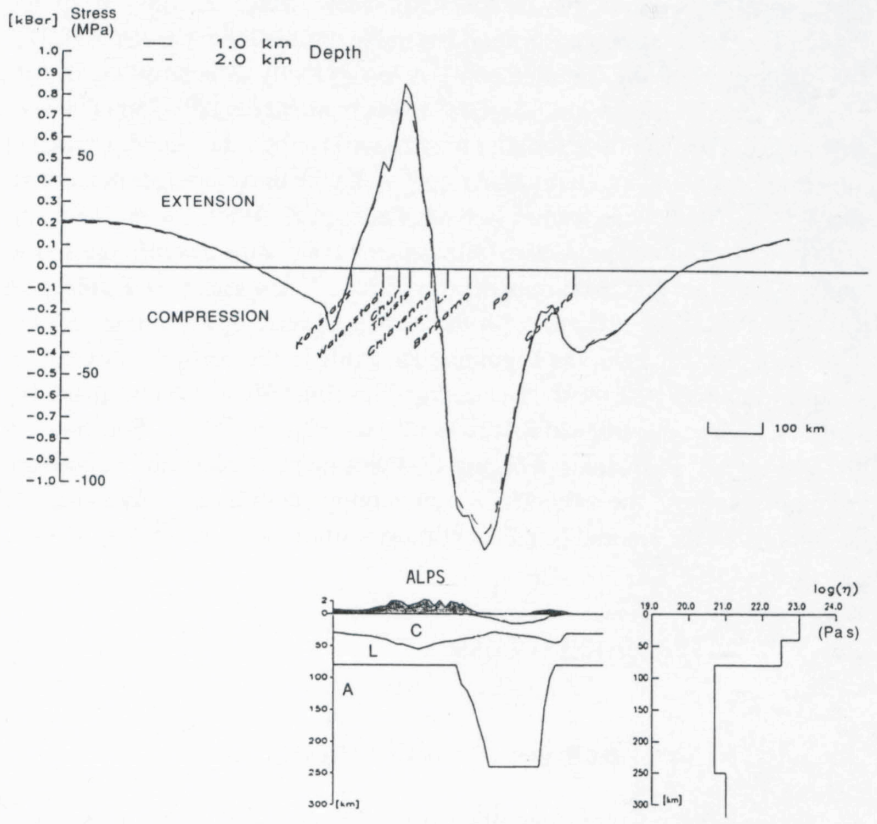

a) Model cross section from the northern foreland of the Alps to the northwestern Apennines (C = crust, L = mantle lithosphere, A = asthenosphere), and viscosity-depth profile (on the right) used in conjunction with the model geometry shown on the left to compute the gravity effect, the vertical movements and the horizontal stress field. Viscosity (η) is given in Pa·s.

b) Observed Bouguer gravity anomaly, corrected for near-surface effects compared to the modelled gravity variations and computed from the following density structure: Po basin, 2300 kg/m^3; Alpine topography, 2670 kg/m^3; Crust (C) 2880 kg/m^3; Mantle lithosphere (L), 3260 kg/m^3; "Lithospheric root", 3320 kg/m^3. The positive residual gravity variation due to the "lithospheric root" within the upper mantle is indicated by the + signs (dashed line on top).

c) Rates of vertical movements, with uplift positive and subsidence negative, computed for the model shown in (a). The modelled uplift (max. 1.2 mm/a) corresponds to the actual observations.

d) Horizontal stress (σ_x, in MPa) computed from the model in (a) at 1 and 2 km depth. Note the pronounced extensional regime in the center of the Alps (cf. also Figures 25-8a and 25-8b).

types of stress regimes are involved in the interaction of the African and Eurasian plates (Figure 25-6b). The dominant one is caused by the increasing spreading rate at the Mid-Atlantic ridge – from north to south – which leads to a gradual counterclockwise rotation of the African plate and results in a right-lateral movement of Africa against Eurasia along the Azores-Gibraltar fracture zone (see e.g. Mueller & Kahle, 1993). Further to the east the plate boundary is characterized predominantly by compressive features due to a north-northwestward oriented stress field. In particular, such compressive stresses prevail in the Alpine region caused by the push of the African plate through a wedge-shaped tip of the Adriatic promontory against central Europe, which is under a SE–NW directed compressional stress as a consequence of the ongoing ocean-floor spreading in the Atlantic Ocean (see Figures 25-6a and 25-6b).

The simplified plate-tectonic model presented so far offers no explanation for well-documented observations published by Pavoni (1975) which exhibit a striking coincidence of the trajectories of maximum horizontal compressive stress (Figure 25-7a) and the directions of maximum crustal shortening (Figure 25-7b) in the Alpine arc and the adjacent Jura Mountains. Figure 25-7b shows the orientation of the trajectories of maximum horizontal shortening (perpendicular to the fold axes) as deduced from an analysis of the Pliocene fold structures in the Alpine arc and its foreland, while Figure 25-7a depicts the trajectories of maximum horizontal pressure (P axes) determined from the focal mechanisms of twenty earthquakes in the Central and Western Alps. Since these trajectories deviate markedly from the dominant stress field in Europe (cf. small inset in Figure 25-6a) only a mechanism specifically characteristic of the Alpine lithospheric structure can provide an explanation for the cause and effect behind these peculiar observations (see Mueller, 1984). In the following section it will be demonstrated that the interaction between "the crustal and the lithospheric roots" is the dominant controlling factor governing the dynamics in the new collision model of the Alps.

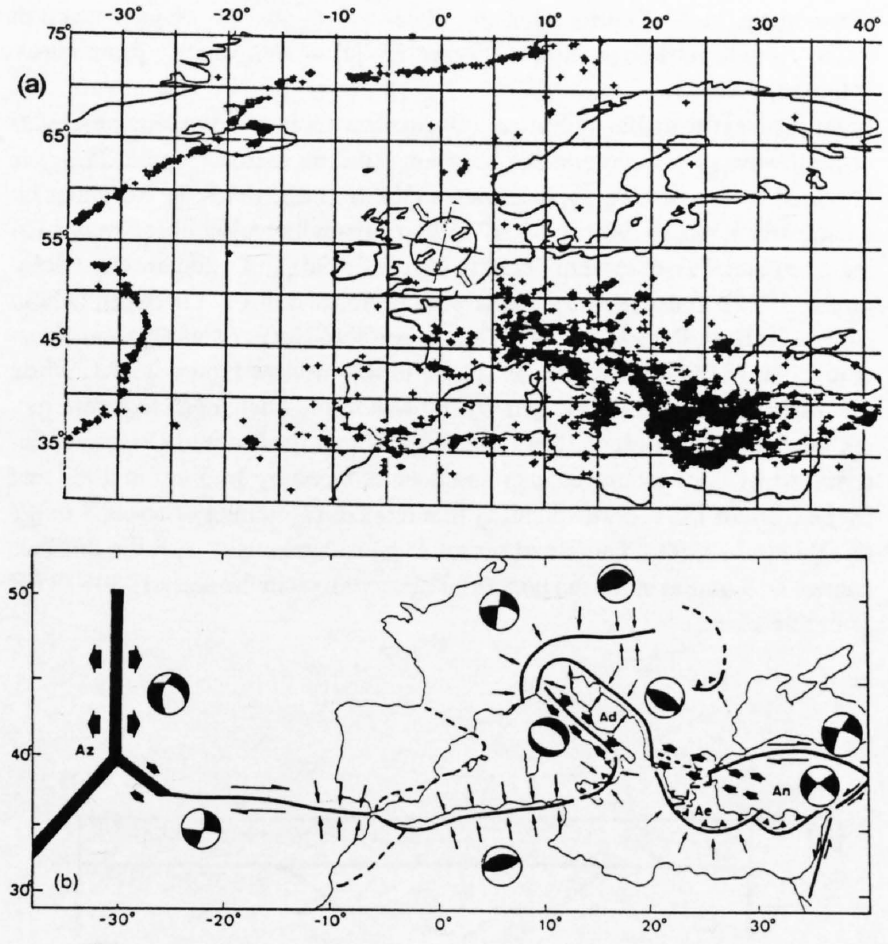

Figure 25-6
Present-day plate pattern and seismic activity.

a) The plate boundaries between North America, Africa and Eurasia as outlined by the recent seismicity (after Waniek et al., 1982). The black + signs represent the epicenters (1970-1980) of nearly 7000 earthquakes with magnitudes less than 5.0. They clearly outline the shape of the "Adriatic promontory" of the African plate (Channell & Horvath, 1976) which extends all the way into the Alpine arc. Also indicated is a simplified seismotectonic scheme for central and northwestern Europe (after Ahorner, 1975).

b) Generalized plate boundaries and seismotectonic stress pattern prevailing in the Mid-Atlantic ridge, the eastern Atlantic as well as in the Mediterranean and Alpine regions (after Udias, 1982). Az = Azores triple junction, Ad = Adriatic promontory. Microplates: Ae = Aegean, An = Anatolian.

25.3.3 Alpine stress regime

Seismic data have shown that the continuing collision process in the Alpine crust-mantle system must have produced a sizable thickening of the crust under the Alps, during which crustal material of lower velocity and density has been forced to a depth almost twice that of its original position. This so-called light "crustal root" is inherently unstable and will, therefore, give rise to isostatic readjustment aided by compressive forces and "wedging" (or "flaking", cf. Oxburgh, 1972) resulting in an asymmetric uplift of the Penninic domain.

As pointed out before the collision of two continental plates will not only lead to the formation of a light "crustal root", but will also produce a cold, dense and deep-reaching "lithospheric root" beneath a mountain chain (cf. Figures 25-2a, 25-3a and 25-3b) which – following Fleitout & Froidevaux (1982, 1983) and Bott (1990) – will induce regional compressive stresses able to maintain the mountain building process without requiring sustaining forces transmitted from far away. This positive feedback is inherently unstable; whenever it reaches a climax, episodic phases of strong compression will be observed accompanied by crustal uplift (see e.g. Kissling et al., 1983).

The geodynamic modelling of mountain belts was taken a stage further by Bott (1990) using finite-element analysis to elucidate the consequences of continent-continent collision and lithospheric thickening, extending the theory developed by Fleitout & Froidevaux (1982, 1983). His models assume that the lithosphere is made up of an elastic upper crustal layer (20 km thick) above a viscoelastic layer (cf. Figure 25-8a) consistent with the rheological behavior of the lithosphere-asthenosphere system to be discussed in the next section. The relief of the "crustal root" is modelled to be in isostatic equilibrium with the surface topography of the mountains, while the mass excess of the denser "lithospheric root" gives rise to a residual gravity anomaly of about + 80 mGal (cf. Figure 25-5b), in good agreement with that observed (Schwendener & Mueller, 1990). If for a symmetric configuration the loads induced from the "crustal root" and the "lithospheric root" are brought together, the tensional stress from the "crustal root" and the compressional stress from the "lithospheric root" more or less cancel out, leaving a negligible horizontal deviatoric stress in the upper crust of the mountain belt itself; but a moderate horizontal compressional stress is present on the flanks, i.e. the northern foreland and the southern hinterland of the Alpine arc. In the more realistic asymmetrical model shown in Figure 25-8a the "lithospheric root" underlies the right (southern) edge of the mountain range. Because of its lateral displacement, the compressional stress from the "lithospheric root" does not cancel the tensional stress from the "crustal root", so that quite large horizontal deviatoric stresses are present in the upper crustal layer, where the earthquake foci are located (Deichmann & Baer, 1990). As can be seen in Figure 25-8a the uppermost central part of the Alpine structure is un-

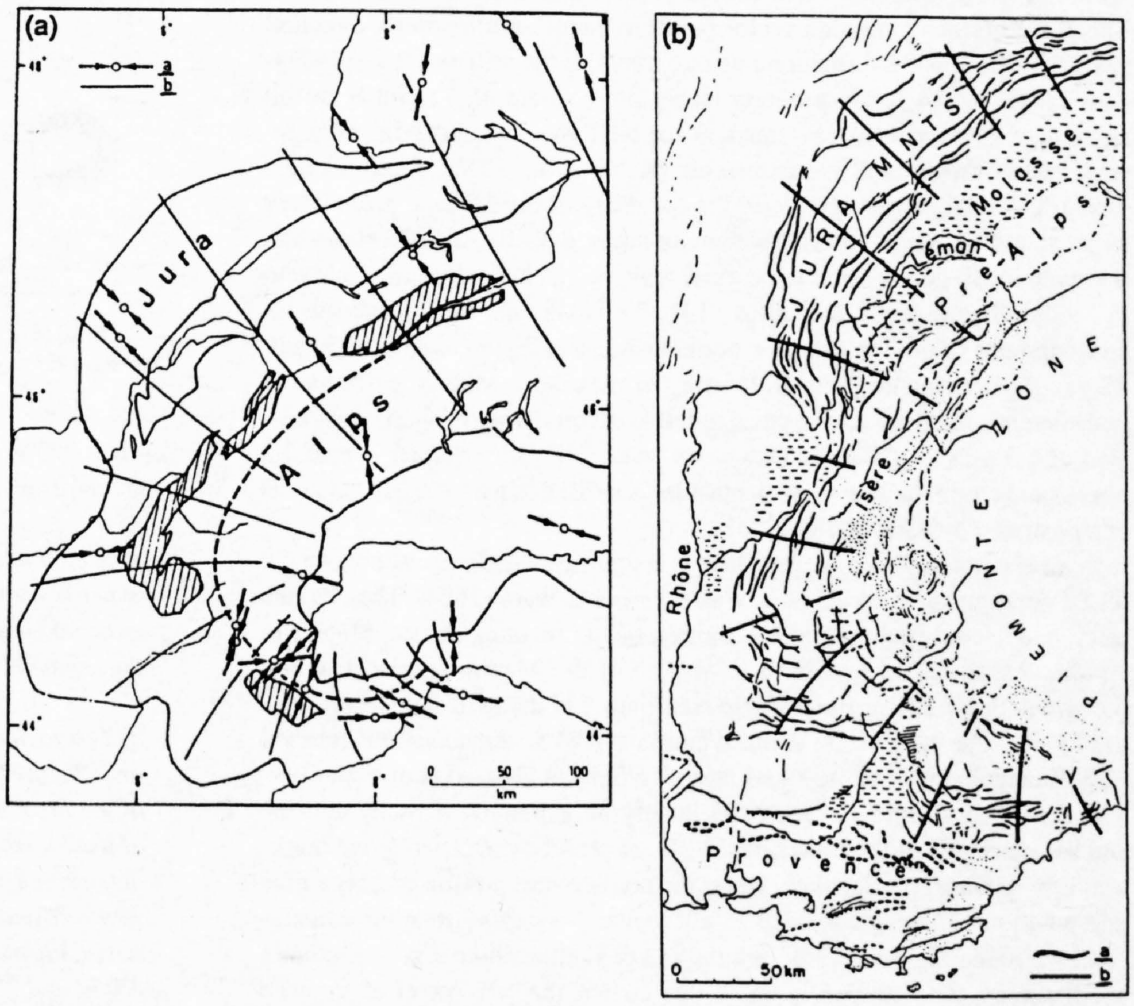

Figure 25-7
Crustal stress field and crustal shortening in the Western Alpine arc.

a) Crustal stress field as determined from the focal mechanisms of 20 earthquakes in the Western Alpine arc and in the Jura Mountains (after Pavoni, 1975). a: P axes of earthquake focal mechanisms; b: trajectories of maximum horizontal compressive stress.

b) Crustal shortening as deduced from a kinematic analysis of the Pliocene fold structures in the Western Alpine arc and in the Jura Mountains (after Pavoni, 1975). a: fold axes; b: trajectories of maximum horizontal shortening.

der tension, thus forming an asymmetric "positive flower structure", while the northern and southern foreland are subjected to moderate and strong compressional stresses, respectively. A very careful analysis of 18 fault plane solutions (Maurer, 1995) indicated different orientations of the principal stress axes to the north and south of the Rhône valley in the Valais (Figure 25-8b). The solutions to the north are mainly of strike-slip type with NW–SE oriented compression, while the focal solutions in the south show normal faulting with N–S oriented extension. This stress pattern can be explained by the combined effect of an asymmetric "lithospheric root" model as illustrated in Figure 25-8a and the vertical extension indicated by the sub-recent faults observed on the surface.

Once formed, the Alpine collision zone appears to function as a self-sustaining system in which the localized forces dominate. The dense "lithospheric root" not only pulls down, but also holds this anomalous zone together and keeps it narrow. Initiation of the system is most readily explained if a subducted slab of oceanic lithosphere was present at the onset of continental collision, as was most likely the case. After some time the "lithospheric root" will narrow to a point where it detaches and contributes no forces to the process anymore, with the result that only the crustal forces remain and dominate the system.

25.3.4 Microplate rotations

Paleomagnetic evidence indicates that the Iberian peninsula, the island chain of Corsica and Sardinia, the Apennine peninsula and the Ionian zone of Western Greece have all undergone rotations in a counterclockwise or clockwise direction to a varying degree (see e.g. Lowrie, 1980). There is strong reason to believe that at least for Italy and Western Greece (Horner & Freeman, 1983) such slow rotations are still in progress. Focal mechanism studies of earthquakes in the Central Alps (Pavoni, 1980) exhibit predominantly left-lateral movement with the axes of maximum horizontal compression perpendicular to the Alpine arc (cf. Figures 25-7a and 25-8b). It has been suggested some time ago (Mueller, 1984) that these sinistral earthquake mechanisms are a counter-reaction of the "rigid" upper crust in the Alps in response to the continuing counterclockwise rotation of the Apennine peninsula.

Recent results of space-geodetic measurements based on several high-precision techniques, such as "Very Long Baseline Interferometry (VLBI)", "Satellite Laser Ranging (SLR)" to the LAGEOS satellite and the "Global Positioning System (GPS)", have greatly enhanced our knowledge and understanding of actual crustal movements. The VLBI data obtained by the European network (Figures 25-9a and 25-9b, after Mantovani et al., 1995) have provided some insight into the current motion of the African plate versus the Eurasian plate in the Central Mediterranean and Adriatic regions.

Of the two similar VLBI interpretations the results of Ward (1994) are taken as the more likely solution, because it is consistent with the SLR and GPS results - in particular with regard to the tracking station at Matera and the observation site at Specchia Cristi in Apulia (cf. Figures 25-9a, 25-9c, 25-9d). There, the horizontal motion vector points in a north-northeasterly direction (28.7°) indicating a deformation rate of 6 mm/a. If the different scales in Figures 25-9a and 25-9c are properly taken into account, this result is in full agreement with the re-interpretation of the NNE movement of Matera as determined by recent SLR measurements (Kahle et al., 1995; Noomen et al., 1996). The relative motions along the boundary of the Adriatic promontory as predicted by Ward (1994) based on an inferred VLBI Adria-Europe rotation pole in Burgundy seem to be quite realistic (with the exception of Noto in Sicily). The recently published SLR results (Figure 25-9c) indicate increasing rates of motion from the northern Adriatic region to Apulia (Figure 25-9a). They compare quite well with the maximum seismic deformation rates determined from earthquakes in the Southern Alps (NW–SE compression of 1.3 mm/a), along the Dalmatian coast (NE–SW compression of 2.2 mm/a) and along the Apennine peninsula (NE–SE extension of 3.1 mm/a) as demonstrated by Kiratzi (1994).

It should be noted, however, that there is a significant difference between the VLBI interpretations by Zarraoa et al. (1994) and Ward (1994). The obvious discrepancy concerns the present motion of the tracking station Matera in Apulia. As discussed by Smith et al. (1994) the Matera site is generally thought to be located on the Adriatic promontory of the African plate (cf. Figure 25-6b). The most recent updated analysis of SLR oberservations (termed SL8.3) compare well to the VLBI interpretations of Zarraoa et al. (1994).

The deformation rates obtained can largely be explained if Sicily and the southwestern part of the Italian peninsula are presently attached to the northwesterly moving African plate, while the northeastern portion of Italy forms part of the Adriatic (or Apulian) "microplate" which is rotating counterclockwise (see Figure 25-9d) with respect to Europe about a pole southeast of Besançon. As has been pointed out earlier, the left-lateral earthquake mechanisms in the Central Alps are, therefore, an obvious counter-reaction to the continuous narrowing (cf. Figure 25-9a) of the Adriatic promontory (Mueller, 1984).

In this context valuable additional information about the dynamic processes in northwestern Greece and the southern Adriatic region (Figure 25-9c) is provided by recent GPS measurements (Kahle et al., 1995), in particular by a comparison of the 1989 and 1993 GPS results with earlier observations using a terrestrial laser system (TLR in Figure 25-9d) and a geodimeter (Balodimos, 1977). These measurements were performed in 1973 between Othoni island (OTHO), Pantokrator (PNTK) on northern Corfu (Kerkyra) and Specchia Cristi (SPEC) in Apulia, as shown in the inset of Figure 25-9d. While the distance between PNTK and OTHO was found unchanged to a centimeter, the distance between OTHO and SPEC across the Strait of Otranto as determined by GPS measurements had been reduced by 14.5 cm in 1989 and by 16.0 cm in 1991, corresponding to a relative shortening of about 8 mm/a (Kahle et al., 1993). This trend seems to be in agreement with the distance change (~ 9 mm/a) since the terrestrial observations in the early 1930's (TER in Figure 25-9d).

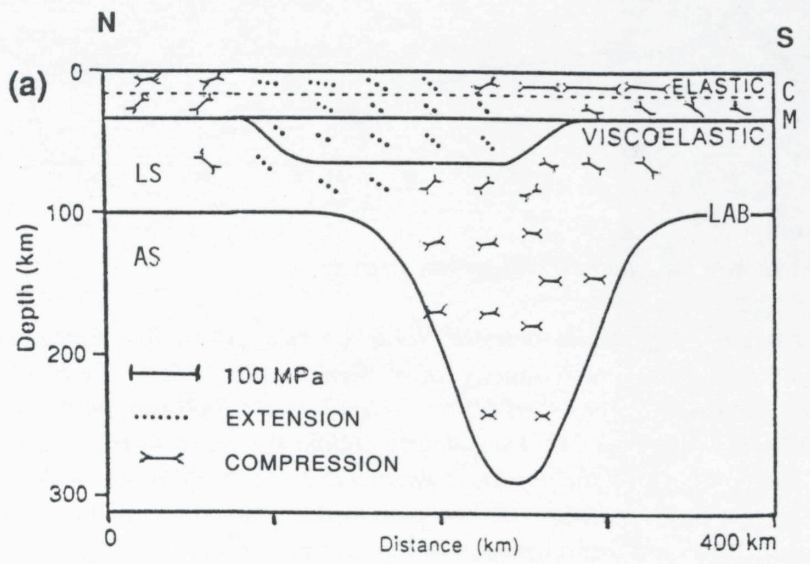

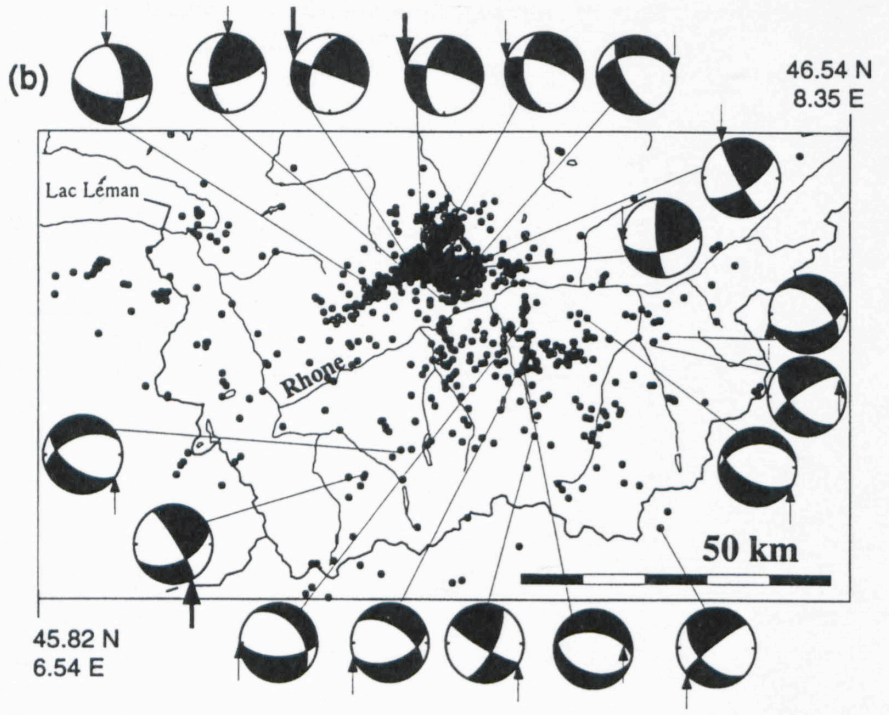

Figure 25-8
Distribution of compressional and tensional stresses in the Swiss Alps.

a) Sketch of stress distributions in a model of the lithosphere with an elastic upper layer overlying a visco-elastic substratum due to the thickening of the crust and mantle lithosphere (simplified after Bott, 1990). Stresses are due to the asymmetrically disposed "crustal and lithospheric roots".

b) Seismicity and focal mechanism solutions (lower hemisphere projection) for 18 stronger earthquakes in the Valais (after Maurer, 1995). The analysis of the resulting stress field reveals markedly different patterns on either side of the Rhône valley. The arrows indicate the actual active fracture planes as determined by the method of stress inversion (after Gephart & Forsyth, 1984). Whereas a strike-slip regime with SE–NW compression prevails in the north, normal faulting with N–S extension is found in the south (cf. Figures 25-5d and 25-8a).

Figure 25-9
Two contrasting geodynamic interpretations of large-scale geodetic measurements (VLBI, SLR, GPS) in the Central Mediterranean region with their constraints and uncertainties (after Mantovani et al., 1995).

a) Motion vectors based on VLBI site velocities in a fixed European reference frame (Ward, 1994). The vectors shown are referred to a frame which minimizes the deformation rates of the sites at Onsala, Effelsberg, Wettzell and Madrid.

b) Motion vectors for the same VLBI observation sites (after Zarraoa et al., 1994). The reference frame in this case fixes the coordinates of Wettzell (Germany), the directions from Wettzell to Onsala (Sweden) and a zero vertical motion at Madrid.

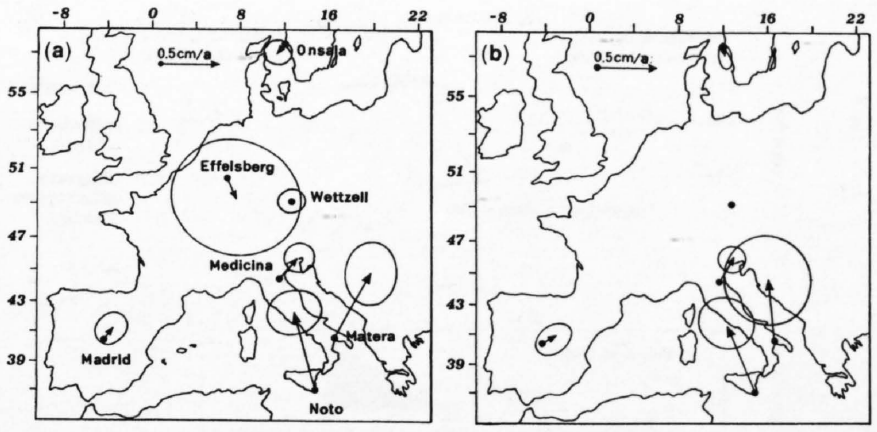

c) Horizontal components of the motion vector solutions for the geodetic stations in the Central and Eastern Mediterranean region. All vectors are relative to Eurasia. The corresponding (SLR) error ellipses represent 3σ-values (after Noomen et al., 1996). Inset (lower left corner): Annual displacement rates in the northeastern Ionian Sea as determined from GPS observations between 1989 and 1993 (Kahle et al., 1995). All motions are relative to Matera in southeastern Italy. The errors represented by the ellipses are 25 times the formal statistical error. As can be seen the station Karitsa in Epirus (Greece) does hardly move at all.

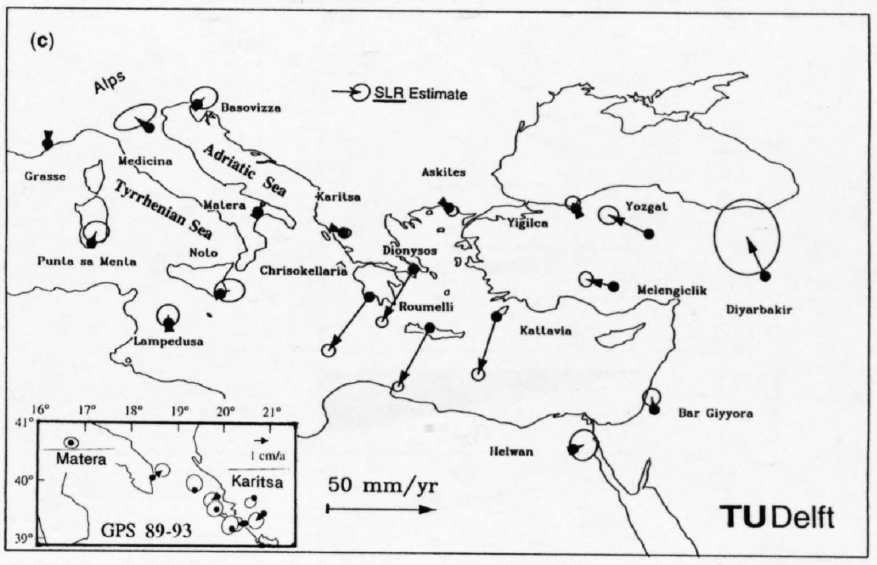

d) Apparent change of distance (shortening of ~ 9 mm/a) between Othoni island (OTHO) and Specchia Cristi (SPEC) in Apulia on the western flank of the Strait of Otranto during the past 60 years. TER = terrestrial observations, TLR = terrestrial laser experiment, GPS = measurements in 1989 and 1991 (after Kahle et al., 1993). The decreasing distance across the Strait of Otranto implies an ongoing counter-clockwise rotation of the Apennine peninsula.

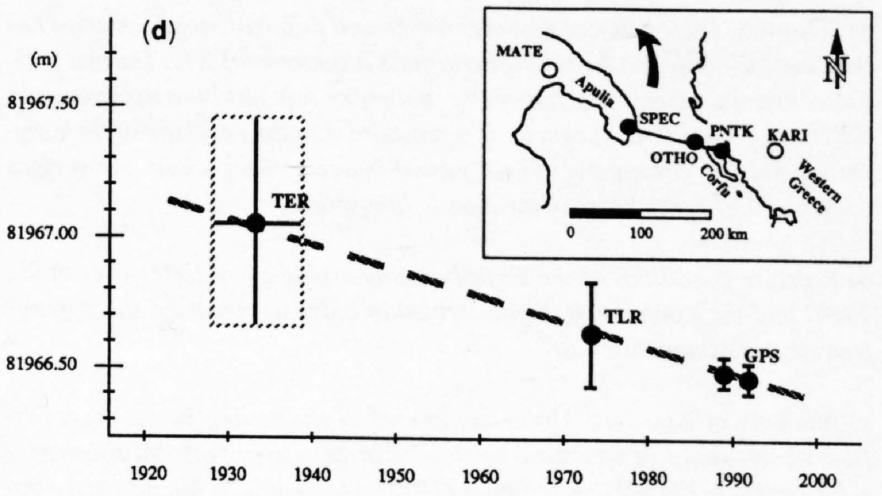

25.4 Lithosphere-asthenosphere evolution

25.4.1 Neo-Alpine evolution model

The existence of the "lithospheric root" and its continuing penetration into the asthenosphere in the course of shortening the Alpine lithosphere lead to an asymmetric exhumation (Figures 25-10a and 25-10c). In order to shed light on the present-day kinematic and thermal structure along the "European Geotraverse (EGT)" through the Central Alps, a model of Alpine evolution has been developed (Okaya et al., 1996) which comprizes the period from 35 Ma to the present, i.e. the so-called Neo-Alpine phase of orogeny. Generally the beginning of this phase is associated with the climax of the Tertiary metamorphic event at about 40–35 Ma (Frey et al., 1980; Hunziker et al., 1989). The model is constrained by tectonic and thermal data, such as deep seismic structure (Figure 15-10a), amounts of lithospheric shortening (Figure 15-10c) and exhumation (Figure 25-10a to 25-10d) as well as metamorphic grade, paleotemperatures and surface heat flow (Okaya, 1993).
Starting at 35 Ma the Neo-Alpine orogeny has been "tuned" step by step to the available observations. In a first modelling step it is assumed that the continuous convergence of the European (northern) plate and the Adriatic promontory of the African (southern) plate, which is characterized by lithospheric thickening and uplift by exhumation (cf. Figure 25-10a), can be described by a constant tectonic mass displacement field (see Figure 25-11a) during the last 35 Ma as a uniform tectonic process. With this simplified model in mind the implications of the present-day large-scale tectonics have been extrapolated back into the geological past.

25.4.2 Mass displacements

Quantification of the mass displacements is based on estimates of the total Neo-Alpine crustal shortening and exhumation. Vertical displacements (i.e. uplift) and exhumation depths are deduced from metamorphic data (Frey et al., 1980) related to the Alpine (Lepontine) metamorphic event at about 35 Ma (Hunziker et al., 1989; Hurford et al., 1989).
As can be seen in Figures 25-10b and 25-10d, the maximum total exhumation amounts to 20-25 km. Neo-Alpine total lithospheric shortening is estimated from data of structural geology to reach about 200 km or slightly more as indicated in Figures 25-10a and 25-10c (cf. Laubscher, 1991) with shortening of 145 to 150 km north of the Insubric Line (IL) on the northern or "European" side (Laubscher, 1991; Pfiffner, 1992), and 50 km south of the Insubric Line (IL) in the Southern Alps or on the "Adriatic/African" side (Laubscher, 1991; Schönborn, 1992). About 25 to 30 km of the northern shortening is compensated in the external massifs (EX) and the remaining 120 km in the Penninic nappes of the Lepontine zone (Figure 25-10c). A detailed, step by step kinematic evolution of this collision is presented by Schmid et al. in Chapters 14 and 22.
Crustal shortening (representing horizontal mass flow) in combination with exhumation depths (implying vertical mass flow) define the position of the present-day surface and outline the Neo-Alpine exhumation volume (Figure 25-10a). All these data have been used to constrain the Neo-Alpine mass displacement field on a lithospheric scale as illustrated schematically in Figures 25-10a to 25-10d. Away from the collision zone, the lithosphere shortens with a constant rate ("rigid push") over the entire lithospheric thickness of 70 ±10 km (Figure 25-10a). Within the collision zone proper it is assumed that

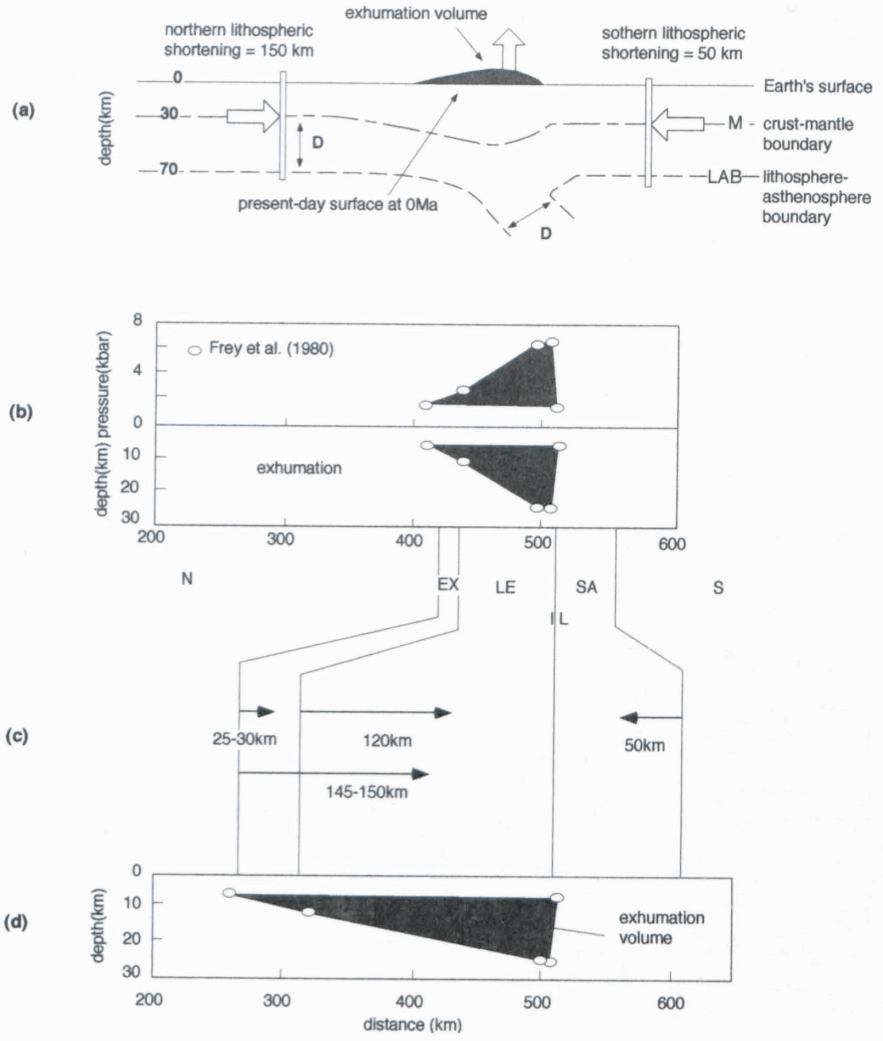

Figure 25-10
Data base to quantify the Neo-Alpine (35 to 0 Ma) large-scale mass displacement field (after Okaya et al., 1996).

a) Schematic illustration of how shortening and exhumation information has been used to constrain the lithospheric mass displacement field. The two horizontal arrows indicate that a uniform shortening rate has been assumed over the entire lithospheric thickness. It is assumed that the envelope of the exhumation volume corresponds to the mirror-image of the present-day surface 35 Ma ago. D = thickness of the mantle lithosphere.

b) Pressure conditions of the Tertiary metamorphic event (after Frey et al., 1980) and the exhumation depth derived in order to constrain the average Neo-Alpine exhumation rate.

c) Amounts of total Neo-Alpine upper-crustal shortening based on results from observations in structural geology. Northern upper-crustal shortening after Laubscher (1991) and Pfiffner (1992), shortening in the external massifs (EX) after Pfiffner (1992), and southern upper-crustal shortening after Schönborn (1992). LE = Lepontine (Penninic domain), IL = Insubric Line, SA = Southern Alps.

d) Compilation of all the Neo-Alpine shortening and exhumation data in order to constrain the original exhumation volume.

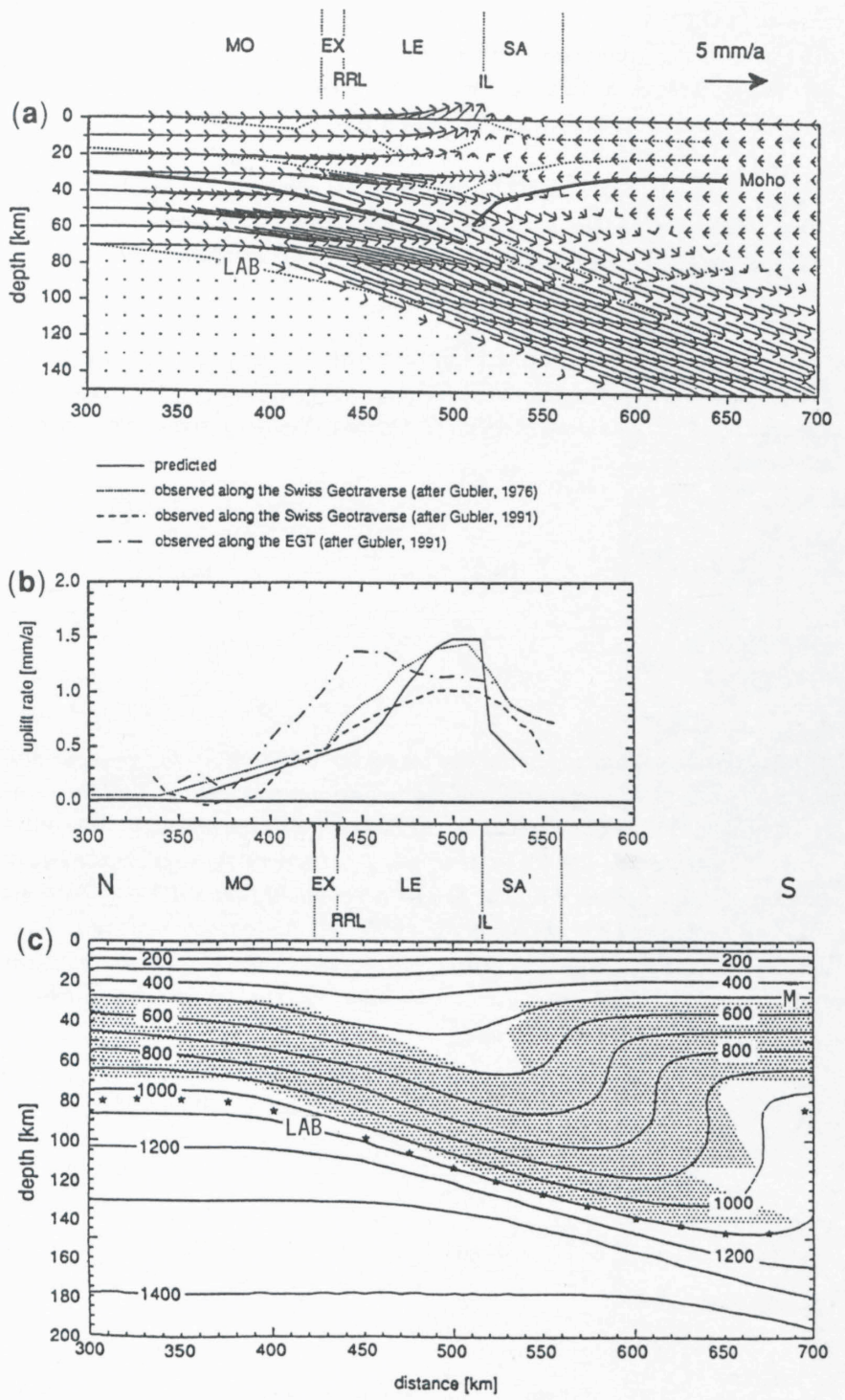

Figure 25-11
Results from kinematic modelling

a) Kinematic modelling results of the Neo-Alpine (35 to 0 Ma) orogeny. The assumed large-scale tectonic mass displacement field along the "European Geotraverse (EGT)" through the Swiss Alps is shown by arrows, while the present configuration is indicated by a dotted line and the crust-mantle boundary ("Moho") is marked by a thick solid line. MO = Molasse basin, EX = external massifs, RRL = "Rhine-Rhône Line", LE = Lepontine, IL = Insubric Line, SA = Southern Alps.

b) Comparison of the present-day uplift rates (mm/a) as derived from geodetic observations (Gubler, 1976, 1991) and the exhumation rates at the surface as given by the kinematic model (cf. Figures 25-10a and 25-11a).

c) Present-day temperature field (isotherms at 100°C intervals). The dots indicate the lithosphere-asthenosphere boundary (LAB), thermally defined as the intersection point of the geotherm with the mantle solidus. The shaded area shows the deformed mantle lithosphere as derived from tectono-kinematic calculations (cf. Figure 25-11a). For an explanation of MO, EX, RRL, LE, IL and SA see also Figure 25-11a and the discussion in the text (after Okaya et al., 1996).

only denser material is being subducted and "decoupled" from the lighter crustal material above or at the crust-mantle boundary (M).
Based on the present-day seismic structural image and its resulting density pattern, as derived from an improved relationship between P-wave velocity and density (Woollard, 1975), the estimated shortening and exhumation rates were used to obtain a mass displacement field describing the Neoalpine orogeny as a uniform process in time (Figure 25-11a). The result shows an overall satisfactory agreement between the observed and calculated relief of the crust-mantle boundary (Moho) and the lithosphere-asthenosphere transition (LAB). This transition zone, as predicted by the kinematic model, cannot simply be compared to the observed base of the lithosphere which represents a zone of incipient partial melting (~ 900° to 1100°C), i.e. it is a thermal "boundary". Outcropping intracrustal boundaries in the core of the mountain belt illustrate exhumation of material from greater depth (cf. near IL in Figure 25-11a). The observed "jump" at the Insubric Line (IL) from the highly metamorphic realm of the Lepontine (LE) to the anchi-metamorphic Southern Alps (SA) is quite well reproduced by the model.
Model results of the last 2 Ma of the Neo-Alpine orogeny yield exhumation rates at the surface which have been compared to the pattern of recent uplift rates (Figure 25-11b) along the EGT and the "Swiss Geotraverse" (Gubler et al., 1992; Gubler, 1991; Gubler, 1976). The calculated uplift rates agree better with the pattern of uplift rates along the "Swiss Geotraverse" from Basel to Chiasso/Como, which transects the high-metamorphic zone of the Lepontine, than along the EGT, where the surface rocks exhibit a lower degree of metamorphism.
The modelled present-day temperature field is shown in Figure 25-11c with the shaded image of the deformed mantle part of the lithosphere superimposed. The asymmetric characteristics of the tectonic setting are clearly reflected in the deep thermal structure. In the upper crust the horizontal temperature variation follows the gross pattern of the predicted surface heat flow (Okaya et al., 1996). At mid-crustal levels the 300°C isotherm (Figure 25-11c) is practically flat from north to south. At greater depth a moderate thickening of the lower crust and the subduction of the European mantle litho-

sphere leads to a conspicuous deformation of the 400° to 1100°C isotherms reaching to a depth of 140 km. The shape of these isotherms describes a negative thermal anomaly which can be explained in terms of a stack of cool, upper-crustal slices piled up in the course of the Neogene collision and subduction of the lower lithosphere.
The reliability of these results was tested by exploring a number of thermo-kinematic models in which the geometry of the mass displacement field was varied (Okaya, 1993). These tests have demonstrated that the thermo-kinematic model presented here yields the best agreement with the combined available geological and geophysical data. The assumed structural geometry and the physical parameters chosen provide sufficiently good constraints on the temperatures in the upper lithosphere, but are not yet good enough to deduce reliably the temperature field in the lower part of the lithosphere. It has, however, become clear that the asymmetric feature of the present-day tectonic structure along the EGT (Figure 25-4b) is also strongly expressed in the thermal structure of the lithosphere (Figure 25-11c).

25.5 Summary and Conclusions

In this brief summary chapter an attempt has been made to unravel and understand the deeper structure, dynamics and evolution (during the past 40 to 35 Ma) of the Alps as a continent-continent collision zone. To this end it is not sufficient to consider only the details of the upper or even the whole crust and extrapolate to greater depth. It has turned out quite clearly that it is necessary to study the entire lithosphere-asthenosphere system to depths of a few hundred kilometers.
The first step in this approach has naturally been rather crude, but has revealed several new features which turned out to be quite surprizing. Various geophysical methods and techniques have been used to elucidate the crust-mantle structure in a synoptic manner. As a result of the still ongoing collision process parts of the lithosphere have apparently been delaminated, leading to "flaking" in the upper crust combined with an asymmetric thickening of the whole crust and the formation of a relatively cold, dense and slowly subsiding "lithospheric root" beneath the Alps. The detached lower crust and mantle lithosphere appear to have penetrated into the asthenosphere to a depth of 130 to 200 km.
The presently measurable subsidence and uplift are due to a superposition of the effects caused by the "dense lithospheric and light crustal roots". From earthquake focal mechanisms a SE–NW directed compressional stress field could be deduced which in the central part of the Alps is interrupted by a zone of extension as postulated by geodynamic modelling. The left-lateral displacements associated with the dominant Alpine stress regime are very likely a reaction to the slow counter-clockwise rotation of the Apennine peninsula as indicated by various recent geodetic observations.

Acknowledgement

Thanks are due to a large number of individuals and institutions who, for more than 10 years, have cooperated unselfishly within the Swiss National Research Project 20 and whose contributions have made it possible to assemble a comprehensive data set about the structure, dynamics and evolution of the Alps. The author wishes to acknowledge the generous financial support by the Swiss National Science Foundation. Special thanks go to the author's colleagues and collaborators at the "Institut für Geophysik der ETH Zürich" for many stimulating discussions and constructive criticism.
Contribution No. 916, ETH-Geophysics, Zürich, Switzerland.